UNIVERSITÄT ZU LÜBECK

From the Institute for Biochemistry
of the University of Lübeck
Director: Prof. Dr. Thomas Krey

Dendritic cell- and T cell-based Immune Therapies against Ebola Virus Infection

Dissertation
for the fulfilment of
the requirements
for the doctoral degree
of the University of Lübeck

from the Department of Natural Sciences

submitted by

Catherine Awuor Olal

from Nairobi, Kenya

Lübeck, 2023

First referee: Prof. Dr. Lars Redecke

Second referee: Prof. Dr. rer. nat Rudolf Manz

Date of oral examination: 13.09.2023

Approved for printing: 22.09.2023

Declaration

I hereby confirm that this thesis has been written by me and that it is the record of work carried out by me or principally by myself in collaboration with others as acknowledged, and that it has not been submitted in any previous application for a higher degree. All references and sources of information have been duly cited and acknowledged.

Hamburg, 2023

Acknowledgement

I would like to thank the following people without whom I would not have been able to complete this dissertation. First, all the past and present members of the virus immunology team at the Bernhard Nocht Institute for Tropical Medicine especially my supervisor Prof. César Muñoz-Fontela. His insight knowledge and guidance steered me through the project. Special thanks to Prof. Lars Redecke for his valuable support and willingness to assist in any way he could throughout my time as a doctoral student. I would like to thank Dr. Julia Port and Monika Rottstegge for their advice regarding assay establishment, analyses and moral support. I would like to thank Dr Emily Nelson and Andras Bencsik for their input and moral support. I would also like to thank Dr. Beatriz Escudero-Pérez for assisting with the animal training in the BSL-4 lab and offering her help whenever needed. Many thanks to the animal facility team at the institute especially Yvonne Richter, Constantin Pretner and Aline Adams and the virology department especially Dr. Lisa Osterreich and Olivia Blake.

Finally, to my family, thank you for all your support without which I would not have been able to achieve this. Asanteni sana kwa mawaidha na fedha. Enyewe Mungu ametutoa mbali na anatupeleka mbali. To my dearly departed father, thank you for always believing in me and encouraging me. This is for you.

Table of Contents

Chapter **Page**

List of figures

List of tables

List of abbreviations

α	anti-
µg	microgram
µl	microlitre
µm	micromolar
Ab	antibody
Ag	antigen
APC	antigen presenting cell
APC	allophycocyanin
AST	aspartate aminotransferase
BDBV	*Bundibugyo ebolavirus*
BOMV	*Bombali ebolavirus*
BSA	bovine serum albumin
BSL-4	biosafety level 4
BUV	brilliant ultraviolet
BV	brilliant violet
CD	cluster of differentiation
cDC	conventional dendritic cell
CFR	case fatality rate
CTL	cytotoxic T lymphocyte
CTLA-4	cytotoxic T lymphocyte associated protein
Cy	cyanine
DC	dendritic cell
DCIR	dendritic cell inhibitory receptor
DC-SIGN	dendritic cell specific intercellular adhesion molecule
DMEM	Dulbecco's modified eagle medium
DMSO	dimethyl sulfoxide
DNA	deoxyribonucleic acid
DPI	day post infection/immunization
EBOV	*Zaire ebolavirus*
EBV	Epstein-Barr virus
EDTA	ethylenediaminetetra acetic acid
ELISpot	Enzyme-linked Immunospot

et al	et alii (and others)
EVD	Ebola virus disease
FBS	foetal bovine serum
Fc	fragment crystallisable
FCS	foetal calf serum
Fig.	figure
FFU	focus forming units
FITC	fluorescein isothiocyanate
FSC	forward scatter
g	gram
g	standard gravity
GFP	green fluorescent protein
Gy	Gray
GP	glycoprotein
h	hour(s)
HEK 293T cells	human embryonic kidney cells
HIV	human immunodeficiency virus
HLA	human leukocyte antigen
HRP	horseradish peroxidase
IFA	Immunofocus assay
IFN	interferon
ISG	interferon stimulated genes
Ig	immunoglobulin
IL	interleukin
IVC	individually ventilated cages
kDa	kilodaltons
L	litre
LC	Langerhans cells
LCMV	Lymphocytic choriomeningitis mammarenavirus
LLOV	*Lloviu cuevavirus*
Ly5.1	natural allelic isoform of CD45 known as CD45.1
mAb	monoclonal antibody
MACS	magnetic-activated cell sorting

MARV	*Marburg marburgvirus*
MHC	major histocompatibility complex
min	minute(s)
ml	millilitre
mM	millimolar
MOI	multiplicity of infection
mRNA	messenger ribonucleic acid
ng	nanogram
NK	natural killer
NP	nucleoprotein
NHP	non-human primate
NK cell	natural killer cell
OVA	ovalbumin
PAMP	pathogen associated molecular pattern
PBS	Dulbecco's phosphate buffered saline
PD-1	programmed cell death protein-1
PE	phycoerythrin
PEI	polyethylenimine
pH	negative decimal logarithm of the H^+ ion concentration
PMA	phorbol 12-myristate 13-acetate
PRR	pattern recognition receptor
P/S	penicillin/streptomycin
RdRp	RNA-dependent RNA polymerase
RESTV	*Reston ebolavirus*
RIG	retinoic-acid inducible gene
RNA	ribonucleic acid
rpm	revolutions per minute
RPMI	Roswell Park Memorial Institute
RT	room temperature
SDS-PAGE	sodium dodecyl sulfate polyacrylamide gel electrophoresis
SEM	standard error of the mean
sGP	soluble glycoprotein
SSC	side scatter

SUDV	*Sudan ebolavirus*
TAFV	*Tai forest ebolavirus*
TCR	T cell receptor
Th	T helper cell
Tfh	T follicular helper cell
Treg	T regulatory cell
TNF	tumour necrosis factor
TLR	toll-like receptor
U	units
UV	ultraviolet
VP	virus protein
VSV	vesicular stomatitis virus
WHO	World Health Organization
WT	wild-type

Abstract

Ebola virus disease (EVD) is a severe and often fatal illness in humans characterized by multi-organ failure and dysfunctional host immune responses. There are currently two approved/licensed vaccines against EVD. These vaccines have been shown to induce a strong humoral immune response. However, the exact correlates of protection are not yet known. Furthermore, the duration of the immune response after vaccination as well as the efficacy linked to such a long-term immune response have not yet been conclusively determined. There is therefore still a need to develop EVD-specific medical countermeasures, both prophylactic and therapeutic.

Vaccines that induce potent cellular immunity are highly desirable in the context of EVD due to the importance of T cells, especially $CD8^+$ T cells, in viral clearance. In this regard, various strategies can be employed with the ultimate goal of inducing EBOV-specific T cells.

One approach that can be used to generate EBOV-specific T cells is the delivery of virus antigens to dendritic cells (DCs). By doing so, antigens are targeted to the immune cell subset responsible for the priming of naïve T cells, thereby bridging innate and adaptive immunity.

In this study, the EBOV nucleoprotein (NP) was conjugated to a monoclonal antibody specific for DEC205; a C-type lectin endocytic receptor found on DCs. Antigen-antibody complexes internalized by DCs via binding to DEC205 result in the cross-presentation of NP-derived peptides to $CD8^+$ T cells, which results in viral clearance. The data herein shows the feasibility of using anti-DEC205 antibodies to deliver virus antigens to DCs. Targeted DCs were able to activate EBOV-specific $CD8^+$ T cells both *in vitro* and *in vivo*. The prophylactic potential of EBOV NP-conjugated anti-DEC205 antibodies in susceptible mice was also evaluated and the data shows that targeting antigens to $DEC205^+$ DCs results in the development and proliferation of antigen-specific memory $CD8^+$ T cells that are protective against lethal EBOV challenge.

Zusammenfassung

Die Ebolavirus-Krankheit (engl. *Ebola virus disease*, kurz: EVD) ist eine schwere und häufig tödlich verlaufende Erkrankung im Menschen, für die Multiorganversagen und eine gestörte Immunreaktion des Wirts charakteristisch sind. Zurzeit gibt es zwei zugelassene Impfstoffe gegen EVD. Diese Impfstoffe induzieren eine starke humorale Immunantwort. Die Dauer der Immunantwort in Folge der Impfung sowie deren Wirksamkeit in Bezug auf eine Langzeitimmunität und die damit korrelierende Protektion sind jedoch noch nicht hinreichend bekannt. Aus diesem Grund besteht nachwievor die Notwendigkeit EVD-spezifische medizinische Gegenmaßnahmen sowohl zur Prävention als auch zur Postexpositionsprophylaxe zu entwickeln. Aufgrund der Bedeutung von T-Zellen für die Virusabwehr, insbesondere von $CD8^+$ T-Zellen, sind solche Impfstoffe im Rahmen einer EVD äußerst erstrebenswert, welche eine starke zelluläre Immunantwort erzeugen. Es können verschiedene Strategien angewendet werden, die zum Ziel haben gegen Ebolavirus (EBOV) gerichtete T-Zellen zu induzieren. Ein möglicher Ansatz diese EBOV-spezifischen T-Zellen zu generieren, ist die Vermittlung von Virusantigenen an dendritische Zellen (engl. *dendritic cells*, kurz: DCs). Auf diese Weise werden Antigene gezielt zu der Population der Immunzellen geleitet, welche für das Priming naiver T-Zellen verantwortlich sind und damit eine Verbindung zwischen der angeborenen und adaptiven Immunantwort herstellen. In dieser Arbeit wurde das EBOV Nukleoprotein (NP) an monoklonale, für DEC205 spezifische Antikörper konjugiert. DEC205 ist ein C-Typ Lektinrezeptor auf DCs, welcher nach Antigenbindung internalisiert und endozytisch prozessiert wird und daher für diese Anwendung geeignet ist. Antigen-Antikörper-Komplexe, welche über DEC205 von DCs internalisiert werden, werden $CD8^+$ T-Zellen als EBOV NP-Peptide kreuzpräsentiert und resultieren so in der Virusbeseitigung. Die Daten dieser Arbeit belegen, dass Anti-DEC205-Antikörper zum Transport von Virusantigenen an DCs verwendet werden können. Anvisierte DCs waren in der Lage EBOV-spezifische $CD8^+$ T-Zellen sowohl *in vitro* als auch *in vivo* zu aktivieren. Darüber hinaus wurde das Potential zur Prophylaxe von EBOV NP-konjugierten Anti-DEC205-Antikörpern in für EVD-empfänglichen Mäusen untersucht. Die Daten zeigen, dass Antigene, welche über DEC205 von DCs internalisiert werden, zur Entwicklung und Vermehrung antigenspezifischer $CD8^+$ T-Zellen führen, die vor einer tödlichen EBOV-Infektion schützen.

1. Introduction

1.1 Family *Filoviridae*

The family *Filoviridae* is composed of 6 virus genera namely *Cuevavirus, Dianlovirus, Ebolavirus, Marburgvirus, Striavirus, and Thamnovirus*. Filoviruses cause severe, often fatal disease in humans. Filoviruses are negative strand RNA viruses with genomes that are approximately 19 kilobases in length. There are various characteristics that determine the inclusion of viruses into the family *Filoviridae* such as the ability to cause viral haemorrhagic fevers in primates, a genome that has a molecular weight of $4.2x10^6$ Da and contains seven genes in the order 3'-UTR-*NP-VP35-VP40-GP-VP30-VP24-L*-5'-UTR. (Kuhn et al., 2010). Filoviruses have a long filamentous morphology.

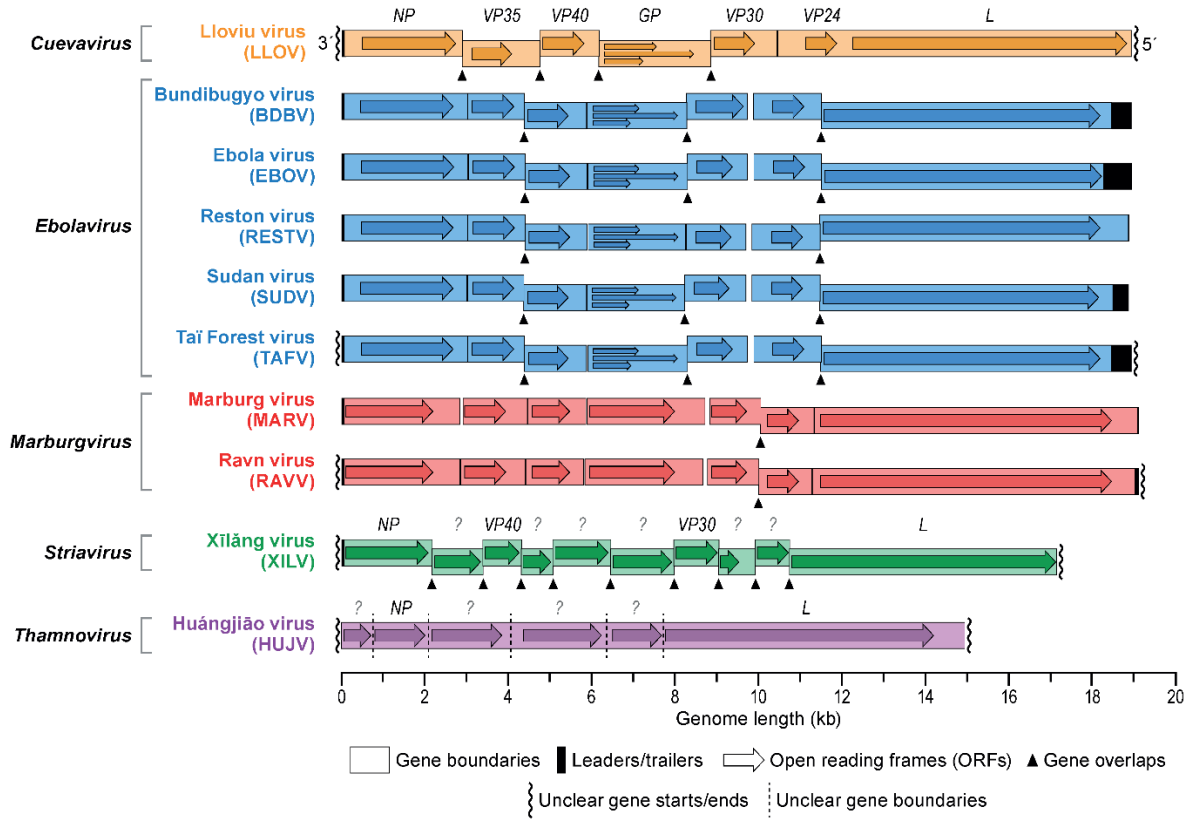

Figure 1. Schematic representation of the filovirus genome organization.

Genome map of known filoviruses illustrating the gene order (from Kuhn et al., 2019).

1.1.1 *Cuevavirus*

The genus *Cuevavirus* has one species known as Lloviu virus (LLOV) which was first discovered in 2011 in dead Schreibers' long-fingered bats (*Miniopterus schreibersii*). It is currently the only filovirus known to be present in Europe (Negredo et al., 2011). In 2016, the virus was found in bat carcasses in Hungary, followed by reports of seropositive Schreiber's bats in Spain (Kemenesi et al., 2018; Ramírez de Arellano et al., 2019). Infectious LLOV was recently isolated from Schreiber's bats in Hungary. They were able to culture the virus and showed that monkey and human cells are permissive to LLOV infection (Kemenesi et al., 2022), which suggests that there is a potential for bat-to-human spillover events.

1.1.2 *Marburgvirus*

The genus *Marburgvirus* includes a single virus species, *Marburg marburgvirus,* whose current members are Ravn virus (RAVV) and Marburg virus (MARV). Marburg virus was discovered in 1967 after an outbreak of haemorrhagic fever among factory workers that had been in contact with African green monkey (*Chlorocebus aethiops*) tissues in Marburg, Germany, and Belgrade, Serbia (Emanuel et al., 2018). Since then, there have been 13 known outbreaks of Marburg virus disease (MVD). MVD outbreaks occur sporadically in remote regions of sub-Saharan Africa. The largest MVD outbreaks occurred in the Democratic Republic of the Congo (DRC) from 1998 to 2000 and in Angola in 2005. The outbreak in Angola had a case fatality ratio of 90 %, one of the highest reported to date for any filovirus outbreak (Amman et al., 2021).

1.1.2.1 Ecology

Cave-dwelling Egyptian rousette bats (*Rousettus aegypticus*) are the natural reservoirs of Marburgviruses. MARV and RAVV have been isolated from/found in Egyptian rousette bats in Kenya, Zambia, South Africa and Sierra Leone (Amman et al., 2020; Kajihara et al., 2019; Kuzmin et al., 2010; Pawęska et al., 2018, 2020; Storm et al., 2018). The presence of antibodies, detection of viral RNA and the culture of the isolated infectious virus in permissive cells have led to proposition of Egyptian rousette bats as the reservoir for MARV (Adjemian et al., 2011; Pourrut et al., 2009; Swanepoel et al., 2007; Towner et al., 2007).

Experimental infection of bats with MARV has shown that oral shedding of the virus may facilitate bat-to-bat transmission through biting and possibly bat-to-primate transmission

(Amman et al 2015). MARV RNA has been detected in the urine of Egyptian rousette bats signalling another potential route of bat-to-bat transmission (Paweska et al., 2015; Schuh et al., 2017).

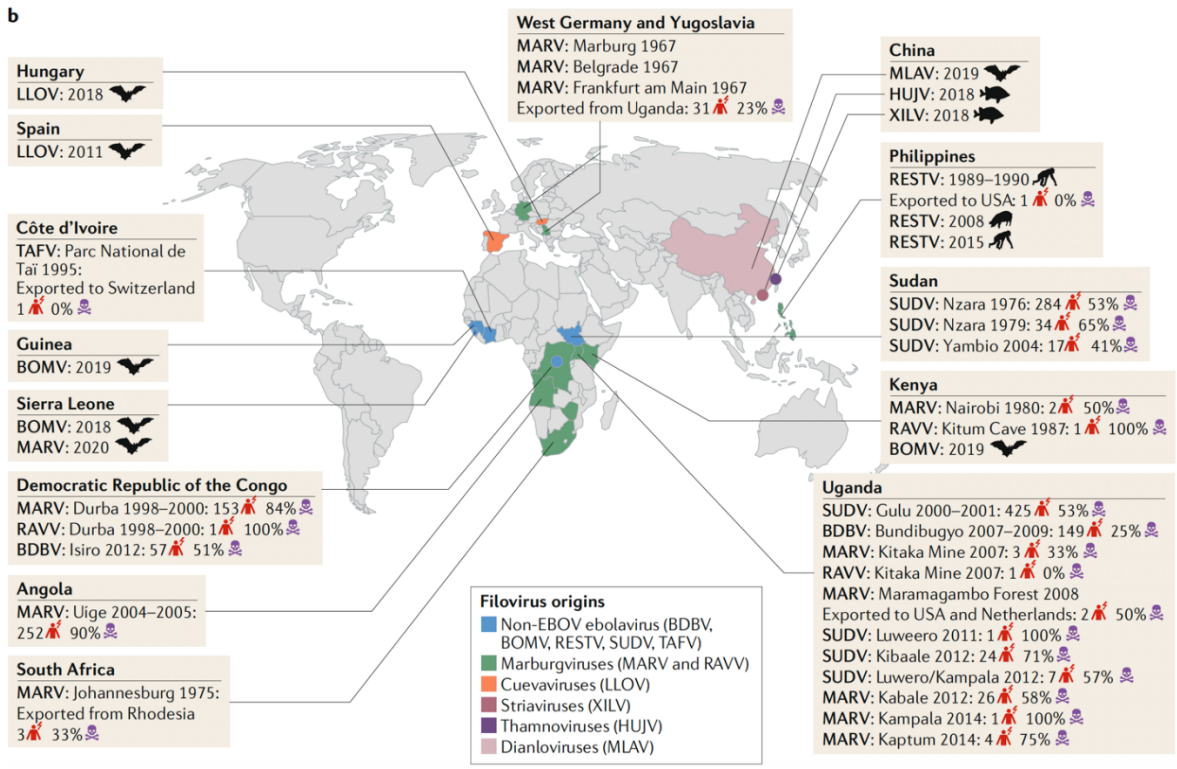

Figure 2. Filovirus outbreaks in the world.

The map illustrates the origin and the geographical distribution of filoviruses in the world. The number of cases and deaths and the case fatality ratios are indicated in the boxes (from Di Paola et al., 2020).

The incidence of MVD corresponds to the geographical distribution of *Rousettus* bats across Africa. It is a zoonotic disease that is endemic in certain regions of Africa particularly the open and dry areas of Eastern and Southern Africa (Brauburger et al., 2012). Bats are thought to maintain the virus in the wild and play an important role in transmission to humans, in particular in cave settings.

1.1.2.2 Molecular biology

Marburg virions are filamentous and have an average diameter of 80 nm with lengths of up to 14,000 nm (Brauburger et al., 2012). The membrane of MARV particles is derived from the host and contains trimers of the glycoprotein (GP). Within is the nucleocapsid which consists of the RNA genome in close association with other proteins. In addition to the glycoprotein, the genome encodes six other proteins namely: the nucleoprotein (NP), viral protein 35 (VP35),

VP24, VP30, VP40 and the L protein (RNA-dependent RNA polymerase) (Brauburger et al., 2012). Table 1 summarises the proteins and their functions and whether they play a role in immune evasion.

Table 1. Summary of Marburg virus viral proteins and their functions

Protein	Molecular mass	Function	Immune evasion
NP	94		
VP35	32	Polymerase cofactor. Essential for replication and transcription	IFN antagonist. Inhibits type I IFN
VP40	38	Budding, particle formation & release	Inhibits IFN signalling by blocking the phosphorylation of Janus kinases
GP	170-200	Attachment; binding to entry receptors, fusion of viral & cellular membrane	GP interferes with the antiviral activity of tetherin. GP2 subunit contains immunosuppressive domain similar to that of retroviruses. Possibility of innate and adaptive immune suppression
VP30	28	Plays a role in viral amplification	
VP24	24	Plays a role in transcription and replication	
L	220	Essential for transcription and replication. Believed to play a part in RNA synthesis, capping and polyadenylation of viral mRNAs	

Table adapted from Brauburger et al., 2012.

1.1.2.3 Pathogenesis

Human-to-human MARV transmission occurs when individuals come into contact with infected bodily fluids such as sweat, tears, stool or saliva (Mehedi et al., 2011). Transmission also occurs through direct contact with infected animals or carcasses e.g., during hunting or, in the case of the 1967 outbreaks, during handling of post-mortem tissues of infected animals. There are reports of infection occurring via breast milk and also via sexual intercourse (Brauburger et al., 2012; Cooper et al., 2018). The virus enters through breaks in the skin and mucosal surfaces. The incubation period ranges from 2-21 days before the manifestation of the initial symptoms with the average incubation period being 5-9 days (Mehedi et al., 2011). The

early stage of the disease is similar to that of other infectious diseases endemic in Africa and begins with flu-like symptoms such as headache, myalgia, lethargy and fever. The disease course worsens beginning at day 5-7 with patients experiencing mucosal bleeding, petechiae, bleeding from venepuncture sites and in some cases the development of a macopapular rash on the face, trunk and extremities. This phase is referred to as early organ phase and commences at day 5-13 post disease onset. Neurological symptoms may also occur during this phase and may include confusion, behavioural changes and delirium. The last stage of the disease is characterised by multiorgan failure, convulsions, metabolic disturbances and diffuse coagulopathy, shock and coma (Brauburger et al., 2012; Cooper et al., 2018). Survivors do not usually progress to the last stage of the disease and typically do not develop the most severe symptoms. However, there are reports of long-term sequalae of infection in survivors such as myalgia, arthritis, psychosis and hepatitis (Mehedi et al., 2011; Cooper et al., 2018; Shifflett and Marzi, 2019).

1.1.2.4 Immune response to MARV and vaccines

MARV has a broad tropism and similar to EBOV, studies have demonstrated that activated monocytes, DCs and Kupffer cells are early targets of MARV infection (Hensley et al., 2011). The immune response to MARV infection has not been extensively characterised but some studies have shown that the responses are similar to those against EBOV and SUDV. MVD is characterised by immune suppression and delayed antibody responses in patients that develop severe disease (Brauburger et al., 2012).

Infected DCs remain immature and fail to produce cytokines important for the activation and polarization of T cells. Infection of endothelial cells, monocytes and macrophages is thought to lead to hyperactivation, which in turn leads to a massive secretion of cytokines which leads to haemorrhage and sepsis like cytokine storm (Bosio et al., 2003; Connor et al., 2015; Schnittler et al., 1993).

Circulating immune cells can be classified into three phases corresponding to clinical disease progression and a robust activation of innate immune cells is observed early after infection. Virus replication is however not strongly limited by the increase in the activation of these cells as evidenced by increasing levels of virus-specific mRNA as the infection progresses. Additionally, administration of IFN-I to infected NHPs did not confer complete protection but did prolong survival (Smith et al., 2013). Interestingly, transcriptional profiling of PBMCs

from aerosol-infected macaques revealed a preponderance of transcripts associated with a T helper cell 2 (Th2) response (Lin et al., 2015).

There are however distinct differences. MARV survivors develop limited $CD8^+$ T cell responses but have better polyfunctional $CD4^+$ T cell responses that are detectable even 2 years after infection. A study of survivors of the 2012 MARV outbreak in Uganda showed that the $CD4^+$ T cell response was skewed to a Th1 effector cell profile and almost all the survivors had measurable IFNγ and IL2 responses (Stonier et al., 2017).

1.1.3 Ebolaviruses

The *Ebolavirus* genus contains six distinct species namely: *Zaire ebolavirus* (EBOV), *Sudan ebolavirus* (SUDV), *Bundibugyo ebolavirus* (BDBV), *Tai Forest ebolavirus* (TAFV), *Reston ebolavirus* (RESTV) and *Bombali ebolavirus* (BOMV). Ebolaviruses have been responsible for haemorrhagic fever outbreaks since their discovery in 1976. The two simultaneous outbreaks of what is now known as Ebola virus disease (EVD) occurred in Yambuku in the Democratic Republic of the Congo and Nzara in South Sudan and resulted in case fatality rates of up to 88 % for EBOV and 53 % for SUDV (WHO, 1978; Richman et al., 1983). Since then, there have been several outbreaks with most of them being caused by EBOV, which is considered the most lethal. The largest EVD outbreak occurred in West Africa between 2013 and 2016 and resulted in approximately 28,600 cases of which 11,300 succumbed to the disease (WHO, 2016).

Other pathogenic ebolaviruses are BDBV, which was identified from clinical isolates in 2008 during an outbreak in Uganda and TAFV of which only a single non-fatal case in Cote d'Ivoire is known (Messaoudi et al., 2015a; Towner et al., 2008; Wamala et al., 2010). RESTV appears to infect humans sub-clinically and is therefore thought to be non-pathogenic (Cantoni et al., 2016; Jahrling et al., 1990). RESTV has been isolated from swine in the Philippines and China. Goldstein et al. recently described the complete genome of a new ebolavirus detected in bats, which they named Bombali ebolavirus (BOMV). They showed that the BOMV GP could mediate entry to cell lines derived from monkeys and humans. Further studies are required to determine the pathogenicity of BOMV (Goldstein et al., 2019).

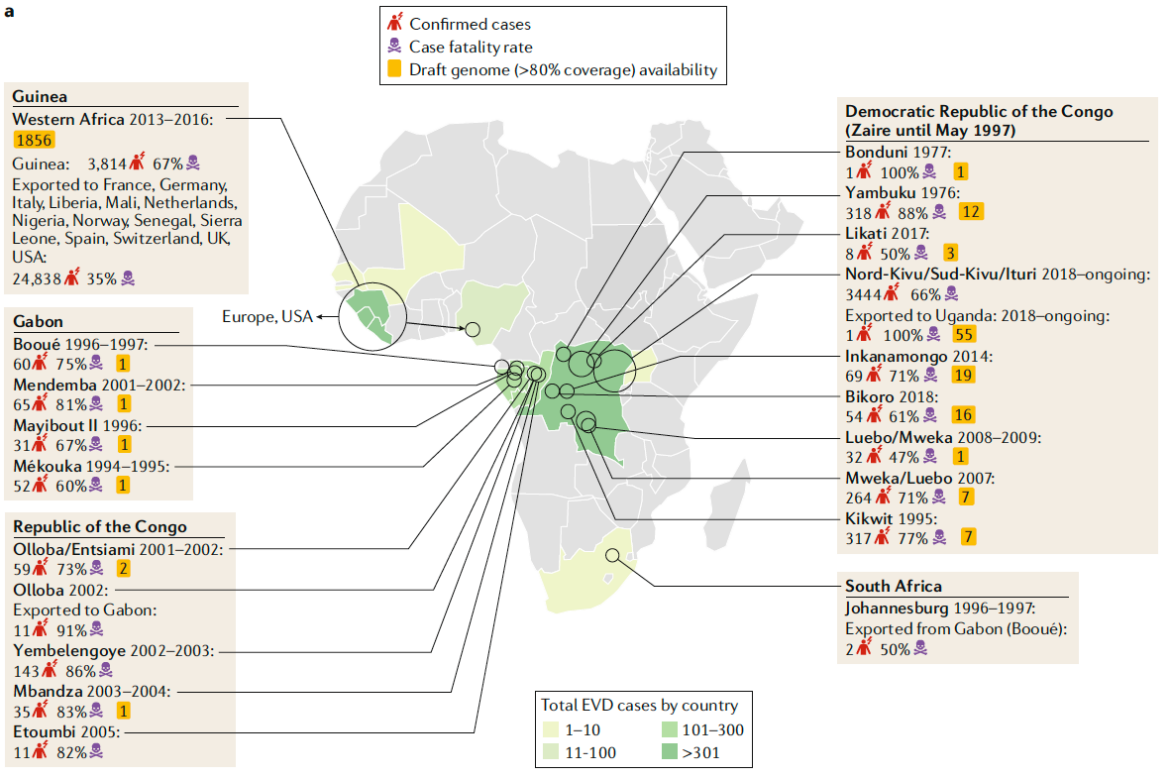

Figure 3. Summary of EBOV outbreaks and the geographical location of their occurrence.
The geographic map of Africa shows the location of EBOV outbreaks and the number of EVD cases by country. The case fatality rates are indicated in the boxes (from Di Paola et al., 2020).

1.1.3.1 Ecology

The natural reservoir for ebolaviruses has not yet been determined but evidence points to bats as the primary host. There is no consensus on the criteria for the definition of natural reservoirs, however there are some commonly accepted characteristics which bats display that make them the primary suspects (Schuh et al., 2017). Antibodies reactive to EBOV antigens as well as EBOV RNA have been detected in bats of various species (Leroy et al., 2005). The first direct link between bats and human infection resulting in an EVD outbreak was reported by Leroy et al., 2009. Bats are involved in the transmission cycle and their interaction with other wild animals in the wild – so called secondary amplifying hosts – serve to maintain circulating filoviruses in the wild.

1.1.3.2 Molecular biology

The genome organization of ebolaviruses is similar to that of marburgviruses. A main difference is that the GP of marburgviruses is attached to the virion, while the GP of ebolaviruses encodes multiple proteins through transcriptional editing by the L protein (Messaoudi et al., 2015b; Mühlberger, 2007). These proteins are $GP_{1,2}$, small soluble glycoprotein (ssGP), and soluble glycoprotein (sGP). The sGP is first synthesised as pre-sGP, a Golgi-specific precursor, which undergoes proteolytic cleavage by cellular proteases such as furin (Zhu et al., 2019). The sGP is the most abundant protein produced from the GP gene and is secreted from infected cells. It plays a role in antigenic subversion by acting as a decoy antigen by binding specific antibodies against $GP_{1,2}$. A study demonstrated that sGP is able to compete for anti-$GP_{1,2}$ antibodies from mice immunized with sGP and interferes with neutralization (Mohan et al., 2012). The role of ssGP in ebolavirus pathogenesis has not yet been elucidated.

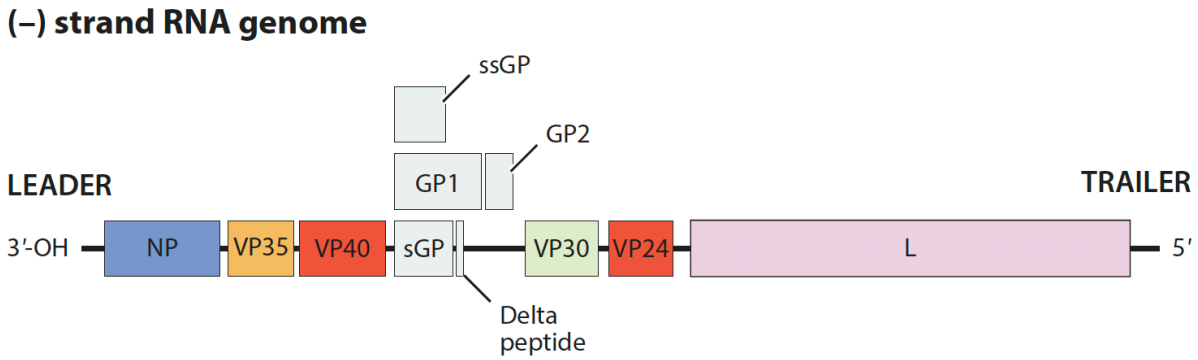

Figure 4. Genome organization of ebolaviruses.
The genomic RNA of Ebola virus (EBOV) is negative sense and is depicted in the 3′-to-5′orientation. GP and sGP are encoded by a single gene due to transcriptional editing (from Furuyama and Marzi, 2019).

The glycoprotein is important for pathogenesis and mediates entry by binding to multiple attachment factors e.g., the asialoglycoprotein receptor on hepatocytes, folate a receptor on epithelial cells and C-type lectins like DC-SIGN on DCs, macrophages and endothelial cells (Alvarez et al., 2002; Rivera and Messaoudi, 2016). The virus then enters cells through macropinocytosis and clathrin-mediated endocytosis (Aleksandrowicz et al., 2011). The glycoprotein is cleaved by cysteine proteases after which it binds to the Niemann-Pick cholesterol transporter 1 (NPC1) receptor (Carette et al., 2011). The acidification of endocytic

vesicles results in the beginning of the process of fusion between the viral and endosomal membranes (Miller et al., 2012). The genome is released into the cytoplasm where replication and transcription occur. EBOV NP is the most transcribed gene while the L protein is the least transcribed gene. The accumulation of the various viral proteins prompts viral replication. The positive-sense antigenome serves as a template for the production of negative-sense genomes. Host ribosomes translate the positive-sense transcripts and the nucleocapsid is thereafter assembled. Particle formation and budding is facilitated by the matrix protein VP40 (Feldmann et al., 2020).

Table 2. Summary of Ebolavirus proteins and their functions

Protein	Molecular mass	Function	Immune evasion
NP	90-104		
VP35	35	Polymerase cofactor. Essential for replication and transcription	IFN antagonist. Inhibits type I IFN Suppression of DC maturation
VP40	35-40	Budding, particle formation & release	Inhibits IFN signalling by blocking the phosphorylation of Janus kinases
GP	150-170	Attachment; binding to entry receptors, fusion of viral & cellular membrane	GP interferes with the antiviral activity of tetherin. GP2 subunit contains immunosuppressive domain similar to that of retroviruses. Possibility of innate and adaptive immune suppression
sGP	50-55	unknown	Antigenic subversion
VP30	27-30	Plays a role in viral amplification	
VP24	24-25	Plays a role in transcription and replication	
L	270	Essential for transcription and replication. Believed to play a part in RNA synthesis, capping and polyadenylation of viral mRNAs	

1.1.3.3. Pathogenesis

Primary EBOV infection occurs in humans via zoonotic spill-over when individuals come into contact with infected animals (e. g. during hunting or whilst handling animal carcasses). The virus enters the body through breaks in the skin and mucosal surfaces. Subsequent human-to-

human transmission is the main driver of virus spread and epidemic amplification. Initial symptoms manifest after an incubation period of 2-21 days (Feldmann and Geisbert, 2011). The first stage of EVD is characterised by malaria or flu-like symptoms such as fever, malaise, headache, myalgia etc. In addition to impaired liver and kidney function, gastrointestinal symptoms such as nausea, vomiting and diarrhoea predominate the second stage. The third stage is characterised by metabolic disturbances and diffuse coagulopathy. In the final stages of disease multiorgan failure is common and bleeding may be observed in a small percentage of patients, and may include melena, hematemesis and petechiae (Baseler et al., 2017; Kortepeter et al., 2011). Severe EVD also involves immune dysregulation whereby pro-inflammatory cytokines, chemokines and other factors are secreted in abundance leading to immune cell hyperactivation and systemic inflammation.

EBOV has a broad tropism and infects multiple cell types such as fibroblasts, epithelial and endothelial cells, hepatocytes, Kupffer cells, macrophages, activated monocytes and dendritic cells (DCs). Antigen-presenting cells such as macrophages and DCs are known to be the early targets of infection. EBOV initially and preferentially replicates in these cells (Geisbert et al., 2003a). Infected cells migrate to the lymph nodes and nodal chains and the virus is released into circulation thus facilitating viral dissemination (Lüdtke et al., 2017; Feldmann et al., 2020) Disease is associated with viral replication and the host immune response to infection.

1.1.3.4 Persistence and recrudescence

Persistence of EBOV in immunologically protected sites in survivors poses another major issue. EBOV has been shown to persist in semen and EBOV RNA has been detected in vaginal fluids, breast milk, semen and urine shortly following the recovery of patients (Den Boon et al., 2019). The virus can be sequestered in immunologically privileged sites such as the gonads eye chamber and conjunctival fluid. Evidence exists of transmission associated with the persistence of EBOV in survivors (Den Boon et al., 2019). EBOV persistence in the male reproductive system may spur transmission from recovered EVD survivors (Caviness et al., 2017). EBOV persistence in survivors may have far reaching consequences not least of which would be the triggering of new infection clusters resulting in the re-ignition of outbreaks (Den Boon et al., 2019). The possibility of the re-emergence of EBOV from survivors underpins the need for better surveillance and redoubling of vaccination efforts in order to reach as many secondary and tertiary contacts as possible (Caviness et al., 2017).

1.1.3.5 Immune response after EBOV infection

An early and well-coordinated innate and adaptive immune response that involves functional DCs and macrophages, natural killer (NK) cells and the induction of antigen-specific T cells, and virus-specific antibodies has been correlated with EVD survival (Muñoz-Fontela and McElroy, 2017). Activation of lymphocytes has been shown to correlate with a decline in viral loads in the second week after symptom onset. The main target of T cell responses is EBOV NP, the most abundantly produced protein during replication and transcription (McElroy et al., 2015). IgM is detected as early as 2 days after the onset of symptoms but can occur generally from 10-29 days post-infection. EBOV IgG is detected from around day 6 after infection and occurs around 19 days after the beginning of symptoms in most patients (Ksiazek et al., 1999; Rowe et al., 1999). Early cytokine responses are correlated with survival (Furuyama and Marzi, 2019). DCs are important immune cells that bridge the innate and adaptive arms of the immune system and are crucial to the activation and functioning of T cells. DC differentiation is impaired after EBOV infection which blocks the upregulation of costimulatory molecules that are necessary for the proper priming of T cells and the induction of an antigen-specific response. By impairing the differentiation of DCs, the activation of lymphocytes is impeded resulting in the elimination of crucial antiviral immune cell subsets that could control EBOV replication (Bosio et al., 2003; Lubaki et al., 2013). Fatal cases have been shown to have a dysregulated immune response that ultimately contributes to the development of a sepsis-like syndrome and organ failure (Wong et al., 2014). The activation of memory T cells without cognate antigens has been observed in viral infections caused by Hepatitis A and B. These cells can cause immunopathology and tissue damage further exacerbating disease (Lee et al., 2022). The release of cytokines by bystander-activated T cells has detrimental consequences on the host and probably contributes to the aberrant immune response observed in fatalities during EVD.

EBOV has evolved a multitude of ways to evade the immune response. Antagonism of the innate immune response results in downstream effects that also interfere with the adaptive immune response, which is crucial for proper antiviral defences. The virus is able to inhibit the production of Type I interferons, the upregulation of co-stimulatory molecules required for adequate priming of T cells by DCs and also interferes with natural killer (NK) cells (Geisbert et al., 2003b). DCs are oftentimes referred to as professional APCs due to the important role that they play in bolstering adaptive immunity. They are the only cells that are known to be capable of priming naïve T cells. EBOV is known to interfere with the ability of DCs to

upregulate costimulatory molecules that are necessary for adequate T cell priming. T cells and NK cells are vital to ensuring viral clearance and studies have shown that there is a decrease in these cell populations in fatal outcomes.

Lymphopenia has been observed during experimental EBOV infection in mice and cynomolgus macaques as well as in samples obtained from infected patients. PBMC samples from fatally infected patients had a higher percentage of $CD4^+$ and $CD8^+$ T cells expressing CD95, a marker for apoptosis. The dearth of $CD4^+$ T cells has a direct effect on the production of EBOV-specific IgM and IgG antibodies due to the role that $CD4^+$ T cells play in B cell isotype class switching (Baize et al., 1999).

DCs play an important role in bolstering adaptive immune responses. It was previously thought that the inactivation of DCs by EBOV would negatively impact the induction of T cells due to poor priming. The outbreak that occurred between 2013 – 2016 enabled more in-depth studies that revealed that there is massive T cell activation in both survivors and individuals that succumb to EVD. CD38 and HLA-DR, surface markers whose upregulation is indicative of T cell receptor engagement were shown to be upregulated on both $CD4^+$ and $CD8^+$ T cells of EVD patients (McElroy et al., 2015; Ruibal et al., 2016). This data suggested that T cells do in fact receive adequate priming by APCs during infection. Ruibal et al. showed in 2016 that the T cells from fatal EVD cases expressed an elevated level of cytotoxic T –lymphocyte-associated protein 4 (CTLA-4) and programmed cell death-1 (PD-1), which are negative regulators of T cell function (McElroy et al., 2015; Ruibal et al., 2016). The upregulation of these molecules on T cells is thought to contribute to T cell dysfunction which may stem from exhaustion (Wherry, 2011; Wherry and Kurachi, 2015). Lymphopenia together with the defective humoral and T cell responses contribute to the pathology associated with EVD.

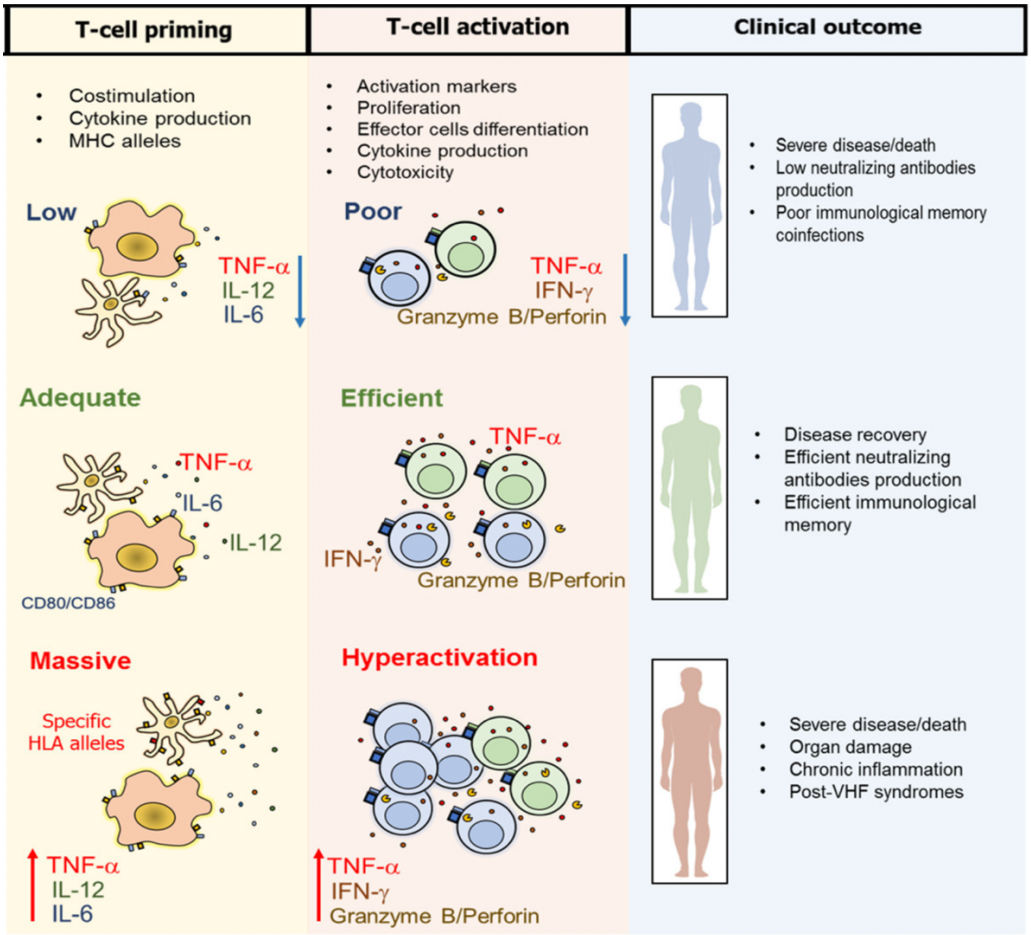

Figure 5. Schematic showing the correlation between T cell priming, activation and clinical outcome.

DCs and activated monocytes and macrophages are the primary targets of filoviruses. The type of clinical outcome is thought to depend on the type of T cell response that is induced during priming. Low expression of co-stimulatory molecules leads to poor T cell priming and activation, reduced proinflammatory cytokine production and lowered cytotoxic potential. The result of these defective response is severe disease and/or death. Efficient priming characterised by the upregulation of co-stimulatory molecules and proper priming leads to the induction of antigen-specific T cells and the production of cytokines. This results in a positive outcome following infection and the formation of long-term immunological memory. T cell hyperactivation can result from massive co-stimulation and the overproduction of proinflammatory cytokines. This leads to severe disease involving chronic inflammation and organ damage (from Perdomo-Celis et al., 2019).

Adequate priming of T cells appears to be correlated with a more efficient adaptive immune response which in turn has a positive effect on the outcome after EBOV infection. Efficient T cell memory coupled with the production of antibodies that have potent neutralizing activity is highly desirable especially in the event of virus persistence.

1.5 Vaccines – currently licensed, in development, need for new ones

Academic laboratories have been working on the development of vaccines against Ebola virus since its discovery in 1976. However, the relatively low industrial interest as well as the sporadic nature of EVD outbreaks has made it difficult to perform clinical trials. This has in turn hampered the efforts to bring vaccines to full licensure. The 2013-2016 west African outbreak, however, cast a spotlight on EVD as a global public health threat and resulted in an increase of efforts and funding to foster vaccine development. Currently, there are about 12 vaccine candidates in different phases of clinical trials. Various vaccine platforms have been utilized for the development of Ebola virus and Marburg virus vaccines. Among these are nucleic acid-based vaccines, viral vectored vaccines and protein-based vaccines.

1.5.1 Nucleic acid-based vaccines

DNA plasmid vaccines expressing EBOV GP and NP, SUDV GP and MARV GP have been tested in small animal models and NHPs and were shown to be safe and protective. They are versatile and easy to manufacture. Codon optimization of the sequences to recapitulate those most often used by humans and the inclusion of promoter regulatory elements was shown to improve protein expression and thereby the immunogenicity (Grant-Klein et al., 2012). Different formulations of the vaccines have been administered to human subjects and have been proven safe. Vaccines based on this platform have not advanced beyond the first phase of clinical trials (Friedrich et al., 2012). Though DNA vaccines have been shown to be efficacious, the antibody titres produced are not long-lasting and drop substantially one year after immunization.

1.5.2 Viral vectored vaccines

Various viruses have been used as vectors to deliver genetic material encoding antigens of interest derived from filoviruses. Viruses including adenoviruses, poxviruses, herpesviruses, lentiviruses are engineered to stimulate immune responses against the proteins generated from the genes encoding the antigen of interest (Travieso et al., 2022). Viral vector vaccines can be designed to be replication deficient or replication competent or only be able to undergo one round of replication. They generally do not cause infection and are therefore safe. They enable the expression of antigens after delivery to cells and can stimulate both humoral and cellular immunity. Replication-deficient vectors are safer than replicating vectors, however, a higher dose is required to generate long-lasting immune responses. Replicating vectors on the other

hand mimic natural infection which results in more well-rounded immune responses (Robert-Guroff, 2007).

1.5.2.1 Vaccinia virus

Poxviruses such as *Vaccinia virus* (VACV) and *Variola virus* belong to the family *Poxviridae* and are unique in that they can accommodate large gene inserts (up to 25 kb). This makes them especially suited for use in the development of multivalent vaccines as multiple antigens can be incorporated. A modified *vaccinia Ankara virus* (MVA) vectored vaccine has been developed for use against filoviral infections. Attenuation of the MVA vector was done by serial passaging in chicken embryo fibroblasts and the vector is replication incompetent (Greenberg et al., 2015; Mayr et al., 1978). The vector is stable and retains immunogenicity even after lyophilization. Two vaccines based on this vector have been developed. One is a monovalent MVA vaccine which encodes the EBOV GP only. The second one known as MVA-BN-Filo is multivalent and encodes EBOV GP, SUDV GP, MARV GP and TAFV NP. Both vaccines have been shown to be efficacious and result in strong humoral responses involving the production of EBOV GP-specific antibodies and T cells (Venkatraman et al., 2019).

1.5.2.2 Recombinant Adenoviruses

Recombinant human and chimpanzee Adenovirus (Ad) serotypes have been used for the development of filovirus vaccines. The earliest adenovirus-based vector used was human adenovirus serotype 5 (Ad5). This vector expresses the EBOV GP and was shown to protect NHPs from lethal EBOV challenge (Sullivan et al., 2006). This vaccine was modified to express the EBOV-Makona GP, which was the major driver of the 2013-2016 outbreak and was shown to be safe and immunogenic but the elicited antibodies were not long-lasting (Matz et al., 2019). There are concerns about pre-existing immunity to the human Ad vectors use, which is thought to dampen the immune response elicited to the vaccine. One strategy used to circumvent this has been the use of human adenoviruses to which there is little or no pre-existing immunity or chimpanzee adenoviruses. A vaccine based on chimpanzee Ad3 confers 100 % protection to NHPs, however, as with the rAd5 based vaccine, the antibody titres are not durable (Reynolds and Marzi, 2017). There is very low seroprevalence to human Ad26 and Ad35, which makes them ideal for use as vectors. Vaccination with these constructs results in robust humoral responses but only Ad26 has been shown to confer protection to NHPs when lethally challenged with EBOV (Matz et al., 2019). A pan-filovirus vaccine expressing EBOV

GP & NP, SUDV GP, MARV NP, two MARV GP and RAVV GP has been developed by Swenson and colleagues. The vaccine also known as CAdVax was shown to be protective when administered in a prime boost regimen to NHPs (Swenson et al., 2008). So far, there are no data on cellular immune responses nor the neutralization capacity of the antibodies elicited by this vaccine (Swenson et al., 2008; O'Donnell and Marzi, 2020).

1.5.2.3 Recombinant vesicular stomatitis virus

Vesicular stomatitis virus (VSV) belongs to the *Rhabdoviridae* family. It is a negative sense non-segmented RNA virus that encodes 5 proteins. Rose et al. engineered wild-type VSV to express antigens from other VSV serotypes in place of the G protein gene (Rose et al., 2000). Various glycoproteins have been shown to be efficiently incorporated into virus particles (Schnell et al., 1996). Recombinant (rVSV) vectors grow to high titres *in vivo* and result in high neutralizing antibody titres against the protein encoded by the pseudotyped gene. In the case of the rVSV-ZEBOV vaccine, the G protein of the rVSV is replaced with EBOV GP. Vaccination with VSV-EBOV confers protection against EBOV challenge in cynomolgus macaques and results in the secretion of high titres of neutralizing antibodies (Jones et al., 2005). Studies have shown that EBOV GP specific antibodies are important for protection and positively correlate with survival (Marzi et al., 2013; Wong et al., 2013). EBOV GP-specific antibodies have been detected up to 1 year after vaccination (Simon et al., 2022). Neutralizing antibody titres are only detectable up to 6 months after vaccination. A high vaccine dose, i.e., $2x10^7$ pfu of rVSV-ZEBOV, elicits EBOV GP specific T cells but generally their T cell response is not robust (Dahlke et al., 2017). A recent study demonstrated that a third of participants who received the vaccine developed immunity to VSV and it remains to be determined whether immunity to the vector could affect vaccine efficacy (Poetsch et al., 2019). rVSV-ZEBOV has been demonstrated to be efficacious and safe in phase 3 clinical trials.

Currently there are two vaccines licensed for use against EBOV (WHO, 2022). The first one, known commercially as Ervebo was licensed in late 2019. It is a replication-competent live, attenuated rVSV that contains the EBOV GP. It has been shown to induce rapid antibody production with high titres observed just fourteen days after infection (Simon et al., 2022). The vaccine however is not protective against other species of ebolaviruses nor Marburg virus. Thus, developing vaccines that offer cross-protection would be highly valuable in the event of outbreaks caused by filoviruses other than EBOV. Additionally, the correlates of protection that ensure immunity after vaccination are not known and are currently being investigated. Gaining more insight into this, would provide scientists with invaluable information that is

necessary for the development of other vaccines or therapeutics that may provide protection from all Ebolaviruses as well as Marburgviruses.

The second vaccine was granted market authorisation by the European medicines' agency in 2020 (WHO, 2022). It comprises a two-dose regimen consisting of MVA-BN-Filo and Ad26.ZEBOV. MVA-BN-Filo is administered first followed by Ad26.ZEBOV 8 weeks later., Though this combination is very effective, the requirement for boosting precludes the use of this vaccine as an emergency vaccine during outbreaks. Another question that has arisen is the duration for which vaccinated individuals have immunity (Marzi and Mire, 2019). How similar or different vaccine induced immunity is to natural immunity also requires further investigation. Waning immunity is also an important factor to consider when determining the effectiveness of vaccine candidates.

1.6 Immune response to filoviruses

The immune system is a tightly regulated system consisting of cells, tissues and humoral components. This complex system can be divided into two major arms, innate immunity and adaptive immunity. The innate immune system is a general alarm-based system that responds rapidly and similarly to all invading pathogens. The adaptive immune response is slower but is antigen-specific. Adaptive immunity comprises the formation of antigen-specific T and B cells as well as antibodies which are capable of immunological memory, that is, responding to re-infection with the same pathogen.

The innate immune system is the first line of defence after encounter with a pathogen and consists of the skin and mucous membranes and immune cells and other proteins. The skin is a strong physical barrier and is inhospitable to many pathogens deterring their entry. Furthermore, the acidic pH of the genital and gastrointestinal tracts and the mucus in the respiratory system all serve to prevent pathogens from gaining a foothold. Breaching this line of defence allows viruses a chance to enter the body and possibly establish infection. Filoviruses enter the body through breaks or abrasions in the skin or through mucosal surfaces. Once inside the body they encounter patrolling immune cells, which begin the process of mounting a pathogen-specific immune response.

1.6.1 Pattern recognition receptors

Pattern recognition receptors (PRR) are found on all nucleated cells. They recognise pathogen associated molecular patterns (PAMP) which are characteristic of pathogens. For example, PRRs such as retinoic acid inducible gene-I (RIG-I) and some types of toll-like receptors

(TLRs) are able to sense double-stranded (ds) and single stranded (ss) RNA which are typical subproducts of viral infections (Herbert and Panagiotou, 2022). PRRs may be located on the cell surface or inside the cell and recognize extracellular or intracellular PAMPs respectively. Intracellular PRRs are present on all cell types and may be membrane bound or free in the cytoplasm (Chan and Gack, 2016). Filoviruses are recognized by intracellular PRRs. 4 types of PRRs have been described so far and these include TLRs, RIG-I-like receptors, nucleotide-binding oligomerisation domain-like receptors (NLRs) and C-type lectin receptors (CLRs).

1.6.1.1 Toll-like receptors

TLRs are the most studied group of PRRs and so far, 10 functional TLRs have been identified in humans (Takeda and Akira, 2005). TLR 1, 2, 4, 5, 6 and 10 are found in the plasma membrane and TLR3, 7, 8 and 9 are found in the endosomal membrane and recognise intracellular pathogens. The endosomal TLRs have the PAMP recognition domain in the endosome and the signalling domain in the cytosol. TLR3 recognises dsRNA and TLR7/8 recognise ssRNA (Herbert and Panagiotou, 2020; Alexopoulou et al., 2001; Heil et al., 2004; Lund et al., 2004). EBOV GP is capable of interacting with and activating cell surface TLR4 leading to the production of proinflammatory cytokines and the suppressor of cytokine signalling 1 (SOCS1) (Okumura et al., 2010). The activation of TLRs leads to conformational changes and the recruitment of adaptor proteins to the signalling domain. A downstream signalling cascade is begun leading to the translocation of transcription factors to the cell nucleus and thereby changes in gene expression (Herbert and Panagiotou, 2020; Takeda and Akira, 2005).

1.6.1.2 Retinoic acid inducible gene-I (RIG-I)- like receptors

RIG-like-receptors are RNA helicase proteins that are involved in the recognition of RNA viruses by the innate immune system. The RLR family includes RIG-I, melanoma differentiation antigen 5 (MDA5) and laboratory of genetics and physiology 2 (LGP2) (Kell and Gale, 2015). They are ubiquitously expressed at low levels in cells and upon viral recognition undergo structural conformational changes leading to a downstream signalling cascade which results in the induction of interferon stimulated genes (ISGs). The activation of RLRs requires tight regulation as an over activation leads to the overproduction of type I interferon (IFN-I) (Rehwinkel and Gack, 2020).

1.6.1.3 Nucleotide-binding oligomerisation domain-like receptors

NLRs are found in the cytosol of macrophages, dendritic cells, epithelial cells and lymphocytes. 22 NLRs have been described. They recognise viral RNA and when activated leads to the secretion of pro-inflammatory cytokines (Herbert and Panagiotou, 2020).

1.6.1.4 C-type lectin receptors

Innate immune cells such as DCs, macrophages and monocytes express CLRs, which are capable of recognising PAMPs. CLRs recognise carbohydrate moieties of pathogens such as mannose, glucan and fucose (Drouin et al., 2020). They are able to bind and internalise viruses and, in the process, activate antiviral immune responses (Monteiro and Lepenies, 2017). The outcome of internalization depends on the specific CLR and the cell on which it is expressed. Internalization via DC-SIGN and DEC-205, for example, leads to degradation by lysosomes while binding to Langerin on Langerhans cells leads to degradation via autophagy (Bermejo-Jambrina et al., 2018). Some viruses have been shown to exploit CLRs and use them to evade degradation, interfere with APC effector functions and facilitate dissemination and transmission (Tortorella et al., 2000)

CLRs can also be exploited by viruses to enhance binding and infection. EBOV GP has been shown to avidly bind DC-SIGN and DC-SIGNR, resulting in enhanced infection of DCs (Simmons et al., 2003). CLRs therefore may play a dual role during viral infections.

CLRs are also involved in antigen presentation on major histocompatibility (MHC) molecules. Antigens endocytosed by DC-SIGN, DEC-205, DCIR and dectin-1 are routed to and presented on MHC II molecules to $CD4^+$ T cells. Once mature, DCs downregulate the expression of CLRs and take up antigen at a lower rate than immature DCS. Mature DCs are more efficient at stimulating T cells. DEC-205 is an exception as the receptor is upregulated on plasmacytoid DCs (pDCs), which still have the capacity to take up antigens even after maturation. Exogenous antigens taken up via this receptor can also be rerouted and presented on MHC I molecules to $CD8^+$ T cells (Idoyaga et al., 2011).

1.6.2 Antigen presenting cells

Antigen presenting cells (APCs) are divided into professional, e.g., DCs, macrophages and B cells, and nonprofessional cells, e.g., fibroblasts and hepatocytes (Eiz-Vesper and Schmetzer, 2020). Professional APCs differ from nonprofessional ones in that they express MHC II molecules. Within professional APCs, DCs are capable of presenting cognate antigens to naïve T cells thereby initiating adaptive immune responses. Additionally, they express PRRs and

costimulatory molecules such as CD40 on DCs and B cells and CD83 and CD86 on DCs, which are required for the stimulation of T cells. In order for T cells to be properly activated, three signals are required as follows: 1. Presentation of antigens by MHC molecules to the T cell receptor (TCR), 2. Upregulation of costimulatory molecules, 3. Secretion of cytokines and chemokines by the APCs which act on T cells and other surrounding cells and secrete cytokines such as IL-12 and IFNα, which are required for differentiation into effector cells and clonal expansion (Cui and Kaech, 2006; Mescher et al., 2006).

DCs and macrophages take up pathogens via phagocytosis whilst B cells take up pathogens through the B cell receptor (BCR).

1.6.2.1 Monocytes and macrophages

Monocytes are the most abundant APCs, making up approximately 10 % of leukocytes in humans and up to 4 % in mice. They circulate in the blood, spleen and bone marrow and act as inflammatory mediators in response to pathogens. They play a role in antiviral defence by phagocytosing and killing pathogens, producing reactive oxygen species and pro-inflammatory cytokines and polarizing T cell responses. Monocytes appear refractive to EBOV GP-mediated entry and thereby EBOV infection, however monocyte-derived macrophages and DCs have been shown to be permissive to EBOV infection and delayed entry is thought to occur during differentiation and associated to expression of DC-SIGN on the surface of activated monocytes (Martinez et al., 2013; Simmons et al., 2002).

1.6.2.2 Dendritic cells in filovirus infections

DCs act as sentinel cells patrolling the portals of entry of pathogens in the body, namely, the skin and the mucosae. Immature DCs reside at these peripheral body sites where they constantly scan for antigens. Once antigens are encountered, they are captured and processed by DCs, which afterwards migrate to the tissue-draining lymph nodes where they encounter and prime cognate T cells. They have been shown to have a superior capability when it comes to antigen presentation and are the only APCs capable of activating naïve T cells (Banchereau and Steinman, 1998). DCs are also capable of rerouting exogenous antigens and presenting them in the context of MHC I molecules to $CD8^+$ T cells, a process termed cross-presentation. In the context of viral infection, cross-presentation is important for the activation of $CD8^+$ T cells against viruses that do not infect DCs (Heath et al., 2004).

The immune response elicited by DCs is largely dependent on the environment in which the antigens are first encountered. In the absence of inflammatory signals or adjuvants, priming of

T cells by DCs may lead to the induction of tolerance (tolerogenic DCs). However, if they receive inflammatory signals during infection or in the form of a vaccine adjuvant, DCs may then drive immunogenic antigen-specific T cell responses (Macri et al., 2016). Even after the resolution of infection, DCs may continue to play a role as they are able to locally re-stimulate effector and memory tissue-resident T cells (Cabeza-Cabrerizo et al., 2021). DCs are consist of different immune cell subsets with overlapping and non-overlapping functions. For example, plasmacytoid DCs are specialized in the production of high amounts of IFN-I in response to infection and langerin$^+$ dermal DCs are specialized in antigen cross-presentation (Flacher et al., 2014). Other DC-like cells are also specialized tissue-resident cells. For example, Langerhans cells, which develop from a foetal liver monocyte precursor, populate the epidermis and express Langerin (CD207), a C-Type-lectin receptor, which is involved in antigen uptake ((Marongiu et al., 2021).

Classical DCs originate in the bone marrow and have recently been shown to be ontogenically distinct from plasmacytoid DCs and Langerhans cells. Currently, 2 subtypes have been defined namely conventional/classical DCs type1 and type2 (cDC1 and cDC2). cDC1s comprise 30 % of total cDCs in the periphery and 40 % in lymphoid organs. They can be distinguished from cDC2s by their expression of CD8aa, CD11c, XCR1, CD103, DEC205 and CD207. cDC1s express Sirpα, CD11b and other macrophage markers such as CD64, but at a much lower level than cDC2s. The differentiation of cDC1s relies on *Batf3, Irf8, Nfil3 and Id2* encoded transcription factors. Batf3 has been shown to be essential for cDC1 development as the deletion of this transcription factor in mice results in the loss of function/dysfunction of cDC1s (Cabeza-Cabrerizo et al., 2021).

DCs have been shown to be fully permissive to EBOV infection and together with activated monocytes and macrophages are the early targets of EBOV in mice and nonhuman primates (Lüdtke et al., 2017). They are crucial for the activation of adaptive antiviral responses due to their role in bridging the innate and adaptive arms of immunity and are vital to survival after EBOV infection. Sufficient priming of T cells after interaction with differentiated DCs is thought to result in a positive outcome following EBOV infection (Perdomo-Celis et al., 2019). On the other hand, they may have a detrimental role to the outcome after infection and are thought to play a role in virus dissemination. DCs have been shown to play a role in virus dissemination.

A study by our group showed that CD11b$^+$ DCs, inflammatory moDCs and alveolar macrophages in the respiratory mucosae of susceptible mice are productively infected

following mucosal exposure to EBOV. EBOV GP was detected on the surface of $CD11b^+$ DCs but not $CD103^+$ DCs as determined by flow cytometry analysis. These cells are believed to support initial viral replication and dissemination (Lüdtke et al., 2017).

Though moDCs have been shown to be early targets of EBOV, the impediment of monocyte entry into infected tissue did not prevent virus dissemination. The fact that EBOV infection impairs DC function together with the migratory properties inherent in DCs points to a role in virus dissemination (Lüdtke et al., 2017). Various studies have shown that DCs have the capacity to transport pathogens to the lymphoid tissues (Cheong et al., 2011; Martín-Fontecha et al., 2009; Martinez et al., 2013). Interestingly migratory cross-presenting DCs expressing CD103 and langerin appear to be spared from infection and the reason as to why remains to be determined (Lüdtke et al., 2017).

EBOV has evolved a number of ways to evade the immune system, one of them being the ability to impair the function of DCs. This in turn contributes to virus dissemination and directly impacts the generation of adequate B and T cell responses. The activation and expansion of antigen-specific T cells is especially important for viral clearance.

1.6.3 B cells – antibodies matter

B cells play an important role during acute viral infections and various modes of action have been described to explain how B cells contribute to protection against viral pathogens. B cells can directly neutralize viruses by binding to viral epitopes or can initiate fragment crystallisable (Fc) receptor functions such as phagocytosis or cytotoxic killing by macrophages and NK cells respectively. Liu et al. have shown that antibody-dependent cellular cytotoxicity (ADCC) contributes to protection and together with Corti et al. postulate that this may be the mechanism by which non-neutralizing antibodies provide protection (Corti et al., 2016; Liu et al., 2017). Antibodies can also opsonize pathogens marking them for targeted removal by the complement system. Natural antibodies (NatAb) also referred to as B1 cells are nonspecific and are produced in response to a variety of pathogens. They are derived from foetal, neonatal and activated B lymphocytes and do not require exposure to foreign antigens to be produced. They consist mostly of secreted immunoglobulin M (sIgM) and have been shown to be necessary for optimal immunity to viral pathogens. They are able to directly bind and neutralize a multitude of viral pathogens limiting viral replication. B2 cells referred to as B cells are specific and once activated can differentiate into plasma cells, which secrete antibodies.

The creation of an antiviral state is achieved by the production of pro-inflammatory cytokines such as IFN-I by cells involved in both innate and adaptive immune responses. This antiviral

state results in an increase in B cell receptor-dependent calcium flux and the upregulation of various B cell receptors. One such receptor is CD69 whose increased expression leads to the inhibition of the signalling of the sphingosine-1-phosphate receptor (S1P1) thus retaining B cells in the lymph nodes. Remodelling of the lymph nodes occurs due to the higher amount of as well as the activation state of B cells thus providing a conducive environment for adaptive immune responses.

Macrophages and $CD8^+$ T cells can be activated by IFNs and the abundant production of these cytokines, which occurs during acute viral infections may negatively impact the B cell response. B cells are permissive to various viruses, e.g., Influenza virus with infection being thought to occur during BCR mediated endocytosis of antigens by antigen specific B cells. Infected B cells may thus be eliminated by activated macrophages and/or $CD8^+$ T cells and this early elimination may lead to a dampening of the humoral response and delays in antibody responses (Lam et al., 2020).

Naïve B cells are found in the follicles of the spleen and the lymph nodes where they are exposed to antigens for the first time. Follicular DCs and $CD169^+$ macrophages are able to present antigens directly to B cells leading to their activation. B cells are also able to take up antigens by both BCR-dependent and BCR-independent mechanisms. The activation of B cells is accompanied by an increase or decrease in the expression of chemokine receptors such as CXCR5, which is downregulated or CCR7, which is upregulated. Downregulation of CXCR5 leads to the retaining of B cells in the follicle while upregulation of CCR7 enhances the migration of B cells to the T cell zone. B cells in the T: B border secrete chemokines such as CCL3 and CCL4, which attract T cells to this zone. Activated B cells engage with CD4 T cells through the peptide-MHC II and T cell receptor (TCR). The immunological synapse is formed and co-receptors on both B and T cells are upregulated and interact with each other beginning the process an antiviral response. This interplay between follicular DCs and macrophages, B cells and T cells is paramount to the generation of an optimal, pathogen-specific and long-lasting humoral response. CD4 follicular helper T (Tfh) cells are also required for the formation of antibody secreting cells and to sustain the germinal centre (GC) responses. CD 4 T helper cells (Th1) and Tfh cells secrete IL21, which is necessary for the differentiation, proliferation and expansion of plasma cells (Miyauchi et al., 2016). Following infection or vaccination with a live virus, B cells differentiate to memory B cells and long-lived plasma cells that can persist for more than 20 years (Lanzavecchia and Sallusto, 2009). EBOV specific memory B cells can be maintained in a survivor and persist for more than a decade after infection (Corti et al., 2016).

Antibodies isolated from survivors are quite efficacious and protect NHPs from lethal challenge when administered up to 5 days after infection (Corti et al., 2016).

mAbs with potent pan-ebolaviruses neutralizing activities that can impede viral entry have been identified and various studies have revealed that the generation of EBOV-specific antibodies after vaccination is essential for protection from lethal EBOV or SUDV infection (Wec et al., 2017).

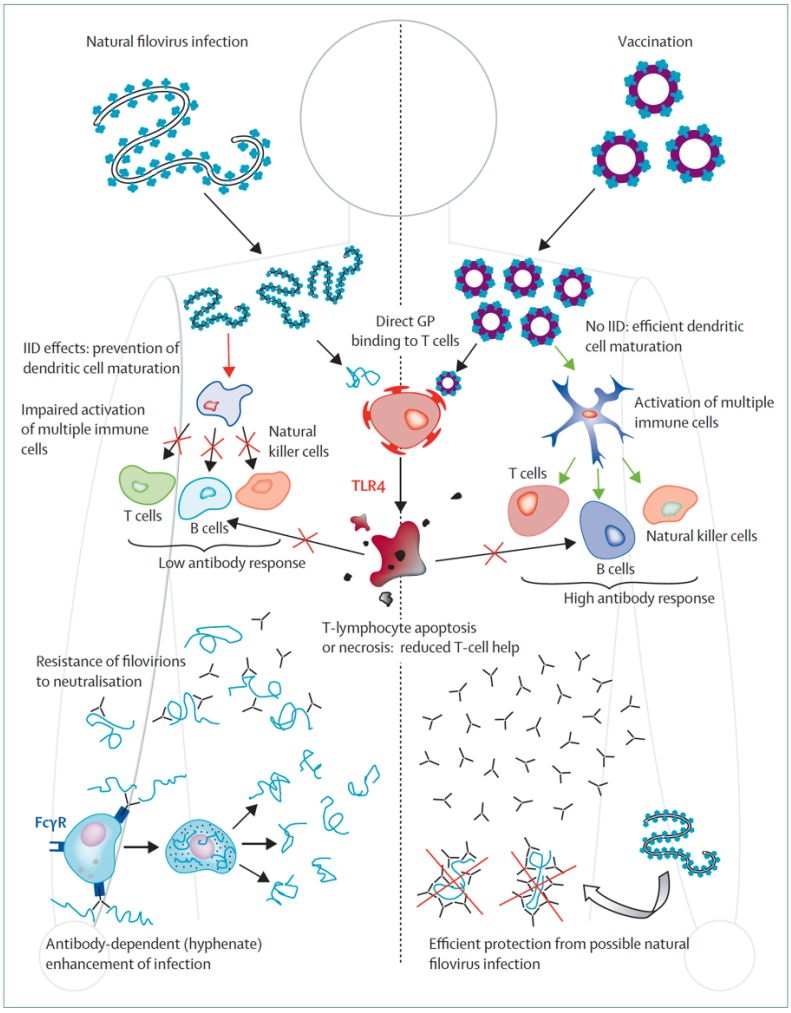

Fig 6. Comparison of the humoral immune response following natural filovirus infection or vaccination.

During natural filovirus infections, the maturation of DCs is suppressed by IIDs in viral proteins VP24 and VP35 resulting in dysregulated T and B cell responses. This state is characterised by a low antibody response lacking the capacity to efficiently neutralise virus. Vectored vaccines and other vaccines, which use the envelope glycoprotein (GP) and lack internal filovirus proteins can induce the maturation of DCs resulting in the proper priming of T cells and thus the activation and proper functioning of various immune cell populations. Such vaccines induce potent neutralising antibodies with strong Fc-

mediated effector functions, which may contribute to protection in the event of natural filovirus infection. IID = interferon-inhibiting domain (from Ilinykh and Bukreyev, 2021).

1.6.4 T cell responses/immunity during filovirus infections: a double-edged sword?

T cell-mediated immunity is an important aspect of the host response to filoviral infections. When T cells interact with APCs and receive the appropriate signals, they become activated and curb the spread of viruses by eliminating infected cells and producing growth factors e.g., cytokines and chemokines that can attract other immune cells to the sites of infection. An adequate T-cell response gives rise to long-lived memory T cells that form a strong defence line in the event of reinfection or exposure to the pathogen after vaccination. Antigen-specific memory T cells are extremely long-lived, are capable of rapidly expanding upon re-infection and, in some instances, have been shown to persist for life. On the other hand, T cells can be detrimental to the host when non-specifically activated. Bystander activation refers to the activation of T cells without antigen recognition. In cases of bystander activation, a stark increase in the levels of circulating inflammatory mediators has been observed mediating adverse effects such as tissue damage. A dysregulated T cell response has been shown to correlate with a more severe disease course during filoviral infections (Ruibal et al., 2016; Muñoz-Fontela and McElroy, 2017)

1.6.4.1 T cell development

The thymus provides a conducive microenvironment where lymphopoeisis can occur (Zúñiga-Pflücker, 2004). Haematopoietic stem cell lymphocyte progenitors migrate from the bone marrow to the thymus and colonise it. These developing T cells also known as thymocytes undergo various differentiation steps during the maturation process in the thymus before they become fully functional (www.immunology.org). Maturation occurs in separate regions of the thymus in the inner medulla or the outer cortex. Early thymocytes do not express CD4 or CD8 co-receptors. These double negative cells can be further delineated based on the expression of CD44 or CD25. $CD25^+$ double negative cells undergo beta selection, which selects for cells that have undergone successful TCRβ rearrangement. The beta chain pairs with a pre-Tα and a TCR is produced. The TCR can then form a complex with CD3 molecules which stops further rearrangement of the TCR chain locus. The cells differentiate and increase expression of CD4 and CD8 after which these double positive cells rearrange the TCRα chain locus and an αβTCR is produced. Only cells that recognize self-antigens and interact with MHC I or MHC II molecules with sufficient affinity are positively selected and survive. In the medulla, the

thymocytes undergo an additional round of selection. At this stage, cells that recognize self-antigens presented by dendritic cells, macrophages, monocytes and other APCs and interact too strongly with MHC molecules are depleted/eliminated or converted into regulatory FOXP3$^+$ CD4$^+$ T cells (Tregs) (Owen et al., 2019). Through this process, the majority of thymocytes die during negative selection. After this step, the co-receptors are down-regulated and single positive cells – CD4$^+$ or CD8$^+$ can exit the thymus and migrate to the periphery (Ceredig and Rolink, 2002; Godfrey et al., 1993; Zúñiga-Pflücker, 2004; www.immunology.org).

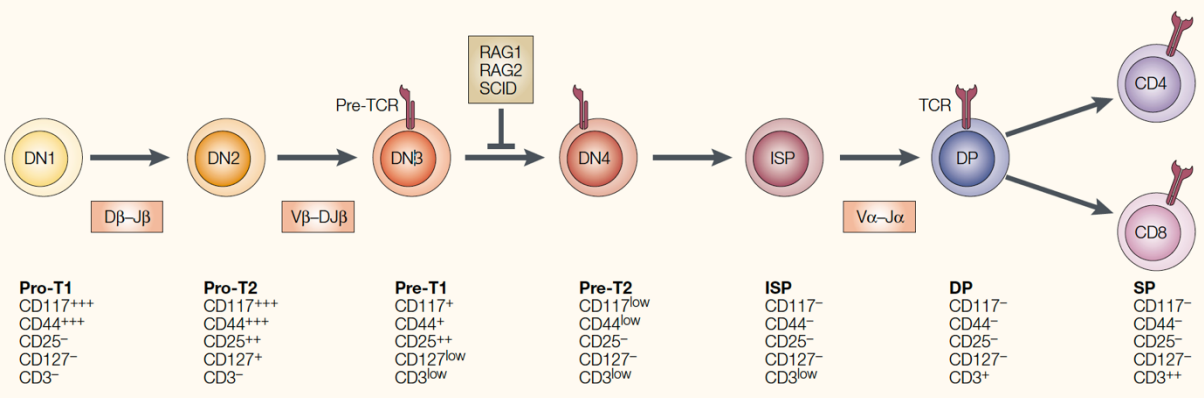

Fig 7. Early T cell development in the thymus.

The scheme shows the development of T cells proceeding from left to right. Gene arrangements are shown in boxes in red and the phenotype of the cells based on surface markers is shown at below. D, diversity; DP, double positive; ISP, immature single positive; J joining; RAG, recombination-activating gene; SCID; severe combined immunodeficiency; SP, single positive; TCR, T cell receptor (Ceredig and Rolink, 2002).

1.6.4.2 CD4 T cell subsets

CD4$^+$ T cells are a vital component of the immune response to filoviruses. Naïve CD4 T cells recognize antigens using the TCR on their surface which interacts with MHC II molecules found on the surfaces of APCs. Antigens are presented to T cells in the context of these MHC molecules and the nature of the stimulus determines the polarization of the T cells (Tao et al., 1997; Saravia et al., 2019). This interaction results in the upregulation of co-stimulatory molecules, which also interact with each other leading to the activation and expansion of the T cells. Co-stimulation is the second signal required for proper activation, differentiation and expansion. Co-stimulatory molecules are thought to also influence the polarization of CD4$^+$ T cells. Both APCs and T cells then secrete cytokines (signal III), which function to provide further stimulation and program the T cells to acquire a particular effector phenotype.

$CD4^+$ T cells differentiate into different effector subsets upon interacting with and receiving the necessary signals from DCs. $CD4^+$ T cell effector subsets defined thus far include Th (T helper) 1, Th2, Th9, Th17, Th22, Treg (regulatory T cells) and Tfh (follicular helper cells). CD4 T cell effector subsets and functional capacities can be defined by the differentiation of naïve cells by different cytokines, and the production of signature cytokines by the CD4 T cells themselves (Saravia et al., 2019). The secreted cytokines can have a pro- or anti-inflammatory effect depending on the antigenic stimulus and thereby the immune response elicited.

Th1 cells are important for antiviral and antibacterial (intracellular) immunity, and secrete IFNγ, TNFα and IL-2, which stimulate innate and T cell responses. Th1 cells have a cytolytic mode of action and are necessary for the clearance of viruses and other obligate intracellular pathogens. Tfh cells are found predominantly in the B cell and follicular zones and germinal centres and produce IL-21 which is necessary for B cell stimulation, and IL-4, which is required for immunoglobulin class switching (Reinhardt et al., 2009). They are essential for the maintenance of germinal centres and promote humoral immunity.

Severe EVD is characterised by hypercytokinemia (or cytokine storm), which has severe consequences for the patients. In the event of a hyperactive and thus detrimental immune response such as the over production of proinflammatory cytokines or activated cytotoxic cells that fail to contract and cause injury to the host, the induction of a regulatory T helper cell response may be advantageous. Tregs are necessary for the maintenance of peripheral tolerance and are beneficial in instances where the immune response requires tempering as well as for the maintenance of immune homeostasis. They secrete inhibitory cytokines such as IL-10 and TGFβ which function to suppress effector cells. Antigen-specific Tregs are able to control disease using other mechanisms such as inhibition of DC maturation, metabolic disruption leading to apoptosis or death of cells due to cytokine deprivation (Vignali et al., 2008).

Ruibal et al., 2016, identified a unique immune signature in EVD patients and showed that EVD fatalities had a higher percentage of $CD4^+$ and $CD8^+$ T cells expressing CTLA-4 and PD-1. Conversely, the T cells from survivors expressed these molecules at a much lower degree and were also shown to mount a robust EBOV-specific T cell response.

The immune response to filovirus infections requires a delicate and intricate balance involving an interplay of different cells. An early and well-coordinated immune response characterised by the production of antibodies and the generation of antigen-specific T cells correlates with a positive outcome during EVD.

Following the resolution of infection, effector cells die through apoptosis during the contraction phase.

A few of the responding cells, however, differentiate into memory cells and are retained in the blood and tissues, forming the basis for the $CD4^+$ T cell memory pool. Memory cells are long-lived and are able to rapidly expand upon a second encounter with the same pathogen. The formation of memory T cells is the foundation for vaccine-induced immunity (Gasper et al., 2014). The removal of the antigenic stimulus signalizes the transition from effector to memory with the transition from effector to memory cells requiring a shift from "a functionally active, highly proliferative effector state to a quiescent, functionally alert memory state" (Gasper et al., 2014). Most of the $CD4^+$ T cell memory pool is maintained in the secondary lymphoid organs (SLOs) with the spleen containing the highest amount of circulating memory cells. IL-7 is necessary for this transition in SLOs and nonlymphoid tissues while IL-15 is required for long term maintenance. T cell memory can be classified into central (T_{CM}) or effector (T_{EM}) memory (Sallusto et al., 1999). T_{CM} express high levels of lymphoid homing receptors e.g., CD62L and CCR7 and migrate between SLOs and the blood. They are highly proliferative and upon reinfection favour the secretion of IL-2 rather than lineage-specific cytokines. T_{EM} cells migrate between the spleen and non-lymphoid tissues and express markers that facilitate homing to target tissues (Gehad et al., 2012; Grindebacke et al., 2009). The contribution of the different CD4 T helper subsets to the response against filovirus infections remains to be elucidated. Lüdtke et al., 2017 showed that both CD4 and CD8 T cells are required to prevent virus dissemination. $CD4^+$ T cells possibly function by stimulating B cell responses leading to the production of anti-EBOV antibodies (Sullivan et al., 2009). This is also evidenced by the fact that the frequency of Tfh cells in circulation correlates with antibody titres after vaccination with rVSV-ZEBOV (Farooq et al., 2016).

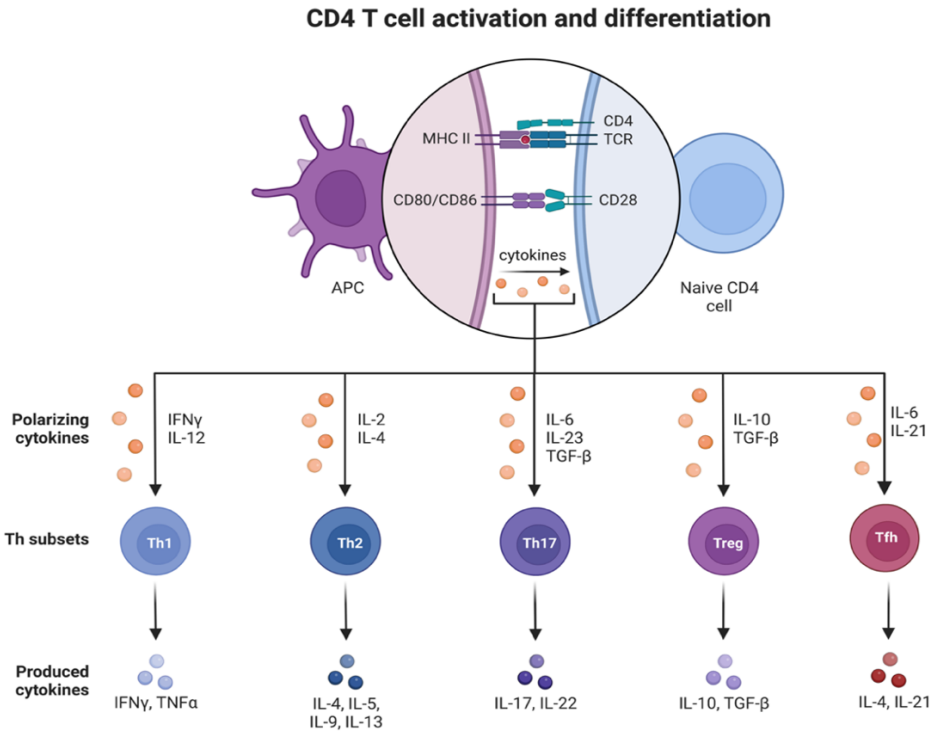

Figure 8. Diagram showing the priming of CD4+ T cells by APCs and the cytokines involved in the polarization of different CD4$^+$ T cell subset.

CD4 T cells are activated upon the recognition of antigen in the context of MHC II molecules and adequate co-stimulation. Rapid clonal proliferation occurs after priming and activated CD4 T cells differentiate and expand into functional effector cells. Effector CD4 T cells can be delineated based on the polarizing cytokine as well as the cytokines they produce. The type of pathogen encountered during priming largely determines the type of effector cell induced. Th, helper T cell; Tfh, T follicular helper cell; Treg, T regulatory cell (Gasper et al., 2014).

1.6.4.3 CD8 T cells – in memory we trust

CD8 T cells are critical players in the response to filoviruses. They express a dimeric co-receptor consisting of one CD8α and one CD8β chain. CD8 T cells recognise antigens expressed in the context of MHC I molecules, which are found on all nucleated cells. Following antigen encounter during infection or after vaccination, CD8 T cells are activated, and undergo clonal expansion. Antigen-specific T cells then differentiate into cytotoxic cells once they receive the third signal, which is the secretion of cytokines by APCs. To become cytotoxic, differentiated CD8 T cells require IL-12 and IFN-I (Curtsinger et al., 2005). In the absence of these polarizing cytokines, CD8$^+$ T cells only express perforin but not Granzyme B (GzB)

(Curtsinger et al., 2005). Once armed, they are able to eliminate virus infected cells in a variety of ways. One mechanism of action is the secretion of cytokines such as IFNγ and TNFα that can activate innate immune cells such as macrophages, which then phagocytose infected cells. Cytotoxic T cells contain cytolytic granules in their lysosomal compartments which when released, can directly kill target cells. Perforin functions by puncturing holes in the membrane of virus-infected cells allowing granzymes to enter. Granzymes are serine proteases that activate caspases, which can then cleave other substrates leading to apoptosis. They can also cleave proteins directly in the absence of caspase activity. Granzymes are able to inhibit viral replication by cleaving viral proteins. Resting CD8+ T cells i.e., naïve and T_{CM} cells do not have cytolytic granules and in the absence of antigenic stimulation, T_{EM} only express GzB for up to one month (Nowacki et al., 2007).

Cytotoxic CD8 T cells can also induce cell death in a FAS/FASL dependent manner.

Similar to CD4 T cells, the CD8 T cell response contracts after resolution of the infection. The contraction phase is in part mediated by cytolytic CD8 T cells, which kill their counterparts in a FAS/FASL dependent manner. A small number of these cells are retained forming a pool of pathogen-specific $CD8^+$ memory T cells.

Antigen-experienced $CD8^+$ T cells can be phenotypically divided into two broad groups namely: short-lived effector cells (SLECs) and memory-precursor effector cells (MPECs). The expression of killer-cell lectin-like receptor G1 (KLRG1) and IL-7 receptor a (IL-7Rα or CD127) are used to delineate these two groups. MPECs mainly express CD127 ($CD127^+KLRG1^-$) while SLECs express KLRG1 ($KLRG1^+CD127^-$). Effector $CD8^+$ T cells are programmed to differentiate into one of the two subsets depending on the invading pathogen, the inflammatory environment as well as the metabolic status. Both MPECs and SLECs arise from a population known as early effector cells (EECs), which are the most abundant type of effector cell prior to the peak of the T cell response (Obar et al., 2011). Plumlee et al., 2015, showed that EECs are driven to differentiate into SLECs or MPECs based on the signals received during priming. Interestingly, these EECs retain plasticity and are not restricted to one fate. Rather, they rely on inflammatory cues and signals from the infectious environment. SLECs are terminally differentiated and are eliminated via apoptosis during the contraction phase as the immune system returns to stasis. MPECs on the other hand are long-lived and are believed to undergo epigenetic changes that maintain them in a poised state ready to quickly respond to antigens following a secondary re-encounter (Yuzefpolskiy et al., 2015).

Introduction

As with $CD4^+$ memory T cells, $CD8^+$ memory T cells are classified into central, effector and tissue resident (T_{RM}) memory cells. Memory cells are able to quickly expand and produce effector molecules including effector cytokines like IFNγ and TNFα and cytolytic granules. $CD8^+$ T_{CM} cells express lymphoid homing markers such as CD62L and CCR7 and have a high expansion potential on antigen re-encounter. T_{EM} cells are mostly found patrolling regions outside of the lymph nodes and are not able to enter the lymph nodes from the blood (Kok et al., 2022). They are able to rapidly execute effector functions but have a lower capacity for proliferation compared to T_{CM} (Behr et al., 2020). T_{RM} cells are found in SLOs and sites of previous antigen encounter or infection such as the lungs, skin, liver, gastrointestinal tract and other non-lymphoid organs. They are permanently domiciled in the tissues and do no traffic to the blood (Wu et al., 2018). T_{RM} cells display an increased expression of markers associated with tissue retention such as CD69 and CD103 (E-cadherin binding αE integrin). They survey the anatomic compartments wherein they are confined for pathogens and upon encounter, induce an antiviral state that draws other immune cells to the site of infection. Jiang et al., 2012, demonstrated that skin infection with vaccinia virus (VACV) results in the generation of potent, effector, long-lived T_{RM} that persist for many months after infection and are able to rapidly protect against re-infection. Circulating T_{CM} cells on the other hand had an impaired ability to clear VACV in the absence of skin T_{RM} cells. T_{RM} cells can provide long term protection against reinfection and vaccine strategies that can induce their production or modulate their activity are therefore highly desirable.

Studies in murine models with EBOV revealed that $CD8^+$ T cells are fundamental for the control of infection. This is supported by data showing that $CD8^+$ T cells are necessary for protection after immunization with viral-like particles (Perdomo-Celis et al., 2019)

An evaluation of PBMC samples from 4 patients revealed that up to 50 % of $CD8^+$ T cells are highly activated and were observed up to 60 days after symptom onset despite the lack of detectable viral RNA in the blood (McElroy et al., 2015).

Characterisation of antigenic epitopes of various viral proteins revealed that EBOV NP is the main driver of T cell responses. Synthetic peptide-based screening and NP-specific mouse mAbs were used to determine antigenic regions of viral proteins. 8 antigenic regions were found with 2 being highly conserved (Changula et al., 2013). Cytokine production was also used to define the immunodominant epitopes of EBOV. A library of overlapping peptides covering all viral proteins with the exception of the L protein was generated. PBMCs were then stimulated with the peptide pools and IFNγ, TNFα and IL-2 production was measured. They

found that of the three patients assessed, all had detectable $CD8^+$ T cell responses with the response to the NP being the most dominant. $CD4^+$ T cells also produced measurable cytokines but at a lower magnitude. Of the three EVD patients, only two had measurable $CD8^+$ T cell responses against EBOV GP (McElroy et al., 2015). Taken together, this indicates that inclusion of the NP antigen in the design of T-cell based vaccines is well advised in view of the critical role that CD8 T cells play in the host defence to filoviruses.

1.7.1 Dendritic cells and T cells – bridging the gap

DCs play a vital role in T-cell mediated immunity and are therefore essential to the development of any T-cell based vaccine. Thus, any successful vaccination strategy needs to engage antigen-presentation by DCs, in particular to ensure T-cell mediated immunity. An important factor to be considered during vaccine design is the ease with which the vaccine can be modified in the event of the emergence of other variants. This is especially pertinent to infectious diseases caused by rapidly mutating pathogens. Antibody-based vaccines can be customised by targeting different receptors or conjugating different proteins in order to induce the desired response.

Dendritic cell targeting refers to the delivery of antigens to specific DC subsets using monoclonal antibodies directed to surface DC molecules as vehicles. In particular, antibodies are commonly specific for endocytic receptors found on the surfaces of DCs and the antigen of interest is coupled to the Fc portion of the heavy chain of the antibody (Bonifaz et al., 2002). The use of monoclonal antibodies ensures that the cargo is optimally delivered to the correct DC subset. After immunization, the antibodies bearing the antigens of interest are internalized and processed by DCs. The entire cargo is degraded and the antigenic peptides are loaded onto MHC I or MHC II molecules.

The rate of internalization and the compartment to which the antigens are trafficked has an effect on the type of T or B cell response elicited. A slower rate of internalization leads to the formation of an antigen depot allowing for prolonged cross-presentation. Trafficking to early endosomes is also preferential due to the reduced rate of proteolysis, which results in more efficient processing for cross-presentation. DCs display a reduced level of proteolysis which may in part explain their superior ability to present antigens compared to other APCs. Exogenous antigens are usually endocytosed and trafficked to late endosomes or lysosomes where they are degraded by proteases in the acidic lumen after which they are loaded onto MHC II molecules. These MHC II-peptide complexes are then transported to the cell surface where the antigens are then presented to $CD4^+$ T cells.

Endogenous antigens arising from virus-derived proteins are degraded via the ubiquitin-proteasome pathway. Ubiquitin covalently attaches to proteins targeting them for degradation by the proteasome. Peptides of approximately 2-25 residues are generated after passing through the proteasome and are then released into the cytosol. Immunodominant epitopes of pathogens, that is, peptides that drive most of the host T-cell response to a specific antigen, are typically more efficiently produced by the immunoproteasome (Kincaid et al., 2012; Sijts et al., 2000). Peptide trimming is done in the cytosol or in the lumen of the endoplasmic reticulum (ER) in order to fit into the groove of MHC I molecules. The peptides are then transported from the cytosol to the ER by the transporter associated with antigen processing (TAP) where further trimming of longer peptides is done by enzymes. The trimmed peptides are then loaded onto growing MHC I molecules done with the help of ER-resident chaperones. These are later on released and the peptide-MHC I complex migrates to the cell surface exposing the groove containing the peptide (Leone et al., 2013). Peptides can also be generated via proteasome-independent pathways.

Exogenous antigens can be rerouted during processing and presented in the context of MHC I molecules to $CD8^+$ T cells leading to the generation of cytotoxic T cells (Heath et al., 2004; Shortman and Heath, 2010). The mechanism of cross-presentation is not yet completely understood, and two pathways have been proposed that may explain how this occurs. In the cytosolic cross-presentation pathway, the endocytosed antigen is ferried from the endosomes to the cytosol followed by degradation via the proteasome. In the vacuolar cross-presentation pathway, antigens are processed in a proteasome and TAP-independent manner. The $CD8\alpha^+$ and $CD103^+$ DC subsets in mice have shown an exemplary capacity for cross-presentation. The $CD8\alpha^+$ DC subset express lower amounts of lysosomal proteases and maintain an alkaline pH in their endosomal lumens in comparison to $CD8^-$ DC subsets, which may in part explain the differences observed in cross-presentation capabilities (Heath et al., 2004).

Different endocytic receptors have different abilities when it comes to inducing a T cell response. *In vivo* targeting to the C-type lectin receptors; DEC205, Clec9A and Clec12A has been done in various studies to investigate their intracellular trafficking capacities and the kind of immune response elicited.

1.7.2 Targeting dendritic cells

The mainstay of vaccination is the ability to induce effective and durable immune responses to virus, bacterial or tumour antigens. The cancer-testis antigen NY-ESO 1 is expressed by a wide

range of tumour types such as neuroblastoma myeloma, metastatic melanoma, bladder, head and neck cancer, prostate, breast and oesophageal cancer etc. (Kumar et al., 2018)

DC based vaccines are at the forefront of immune based interventions being tested against various cancers. Peptide pulsing of DCs with NY-ESO-1 has been promising. However, the process is laborious and expensive and there is evidence that *in vitro* manipulated DCs have a lower immune-stimulatory potential (Pugholm, Varming and Agger, 2016). The DC targeting platform has also been used to develop a vaccine against cancers bearing NY-ESO-1. A study by Dhodapkar et al. showed that targeting DCs with the NY-ESO-1 antigen resulted in the induction of antigen-specific humoral and immunity. The phase 1 trial evaluated the safety, immunogenicity and efficacy of CDX-1401 (anti-human DEC205 monoclonal antibody fused to the full-length NY-ESO-1) against malignancies refractory to other interventions. Out of the 45 patients who received the therapy, thirteen experienced a stabilization in disease, two had approximately 20 % shrinkage of tumour legions and six who received immune checkpoint inhibitors in addition to CDX-1401, had objective tumour regression (Dhodapkar et al., 2014). CDX-1401 is undergoing clinical trials against stage II-IV melanoma and ovarian, fallopian tube and peritoneal carcinomas (Thomas et al., 2018). Another study also demonstrated the utility of targeting tumour-specific antigens to DEC205$^+$ DCs. Targeting melanoma antigens to DEC205 in vivo resulted in melanoma specific T cells when administered together with CpG adjuvant. The mice were protected against challenge with tumour cells and the growth of an established tumour was diminished (Mahnke et al., 2005a).

Infectious diseases such as Malaria, Leishmania, HIV, Dengue, Influenza and Herpes may benefit greatly from vaccines based on the DC targeting platform due to the requirement for T cell mediated immunity. Indeed, various studies have been published over the last decade detailing the use of antibody-mediated delivery of different viral and bacterial epitopes to DCs to improve the efficiency of antigen presentation and cellular immunity.

Targeting the HIV gag P24 to CD8a$^+$ DCs has been shown to result in a robust T cell response comprising of Th1 and CD8 T cells. Targeting DCs with HIV gag P24 together with Poly IC elicited multifunctional and high cytokine secreting CD4$^+$ T cells that persisted several weeks after immunization. HIV specific CD4$^+$ T cells that secrete IFNY and IL-2 are associated with a better clinical outcome (Idoyaga et al., 2011; Trumpfheller et al., 2008)

Antibody-mediated delivery of Dengue virus non-structural protein 1 (NS1) to DEC205$^+$ DCs or DCIR$^+$ DCs resulted in the generation of Dengue NS1 specific IgG antibodies. However, the number of IFNγ producing T cells was considerably higher after targeting the NS1 antigen to DEC205$^+$ DCs. Mice that were immunized with the anti-DEC205$^+$ antibodies were also

partially protected from intracranial challenge with Dengue virus in contrast to those that were immunized with the anti-DCIR$^+$ antibodies (Pereira et al., 2020).

Other studies on Epstein Barr virus have shown that targeting a virus antigen to DEC205$^+$ DCs elicited strong EBV-specific effector memory T cells. The generated CTLs possessed cytotoxic activity against EBV and mice immunized with antiDEC205 BZLF1 showed significant improvement in survival compared to control mice (Ahmed et al., 2021).

A vaccine that comprises anti-human DEC205$^+$ antibodies fused to a Flu matrix protein (FluM1) and administered to humanized mice, elicited strong human CD8$^+$ T-cell responses in vivo (Graham et al., 2016).

1.7.3 Targeting antigens to DEC-205

DEC-205 is expressed by thymic epithelial cells, dermal and CD8$^+$ DCs and LCs.

Targeting to the DEC-205 receptor initiates a robust CD8$^+$ T cell response (Bonifaz et al., 2002). In the presence of an adjuvant, immunization with anti-mouse DEC205 (αmDEC-205) antibodies results in the cross-presentation of antigens and the proliferation of T cells that are specific to ovalbumin (OVA), a model antigen routinely used in immunological studies. The TCR of OVA-specific T cells has been engineered to recognise OVA residues presented in the context of MHC I molecules (OT-I T cells) or MHC II molecules (OT-II T cells). Following DEC-205 targeting, OT-I T cells robustly proliferate and later acquire an effector cell phenotype. There is also an induction of a strong humoral response depending on the targeting antibodies used. Interestingly, the omission of an adjuvant results in the induction of CD25$^+$ Tregs and peripheral tolerance (Bonifaz et al., 2002). Tolerogenic DEC-205 targeted DCs are still able to prime T cells and induce the expansion of antigen-specific T cells. However, these T cells do not differentiate into effector cell but rather they convert into Tregs or enter an anergic state and are depleted afterwards (Hawiger et al., 2001). Targeting antigens to other CLRs such as Clec9A or Clec12A has been also shown to result in priming of both CD4$^+$ and CD8$^+$ T cells. This further supports the idea that targeting antigens to CLRs on the surface of DCs can be used to harness DC function to induce either immunity or tolerance.

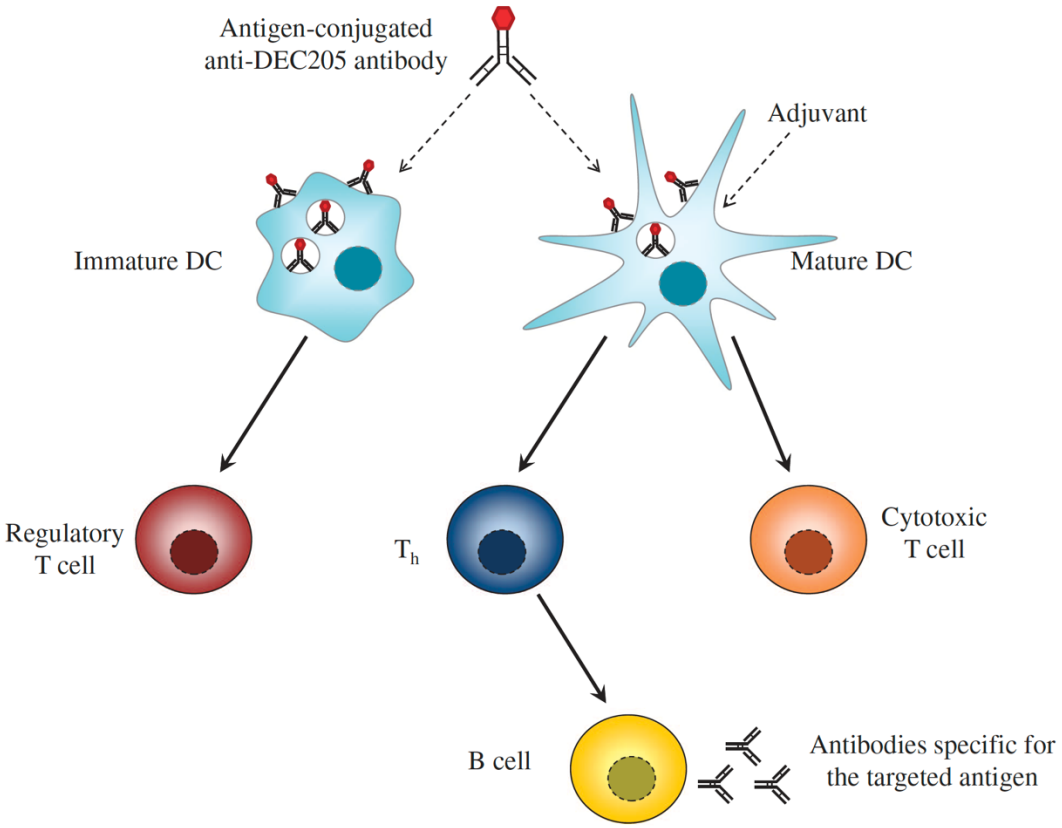

Figure 9. Principle of targeting antigens to DCs.

Immunization of mice with antigen-conjugated anti-DEC205 antibodies in the absence of adjuvants leads to the induction of regulatory T cells. Supplying adjuvant during the immunization results in a robust cytotoxic t cell response and the induction of effector $CD4^+$ T including T helper cells that support the humoral response (from Macri et al., 2016).

1.8 Aim of the study

Fatal EVD is characterised by multi-organ failure and dysregulated immune responses. Survivors of EVD have been shown to mount a well-coordinated immune response involving the generation of potent neutralizing antibodies that can mediate Fc effector functions as well as antigen-specific T cells. The current vaccines licensed against EVD elicit robust humoral immune responses but poor T cell immunity. The induction of antigen-specific immunity can prevent severe disease and the generation of a cytotoxic T cell response is crucial to the containment of viral infections. The induction and maintenance of memory T cells is the basis for protective vaccination against disease and can protect against reinfection.

Targeting antigens to DEC205$^+$ DCs is a useful strategy for inducing potent and durable cytotoxic T cell responses and boosting vaccine immunogenicity and efficacy.

The aim of this thesis is to investigate whether targeting EBOV NP to cross-presenting DEC205$^+$ DCs using monoclonal antibodies bearing the EBOV NP can improve immunity against filovirus infections. The four main objectives are:

1. To determine the ability of DEC205$^+$ DCs to activate EBOV NP-specific CD8$^+$ T cells after antigen delivery and whether targeting EBOV NP to DCs will induce an antigen-specific multifunctional T cell response. The induction of EBOV NP-specific CD8$^+$ T cells after immunization with αmDEC205 EBOV NP will be assessed together with the ability of these cells to secrete effector cytokines that are associated with protective immunity.
2. To assess whether targeting EBOV NP to DEC205$^+$ DCs enhances the generation of antigen-specific T cells and if these cells facilitate viral clearance and improve the outcome after EBOV infection.
3. To characterize the T cell response following infection using a novel recombinant EBOV harbouring the model antigen OVA. This virus will facilitate the identification and characterisation of infection-specific T cells. Here, the ability of targeting antibodies to enhance the proliferative expansion and differentiation of antigen-specific CD8$^+$ T cells into effector populations will be evaluated and the generation of CD8$^+$ T-cell memory will be examined.
4. To evaluate whether immunization with the targeting antibodies confers protection to mice infected with SUDV and MARV.

To fulfil these objectives, vaccine studies will be performed in a susceptible immunocompetent mouse model in the BSL-4 laboratory at the Bernhard Nocht Institute for Tropical Medicine in Hamburg. These studies will include immune assays and multi-parametric flow analyses.

The ultimate goal is to provide insight on the capacity of the DC targeting platform to enhance protective immunity and to lay the groundwork for further development of DC-targeted vaccines against filoviruses.

2. Materials

2.1 Reagents

Table 3. List of reagents

Reagent	Company
Acetic acid	Roth
3-amino-9-ethylcarbazole (AEC) chromogen	BD Biosciences
AEC substrate	BD Biosciences
Ammonium sulphate	Roth
Ampicillin	Thermo Fisher scientific
Bovine serum albumin (BSA)	Sigma
Collagenase D	Roche
Complete Freund's adjuvant (CFA)	Sigma
Dimethyl sulfoxide (DMSO)	Roth
DNase I	Sigma
Dulbecco's Modified Eagle Medium (DMEM)	Sigma
Dulbecco's Phosphate Buffered Saline (PBS)	Sigma
Ethylenediaminetetraacetic acid (EDTA)	Roth
Ethanol	Roth
Foetal calf serum (FCS)	Gibco
GolgiPlug™ Protein Transport Inhibitor	BD Biosciences
HEPES	Gibco
HRP-streptavidin	BD Biosciences
HyPure Endotoxin free water	Hyclone
Ionomycin	Sigma
Isoflurane	Abbvie
Isopropanol	Thermo Fisher Scientific
L-Glutamine (200 mM)	Gibco
Lipofectamine® 2000	Invitrogen
Methyl cellulose	Roth
MHC Dextramer	Immudex
Nutridoma SP	Roche

Opti-MEM	Gibco
Paraformaldehyde (PFA)	Biocyc GmbH CO & KG
Penicillin/Streptomycin	Gibco
Peptide - EBOV NP_{44-52} YQVNNLEEI	JPT peptide tech.
Peptide – EBOV NP LSFASLFLPKLVVGE	JPT peptide tech.
Phorbol 12-myristate 13-acetate (PMA)	Sigma
Polyethylenimine	Polysciences
Propanol ≥99.8 %	Roth
Protease inhibitors (complete, EDTA free)	Roche
Protein G IgG binding buffer	GE Healthcare
Protein G Sepharose beads	GE Healthcare
Purified Rat Anti-mouse CD16/CD32 (Mouse FC block)	BD Biosciences
RBC lysis buffer	Biolegend
Recombinant murine IL-2	Peprotech, Miltenyi
Roswell Park Memorial Institute medium (RPMI) 1640	Gibco
Sodium hydroxide	Roth
Sulphuric acid	Sigma Aldrich
TransIT-LT1	Mirus Bio LLC
Tetramethylbenzidine (TMB)	Mikrogen Diagnostics
Tris	Applichem
Trypsin TrypLE™	Gibco
Tween-20	Roth
Ultra-low IgG Fetal Bovine Serum	Gibco

2. 2 Buffers and media

2.2.1 Buffers

Spleen processing buffers	
RBC lysis buffer 1X	in endotoxin free H_2O
Wash buffer	in PBS 0.1 % BSA 2 mM EDTA
Antibody production & purification	
Protein G IgG binding buffer	GE healthcare
IgG elution buffer	20 mM sodium phosphate
Flow cytometry & magnetic bead enrichment buffers	
EDTA buffer	0.5 M in ddH_2O, pH 7.2
MACS buffer	in PBS 0.5 % BSA 1 % FCS 2 mM EDTA
Sorting buffer	in PBS 2 % FCS

2.2.2 Solutions

Saturated ammonium sulphate solution	in endotoxin free H_2O 4.3 M $(NH_4)_2SO_4$

2.2.3 Media

DMEM-10	in DMEM 10 % ultralow IgG FBS 100 U/ml P/S 2 mM L-glutamine
RPMI-2	in RPMI 1640 2 % FCS 100 U/ml P/S

	2 mM L-glutamine
RPMI-10	in RPMI 1640 10 % FCS 100 U/ml P/S 2 mM L-glutamine
Lung and spleen digestion medium	in RPMI-2 2 mg/ml collagenase type D 50 µg/ml DNase I
Freezing medium	90 % FCS 10 % DMSO

2.3 Cell lines

Human embryonic kidney (HEK293T) cells were used for antibody production.

Vero E6 cells were used for virus propagation and amplification.

Huh7 cells (hepatocyte derived cellular carcinoma) were used for virus rescue. The line was established by Nakabayshi, H and Sato, J in 1982.

2.4 Plasmids

Plasmids encoding the heavy and light chains of the isotype control and anti-mDEC205 OLLAS OVA (αmDEC205: OVA) antibodies were provided by Prof. Ralph Steinman (Rockefeller University, USA). Cloning, to insert the EBOV NP protein into the heavy chain of anti-mDEC205 OLLAS EBOV NP (αmDEC205: EBOV NP) was performed in our lab by Prof. César Muñoz-Fontela.

2.5 Mice

Mice were obtained from Jackson laboratories and were housed in the animal facility of the Bernhard Nocht Institute for Tropical Medicine. The mice were housed in individually ventilated cages and fed and watered ad-libitum.

The age and gender of the mice used varied depending on the experiments performed as described in the Methods section. Briefly, the different strains of mice used were.

1. C57BL/6J
2. B6.SJL-*Ptprc*^{a} *Pepc*^{b}/BoyJ (C57BL/6 Ly5.1)

3. IFNαβR-/-
4. C57BL/6-Tg (TcraTcrb)1100Mjb/Crl (OT-I).

2.6 Antibodies

2.6.1 DC targeting antibodies

Table 4. List of antibodies used for DC targeting

Antibody	Clone	Company
Iso OLLAS – Isotype control	-	In-house
Anti-mDEC205 OLLAS OVA	-	In-house
Anti-mDEC205 OLLAS EBOV NP	-	In-house
InVivoMab anti mouse CD40	FGK4.5/FGK45	Biocell

2.6.2 ELISpot antibodies

Table 5. List of antibodies used for ELISpot

Antibody	Clone	Company
Anti-mouse IFN-γ (capture) antibody	-	BD Biosciences
Biotinylated anti-mouse IFN-γ (detection) antibody		BD Biosciences

2.6.3 Immunofocus assay

Table 6. List of antibodies used for virus detection

Antibody	Clone	Company
Polyclonal mouse αEBOV primary antibody	-	In-house
Sheep αmouse (IgG H+L) HRP-conjugated	-	Jackson Immuno Research Laboratories, Inc

2.7 Kits

Table 7. List of kits

CD3ε Microbead kit (mouse)	**Miltenyi**
CD8α T cell isolation kit (mouse)	Miltenyi
CellTrace™ Violet cell proliferation kit	Thermo Fisher Scientific
Compensation beads anti-rat & anti-hamster	BD Biosciences
Endotoxin free Maxi-Prep kit	Qiagen, Macherey-Nagel
Fixation and permeabilization kit	BD Biosciences
Pan T cell isolation kit II	Miltenyi
Zombie NIR™ Fixable Viability Kit	Biolegend

2.8 Equipment

Table 8. List of machines and equipment

Machine	**Company**
AID ELISpot reader	Advanced Imaging Devices GmbH
BD LSRFortessa™	BD Biosciences
BD FACSAria™ III	BD Biosciences
Caesium irradiator	-
Cytek SpectroFlo Aurora	Cytek Biosciences
ELISA reader	Tecan - Infinite 200 Pro
FastPrep-24 5G	MP Biomedicals
Fuji DRICHEM Analyzer	Fujifilm
MACS separators	Miltenyi
MACSMix tube rotator	Miltenyi
NanoDrop spectrophotometer	Thermo Fisher Scientific

2.9 Computer software

Table 9. List of computer programs and software

Program/Software	Company
FlowJo, V10.9	FlowJo LLC
GraphPad Prism	GraphPad Software, Inc
Biorender	Biorender
Microsoft Office	Microsoft Corporation
Mendeley	Elsevier

3. Methods

3.1 Antibody production

The antibody production protocol was already described in a previous work. To recapitulate, 3 antibodies were produced and purified and used afterwards for DC targeting. These are: Iso OLLAS, αmDEC205: OVA and αmDEC205: EBOV NP. HEK293T cells were transfected with different combinations of plasmids as indicated below:

Plasmid	Fragments
Iso kappa	Light chain containing non-mDEC205 variable region
Iso OLLAS	Heavy chain
DEC kappa	Light chain mDEC205 variable region
DEC OLLAS OVA	Heavy chain containing OVA
DEC OLLAS EBOV NP	Heavy chain containing EBOV NP

1. Iso kappa + Iso OLLAS → Isotype control antibody
2. DEC kappa + DEC OLLAS OVA → αmDEC205 OVA
3. DEC kappa + DEC OLLAS EBOV NP → αmDEC205 EBOV NP

3.1.1 Plasmid DNA preparation

Plasmid DNA was extracted and purified using the Qiagen Endofree® Plasmid Maxi Kit or Macherey-Nagel Nucleobond® Xtra Maxi EF according to the manufacturer's instructions. Endotoxins can inhibit transfection therefore an endotoxin removal step is included in the kit. The concentration of the DNA was subsequently measured on a NanoDrop spectrophotometer.

3.1.2 Transfection

$8x10^6$ cells/plate were seeded in 30 15 cm tissue culture dishes 20-24 h before transfection in order to achieve 70 % confluence at the time of transfection. The transfection media was DMEM supplemented with 10 % low IgG FCS and 1 % L-glutamine without antibiotics. 300 µg of the light chain DNA and 300 µg of the heavy chain DNA for the different hybrid antibody

combinations were placed in 18.75 ml of Opti-MEM. 1800 µl of PEI or 1200 µl of TransIT-LT1 transfection reagents were also added to 18.75 ml of Opti-MEM. The diluted DNA and diluted PEI/TransIT-L1T were left at room temperature for 5 min and then gently mixed. An additional 15 min was allowed for PEI/DNA or Transit LT/DNA complexes to form after which the complexes were added drop wise to each plate. The plates were placed in an incubator at 37 ˚C and 5 % CO_2 for 5 h. The transfection medium was aspirated and replaced with fresh DMEM supplemented with 1 % L-glutamine and 1 % Nutridoma SP. The plates were placed in the incubator for 5 days.

3.1.3 Ammonium sulphate precipitation

Ammonium sulphate is an inorganic salt that is highly soluble and can stabilize protein structure. At low salt concentrations (<0.15M) the addition of more salt tends to increase the solubility of proteins as ions shield the protein molecules from the charges of other molecules; this trend is termed 'salting-in' (www.info.gbiosciences.com). At a high salt concentration, the protein will precipitate out of the solution in a process known as 'salting-out'. Removal of the salt by chromatography or dialysis is required later.

Five days after transfection, the supernatant was harvested into 250 ml tubes. The supernatant was centrifuged for thirty min at 800 g, 4 ˚C, in order to remove dead cells and was then filtered through a 0.22 µm filter after which protease inhibitors were added. Ammonium sulphate was carefully added in an amount equal to 60 % of the supernatant in weight to facilitate protein precipitation. The samples were then placed in the cold room and stirred overnight at 150 rpm. The next day the samples were centrifuged at 2900 g with the brakes off. The supernatant was discarded and the pellets were resuspended in PBS. Freshly prepared saturated ammonium sulphate solution was slowly added to the samples under constant stirring. The samples were gently stirred for 45 min at room temperature followed by 10 min at 4 ˚C and then centrifuged for 20 min at 4 ˚C. The pellet was re-suspended in 2.5 ml PBS and added to PD-10 columns.

The process of salting out proteins results in the samples having a high salt concentration. The salt has to be removed before the protein samples can be used in downstream applications. PD-10 desalting columns contain sephadex G-25 resin to facilitate rapid buffer exchange and desalting by gravity flow (GE healthcare).

3.1.4 IgG purification

The purification of IgG and IgG subclasses is based on the high affinity of protein G for the FC region of polyclonal and monoclonal IgG antibodies. Protein G is found in the cell walls of

group g streptococcal bacteria. It can bind immunoglobulins and is routinely used for the purification of monoclonal and polyclonal antibodies from culture supernatant, tissue ascites and sera.

Protein G IgG binding buffer (20 mM sodium phosphate pH 7.2) was added to the desalted samples and placed on ice for thirty min. The samples were then centrifuged, and the supernatant was added to protein G Sepharose beads. The protein samples were then incubated at 4 ˚C in the cold room overnight.

24 h later, the protein samples were centrifuged, and the supernatant was discarded. 5 ml binding buffer was added to the Protein G beads bound to the protein. Chromatography columns were equilibrated by washing with the binding buffer three times, after which the sample was added and allowed to enter the resin by gravity flow. The protein was then eluted into tubes containing 1 M Tris-HCl for neutralization.

3.1.5 Buffer change and sample concentration

An Amicon Ultra-15 Ultracel 10,000 centrifugal filter unit was used for buffer exchange and to concentrate the protein. This was done by centrifuging the samples in PBS four times at 2900 g, 4 ˚C for 20 min. The protein sample was then harvested from the tube and transferred into a cryotube.

The Nano-drop spectrophotometer was set to the IgG setting and the antibody concentration was measured.

3.2 Ethics statement

All animal experiments were performed in accordance with the prescribed rules and regulations of the German Society for Laboratory Animal Science. The experiments were approved by the Committee on the Ethics of Animal Experiments of the federal state of Hamburg. Animal experiments were performed as described in permit numbers 117/2018 and 011/2020 in strict adherence with the ethical regulations outlined by the animal welfare authorities.

3.2.1 Humane endpoint criteria

Mice were housed in individually ventilated cages and fed and watered ad libitum. Mice were housed in rooms with controlled humidity and temperature and were regularly monitored for adverse effects after immunization. Mice were transferred to the BSL-4 laboratory five to seven days before the beginning of experiments to allow acclimatisation. Following infection,

temperature and weight measurements were taken daily and their wellness scored using the scale shown in table 4. Mice that reached the humane endpoint criteria were euthanised.

Table 10. Humane endpoint criteria after immunization

Observation/finding	Scoring
Body weight	
No change	0
Reduction > 5 %	1
Reduction > 10 %	2
Reduction > 20 %	3
General condition	
Smooth and shiny fur, clean orifices	0
Dull and ruffled fur, cloudy eyes	1
Dirty or moist orifices, abnormal posture, high muscle tone, dehydration	2
Cramps, lameness, abnormal breathing, animal cold to the touch	3
Spontaneous behaviour	
Normal behaviour – sleep, reaction to touch and gentle blowing, curiosity, social contact	0
Abnormal behaviour, reduced mobility or hyperkinesis	1
Isolation, apathy, expression of pain, pronounced hyperkinesis i.e., repetitive behaviour, coordination disturbance	2
Auto mutilation	3
Evaluation and measures to be taken	Total points
No burden	0
Low burden – observe carefully (1x daily), add heat supply, wet food, therapy such as zinc oxide	1
Medium burden – observe carefully (2x daily)	2

High burden – euthanise animal	3

Table 11. Humane endpoint criteria after infection

Observation/finding	**Scoring**
Body weight	
No change	0
Reduction > 5 %	1
Reduction > 10 %	2
Reduction > 20 %	3
General condition	
Smooth and shiny fur, clean orifices	0
Dull and ruffled fur, cloudy eyes	1
Dirty or moist orifices, abnormal posture, high muscle tone, dehydration	2
Cramps, lameness, abnormal breathing, animal cold to the touch	3
Spontaneous behaviour	
Normal behaviour – sleep, reaction to touch and gentle blowing, curiosity, social contact	0
Abnormal behaviour, reduced mobility or hyperkinesis	1
Isolation, apathy, expression of pain, pronounced hyperkinesis i.e., repetitive behaviour, coordination disturbance	2
Auto mutilation	3
Body temperature	
36.1 – 37.9 ˚C	0
38.0 – 38.9 ˚C	1
33.0 – 36.0 ˚C	1
30.1 – 32.9	2
>40 ^{0}C	2

<30	3
Evaluation and measures to be taken	**Total points**
No burden	0
Low burden – observe carefully (1x daily), add heat supply, wet food, therapy such as zinc oxide	1
Medium burden – observe carefully (2x daily), add heat supply, wet food, therapy such as zinc oxide. If symptoms worsen during 2nd observation – euthanise animal.	2
High burden – euthanise animal	3

3.3 Generation of chimaeras

Wild-type lab mice (C57BL/6J) are not susceptible to EBOV infection. Ebolaviruses and marburgviruses are able to infect and replicate in murine cells but the type I IFN response mediates protection enabling the mice to survive the infection. One of the parameters that can be used to determine how effective a vaccine is, is survival. It is therefore necessary to use a mouse model which is susceptible to EBOV infection. Wild-type (WT) haematopoietic cells are transferred to irradiated IFNαβ receptor knockout ($IFNAR^{-/-}$) mice. The resultant mice are referred to as WT → $IFNAR^{-/-}$ mice. These chimeric mice were developed in our lab and infection with EBOV results in 50 – 60 % lethality. The model also allows for the evaluation of the resultant immune response, which is crucial for vaccine studies.

3.3.1 Irradiation

6 - 8-week-old $IFNAR^{-/-}$ mice from Jackson Laboratories were irradiated twice at 550 rad 5 h apart using a cesium-137 irradiator. The mice were provided with water and food ad libitum. Enrofloxacin, a fluoroquinolone antibiotic sold under the trade name Baytril by the Bayer Corporation was added to the water for one month after irradiation. It is bactericidal and active against a wide range of both gram positive and negative bacteria.

3.3.2 Bone marrow cell isolation

One day after irradiation, $2x10^6$ cells from donor mice were adoptively transferred via retroorbital injection to the irradiated mice.

2 B6.SJL-*Ptprc*^{a} *Pepc*^{b}/BoyJ (C57BL/6 Ly5.1) were used for every 10 IFNAR$^{-/-}$ mice that were irradiated. Bone marrow cells were obtained as follows: the mice were humanely euthanized using an overdose of isofluorane followed by cervical dislocation and the femurs were obtained. The tissue and muscle were removed with scissors and by rubbing with sterile gauze. The cleaned femurs were placed in ice-cold PBS and transferred to a biosafety II cabinet. The femurs were dipped in 70 % ethanol to remove excess muscle fibres and any lingering contaminants and then dipped in sterile PBS to remove the ethanol. The bones were then placed in 5 ml RPMI-10 contained in another cell culture dish. Both ends of the femurs were cut using scissors. A 30-gauge insulin syringe was used to aspirate 1 ml of the RPMI-10 media and holding the femur with forceps, the bone marrow was flushed out into the cell culture dish. This was done repeatedly until the bones were white. A 70 µM cell strainer was placed on top of a 50 ml conical tube and the bone marrow suspension was passed through it. The cell culture dish and strainer were rinsed twice with RPMI-10 to get all the leftover marrow. Cells were washed by centrifuging for 5 min at 500 g and re-suspended in 10 ml of 1x RBC lysis buffer. RBC lysis was done for 5 min at room temperature with periodic shaking. The reaction was stopped with 30 ml PBS. The cells were spun down twice and the pellet was re-suspended in 1 ml PBS for counting. The cell number was adjusted to $2x10^{6}$ cells/100 µl and the suspension was kept on ice until about 30 min before being injected into the recipient mice. Cell viability was greater than 90 % as determined by a Luna II cell counter for all experiments.

3.3.3 Evaluation of engraftment

Engraftment of the donor cells in the peripheral blood was determined 7 - 8 weeks after transplantation by flow cytometry.

Blood from the tail veins of irradiated and transplanted mice (WT → IFNAR-/-) was collected into 1 ml EDTA tubes to prevent clotting. 500 µl of a 1x RBC lysis buffer solution was added to each sample. 5 min later, the samples were transferred to 2 ml tubes containing 1 ml PBS. The samples were centrifuged for 5 min at 720 g. In the meantime, fixable viability dye was prepared by diluting 1:1000 in PBS. The cell pellet was re-suspended by adding 100 µl of the dye and staining both for the fixable viability dye and other surface markers was done as described in section 3.4.1. Cells were either acquired on an LSR II cytometer or an LSR Fortessa.

Chimeric mice that had a reconstitution of donor haematopoietic cells of more than 85 % were used in subsequent experiments.

3.4 Flow cytometry staining

3.4.1 Surface marker staining

Single cell suspensions were prepared from the spleen, lungs or other organs as indicated. At the final step, the cell suspensions were re-suspended in PBS, transferred to a 2 ml Eppendorf tube and centrifuged at 500 g for 5 min at 4 ˚C on a table top centrifuge.

Fixable viability dyes depend on the reaction of fluorescent reactivity dyes with amines, which are proteins found in cells. The dyes are unable to penetrate live cell membranes and only surface proteins react with the dyes resulting in dim staining. However, when cells are apoptotic or dead, the reactive dyes can penetrate the cell membrane and thus stain both the interior and the exterior amines resulting in a higher intensity of staining. Live cells can be discriminated from dead cells since the fluorescence intensity is typically greater than 50-fold. Additionally, the staining pattern is not lost after fixation with formaldehyde due to the fact that the dye forms covalent bonds with the proteins. Zombie Near-Infrared (Nir) dye was used in all experiments. Zombie Nir was diluted 1:1,000 in PBS and 100 µl was added to each tube containing the pelleted cells. The cells were gently pipetted up and down to ensure that all the cells were re-suspended and thereafter the tubes were vortexed. The cells were incubated at 4 ˚C for 30 min in the dark or at room temperature (22 ˚C) for 20 min in the dark in the BSL-4 lab due to time restrictions. The cells were washed by adding 1 ml PBS and centrifuging at 500 g for 5 min at 4 ˚C. In the meantime, FC block (purified rat anti-mouse CD16/32) was prepared by diluting 1:100 in PBS. Immune cells such as neutrophils, macrophages, Natural Killer cells, monocytes and to a lesser extent, dendritic cells express a variety of Fc receptors on their surface. These cells are able to bind the Fc portion of the flow cytometry staining antibodies, which can lead to increased background or false positive signals. The addition of FC block saturates the receptors thereby lessening or removing the possibility of unwanted antibody binding thereby improving specificity of the staining. 50 µl of Fc block was added to each tube and the cells were re-suspended by pipetting followed by brief vortexing. Incubation was done for a period of 15 min at 4 ˚C followed by an additional wash step as mentioned above. Fluorescent conjugated antibodies that bind to the surface markers were diluted to a previously determined working concentration as detailed in the various panels shown in section 3.4. 50 µl of the antibody master mix was added to the cells. The cells were gently pipetted up and down to re-suspend them and immediately thereafter vortexed to ensure homogenous labelling. The cells were incubated for 25 min at 4 ˚C in the dark. The cells were washed twice with PBS and re-suspended in 300 - 500 µl for acquisition on a flow cytometer.

3.4.2 Intracellular staining

The cells are fixed in suspension before intracellular staining to ensure the stability of soluble antigens or transiently expressed antigens thus retaining the antigens of interest. Cell permeabilization allows the cell membrane to become permeable thus facilitating the passage of large molecules such as antibodies through the plasma membrane to the cell interior.

Intracellular staining was done after surface staining as follows: After washing with PBS, the cell pellet was re-suspended with 100 µl of a 4 % paraformaldehyde solution. The cells were incubated for 30 min at 4 ˚C. 1X permeabilization wash was prepared by diluting the 10x concentrate 1:10 in distilled water. 1 ml of the 1X permeabilization wash was added and the cells were washed twice for 5 min at 500 g, 4 ˚C. The cells were re-suspended in the residual permeabilization wash and a predetermined amount of intracellular fluorophore-conjugated antibodies was added. Incubation was done in the dark for 30 min at room temperature followed by washing twice with PBS. The cells were re-suspended in 200 – 400 µl PBS for acquisition on a flow cytometer.

In cases where fixation and permeabilization was done inside the BSL-4, the cells were incubated with 2 ml 4 % PFA for 45 min. The samples were transferred from the BSL-4 lab to a BSL-2 lab. The samples were centrifuged for 5 min at 500 g to pellet the cells. 1 ml of the 1X perm wash was added to the cells and the cells were incubated for 5 min followed by centrifugation for 5-7 min at 500 g, 4 ˚C. Cells were washed twice with the perm wash. After centrifugation, the cells were then re-suspended in the residual permeabilization wash and a predetermined amount of intracellular fluorophore-conjugated antibodies was added. Incubation was done in the dark for 30 min at room temperature followed by washing twice with PBS. The cells were re-suspended in 200 – 400 µl PBS for acquisition on a flow cytometer.

3.4.3 Tetramer staining

Tetramer staining is used to detect and determine the proportion of antigen-specific T cells after immunization/vaccination or after infection within blood or tissue samples. The interaction between a peptide MHC complex and a cognate T cell receptor is of too low affinity to be easily detected by flow cytometry. Tetramers are made of 4 MHC molecules bound to a specific peptide. This allows the detection of T cells that are able to recognize the peptide bound to the MHC molecules. They mimic the antigen presenting complex on cells. The tetramers are labelled with fluorophores which enables the visualization of antigen-specific T cells through flow cytometry. 4 monomeric peptide MHC are complexed to form a multimer followed by biotinylation of the carboxy-terminus of one chain of the MHC molecule. The

peptide MHC complex is then bound to streptavidin, which has four biotin binding sites. 4 MHC molecules are thereby linked in a complex and this increases the avidity and therefore the efficiency with which antigen specific T cells are detected.

Tetramer staining was done after the addition of the Fc block. After the incubation period cells were washed with PBS for 5 min at 500 g. The PBS was discarded first by decanting followed by gently pipetting out taking special care not to disturb the cell pellet. The cell pellet was re-suspended in 50 µl of PBS supplemented with 5 % FCS. 10 µl of the tetramer was added to each sample and the cells were incubated for 10 min at room temperature in the dark. The antibody master mix was prepared and 50 µl of surface staining antibodies were added to the cells after which they were incubated for an additional 15 min. After the incubation period, the cells were washed with PBS and re-suspended in 300 - 500 µl for acquisition on a flow cytometer.

In cases where tetramer staining was performed in the BSL-4 lab and subsequent intracellular staining was done, the samples were treated as follows: cells were fixed and permeabilized by incubating them with 2 ml of 4 % PFA for 45 min after tetramer and surface staining. The samples were transferred from the BSL-4 lab to a BSL-2 lab and centrifuged for 5 min at 500 g to pellet the cells. 1 ml of 1X perm wash was added to the cells and the cells were incubated for 5 min followed by centrifugation for 5-7 min at 500 g, 4 ˚C. Cells were washed twice with the perm wash. After centrifugation, the cells were re-suspended in the residual perm wash and a predetermined amount of intracellular fluorophore-conjugated antibodies was added. Incubation was done in the dark for 30 min at room temperature followed by washing twice with PBS. The cells were re-suspended in 200 – 400 µl PBS for acquisition on a flow cytometer.

3.4.4 Flow cytometry staining panels

Table 12. Flow cytometry panel used for the identification of target cells

Antigen	Clone	Conjugated fluorophore	Dilution/amount	Company
DEC205	YEKTA	PerCP-eFluor710	1:200	eBioscience
LY51	6C3	FITC	1:200	Biolegend
CD8α	53-6.7	PE-Cy7	1:200	Biolegend
SIRPα	P84	PE-Texas Red	1:100	Biolegend
MHC II	M5/114.15.2	AF700	1:200	
DEC205 (immunization)	YEKTA	APC	5 µg/mouse	Biolegend
CD11c	N418	BV786	1:200	Biolegend
CD64	X54-5/7.1	BV711	1:200	Biolegend

CD24	M1/69	BV605	1:200	Biolegend
CD11b	M1/70	BV510	1:200	
XCR1	ZET	BV421	1:200	Biolegend
CD3ε	145-2C11	BUV395	1:200	Biolegend
CD4	GK1:5	BUV737	1:200	BD Biosciences
Zombie NIR	-		1:1000	Biolegend

Table 13. Flow cytometry panel used to determine the frequency T cells secreting effector cytokines and degranulation

Antigen	Clone	Conjugated fluorophore	Dilution/amount	Company
CD3ε	145-2C11	BUV395	1:200	Biolegend
CD4	GK1.5	BUV737	1:200	BD Biosciences
CD8α	53-6.7	PE-Cy7	1:200	Biolegend
IFNγ	XMG1.2	PE	1:100	eBioscience
CD25	PC61.5	BV711	1:200	BD Biosciences
CD28	37.51	-	2 µg/ml	BD Biosciences
CD44	IM7	BV510	1:200	Biolegend
CD62L	MEL-14	BV785	1:200	Biolegend
CD49	R1-2		2 µg/ml	BD Biosciences
CD69	H1.2F3	BV609	1:200	Biolegend
CD107α	14DB	APC	1:100	Biolegend
NK1.1, B220 (dump)	RA3-6B2	PerCP-Cy5.5	1:200	Biolegend
Zombie NIR	-		1:1000	Biolegend

Table 14. Flow cytometry panel used for the identification of antigen-specific $CD8^+$ T cell

Antigen	Clone	Conjugated fluorophore	Dilution/amount	Company
CD3ε	145-2C11	BUV395	1:200	Biolegend
CD4	GK1.5	BUV737	1:200	BD Biosciences
CD8α	53-6.7	PE-Cy7	1:200	Biolegend
NP tetramer	-	PE	10 µl/test	Immudex
CD25	PC61.5	BV711	1:200	eBioscience
CD44	IM7	BV510	1:200	Biolegend
CD62L	MEL-14	BV785	1:200	Biolegend
CD69	H1.2F3	BV609	1:200	Biolegend

NK1.1, B220 (dump)	RA3-6B2	PerCP-Cy5.5	1:200	Biolegend
Zombie NIR	-		1:1000	Biolegend

Table 15. Flow cytometry panel used to determine the frequency of expanded, effector and memory T cells

Antigen	Clone	Conjugated fluorophore	Dilution/amount	Company
CD3ε	145-2C11	BUV395	1:200	Biolegend
CD4	GK1.5	BUV737	1:200	
CD8α	53-6.7	PE-Cy7	1:200	Biolegend
SIINFEKL tetramer	-	PE	10 µl/test	Immudex
CD25	PC61.5	BV711	1:200	eBioscience
CD44	IM7	BV510	1:200	Biolegend
CD62L	MEL-14	BV785	1:200	Biolegend
CD69	H1.2F3	BV609	1:200	Biolegend
CD103	1AH2	FITC	1:200	Biolegend
CD127	A7R34	BV650	1:200	Biolegend
KLRGI	2F1	APC	1:200	Biolegend
Granzyme B	GB11	Pacific Blue	5 µl/test	Biolegend
NK1.1, B220 (dump)	RA3-6B2	PerCP-Cy5.5	1:200	Biolegend
Zombie NIR	-		1:1000	Biolegend

3.5 DC targeting of bulk splenocytes

3 C57BL/6J mice were immunized subcutaneously with 100 µg of EBOV NP peptide and complete Freund's adjuvant (CFA). 21 days later the mice received a boost with the same peptide and incomplete Freund's adjuvant in a 1:1 (v/v). 14 days later, the mice were sacrificed using an overdose of isofluorane followed by cervical dislocation.

3.5.1 Enrichment of antigen-specific $CD8^+$ T cells and labelling with a cell trace dye

The spleens from the EBOV NP immunized mice or 2 OT-I mice were placed in ice cold PBS and mashed through a 70 µM cell strainer using the back-end of a sterile syringe plunger into a 50 ml falcon tube containing 5 ml PBS. The cell strainers and were rinsed with 10 ml PBS and the cell suspensions were centrifuged for 5 min at 500 g. Erythrocytes were lysed by adding 5 ml of a 1x solution of erythrocyte lysis buffer and incubating for 5 min at room temperature with periodic shaking. The reaction was stopped by adding 25 ml of PBS. The cells were washed once by centrifuging the suspension for 5 min at 500 g. The cell pellets were re-

suspended in 1 ml PBS and cells were counted on a Luna II counter. After an additional wash step, the cells were re-suspended in PBS at a concentration of $1x10^6$ cells in 1 ml. $5x10^6$ cells in total were labelled. Cells were labelled using a CellTrace™ proliferation dye. A 5 mM CellTrace™ Violet stock solution was prepared by adding 20 µl of DMSO to the vial. 5 µl of the stock solution was added to each of the cell suspensions to achieve a final working concentration of 5 µM. The cells were incubated at 37 °C for 30 min protected from light.
Excess dye was washed off by adding > 25 ml RPMI-10 media and centrifuging for 5 min at 500g. Centrifugation was done twice after which the cells were re-suspended in fresh RPMI-10 media at a concentration of $1x10^6$ cells/100µl.
The cells were then seeded in a 96 well round bottom plate and 5 µg of either the isotype control, anti-mDEC205 conjugated to EBOV NP (αmDEC 205 EBOV NP) or anti-mDEC 205 conjugated to OVA (αmDEC205 OVA) were added with or without αCD40 adjuvant. 6 days later, the cells were harvested and FACS staining was done as detailed in section 3.5.1. Measurement was done on the LSR Fortessa.

3.5.2 DC targeting of bone marrow derived dendritic cells

3.5.2.1 Isolation and generation of bone marrow derived dendritic cells

C57BL/6J mice were humanely euthanized as previously described and the femurs were obtained. The tissue and muscle were removed with scissors and by rubbing with sterile gauze. The cleaned femurs were placed in ice-cold PBS and transferred to a biosafety II cabinet. The femurs were dipped in 70 % ethanol to remove excess muscle fibres and any lingering contaminants and then dipped in sterile PBS to remove the ethanol. The bones were then placed in 5 ml RPMI-10 contained in another cell culture dish. Both ends of the femurs were cut using scissors. A 30-gauge insulin syringe was used to aspirate 1 ml of the RPMI-10 media and holding the femur with forceps, the bone marrow was flushed out into the cell culture dish. This was done repeatedly until the bones were white. A 70 µM cell strainer was placed on top of a 50 ml conical tube and the bone marrow suspension was passed through it. The cell culture dish and strainer were rinsed twice with RPMI-10 to get all the leftover marrow. Cells were washed by centrifuging for 5 min at 500 g and re-suspended in 10 ml of 1x RBC lysis buffer. RBC lysis was done for 5 min at room temperature with periodic shaking. Cells were spun down twice and the pellet was re-suspended in 1 ml RPMI-10. The cell number was adjusted to $1x10^6$ cells per ml and 1 ml of cells were seeded in each well of a 6-well plate. 50 ng/ml of granulocyte-monocyte colony stimulating factor (GM-CSF) was added to the cells and the plate

was placed in the incubator (37 ˚C, 5 % CO_2). 3 days later, 2 ml of RPMI-10 media containing 50 ng/ml GM-CSF was added to the existing culture. 6 days later the bone marrow derived DCs were harvested, washed and the cell number was adjusted to $5x10^5$ cells per 100 µl.

3.5.2.2 Magnetic isolation and labelling of $CD8^+$ T cells

The spleens from the immunized mice and OT-I mice were processed as described in section 3.3.1. After counting, cells were re-suspended in MACS buffer (PBS, 2 mM EDTA, 0.5 % BSA) and magnetic labelling and separation was done using the $CD8^+$ T cell isolation kit (Miltenyi) as described in the manufacturer's protocol. The cell suspension consisting of negatively isolated or "untouched" $CD8^+$ T cells was centrifuged once at 500 g for 5 min. The cell pellet was re-suspended in PBS at a concentration of $1x10^6$ cells in 1 ml and CellTrace™ Violet labelling was done as previously described. After labelling and washing the cells were re-suspended in RPMI-10 at a concentration of $1x10^6$ cells per 100 µl. $2x10^5$ labelled $CD8^+$ T cells were co-cultured with bone marrow derived dendritic cells.

3.6 Assessment of cross-presentation *in vivo*

2 C57BL/6J Ly5.1 (B6.SJL-*Ptprc*^{a}*Pepc*^{b}/BoyCrl) donor mice were subcutaneously immunized with 100 µg of EBOV NP peptide – YQVNNLEEI together with complete Freund's adjuvant. This is a congenic mouse strain that has a different pan leukocyte marker from wild-type C57BL/6J inbred strains. They are routinely used in immunological research for adoptive transfers.

28 days later, the Ly5.1 donor mice were subcutaneously immunized with 100 µg of the EBOV NP peptide together with incomplete Freund's adjuvant. After 14 days the spleens were harvested and processed as described in previous sections.

3.6.1 Enrichment of antigen-specific $CD8^+$ T cells and labelling with a cell trace dye

$CD8^+$ T cells were isolated from the splenocytes of the immunized mice and labelled with CellTrace™ Violet. Cells were re-suspended in sterile PBS at a concentration of $5x10^6$ cells/100µl.

$CD8^+$ T cells were also isolated from the spleens of OT-I mice, processed and labelled with CellTrace™ Violet.

3.6.2 Adoptive transfer and assessment of antigen specific CD8$^+$ T proliferation

2 C57BL/6J Ly5.2 recipient mice were used per group with 6 groups in total – isotype control group, αmDEC205 EBOV NP group and αmDEC205 OVA group with or without 25 µg αCD40 adjuvant. The isolated and CellTrace^{TM} Violet CD8$^+$ T cells were transferred to the recipient mice via retroorbital injection. Approximately 24 h later, the mice were subcutaneously immunized with either the isotype control antibody or the targeting antibodies with or without αCD40. 4 days later, the recipient mice were sacrificed and the spleens obtained and processed. FACS staining was done as described in section 3.4.1.

3.7 *ex vivo* DC targeting

3.7.1 Identifying target cells

WT → IFNAR$^{-/-}$ mice were intraperitoneally immunized with 10 µg of an antimDEC205 antibody conjugated to APC. 30 min later, the mice were humanely euthanized using an overdose of isoflurane followed by cervical dislocation. The following organs were harvested: thymus, spleen, liver, lungs and brachial, mesenteric and mediastinal lymph nodes. The organs were placed in sterile PBS and kept on ice or at 4 ˚C until further processing.

All the harvested organs except the lymph nodes were enzymatically digested by placing them in 2 ml of RPMI media containing 2 % FBS 2 mg/ml collagenase and 50 µg/ml DNase I. The organs were cut into small pieces and incubated for 30 min at 37 ˚C while shaking at 400 rpm on a thermal block. The enzymatic process was stopped by adding RPMI media containing 10 % FCS, 1 % penicillin/streptomycin and 1 % L-Glutamine. The cell suspension was passed through a 70 µM cell strainer and cells were pelleted by centrifugation at 500 g for 5 min. Erythrocytes were lysed by adding 5 ml of a 1x solution of erythrocyte lysis buffer and incubated for 5 min at room temperature with periodic shaking. The reaction was stopped by adding 25 ml of PBS. The cells were washed twice with PBS by centrifuging the suspension for 5 min at 500 g. FACS staining was performed as detailed in section 3.3.1.

3.7.2 Assessment of the T cell response after targeting

C57BL/6J mice were intraperitoneally immunized with either 10 µg of an isotype control, αmDEC 205 EBOV NP or αmDEC 205 OVA with or without 50 µg poly IC and 25 µg αCD40. 14 or 28 days later, the mice were humanely sacrificed using an overdose of isoflurane followed by cervical dislocation. The spleens were obtained and mashed through a 70 µM cell strainer into a 50 ml falcon tube containing 5 ml PBS. The cell strainers were rinsed with 10 ml PBS and the cell suspensions were centrifuged for 5 min at 500 g. Erythrocytes were lysed by adding

5 ml of a 1x solution of erythrocyte lysis buffer and incubating for 5 min at room temperature with periodic shaking. The reaction was stopped by adding 25 ml of PBS. The cells were washed once by centrifuging the suspension for 5 min at 500 g. The cell pellets were re-suspended in 1 ml RPMI -10 media and cells were counted on a Luna II cell counter. After an additional wash step with RPMI -10 media, the cells were re-suspended at a concentration of $1x10^6$ cells/100 µl.

3.7.3 Peptide re-stimulation of T cells

To determine the functionality of antigen specific T cells, $1x10^6$ cells per well were seeded in a 96 well round bottom plate and a master mix containing 5 µg/ml of EBOV NP peptide (YQVNNLEEI) or OVA peptide (SIINFEKL), 2 µg/ml αCD28 and 2 µg/ml αCD49d was added. CD107a is transiently expressed on the surface following activation and the staining antibody was therefore added at the beginning. PMA was used as a positive control. 1 h later, 1 µl/ml of Golgiplug™ was added. Golgiplug™ contains brefeldin A which is a protein transport inhibitor. Cytokines produced by T cells are detectable due to their accumulation in the Golgi complex after incubation with brefeldin A.

The plate was placed at 37 ˚C, 5 % CO_2 and the cells were stimulated for 6 h. The plate was thereafter wrapped in parafilm and aluminium foil and put in the refrigerator at 4 ˚C overnight. FACS staining was done the next day as detailed in section 3.3.2.

3.7.4. Tetramer staining of antigen-specific T cells

3 WT → $IFNAR^{-/-}$ mice per group were immunized intraperitoneally with 10 µg of the isotype control antibodies, αmDEC205 EBOV NP or αmDEC205 OVA antibodies. Some mice received 25 µg αCD40 and 50µg Poly IC. 14 or 28 days later, the mice were humanely sacrificed and the splenocytes obtained. A fraction of the cells was re- stimulated with EBOV NP peptide 1 (YQVNNLEEI) and peptide 2 (LSFASLFLPKLVVGE) or OVA SIINFEKL peptide. The rest of the cells were stained for various surface markers to determine the activation status as well as to determine the proportion of antigen specific (EBOV NP) T cells by tetramer staining.

3.8 DC targeting *in vivo*

3 WT → $IFNAR^{-/-}$ mice per group were immunized intraperitoneally with 10 µg of the isotype control antibodies, αmDEC205 EBOV NP or αmDEC205 OVA antibodies with or without adjuvant (25 µg αCD40 and 50µg Poly IC). 14 or 28 days later, the mice were humanely

euthanized and the splenocytes were processed as described in previous sections. IFNγ secretion by the cells was determined using an enzyme-linked immunosorbent (ELISpot) assay.

3.8.1 Determining T cell functionality

The ELISpot is an assay that enables the detection of cytokines or other secreted products from a single responding cell. The type of cytokine as well as the number of cells producing the cytokine can be determined. It is a very sensitive assay and enables the analysis of rare cell populations such as antigen-specific T cells.

To order to determine the functionality of T cells from immunized mice, an ELISpot assay was performed.

96-well ELISpot plates were briefly activated (approximately 45 seconds) with 15 µl/well 35 % ethanol. The plates were washed by adding 200 µl PBS followed by inverting and flicking the plate to remove the PBS. This was done three times. The capture antibody (anti-mouse IFNγ) was diluted in PBS to achieve a final working concentration of 5 µg/ml and added to the wells. The plate with the capture antibody was stored in the fridge overnight. The next day, the wells were washed with 200 µl PBS and blocked with 200 µl of a 1 % BSA PBS solution for 1 h 30 min. During the blocking period, the peptides were prepared by diluting them to the appropriate working concentration in RPMI-10. The blocking solution was discarded and the plate was washed once with 200 µl PBS. The peptides were added to the appropriate wells at a concentration of 10 µg/well in 100 µl RPMI-10.

Freshly isolated splenocytes from immunized mice were prepared and re-suspended at a concentration of $5x10^5$ cells in 100 µl. 100 µl of each cell suspension was added to the wells containing the peptides. The plate was placed in the incubator at 37 °C, 5 % CO_2.

25 h later, the cell suspension was aspirated, and the wells were washed 5 times with 200 µl PBS. The detection antibody was diluted in 0.1 % BSA in PBS to achieve a final working concentration of 1 µg/ml. 50 µl of the detection antibody (anti-IFNγ-Biotin) was added to each of the assay wells and incubated for 2 h at room temperature.

The detection antibody was discarded after the incubation period and the wells were washed 5 times with PBS. Streptavidin-Horse radish peroxidase (HRP) is an enzyme that is used for the detection of biotinylated antibodies. It binds to biotin with high affinity and acts on soluble substrates such as 2,2'-azino-bis (3-ethylbenzothiazoline-6-sulfonic acid (ABTS) or Tetramethylbenzidine (TMB) resulting in a colorimetric reaction.

Streptavidin - HRP was diluted in PBS (1:400) and 50 µl was added to the wells and the plate was incubated for 45 min at room temperature. The plate was then washed 5 times with PBS

and 100 µl of AEC substrate mix (20 µl of AEC chromogen in 1 ml of AEC substrate) was added per assay well. Spot development was monitored and once the spots were clearly visible by the naked eye, the reaction was stopped by the addition of distilled water. The plate was air-dried overnight in the dark. Spots were enumerated using an AID ELISpot reader.
In some experiments only αCD40 was used as an adjuvant. Some of the cell suspension was also set aside for tetramer staining.

3.9. *In vivo* DC targeting with and without adjuvant

To evaluate the prophylactic potential of the targeting antibodies, 2-4 WT → IFNAR$^{-/-}$ mice/group were immunized intraperitoneally with 10 µg of either the isotype control antibody or αmDEC 205 EBOV NP with or without adjuvant (50 µg Poly IC and 25 µg αCD40). Only 2 mice were immunized with the isotype control and the adjuvant. the rest of the groups had 4 mice. 28 days later, the mice received a boost with 10 µg of the antibodies and the adjuvant. 14 days later, the mice were intranasally infected with 10,000 FFU of EBOV Mayinga in 20 µl PBS. The mice were transferred to the BSL-4 lab 5-7 days before infection and were monitored for a total of 21 days after infection. The mice were housed in individually ventilated cages (IVC) in a regulated environment (23 ˚C ± 2 ˚C, 50 % relative humidity and under a light dark cycle of 12 h) and were fed and watered ad libitum. They were provided with enough bedding and nesting material, boxes and tubes (paper rolls) to enrich their environment. In order to determine viral titres in the blood, about 30 µl of blood was obtained from the tail vein every 3 days at day 3, 6, 9, 11, 15 and 18. Blood was collected by making an oblique incision into the tail vein and letting the drops fall into tubes treated with anti-coagulants such as ethylene diamine tetraacetic acid (EDTA) or lithium heparin to prevent coagulation. Bleeding was stopped by compressing the wound with cellulose swabs. Shortly after collection, the blood was diluted 1:50 in DMEM and stored in a -80 ˚C freezer for later processing. About 10 µl of the blood was pipetted into tubes containing separating gel to obtain serum. Serum was used to determine aspartate aminotransferase (AST) levels. Mice were humanely sacrificed when they reached the previously determined criteria for euthanasia based on the scoresheet. At day 21, the surviving mice were surgically anesthetised using isoflurane and blood was collected by cardiac puncture. The mice were immediately sacrificed by cervical dislocation after the cardiac puncture. 500 µl -1 ml of blood was collected at endpoint. The spleen, liver, lungs and kidney were also collected at endpoint in order to determine viral titres in the organs.

3.9.1 Titration of virus in the organs

Infectious virus particles in the organs of infected mice were determined by an immunofocus assay. Also known as a focus forming assay, it is an immunostaining technique in which infectious virus particles are detected before plaques are formed or in cases where plaques are not formed.

Organ samples were weighed and placed in tubes containing 1 ml DMEM supplemented with 2 % FBS and containing 1.4 mm ceramic spheres lysing matrix D (MP Bio). The organs were mechanically homogenized using the FastPrep^{TM} bead beating system using a FastPrep-24 5G instrument. Samples were stored in the -80^{0}C freezer until further processing.

One day before organ titration, Vero E6 cells were seeded at a concentration of 1.5x10^5/well or 3.6x10^6 /plate to achieve 95-100 % confluence after 18-24 h. On the day of titration, the cells were transferred to the BSL 4 lab. Serial 10-fold dilutions of the organ samples were prepared and added to the cells in the 24-well plate to facilitate adsorption. The plates were placed in the incubator at 37 ˚C and 5 % humidity for 1 h. After the time had lapsed, the inoculums were discarded and the overlay media containing DMEM supplemented with 10 % FBS and methyl cellulose was added. The cells were incubated for 7 days at 37 ˚C and 5 % humidity. On day 7, the cells were inactivated using 4 % paraformaldehyde (PFA) for 1 h and taken out of the BSL-4 laboratory. The plates were washed 5 times with water to remove residual PFA and briefly dried on an absorbent mat. Permeabilization was done with 400 µl 0.5 % Triton X-100 in PBS followed by blocking with 200 µl 5 % FCS in PBS for 1 h after washing with water. The plates were washed with water 3 times after the blocking step after which 200 µl of anti-EBOV polyclonal antibody (1:5,000 in PBS) was added to each well. The cells were incubated overnight at 4 ˚C. Plates were washed with water and 200 µl (1:5,000) of the secondary antibody - peroxidase conjugated sheep anti-mouse H+L was added. Incubation was done for 1 h at room temperature in the dark. The plates were washed once more and focus forming units (FFUs) were revealed by the addition of 200 µl of tetramethylbenzidine (TMB) substrate.

3.9.2 Titration of virus in the blood

Blood samples collected on different days as previously described were serially diluted. The samples were added to Vero E6 cells at 100 % confluence prepared one day prior to virus titration. The cells were incubated with the inoculum for 1 h at 37 ˚C and 5 % humidity. The inoculum was discarded, and the overlay media was added to the wells. The cells were incubated for 7 days at 37 ˚C and 5 % humidity after which they were inactivated using 4 %

paraformaldehyde (PFA) for 1 h and taken out of the BSL-4 laboratory. Immunostaining was performed as described in section 3.9.1.

3.9.3 Assessment of clinical parameters

Aspartate transaminase or aspartate aminotransferase (AST) is an enzyme that is released when there is liver damage. Liver damage occurs after infection with Ebola virus.

ASTs levels in the serum were determined using a FUJI DRI-CHEM analyser. The serum samples were diluted 1:10 in 0.9 % sodium chloride. Fuji Dri-Chem GOT/AST P-III slides were warmed up to room temperature prior to starting. 10 µl each sample was added to a slide which was set on the analyser. The sample ID was input and the AST levels in the mouse sera were measured.

3.9.4 *In vivo* DC targeting with Poly IC and αCD40 adjuvant

In other experiments, the prophylactic potential of DEC205 antibodies were evaluated only in the presence of the adjuvant. 14 mice per group were immunized with 10 µg of either the isotype control antibody or αmDEC 205 EBOV NP with 50 µg Poly IC and 25 µg αCD40. 28 days later, the mice received a boost with 10 µg of the antibodies and the adjuvant. 14 days later, the mice were infected intranasally with 10000 FFU of EBOV strain Makona in 20 µl PBS. The mice were transferred to the BSL-4 lab 5-7 days before infection and were monitored for a total of 21 days after infection. Serial sacrifices of 3 mice per group were done at day 3 and day 7 post infection. The spleen, liver, lungs and kidneys were collected and stored in the -80 ˚C freezer to assess viral titres in the organs. Blood was collected from the lateral tail veins at 3-day intervals in tubes containing lithium-heparin. Shortly after collection, the blood was diluted 1:50 and stored in a -80 ˚C freezer for later processing. The rest of the blood collected in the lithium-heparin tubes was centrifuged at 10,000 g for 2 min in order to obtain serum for the assessment of AST levels. Mice were humanely sacrificed when they reached the previously determined criteria for euthanasia based on the scoresheet. At day 21, the surviving mice were surgically anesthetised using isoflurane and blood was collected by cardiac puncture. The mice were immediately sacrificed by cervical dislocation after the cardiac puncture. 500 µl - 1 ml of blood was collected at endpoint. The spleen, liver, lungs and kidney were also collected at endpoint in order to determine viral titres in the organs.

3.9.5 DC targeting with αCD40 adjuvant

In order to determine the prophylactic potential of the targeting antibodies and whether αCD40 adjuvant alone was enough to rescue mice from lethal EBOV challenge, mice were immunized with either 10 µg of the isotype control or αmDEC205 EBOV NP together with 25 µg of αCD40. The immunization regimen was the same as described in section 3.9.4. Mice were infected intranasally with 10,000 FFU in 20 µl PBS of EBOV Mayinga. The mice were monitored for a period of 21 days and were humanely sacrificed in cases where the criteria for euthanasia were reached before the end of the experiment. Blood was collected from the lateral tail veins at 3-day intervals in tubes containing lithium-heparin. Shortly after collection, the blood was diluted 1:50 and stored in a -80 ˚C freezer for later processing. The rest of the blood collected in the lithium-heparin tubes was centrifuged at 10,000 g for 2 min in order to obtain serum for AST level assessment. At day 21, the surviving mice were surgically anesthetised using isoflurane and blood was collected by cardiac puncture. The mice were immediately sacrificed by cervical dislocation after the cardiac puncture. 500 µl - 1 ml of blood was collected at endpoint. The spleen, liver, lungs and kidney were also collected for the determination of viral titres in the organs.

3.9.5.1. Detection of IgG antibodies after infection

A 96-well NUNC Maxisorp microplate was coated overnight at 4 ˚C with 1 µg/ml EBOV NP peptide in PBS. A solution of 5 % skim milk in PBS was used for blocking. Blocking was done for 1 h at 37 ˚C. In the meantime, dilutions of mouse sera were prepared by diluting them 1:100 in 2.5 % skim milk in PBST. After blocking, the wells were washed once with 0.05 % tween-20 in PBS (PBST). The serum samples were then added to the wells. The plate was incubated for 1 h at 37 ˚C. The wells were washed 3 times with 200 µl/well PBST after which the secondary antibody – HRP conjugated goat anti-mouse IgG H+L diluted 1:10,000 in 2.5 % skim milk-PBST buffer was added to the wells. The samples were incubated at 37 ˚C for 1 h. After the incubation period, wells were washed thrice with 200 µl/well PBST by repeatedly filling and dumping and flicking the solution into a receptacle. A 1X solution of the substrate was prepared by mixing 1 ml of the hydrogen peroxide solution with 9 ml of the TMB solution. 100 µl was added to each well and the plate was incubated for 10 min at room temperature. The reaction was stopped by the addition of 100 µl of 1M sulphuric acid to each well. The OD was measured at a wavelength of 450 nm and 620 nm was used as a reference wavelength.

3.9.6 Generation of OVA-expressing EBOV

For cloning of the full-length EBOV genome plasmid, the OVA gene was inserted as an additional transcriptional unit after the NP gene duplicating the NP/VP35 non-coding region within the cassette vector pKan_rgZ1.2-DrdI-NruI-iORF (Groseth et al., 2012). Subcloning of this gene cassette into the full-length genome plasmid pAmp-rgZ-dSXBS was done via restriction enzymes *Drd*I and *Nru*I using standard cloning methods.

3.9.6.1 Virus rescue and stock production

The full-length cloning plasmid is based on Zaire ebolavirus rec/COD/1976/Mayinga-rgEBOV (GenBank accession number KF827427.1, rgEBOV) (Shabman et al., 2013). Rescue of rgEBOV-iOva was done as previously described by Hoenen and Feldmann, 2017. In brief, Huh7 cells seeded in a 6-well plate at a confluency of 50 % were transfected with expression plasmids for the EBOV proteins NP (125 ng/well), VP35 (125 ng/well), VP30 (75 ng/well), and L (1,000 ng/well), as well as expression plasmids for T7-polymerase (250 ng/well) and the full-length genome plasmid (250 ng/µ). Medium was exchanged 24 h post transfection against 4 ml per well of DMEM supplemented with 5 % fetal calf serum, 100 U/ml penicillin, 100 µg/ml Streptomycin and 1x GlutaMAX. After one week 500 µl supernatant was used to infect Vero E6 cells seeded in a 6-well plate at 90 % confluency. Cells were checked for cytopathic effect 13 days after passaging of the supernatant. One virus clone was then amplified on Vero E6 cells and its sequence confirmed via Sanger sequencing. Virus titers were determined by 50 % tissue culture infectious dose ($TCID_{50}$) assay. The rescue of infectious virus was performed under BSL-4 conditions at the Friedrich-Loeffler-Institut (Federal Research Institute of Animal Health, Greifswald Insel-Riems, Greifswald, Germany) following approved standard operating procedures.

3.9.6.2 Multicycle replication

To determine whether the recombinant virus replicates well, multicycle replication kinetics were performed. $1x10^5$ Vero E6 were seeded in each well of a 24- well plate in order to achieve 70 % confluence after 18-20 h. The next day, the plates were transferred to the BSL-4 lab. The media (5 % DMEM) was discarded, and PBS was added to rinse the wells. The cells were infected at an MOI of 1 or 0.1 with the wild-type virus, EBOV OVA or EBOV GFP, another recombinant virus. 1 h later the inoculums were removed, and 1 ml media supplemented with 2.5 % DMEM was added to each well. The plates were placed in the incubator at 37 °C and 5

% humidity. 1 ml supernatant (for each duplicate) was collected from each well every day for a period of 7 days and stored in the -80 ˚C freezer to determine the kinetics of replication.

3.9.6.3 Viral titration

Vero E6 cells were seeded at a concentration of $1.5x10^5$/well or $3.6x10^6$ /plate to achieve 95-100 % confluence after 18-24 h. The next day, the cells were transferred to the BSL 4 lab. Seral 10-fold dilutions of the supernatant of infected cells were prepared and added to the cells in the 24-well plate to facilitate adsorption. The plates were stored in the incubator at 37 ˚C and 5 % humidity for 1 h. After the time had lapsed, the inoculums were discarded and DMEM supplemented with 5 % FBS and methyl cellulose (overlay media) was added. The cells were incubated for 7 days at 37 ˚C and 5 % humidity. On day 7, the cells were inactivated using 4 % paraformaldehyde (PFA) for 1 h and taken out of the BSL-4 laboratory. The plates were washed with 5 times with water to remove residual PFA and briefly dried on an absorbent mat. Permeabilization was done with 400 µl 0.5 % Triton X-100 in PBS followed by blocking with 200 µl 5 % FCS in PBS for 1 h after washing with water. The plates were washed with water 3 times after the blocking step after which 200 µl of anti-EBOV polyclonal antibody (1:5,000 in PBS) was added to each well. The cells were incubated overnight at 4 ˚C. Plates were washed with water and 200 µl (1:5,000) of the secondary antibody - peroxidase conjugated sheep anti-mouse H+L was added. Incubation was done for 1 h at room temperature in the dark. The plates were washed once more and focus forming units (FFUs) were revealed by the addition of 200 µl of tetramethylbenzidine (TMB) substrate.

3.9.7 *In vivo* DC targeting with αmDEC OVA and EBOV OVA

To enable the assessment of the T cell response after antibody mediated delivery of antigens to DCs, 13-14 mice per group were immunized with 10 µg of the isotype control antibody or αmDEC 205 OVA and 25 µg αCD40 adjuvant. 28 days later, the mice were boosted with 10 µg of the antibodies and 25µg αCD40. After 14 days, the mice were infected with 10,000 FFU in 20 µl PBS of EBOV OVA. Serial sacrifices of 2-3 mice per group were done at day 3 and day 7 post infection. The mice were euthanized using an overdose of isoflurane and cervical dislocation after which blood was collected from the inferior vena cava. The spleens and lungs were obtained and cut into 2 pieces. One piece each of the lungs and the spleen were placed in separate 2 ml Eppendorf tubes containing ice cold PBS for further processing for FACS analyses while the other pieces together with the liver and kidneys were placed in 2 ml Eppendorf tubes and stored in the -80 ˚C freezer for the assessment viral titres in the organs at

a later point. Blood was collected from the lateral tail veins into tubes containing lithium-heparin at 3-day intervals. Shortly after collection, the blood was diluted 1:50 and stored in a -80^0C freezer for later processing. The rest of the blood collected in the lithium-heparin tubes was centrifuged at 10,000 g for 2 min and stored at -80 °C in order to obtain serum for the assessment of AST levels. Mice were humanely sacrificed when they reached the previously determined criteria for euthanasia based on the scoresheet. At endpoint, the spleen, liver, lungs and kidney were collected for the determination of viral titres in the organs.

3.9.7.1 Processing of spleen and lungs

The PBS from the tubes containing the lung samples was discarded and 1 ml RPMI media supplemented with 2 % FBS, 2 mg/ml collagenase D and 50 µg/ml DNase I was added. The lungs were cut up into small pieces and an additional 1 ml of RPMI containing collagenase and DNase I was added. The lung samples were placed in a thermal block and incubated for 30 min at 37 °C while shaking at 400 rpm. The enzymatic process was stopped by adding RPMI-10. The lung pieces were mashed through a 70 µM cell strainer using the back-end of a sterile syringe plunger into a 50 ml falcon tube containing 5 ml PBS. The cell strainers were rinsed with 10 ml PBS and the cell suspensions were centrifuged for 5 min at 500 g. Erythrocytes were lysed by adding 5 ml of a 1x solution of erythrocyte lysis buffer and incubating for 5 min at room temperature with periodic shaking. The reaction was stopped by adding 25 ml of PBS. The cells were washed once by centrifuging the suspension for 5 min at 500 g. The cell pellets were re-suspended in 1 ml PBS and a half of this suspension was transferred to a different 2 ml tube, spun down and surface marker and tetramer staining was done as described in sections 3.4.1 and 3.4.3. The rest of the cells were spun down and re-suspended in 10 % DMSO in FBS. The spleens from the immunized and infected mice were mashed through a 70 µM cell strainer using the back-end of a sterile syringe plunger into a 50 ml falcon tube containing 5 ml PBS. The cell strainers were rinsed with 10 ml PBS and the cell suspensions were centrifuged for 5 min at 500 g. Erythrocytes were lysed by adding 5 ml of a 1x solution of erythrocyte lysis buffer and incubating for 5 min at room temperature with periodic shaking. The reaction was stopped by adding 25 ml of PBS. The cells were washed once by centrifuging the suspension for 5 min at 500 g. The cell pellets were re-suspended in 1 ml PBS and a half of this suspension was transferred to a different 2 ml tube, spun down and surface marker and tetramer staining was done as described in section 3.4.3. The rest of the cells were spun down and re-suspended in 10 % DMSO in FBS. These cells were placed in a Mr. Frosty and stored in the -80 °C freezer. 1 day later, the cells were transferred from the Mr. Frosty to another rack in the freezer.

After the tetramer staining, the samples, the samples were washed with PBS and centrifuged for 5 min at 500 g. The samples were re-suspended in 2 ml 4 % PFA and incubated for 45 min in the BSL-4 lab. The samples were then taken out of the BSL-4 lab, spun down and re-suspended in 1 ml permeabilization wash (BD Biosciences). The samples were incubated with the permeabilization wash for 5 min at room temperature and centrifuged for 10 min at 500 g. The cells were washed again with the permeabilization wash after which intracellular staining was done as described in section 3.4.2.
Cells were acquired on a Cytek Aurora cytometer.

3.10. Evaluation of the cross-protective capacity of αmDEC 205 EBOV NP

To evaluate whether the targeting antibodies could confer cross-protection, DC targeting was performed as described in previous sections. Briefly, 8 mice per group were immunized with 10 µg of the isotype control or αmDEC 205 EBOV NP together with 25 µg of αCD40. The immunization regimen was the same as described in section 3.9.4. Mice were infected intranasally with 10,000 FFU in 20 µl PBS of SUDV Gulu strain or MARV Musoke.

3.10.1. DC targeting *Ebolavirus spp.*

After the immunization regimen, mice were infected with 10,000 FFU in 20 µl PBS of SUDV Gulu strain. The mice monitored for a period of 21 days and were humanely sacrificed in cases where the criteria for euthanasia were reached before the end of the experiment. Blood was collected from the lateral tail veins at 3-day intervals in tubes containing lithium-heparin. Shortly after collection, the blood was diluted 1:50 and stored in a -80 °C freezer for later processing. The rest of the blood collected in the lithium-heparin tubes was centrifuged at 10,000 g for 2 min in order to obtain serum for AST level assessment. At day 21 after infection, surviving mice were euthanized using an overdose of isoflurane and cervical dislocation after which blood was collected from the inferior vena cava. The spleen, liver, lungs and kidney were also collected at endpoint in order to determine viral titres in the organs.

3.11 Determination of FFU units for infection

To determine the amount of focus forming units required to induce 100 % lethality, 4-6 IFNAR$^{-/-}$ mice were intranasally infected with either 1000 or 10000 FFUs in 20 µl PBS of MARV Leiden strain or MARV Musoke strain. 5 mice were mock infected with 20 µl PBS. The mice were monitored for up to 20 days and were humanely sacrificed in cases where the criteria for euthanasia were reached before the end of the experiment. Blood was collected from the lateral

tail veins at 3-day intervals in tubes containing lithium-heparin. Shortly after collection, the blood was diluted 1:50 and stored in a -80 °C freezer for later processing. The rest of the blood collected in the lithium-heparin tubes was centrifuged at 10,000 g for 2 min in order to obtain serum for AST level assessment. At day 21 after infection, surviving mice were euthanized using an overdose of isoflurane and cervical dislocation after which blood was collected from the inferior vena cava. The spleen, liver, lungs and kidney were collected at endpoint in order to determine viral titres in the organs.

3.11.1 Determination of the best route of infection

To determine the best route of infection, 4 IFNAR$^{-/-}$ mice per group were infected with 10,000 FFUs of MARV Leiden or Musoke using different routes. Infections were done in a total volume of 100 µl in PBS. In the case of MARV Musoke, mice were infected with only 10,000 FFUs. 4 mice were mock infected with 100 µl PBS. The mice were monitored for up to 20 days and were humanely sacrificed in cases where the criteria for euthanasia were reached before the end of the experiment. Blood was collected from the lateral tail veins at 3-day intervals in tubes containing lithium-heparin. Shortly after collection, the blood was diluted 1:50 and stored in a -80 °C freezer for later processing. The rest of the blood collected in the lithium-heparin tubes was centrifuged at 10,000 g for 2 min in order to obtain serum for AST level assessment. At day 21 after infection, surviving mice were euthanized using an overdose of isoflurane and cervical dislocation after which blood was collected from the inferior vena cava. The spleen, liver, lungs and kidney were collected at endpoint in order to determine viral titres in the organs.

3.11.3 DC targeting

To determine the ability of the targeting antibodies to confer protection to MARV, WT → IFNAR$^{-/-}$ mice were immunized with 10 µg of the isotype control or αmDEC 205 EBOV NP together with 25 µg of αCD40. The immunization regimen was the same as described in section 4.1. Mice were infected intraperitoneally with 10,000 FFU MARV Musoke. The mice were monitored for a period of 21 days and were humanely sacrificed in cases where the criteria for euthanasia were reached before the end of the experiment. Blood and organs were collected and processed as described in previous sections. After 21 days, surviving mice were humanely euthanized using an overdose of isoflurane and cervical dislocation after which blood was collected from the inferior vena cava.

3.12 Statistical analysis

Where applicable, statistical analysis of data was done using GraphPad Prism software. Differences in cytokine secretion, frequency of expanded responder $CD8^+$ T cells, and frequency of effector memory T cells as well as differences in viral titres in the organs and blood were determined using non-parametric tests namely student's t-test. Differences in antibody titres were analysed using non-parametric Mann-Whitney U test. The Kruskall-Wallis test with Dunn's multiple comparison test was used for group analyses where the number of groups was greater than 2. The levels of significance are represented as follows: ns (not significant) when $p > 0.05$, *$p \leq 0.05$, **$p \leq 0.01$, ***$p \leq 0.001$, ****$p \leq 0.0001$.

4. Results

4.1 Antibody-mediated delivery of EBOV NP results in the proliferation of NP-specific T cells

The induction of antigen-specific $CD8^+$ T cells after EBOV infection has been associated with survival (McElroy et al., 2015; Ruibal et al., 2016). Considering that the EBOV NP is the main driver of the host T-cell response (McElroy et al., 2015), the effect of antibody-mediated delivery of NP antigen to $DEC205^+$ DCs and whether this would result in the generation of functional antigen-specific T cells was determined.

First, the effect of DEC-205 targeting *in vitro* was tested. A source of NP-specific CD8 T cells was needed and to this end, C57BL6/J were subcutaneously immunized with 100 µg of an EBOV NP peptide (YQVNNLEEI) together with complete Freund's adjuvant (CFA). CFA contains inactivated mycobacteria, which attracts APCs such as macrophages to the site of injection to enhance the immune response. Incomplete Freund's adjuvant, which does not contain mycobacteria was used for the boost to minimize the side effects associated with CFA. To test the feasibility of antibody-mediated delivery of EBOV NP and whether targeting of $DEC205^+$ DCs would result in the proliferation of $CD8^+$ T cells, $CD8^+$ T cells from mice immunized with the EBOV NP peptide were labelled with CellTrace Violet™ (CTV) proliferation dye to enable the tracking of proliferation and co-cultured with bone marrow derived DCs (BM-DCs) obtained from naïve mice.

EBOV NP-specific $CD8^+$ T cells proliferated *in vitro* after being co-cultured with BM-DCs and αmDEC205 EBOV NP in the presence of αCD40 adjuvant (figure 10 C) but not when the isotype control antibody was added (figure 10 B).

A

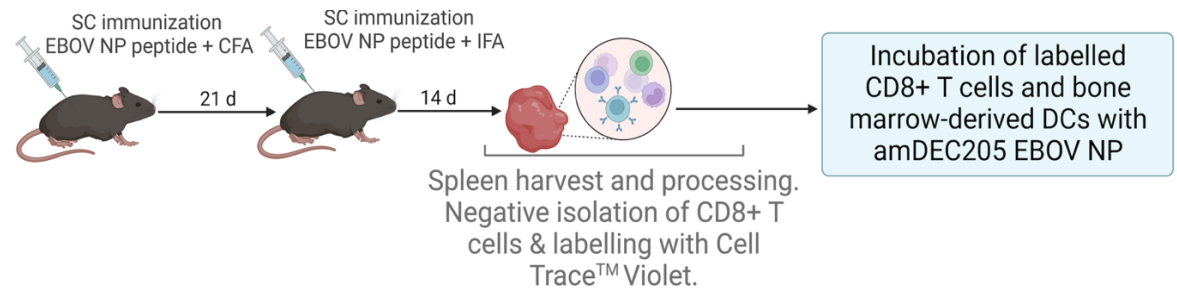

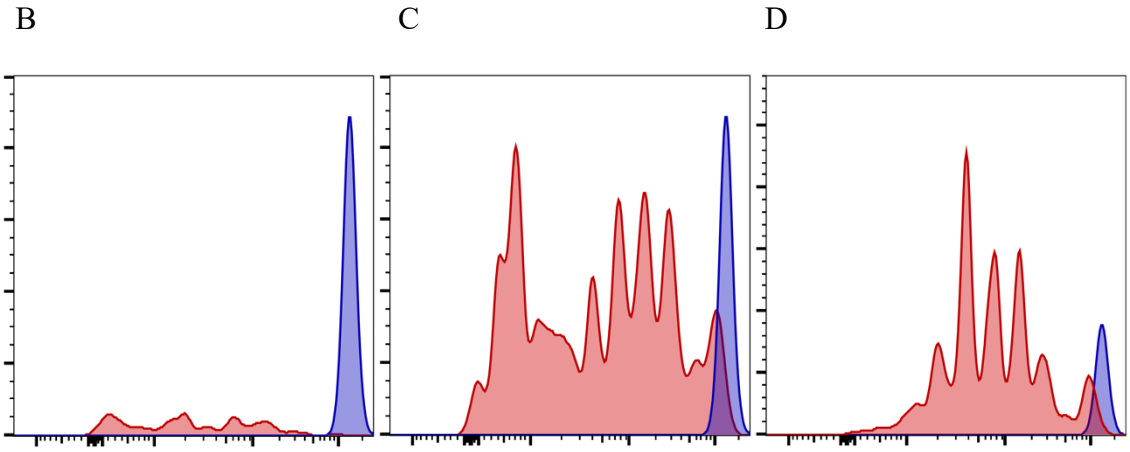

Figure 10: CD8$^+$ T cells from immunized mice proliferate after *in vitro* DC targeting with αmDEC205 EBOV NP.

Male C57BL/6J mice were subcutaneously immunized with 100 µg of EBOV NP peptide YQVNNLEEI and complete Freund's adjuvant (CFA). 21 days later, the mice were boosted with 100 µg of the same peptide and incomplete Freund's adjuvant (IFA). 14 days after the boost, the mice were humanely euthanized and splenocytes obtained. CD8$^+$ T cells were negatively isolated from the splenocytes and labelled with CellTrace Violet^{TM}. Labelled CD8$^+$ T cells were then incubated with bone marrow-derived DCs from isolated from naïve mice and cultured with GM-CSF for 6 days. 5 µg of either the isotype control or αmDEC205 EBOV NP were added with or without αCD40. As a positive assay control, OT-I T cells were incubated with αmDEC205 OVA. Proliferation of the CD8$^+$ T cells was assessed 4 days later by flow cytometry. Experimental scheme (A). Flow cytometry histogram plots showing proliferation after incubation with the isotype control (B), αmDEC205 EBOV NP (C) and αmDEC205 OVA (D).

To assess the feasibility of antibody-mediated delivery *in vivo*, C57BL/6 Ly5.1 (CD45.1) mice were subcutaneously immunized with the EBOV NP peptide and CFA followed by a boost with the peptide and IFA 21 days later as shown in figure 11A. T cells were isolated from the splenocytes of naïve mice and labelled with CTV and transferred to naïve C57BL/6J mice. The recipient mice were immunized with the isotype control antibody or αmDEC205 EBOV NP with or without αCD40. The labelled T cells that were transferred to the recipient mice proliferated when mice were immunized with the targeting antibody and only in the presence of the adjuvant but not the isotype control antibody (figure 11 B and C).

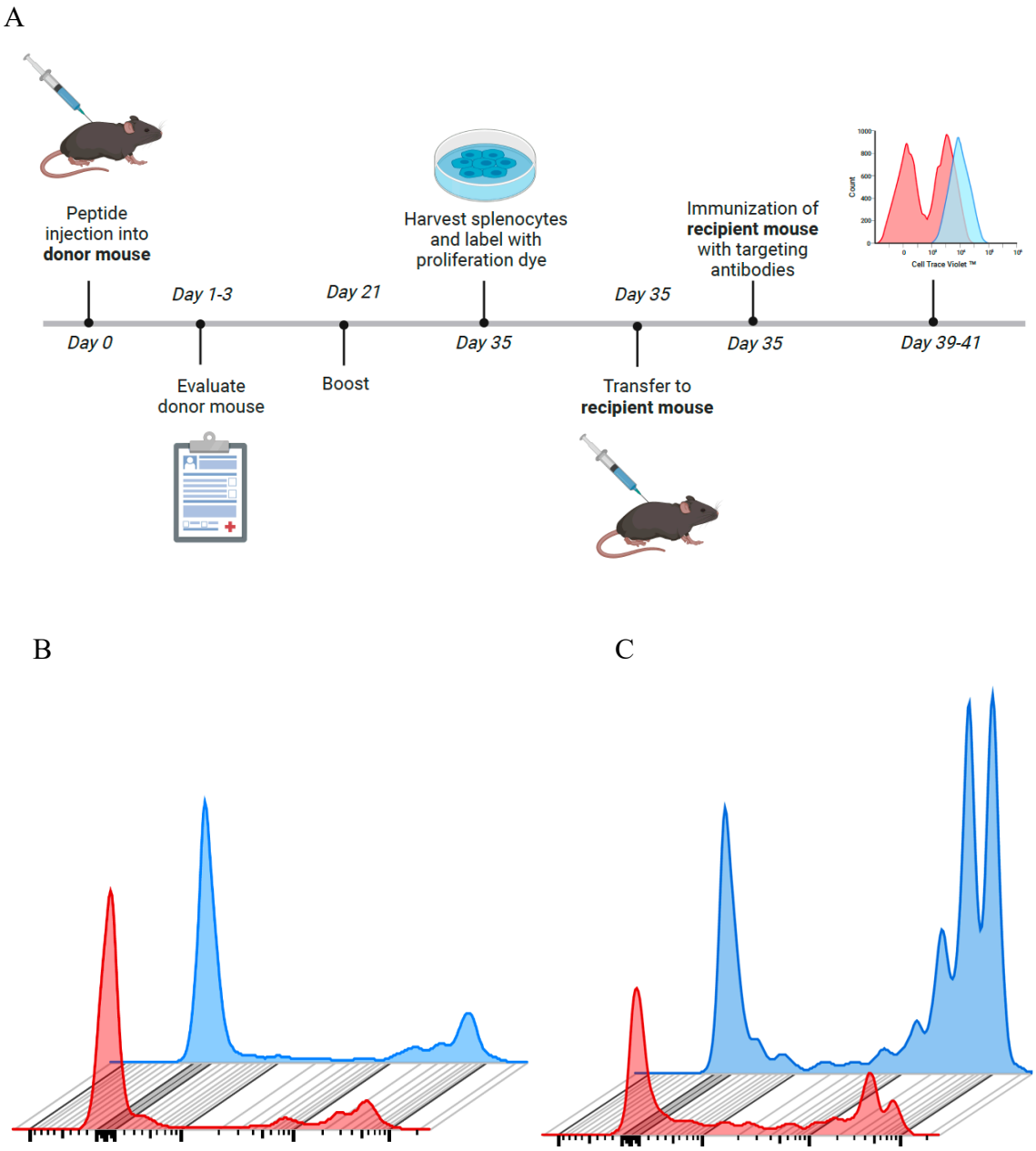

Figure 11: CD8$^+$ T cells from immunized mice proliferate after *in vitro* DC targeting with αmDEC205 EBOV NP in the presence of adjuvant.

Male C57BL/6 Ly5.1 (donor) mice were subcutaneously immunized with 100 µg of EBOV NP peptide YQVNNLEEI and complete Freund's adjuvant (CFA). 21 days later, the mice were boosted with 100 µg of the same peptide and incomplete Freund's adjuvant (IFA). 14 days after the boost, CD8$^+$ T cells were obtained from the splenocytes and labelled with CTV. The T cells were then transferred to recipient mice C57BL/6J mice which have T cells bearing the CD45.2 congenic marker. 1 day later, recipient mice were intraperitoneally immunized with 10 µg of the isotype control or αmDEC205 EBOV NP. 4 days later, proliferation was assessed by flow cytometry. B, Histogram plots showing proliferation after gating on CD8+ T cells from recipient mice immunized with the isotype control (red) or αmDEC205 EBOV NP (Blue) without the adjuvant. C, Histogram plots showing proliferation after gating on CD8$^+$

T cells from recipient mice immunized with the isotype control (red) or αmDEC205 EBOV NP (Blue) with adjuvant.

4.2 Identification of target cells

One of the most commonly used mice in laboratories are C57BL/6J mice. These mice can be infected by EBOV but do not succumb to disease caused by infection with ebolaviruses or marburgviruses. On the other hand, EBOV causes 100 % lethality in IFNAR$^{-/-}$ mice which have the same genetic background but lack the cell surface receptor shared by multiple variants of IFNα and the single forms of IFNβ and IFNω (Meager, 1998). In addition, IFNAR$^{-/-}$ mice display the morbidity and viremia associated with infection with ebolaviruses and marburgviruses. Due to the important role that IFN-I plays in innate and adaptive immunity these mice are not suitable for immunological studies. To circumvent this issue, our laboratory has engineered a bone marrow chimeric model in which wild-type bone marrow progenitor cells from C57BL/6J donor mice are transplanted into irradiated IFNAR$^{-/-}$ recipient mice. This results in mice in which the IFN-I deficiency is limited to the radio-resistant compartment. The partial IFN-I deficiency allows viral replication to occur with the resultant WT →IFNAR$^{-/-}$ chimaera rendered susceptible to EBOV disease. These mice are also able to mount an adaptive immune response driven by the wild-type immune cells of hematopoietic origin, which makes them ideal for vaccination studies or other studies of the immune response to ebolaviruses or marburgviruses. EBOV causes 50-60 % lethality in this model. (Lüdtke et al., 2017; Oestereich et al., 2016).

Therefore, these mice were used for subsequent experiments in the BSL-2 and BSL-4 lab to identify target cells, determine T cell functionality after antibody-mediated delivery of EBOV NP and to evaluate the protective capacity of αmDEC205 antibodies.

Various groups have utilized different routes to administer DC targeting antibodies. Administration into the peritoneal cavity allows for a quicker onset of effects after injection, which enables the observation of the effects much faster. Injection via this route ensures that the antibodies are distributed to multiple organs at a similar time. In order to identify target cells, and to assess the nature of DCs targeted by αmDEC205 antibodies, WT → IFNAR$^{-/-}$ mice were immunized with αmDEC205 antibodies conjugated to APC. 30 min after inoculation, the mice were euthanised and the lymph nodes, spleen, liver and lungs were harvested. Single cell suspensions were prepared for the staining of surface markers and flow cytometric analysis. Using another antibody against DEC-205 conjugated to PercP-eFluor 710 allowed for the

characterisation of DEC205$^+$ DCs that may have not been stained by the APC conjugated αmDEC205 antibodies. This technique allowed the discrimination of cDC1 from other DC subsets. The injected antibodies were able to rapidly bind to DEC205$^+$ DCs in the lymph nodes and spleen indicating that this route of administration was feasible and that CD8α$^+$-expressing cDC1s, one of the major subsets involved in cross-presentation of antigens was successfully targeted after IP injection of the targeting antibody.

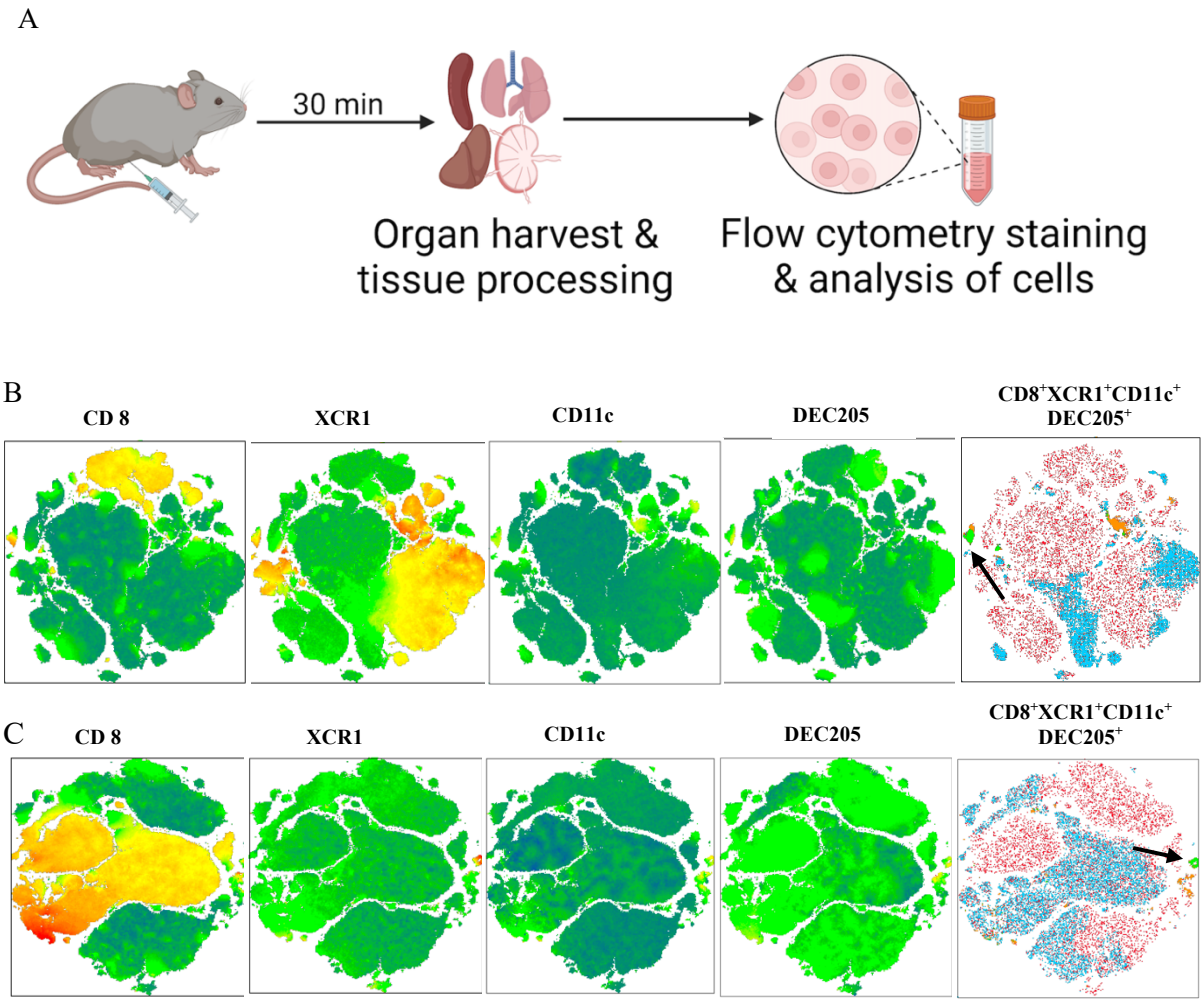

Figure 12: αmDEC205 antibodies conjugated to APC are able to rapidly bind cross-presenting DCs in WT → IFNAR$^{-/-}$ mice.

WT → IFNAR$^{-/-}$ mice were immunized with 5 µg of αmDEC205-APC (n=2). 30 min later the spleen, lungs, lymph nodes and liver were obtained, processed and the cells stained for flow cytometry analysis. (A) Schematic of the experiment. (B) t stochastic neighbourhood embedding (tSNE) of DEC205$^+$ cells in the spleen and (C) draining lymph nodes built on CD8, XCR1, CD11c and MHC II.

4.3 Antibody-mediated delivery of EBOV NP results in the induction of functional NP-specific T cells

The differentiation of $CD8^+$ T cells to cytotoxic T cells after priming by DCs is characterised by the release of cytokines such as IL-2, IFNγ and TNFα. Together with the secretion of cytotoxic granules, these CTLs can mediate the killing of virus infected cells. To assess whether targeting EBOV NP to DCs would result in the induction of EBOV NP specific T cells and whether these T cells were functional, the secretion of various cytokines such as IL-2, IFNγ and TNFα was measured.

4.3.1 Tetramer positive (EBOV NP-specific) T cell induction after immunization with αmDEC205 EBOV NP

In order to determine whether targeting EBOV NP to $DEC205^+$ DCS led to the generation of EBOV NP-specific T cells, mice were immunized with αmDEC205 EBOV NP and the presence of EBOV NP-specific CD8 T cells determined via MHC class I tetramer staining. MHC tetramers enable the detection, visualization and quantification of antigen-specific T cells. Tetramers consist of four MHC molecules complexed with the peptide of interest and are labelled with a fluorophore, which allows the visualization of tetramer-bound T cells via flow cytometry. They mimic peptide-MHC complexes and are multimerized to enable them to bind to more than one TCR i.e., four. These multimerized complexes have slower dissociation rates, which makes them more suitable for flow cytometry staining (Altman et al., 1996). The principle of tetramer staining is described in more detail in section 3.4.3.

Flow cytometric analysis of splenocytes showed that EBOV NP-specific T cells were detectable at 14- and 28-days post immunization indicating that EBOV NP was successfully delivered to $DEC205^+$ DCs and was cross-presented to $CD8^+$ T cells (figure 13 B and C).

A

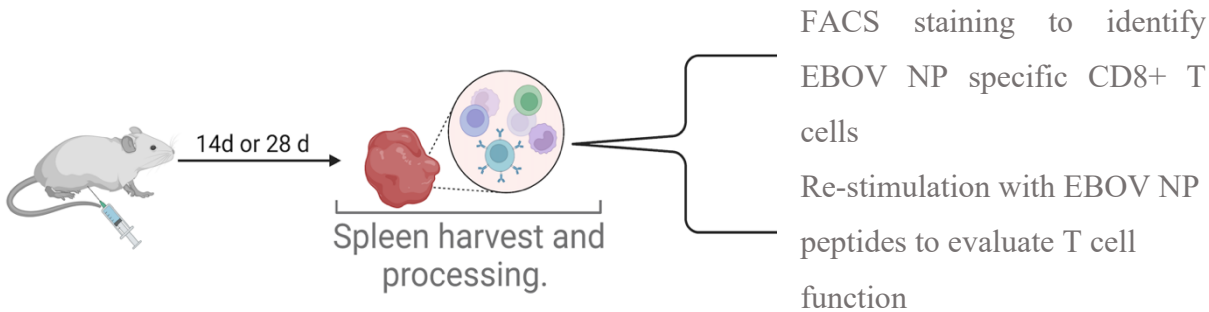

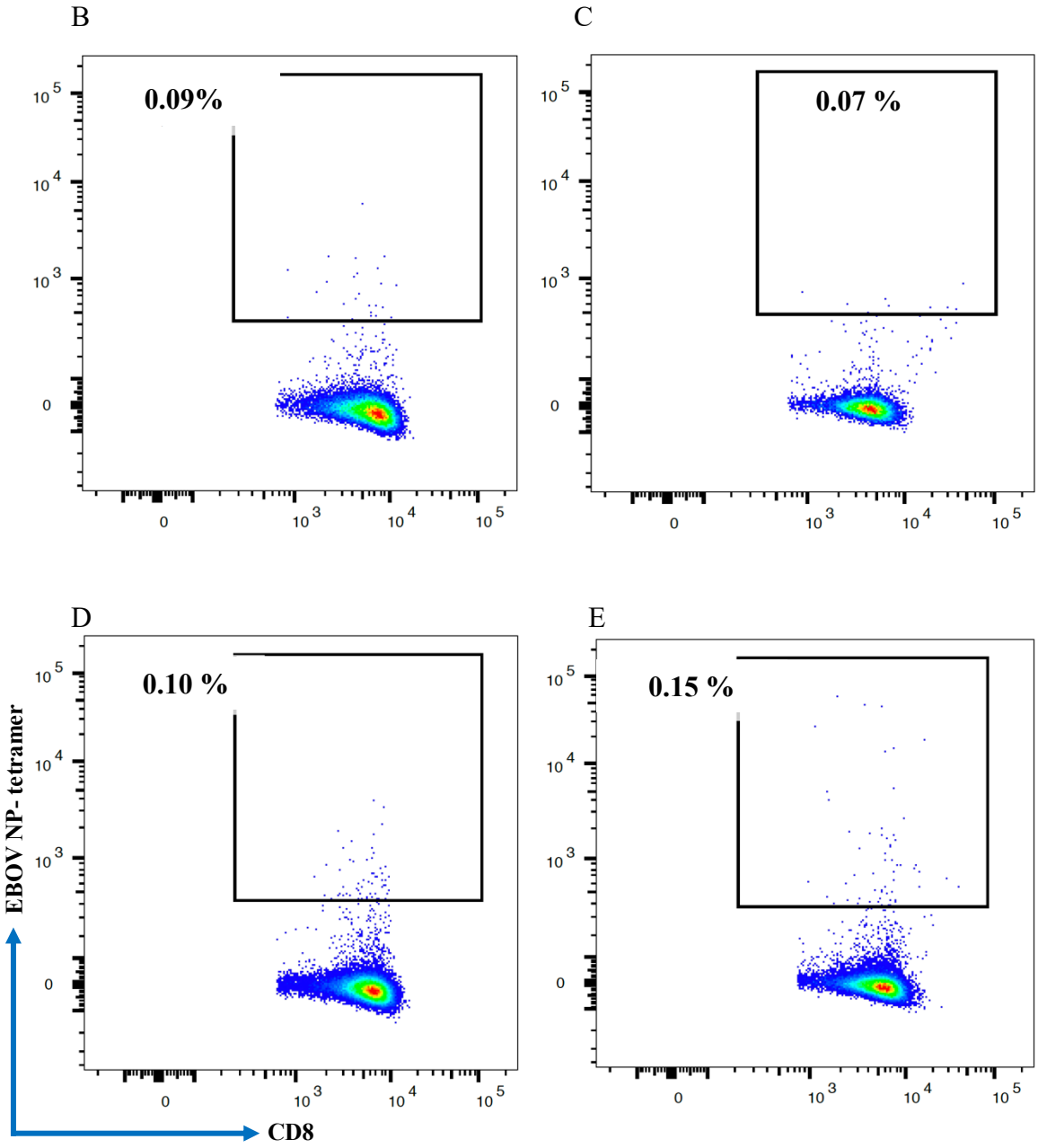

Figure 13: Antibody-mediated delivery of antigen to DEC205^{+} DCS leads to the induction of EBOV NP specific CD8^{+} T cells.

WT → IFNAR$^{-/-}$ mice were immunized intraperitoneally with 10 µg of the isotype control or αmDEC205 EBOV NP together with αCD40. 14 or 28 days later, the mice were sacrificed and the splenocytes obtained and stained for flow cytometric analysis. Schematic showing the experimental procedure. Representative dot plots show the percentage of EBOV NP specific T cells from total CD8^{+} T cells in bulk splenocytes. (B) and (C), isotype control 14- and 28-days post immunization. (D) and (E) αmDEC205 EBOV NP 14- and 28-days post immunization, respectively.

4.3.2. CD8$^+$ T cells from αmDEC205 EBOV NP immunized mice are functional

The presence of antigen-specific T cells does not always translate to function. One way of determining the function of antigen-specific T cells is by measuring the amount of effector molecules secreted. Antigen-specific CD8$^+$ T cells are activated, expand and differentiate into effector cells upon antigen recognition and after interaction with DCs. A small subset of these cells differentiates into memory precursors, which are retained in the body following vaccination or infection and have the ability to give rise to effector cells or memory cells following a secondary encounter with the antigen or, in the case of vaccination, the first encounter with a pathogen. Effector T cells secrete various cytokines following encounter with their cognate antigen. IFNγ is used to track CD8$^+$ T cell responses and is a major readout used to determine the presence of effector or effector memory T cells and thereby vaccination success.

To determine the functionality of T cells after DC targeting, mice were immunized with the targeting antibodies and the splenocytes were obtained 14 and 28 days after immunization as described in figure 13 A. The splenocytes were then re-stimulated *ex vivo* with peptides namely, EBOV NP peptide YQVNNLEEI, which is MHC I restricted and LSFASLFLPKLVVGE, which is MHC II restricted. Brefeldin A, a reagent that inhibits cytokine release and therefore allows the detection of cytokine expression by flow cytometry and mouse anti-CD28 and anti-CD49d antibodies were also added to activate costimulatory molecules thus enhancing the secretion of cytokines. Anti-mouse CD107, a marker for degranulation was also included. Figure 14 shows the percentage of CD8 T cells that expressed IFNγ, IL2 and CD107a. Cytotoxic T cell and NK cells express of CD107a when activated the degranulation of CD8$^+$ T cells can be used as a measure of the ability of CD8$^+$ T cells to exert cytotoxic functions.

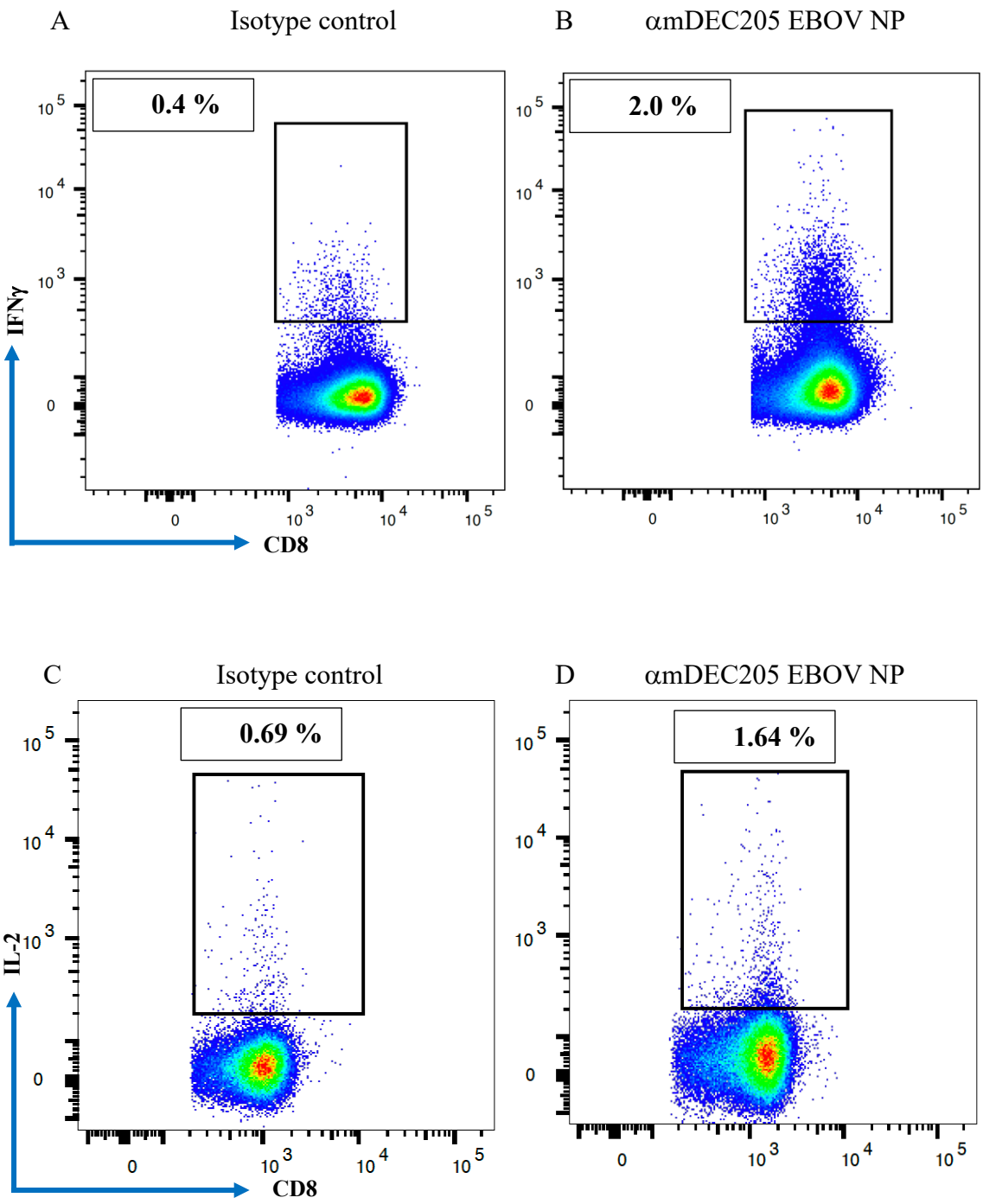
A
Isotype control
0.4 %
B
αmDEC205 EBOV NP
2.0 %
IFNγ
CD8
C
Isotype control
0.69 %
D
αmDEC205 EBOV NP
1.64 %
IL-2
CD8

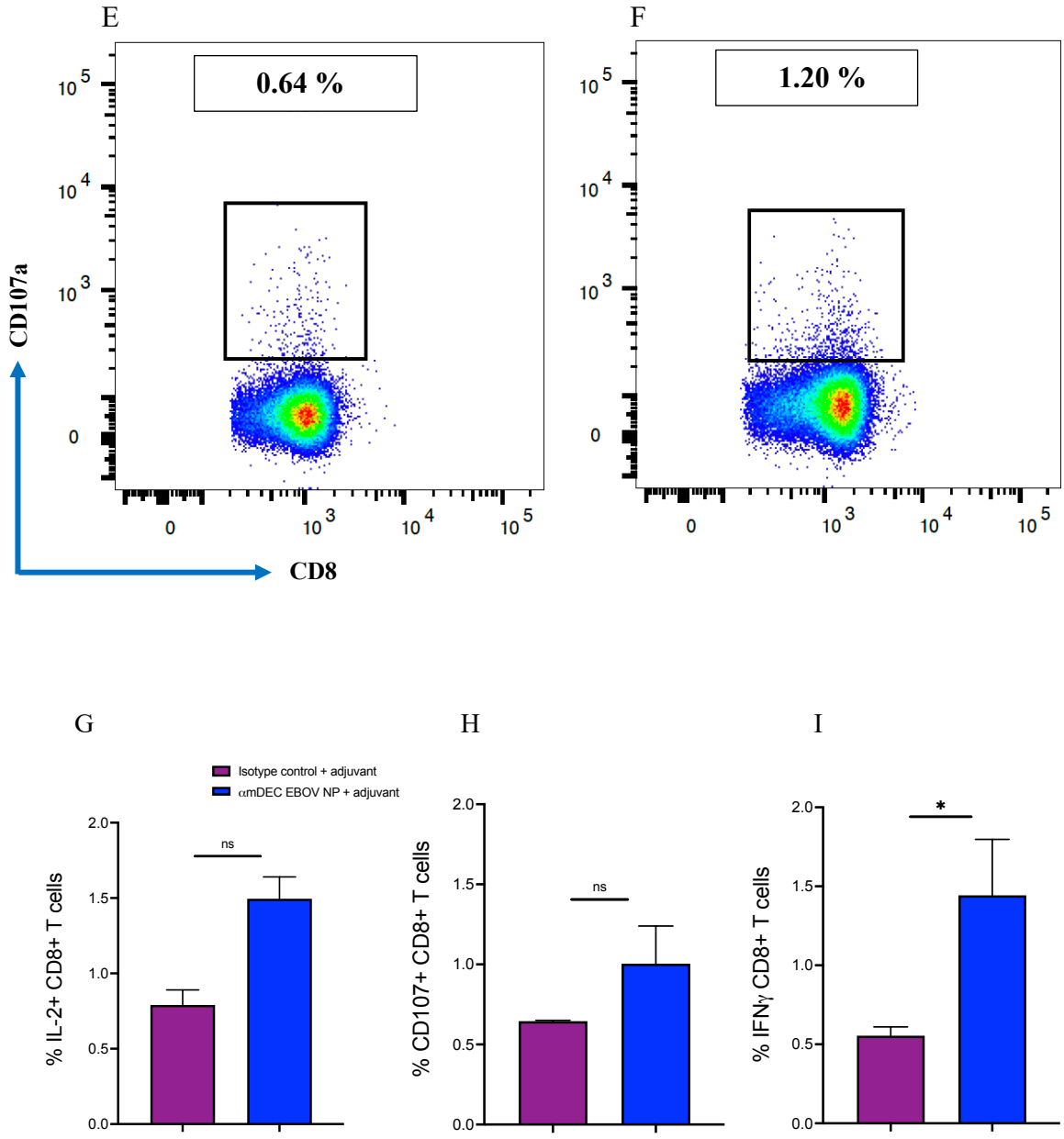

Figure 14: CD8$^+$ T cells secrete cytokines and degranulate after targeting EBOV NP to DEC205$^+$ DCs.

Mice (n=2-4) were immunized as described in figure 13. Splenocytes were obtained and re-stimulated with EBOV NP peptide - YQVNNLEEI. The frequency of T cells expressing IFNγ and IL-2 and CD107a were determined by intracellular cytokine staining after peptide re-stimulation. Representative flow cytometry plots showing the percentage of CD8$^+$ T cells expressing IFNγ (A & B) IL-2 (C & D) or CD107a 28 days post immunization (E & F). Bar graphs represent mean values ± SEM of IL-2 (G), CD107a (H) and IFNγ (I). Statistical significance was calculated using student's t-test (ns – not significant, *$p \leq 0.05$, **$p \leq 0.01$, ***$p \leq 0.001$).

The percentage of $CD8^+$ T cells expressing IFNγ was significantly higher compared to the control group (figure 14 A, B, I) with the frequency of IFNγ expressing $CD8^+$ T cells being more than double that of the control group (figure 14 I). Though not significant, $CD8^+$ T cells from mice immunized with αmDEC205 EBOV NP expressed higher amounts of IL-2 and CD107a in comparison to the mice that were immunized with the isotype control group (figure 14 C-H).

Due to the high background staining observed during intracellular cytokine staining and in view of the differences in the percentages of tetramer-specific T cells, a different assay was used to investigate whether there would be a significant difference in IFNγ expression between the control and the experimental groups. The ELISpot assay is a quantitative assay that measures the frequency of cytokine secretion. It has a lower limit of detection compared to flow cytometric techniques and is routinely used to measure vaccine responses. WT → $IFNAR^{-/-}$ mice were immunized as previously described in figure 13A. The splenocytes were obtained 14 or 28 days after immunization and re-stimulated with the same peptides as described in section 4.3.2. IFNγ secretion was detected using ELISpot. The amount of IFNγ secreting cells were measured 25 h after culture of the splenocytes with the peptides.

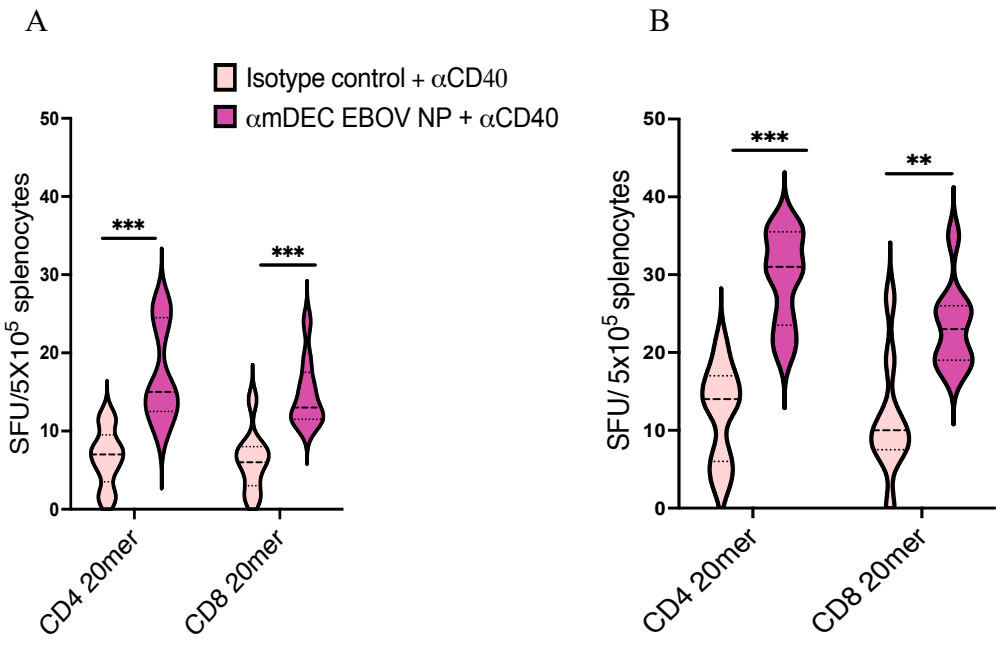

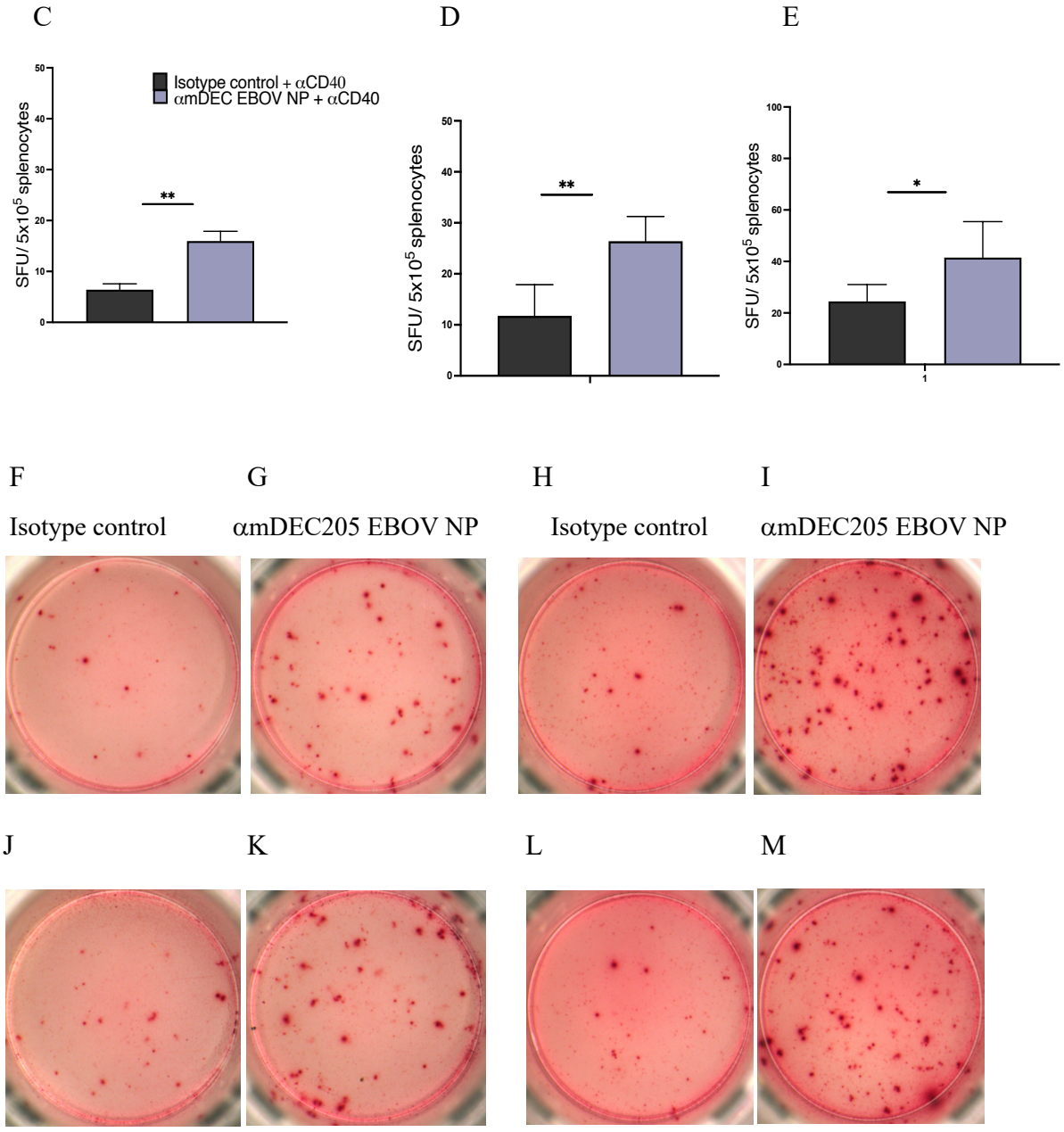

Figure 15: CD8$^+$ T cells from mice immunized with αmDEC205 EBOV NP secrete IFNγ after re-stimulation with EBOV NP peptides.

WT → IFNAR$^{-/-}$ mice were immunized as described in figure 13. Splenocytes were obtained and re-stimulated with EBOV NP peptide AGQFLSFASLFLPKLVVGEK (MHC II, CD4) or RVIPVYQVNNLEEICQLIIQ (MHC I, CD8) restricted peptides. T cells secreting IFNγ were determined via an ELISpot assay. Spot forming units were enumerated and are represented as spot forming units (SFU) per 5x10^5 cells. Graphs show the number of SFU/5x10^5 after incubation with either MHC I or MHC II peptides (figure 15 A and B). Bar graphs represent mean values ± SEM and show total IFNγ-secreting CD4$^+$ and CD8$^+$ T cells (figure 15 C-E).

Images show IFNγ-secreting T cells in the form of spots at day 14 post immunization (figure 15 F, G, H, I) and day 28 post immunization (figure 15 J, K, L, M). F,G, J, K – MHC II restricted peptide, H, I, L, M – MHC I restricted peptide. Bar graphs represent mean values ± SEM and show both IFNγ-secreting $CD4^+$ and $CD8^+$ T cells. Statistical significance was calculated using Mann-Whitney U test (A & B) and unpaired Student's *t*-test (C-E). (ns – not significant*$p \leq 0.05$, **$p \leq 0.01$, ***$p \leq 0.001$).

IFNγ production was detectable after the restimulation of splenocytes with both the MHC I and MHC II restricted EBOV NP peptides. IFNγ secretion by T cells obtained from αmDEC205 EBOV NP immunized mice was significantly higher than that observed for the isotype control immunized mice.

4.4 Evaluation of the protective capacity of αmDEC205 EBOV NP

The induction of EBOV specific T cells is associated with a positive outcome during EVD. Survivors are able to mount a response that involves both humoral and T cell immunity.
Having shown that targeting EBOV NP to DCs results in the induction of functional EBOV NP-specific T cells, it was hypothesised that immunizing mice with αmDEC205 EBOV NP would improve the outcome after EBOV infection. The prophylactic potential of immunization with αmDEC205 EBOV NP was therefore evaluated.

4.4.1 DC targeting with Poly IC and CD40 agonist as adjuvants results in protection after EBOV infection

An important factor to consider during targeting to DCs is the kind of response that is desired. Targeting antigens to C-type lectin receptors such as DEC205 and Clec9A allows tailoring of the immune response to suit the need at hand, i.e., directing the response towards immunity or tolerance based on the presence or absence of adjuvants. In diseases associated with immune pathology, the induction of regulatory T cells that can dampen the immune response may be desirable. In other instances, there might be a deficiency in the induction of a pro-inflammatory response that can contribute to the control of viral replication and limit further spread of the virus. Indeed, EBOV and MARV are known to inhibit DC maturation leading to the inadequate priming of T cells and therefore a lack of antigen-specific T cells that may mediate protection. In the absence of an adjuvant, DCs remain immature and targeting antigens to $DEC205^+$ DCs leads to the induction of Tregs. Conversely, providing an adjuvant leads to the maturation of DCs which in turn are able to polarize T cells towards immunity leading to the induction of $CD4^+$ T helper cells with a Th1 phenotype and CTLs.

Adjuvants augment the immune response to antigens and improve the efficacy of vaccines. CD40 is a 45-50 kDa transmembrane glycoprotein belonging to the tumour necrosis factor (TNF)/TNF receptor (TNFR) family. Its natural ligand is CD40L (CD154), which is expressed on activated $CD4^+$ T cells (Borrow et al., 1996). CD40 is expressed by APCs such as DCs, monocytes, macrophages and non-immune cells such as endothelial and epithelial cells. CD40 ligation on the surface of APCs enhances the expression of MHC and costimulatory molecules and induces the activation of T cells and the production of proinflammatory cytokines (Khalil and Vonderheide, 2007). CD40 agonists can be used to activate DCs and other cells of the myeloid compartment that highly express this molecule (Grewal and Flavell, 1998; Grewal et al., 1995, 1996). Its potential as an immunotherapy target to enhance anticancer responses has been investigated and various formulations have been tested in phase 1 clinical studies to determine the efficacy of CD40 agonists against tumours (Vonderheide, 2020).

Studies show that the administration of CD40 agonists leads to the expansion of $CD8^+$ T cells that require priming by cross-presenting DCs (Bonifaz et al., 2004).

Poly-inosinic-poly-cytidylic (Poly IC) acid is a synthetic double-stranded (ds) RNA that activates innate immune cells in a similar manner to pathogenic elements mimicking a viral infection. It is recognised by endosomal TLR3. Downstream signalling upon the recognition of Poly IC results in the production of IFN-I (Alexopoulou et al., 2001). Recognition of poly IC can also lead to the activation of NF- κB and AP-1 transcription factors, which results in the production of TNFα, IL 6 and CXCL10 which are pro-inflammatory cytokines (Kato et al., 2008; Kawai and Akira, 2008).Combining Poly IC with an antigen can be used to modulate and optimize the elicited immune response (Longhi et al., 2009; Trumpfheller et al., 2008).

Thus, in order to determine which adjuvants could optimally enhance the immune responses elicited by αmDEC-205 EBOV NP targeting antibodies the effect of immunization with either Poly IC in combination with CD40 agonist or CD40 agonist alone was compared.

Male and female WT → $IFNAR^{-/-}$ mice were immunized with 10 µg of αmDEC205 EBOV NP, 50 µg of Poly IC and 25 µg of αCD40 according to the immunization regimen shown in the schematic below. The optimal amount of targeting antibodies to be used in the immunization regimen was determined in prior experiments (data not shown). To compare the virus titres in the organs, mice were serially sacrificed on day 3 and 7 after challenge with EBOV.

A

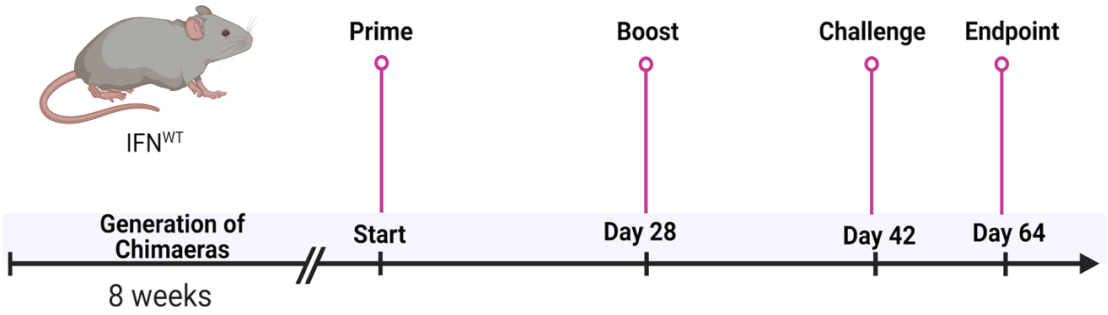
IFN^{WT}
Prime
Boost
Challenge
Endpoint
Generation of Chimaeras
8 weeks
Start
Day 28
Day 42
Day 64

B

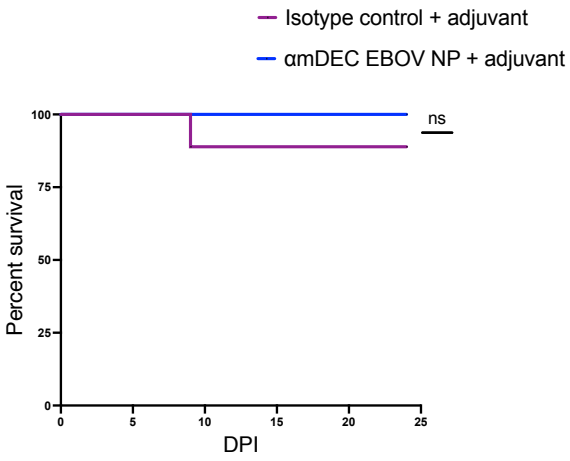
Isotype control + adjuvant
αmDEC EBOV NP + adjuvant
ns
Percent survival
DPI

C

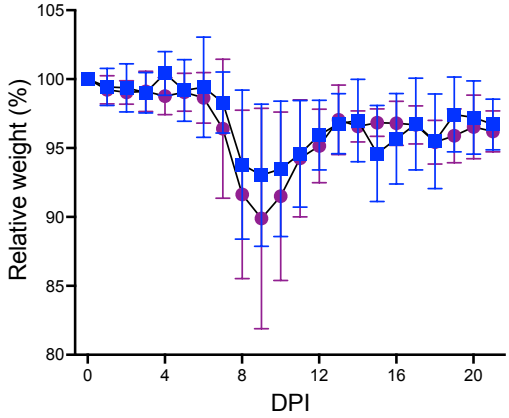
Relative weight (%)
DPI

D

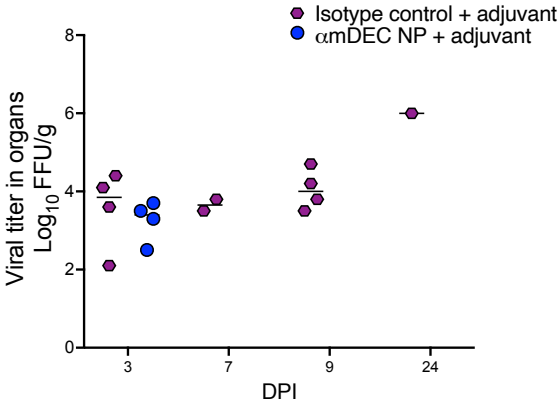
Isotype control + adjuvant
αmDEC NP + adjuvant
Viral titer in organs
Log10 FFU/g
DPI

E

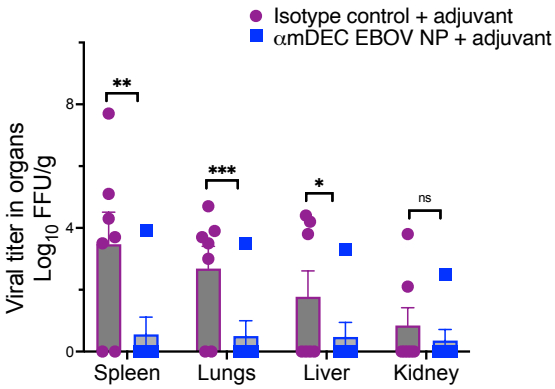
Isotype control + adjuvant
αmDEC EBOV NP + adjuvant
Viral titer in organs
Log10 FFU/g
**
***
*
ns
Spleen
Lungs
Liver
Kidney

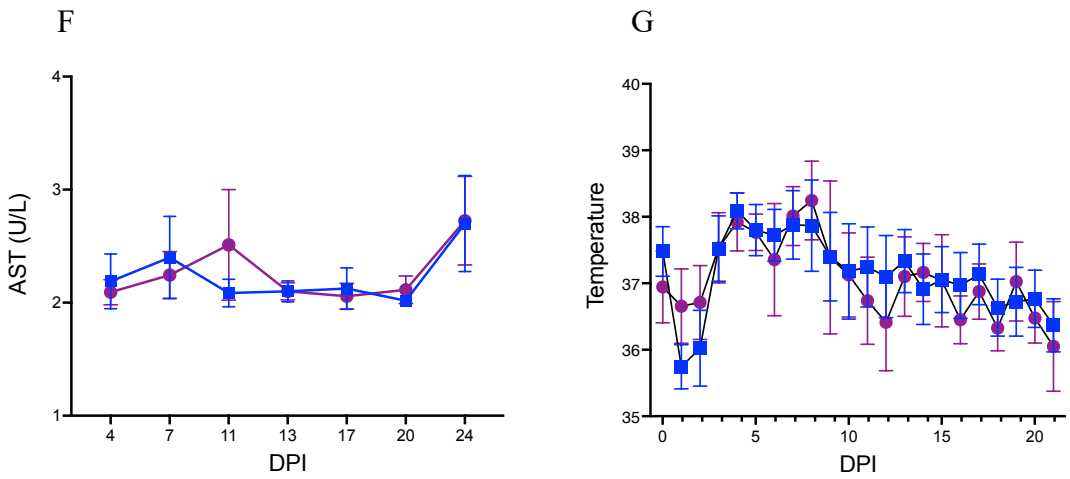

Figure 16: Targeting EBOV NP to DEC205^{+} DC results in 100 % survival of immunized mice and reduced viral titers in organs.

Male and female WT → IFNAR$^{-/-}$ mice (n = 12) were immunized with either the isotype control or αmDEC205 EBOV NP together with 50 µg Poly IC and 25 µg αCD40 according to the immunization regimen shown in the schematic (A). At 28 days post immunization, the mice received a boost with antibodies and the same amounts of the adjuvants and 14 days later were infected intranasally with 10000 FFU EBOV (Makona). 2 mice from each group were sacrificed at 3 and 7 ds post infection. Mice were monitored for up to 24 days and blood was obtained at intervals of 3-4 days to determine viremia and liver enzyme levels. Graphs show Kaplan Meier survival curves (B), weight (C), viral titers in the organs at 3 and 7 days after infection (D), viral titers in the the spleen, liver, lungs and kidney at endpoint (E), liver AST levels (F) and temperature (G). Values are reported as mean ± SEM. Statistical significance was determined using Mantel-Cox test (B) or unpaired Student's *t*-test (C-G). (ns – not significant, *$p \leq 0.05$, **$p \leq 0.01$, ***$p \leq 0.001$).

EBOV infection causes 50 % lethality in the WT → IFNAR$^{-/-}$ chimaera model, which makes it a suitable model for evaluating immune respones to EBOV infection and by extension vaccine studies. 100 % of the mice that were immunized with αmDEC205 EBOV NP and subsequently challenged survived (figure 16 B). Though there were no significant differences in survival nor weight between the groups, mice that received the isoytpe control were unable to clear the virus, with virus being detectable up to 24 days after infection in the organs assessed (figure 16 D and E). The isotype control group had a slightly higher elevation in AST levels, which implies more damage to the liver (figure 16 F).

4.4.2 DC targeting with αmDEC205 EBOV NP and CD40 agonist protects susceptible mice from lethal EBOV infection

The results in section 4.4.1 indicated that targeting EBOV NP to DEC205$^+$ DCs had an overall positive effect on the outcome after EBOV infection with significant differences in viral titres in the organs between the control and experimental group. Due to the limitations of the chimeric mouse model, it was important to minimize or exclude any factors that may have a confounding effect on the data. Poly IC activates all innate immune cells in a non-specific manner which leads to a general antiviral effect (Martins et al., 2016). Indeed, this might explain why the mice immunized with the isotype control antibody and poly IC were protected against EBOV challenge. To test this hypothesis, Poly IC was therefore omitted in subsequent experiments and αCD40 alone was used as adjuvant.

The use of CD40 agonists for immunotherapy has been extensively studied and different formulations have been advanced to clinical trials with promising results (Forero-Torres et al., 2006; Tai et al., 2004; Vonderheide, 2007). CD40 agonists have been shown to enhance the immune response to antigenic stimulation when administered as adjuvants (Ahonen et al., 2004; Diehl et al., 1999). Binding of CD40 on the surface of APCs results in the upregulation of MHC molecules and CD80/86 and stimulates the production of pro-inflammatory cytokines such as IL-12, IL-6, TNFα, and IFNγ (Li and Wang, 2020). CD40 agonists can also enhance cytotoxic T cell responses and have been shown to improve the efficacy of vaccines in mice associated with the expansion of antigen-specific CD8$^+$ T cells (Vonderheide et al., 2020). The fact that αCD40 agonists have been tested in phase 1 clinical trials with promising results and have been shown to be effective in combination with other therapeutics motivated us to test αCD40 agonist alone as an adjuvant in subsequent immunization experiments.

The immunization regimen was the same as shown in figure 16A.

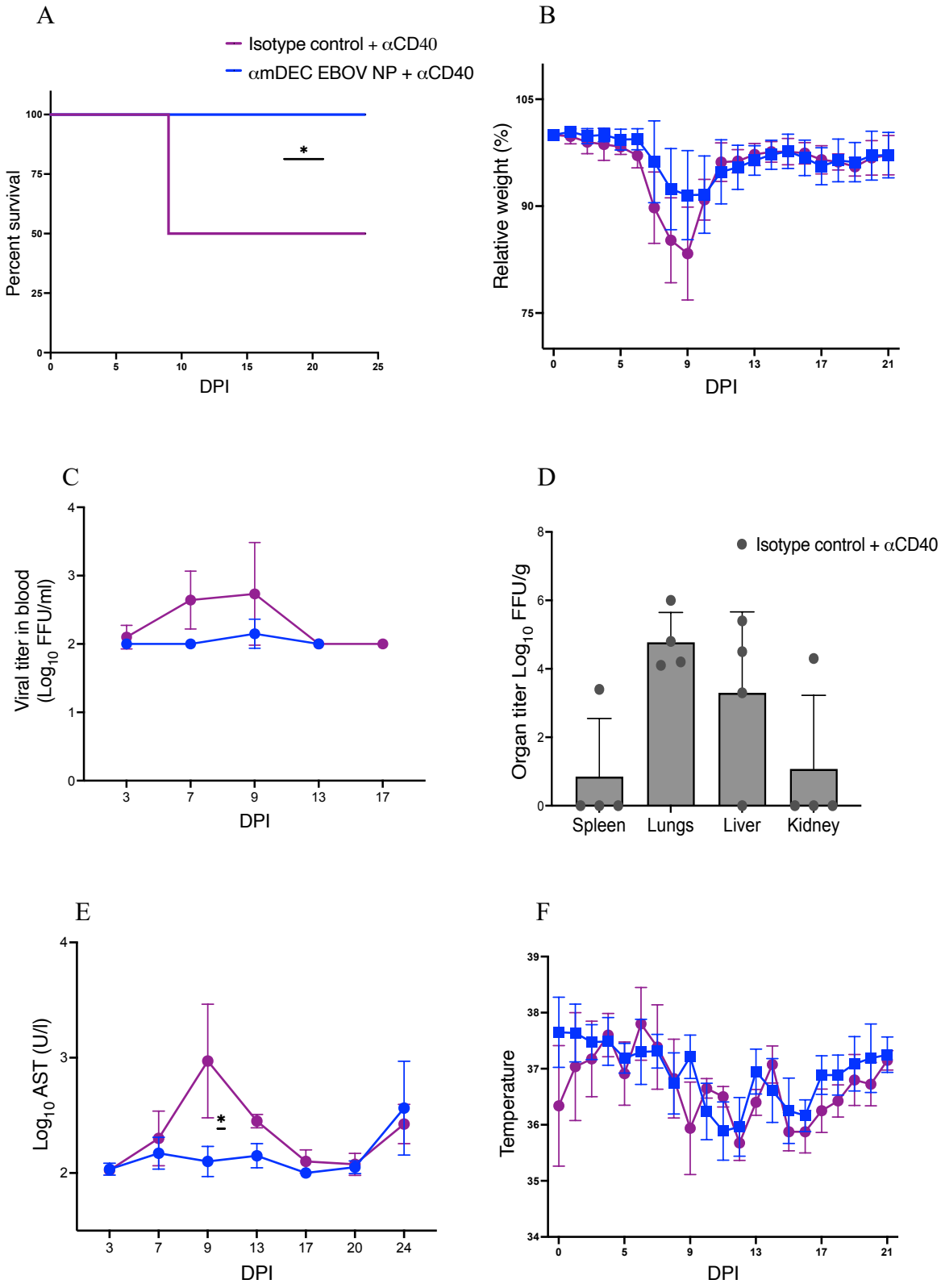

Figure 17: Targeting EBOV NP to DEC205^{+} DCs with αCD40 as an adjuvant results in 100 % survival of immunized mice and reduced viral titers in organs.

Male and female WT → IFNAR$^{-/-}$ mice (n = 8) were immunized with either the isotype control or αmDEC205 EBOV NP together with 25 µg αCD40 according to the immunization regimen shown in

the schematic (A). At 28 days post immunization, the mice received a boost with the targeting antibodies and 25 µg αCD40. 14 days later, mice were infected intranasally with 10,000 FFU EBOV Mayinga. Mice were monitored for 21 days and those that recahed humane endpoint criteria were euthanised. Blood was obtained at intervals of 3-4 days to determine viremia and liver enzyme levels. Graphs show Kaplan Meier survival curves (A), weight (B), viremia (C) viral titers in the the spleen, liver, lungs and kidney at endpoint (D), liver AST levels (E) and temperature (F). Values are reported as mean ± SEM. Statistical significance was determined using Mantel-Cox test (A) or unpaired Student's *t*-test (B-F). (ns – not significant, *$p \leq 0.05$, **$p \leq 0.01$, ***$p \leq 0.001$).

Immunization with the targeting antibodies and using αCD40 alone as an adjuvant rescued mice from lethal EBOV infection. Mice in the control group lost slightly more weight (figure 17 B) and 50 % had to be euthanised due to reaching humane endpoint criteria (figure 17 A). The animals in the control group had higher AST levels as measured in the serum compared to the experimental starting at day 3 after infection. The highest AST levels were measured at day 9 post infection with signigficantly higher levels observed in the isotype control group indicating liver damage (figure 17 D). Furthermore, mice immunized with the isotype control developed higher levels of viremia and had detectable virus in the spleen, lungs, liver and kidneys. The mice immunized with αmDEC205 EBOV NP on the other hand had lower viremia and AST levels and were able to clear the virus by day 13 post infection (figure 17 C & D).

4.5 Characterisation of the T cell response after DC targeting using the model antigen - OVA

The results described in previous sections indicated that antigen delivery to DCs via monoclonal antibodies could be a viable vaccination strategy against EBOV infection. Understanding the elicited response not only after vaccination but also after infection is essential to determining the correlates of protection.

Next, the T cell response after infection was assessed. The endogenous T cell responses, though present after infection proved difficult to characterise due to the low frequency of EBOV NP-specific T cells and the high background observed with tetramer staining. Therefore, in order to better understand the processes involved in elaborating a positive outcome after infection, a recombinant OVA-expressing EBOV was generated.

The OT-I-OVA system is a tool that is extensively used in immunological studies. The OT-I mouse model contains transgenic inserts for mouse TCR genes that can recognize OVA, an inert T-cell dependent antigen routinely used in studying antigen-specific T cell responses.

4.5.1 Generation of recombinant OVA-expressing EBOV

The OVA gene was inserted as an additional transcriptional unit after the NP gene duplicating the NP/VP35 non-coding region within the cassette vector plasmid as described in the methods section. This gene was subsequently sub-cloned into the full-length EBOV plasmid using restriction enzymes D*rd*I and *Nru*I (Groseth et al., 2015).

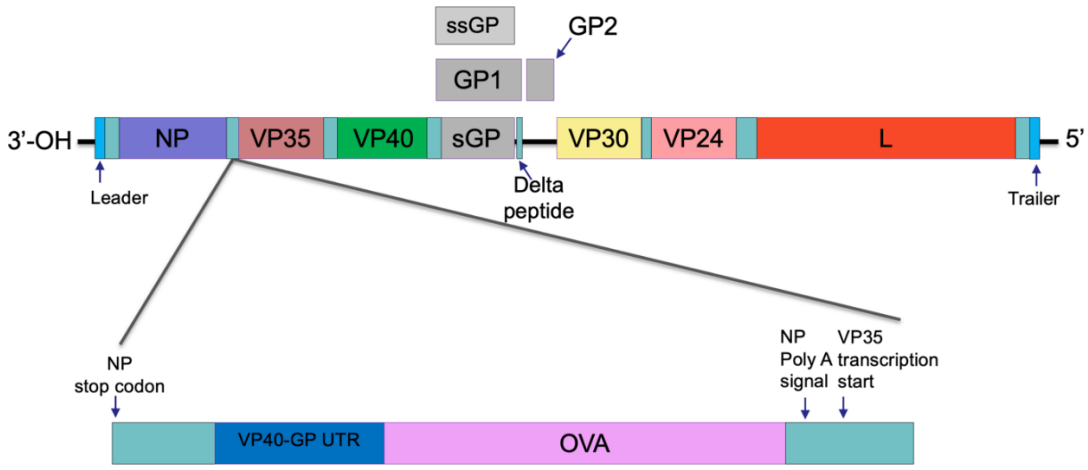

Figure 18: Schematic showing the genome organisation of EBOV and the location of the inserted gene.

4.5.2 Rescue of recombinant EBOV OVA and stock production

Full-length EBOV clone plasmid contains a cDNA copy of the complete EBOV genome in cRNA orientation, which allows expression in mammalian cells.

The full-length plasmid used for cloning is based on Zaire ebolavirus rec/COD/1976/Mayinga-rg-EBOV (Shabman et al., 2013). Viral RNA synthesis requires the viral NP, VP35, VP30 and L proteins together known as the ribonucleoprotein complex (RNP) or RNP proteins. The RNP proteins recognize the cRNA as a template for replication into the vRNA genome, which can then be transcribed into mRNAs allowing for virus rescue of the recombinant virus (Hoenen and Feldmann, 2017).

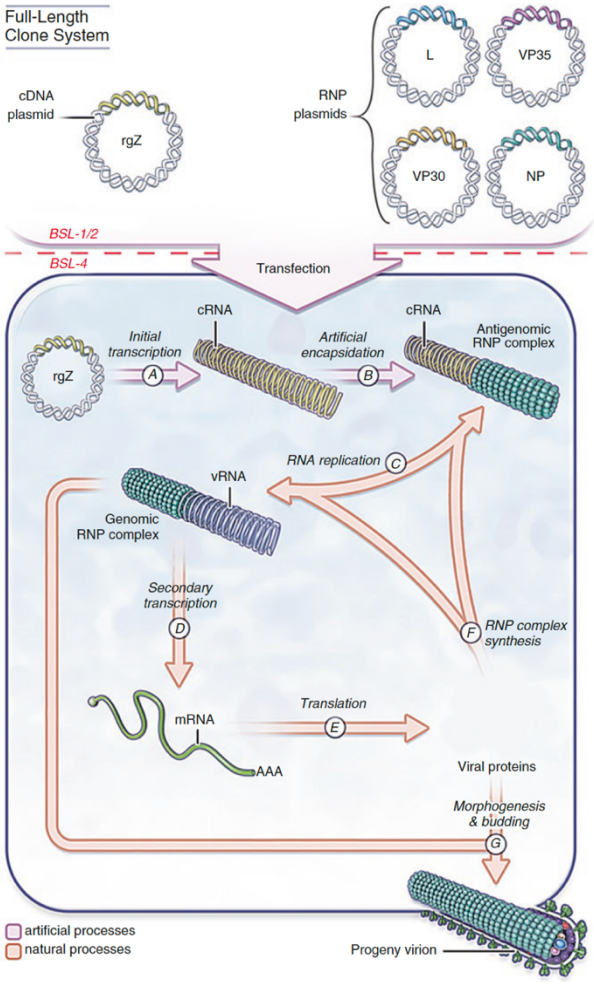

Figure 19: Schematic showing the components necessary for virus replication and transcription and required for virus rescue from Hoenen and Feldmann, 2017.

Cells are transfected with the full-length EBOVplasmid (rgZ) and plasmids encoding L, VP35, VP35 and NP. Transcription results in a full-length genome (cRNA), which is encapsidated and is used as template for replication and transcription (from Hoenen and Feldmann, 2017; Hoenen et al., 2011).

Virus rescue was performed by transfecting Huh7 cells with expression plasmids for the EBOV proteins NP, VP35, VP30 and L together with expression plasmids for T7-polymerase and the full-length EBOV genome plasmid. One week after transfection, supernatant was harvested and used to infect Vero E6 cells, which were monitored for 14 days. At 14 days, the cells were assessed to determine whether there was cytopathic effect (CPE). Infection of permissive cells in this case, Vero E6 cells leads to the production of viral progeny. CPE is a good indicator for viral invasion and is characterised by structural or morphological changes in host cells. This could be rounding of the infected cells, formation of syncytia or the appearance of inclusion

bodies. One virus clone that clearly caused discernible CPE was chosen for further experiments. The clone was amplified on Vero E6 cells and the sequence confirmed by Sanger sequencing. Virus rescue was done under BSL-4 containment. In the absence of the expression plasmid for the L protein, Vero E6 cells remain healthy and adhere to the culture vessel as a result of restrictive infection i.e., the virus genes necessary for replication are not transcribed nor translated (figure 20 A). Figure 20 B shows an image of the cells infected with the virus clone chosen for stock production where the expression plasmid for the L protein was added. The first stage of CPE is clearly discernible as evidenced by the rounding of infected cells.

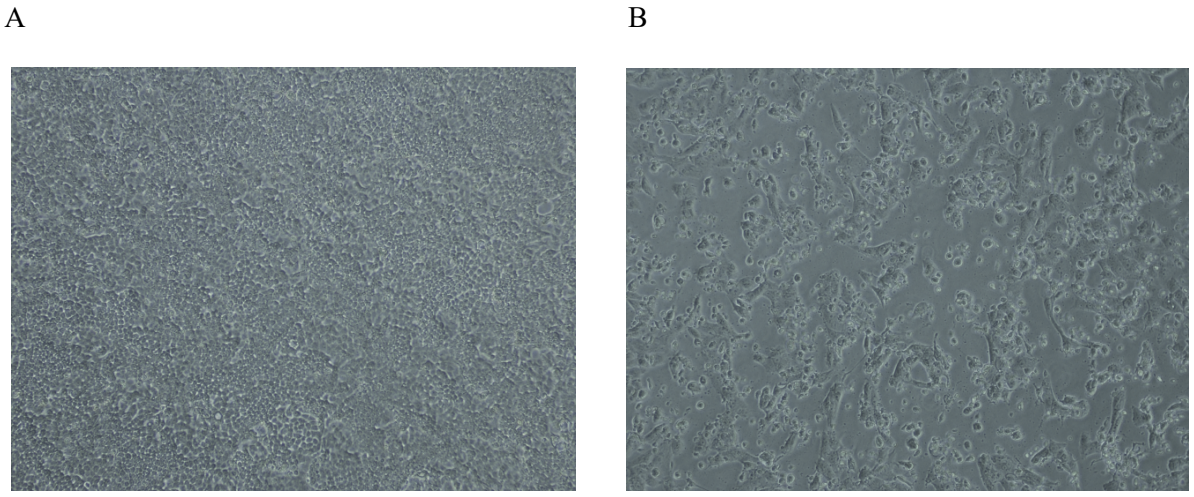

Figure 20: EBOV OVA replicates in Vero E6.

Vero E6 cells were infected with a recombinant EBOV OVA virus clone and monitored for the development of CPE at 14 days post infection. A, Mock control in which the expression plasmid for the L protein was not added during transfection. B, image showing cells that were infected with the virus clone obtained after transfection with all the components of the RNP complex.

4.5.2.1 Assessment of the growth kinetics of recombinant EBOV OVA

The OVA ORF was inserted after the NP gene and therefore it stands to reason that all downstream viral genes may be downregulated resulting in the attenuation of the growth of EBOV OVA. To determine the growth properties of the newly rescued recombinant virus, Vero E6 cells were infected at a multiplicity of infection of 1 and supernatant collected at various time points after infection and immunofocus staining was then performed. The focus forming units were clearly visible and easy to quantify. The growth kinetics are similar to that of the wild-type virus and another recombinant virus EBOV GFP albeit EBOV OVA grew to slightly

lower titres compared to the other two between day 2 and day 6. The virus titres were essentially identical at day 7 post infection.

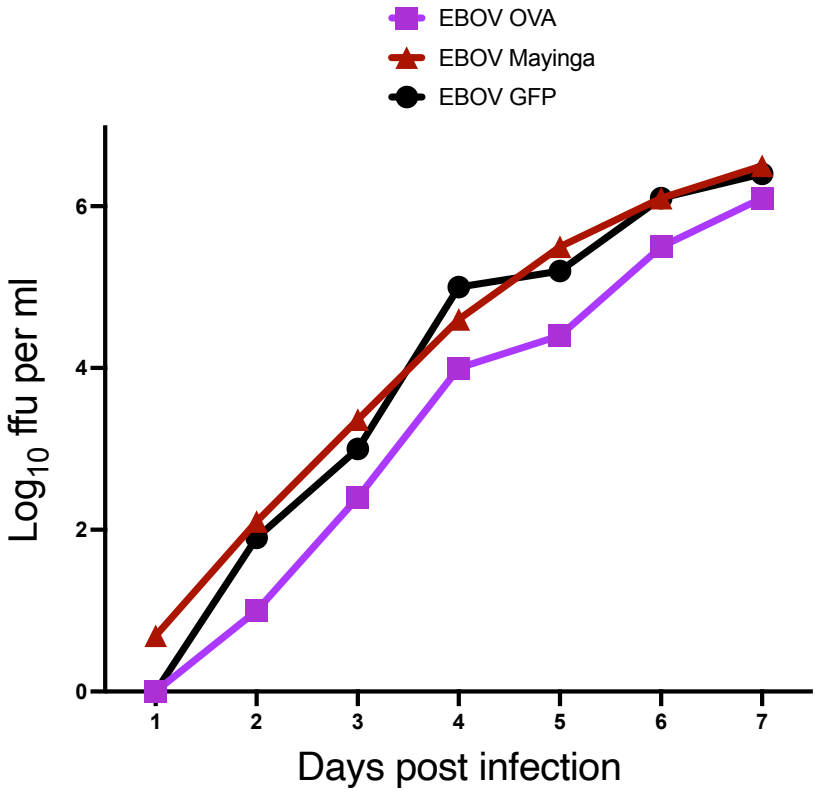

Figure 21: Multicycle growth kinetics of EBOV Mayinga, EBOV OVA and EBOV GFP.
Vero E6 cells were infected at a MOI of 1 and virus titres in the supernatants were determined by immunofocus assay at the time points indicated on the graph.

4.5.3 Targeting DCs with αmDEC205 OVA protects mice after challenge with EBOV OVA

The main goal of vaccination is to induce the development of memory T cells that can provide protection in the event of infection. Various studies have shown that memory T cells can persist for years after infection, in some instances for life. In mice, memory T cells that are still present after the contraction phase have been shown to persist for the life span of the host (Homann et al., 2001). The low number of naïve precursor T cells and antigen-specific T cells generated during the endogenous response poses a hurdle to the characterisation of the T cell response after vaccination. The OT-I mouse model enables the detection and characterisation of antigen-

specific T cells. A large number of cells can be transferred which facilitates the characterisation of the response to vaccination and infection.

To identify and characterise the T cell response and further to determine whether the induced T cells are functional, adoptive transfer experiments of OT-I T cells were performed. WT → IFNAR$^{-/-}$ chimaeras were immunized with the isotype control or αmDEC205 OVA and αCD40 according to the established immunization regimens described in previous sections. One day after the prime dose, 4x10^{6} OT-I T cells were transferred to immunized mice. At day 28, the mice were immunized again and were infected with EBOV OVA 14 days later. 3 mice from each group were euthanized at day 3 and 7 post infection to analyse the kinetics of the antigen-specific T cell response.

A

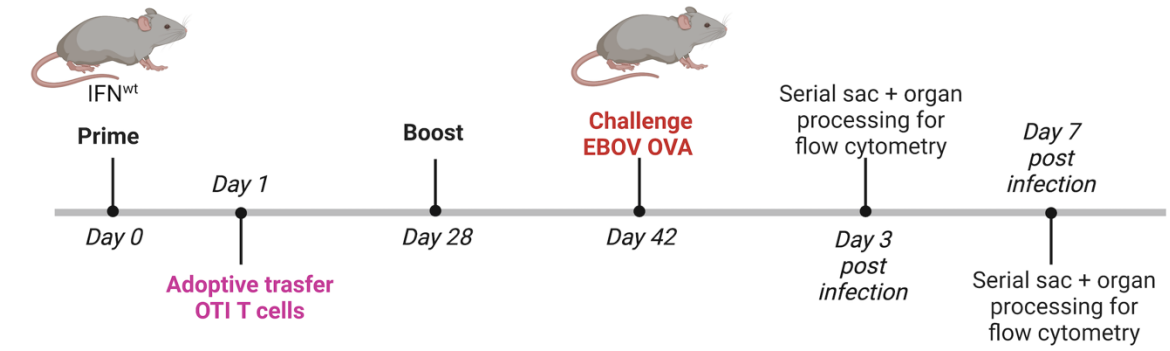

B

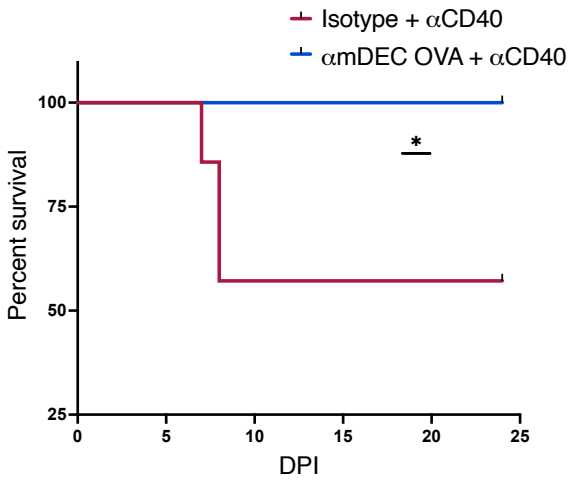

C

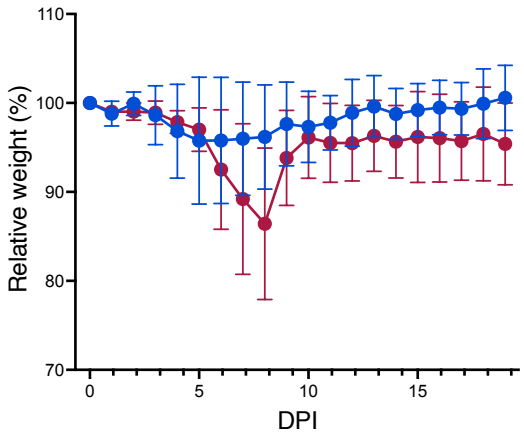

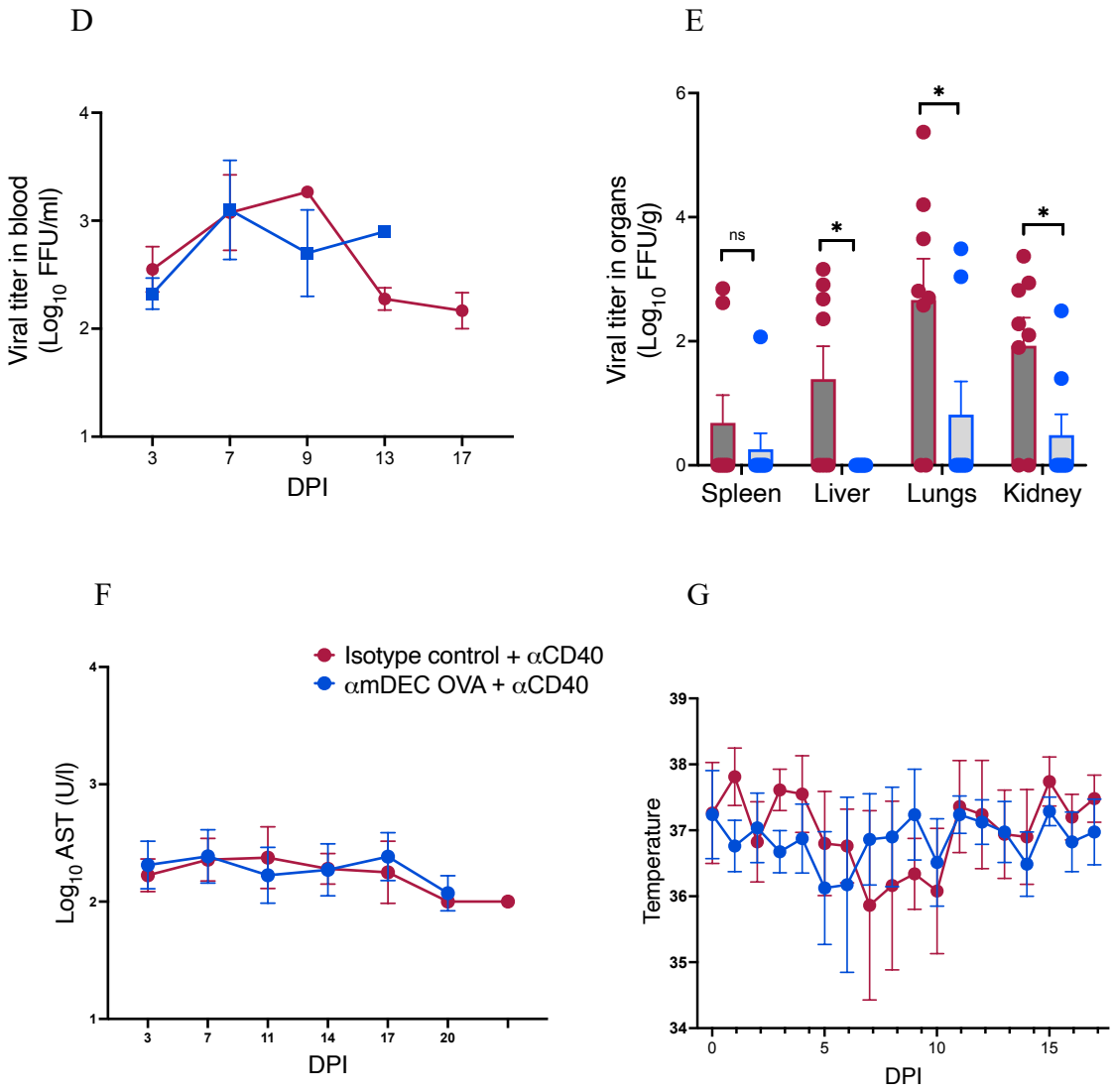

Figure 22: Targeting OVA to DEC205^{+} DCs results in 100 % survival and lower viral titres in the organs.

Male and female WT → IFNAR$^{-/-}$ mice (n = 14) were immunized with either the isotype control or αmDEC205 OVA together with 25 µg αCD40 according to the immunization regimen shown in the schematic (A). 1 day later, 4x10^{6} OT-I T cells were transferred to the mice. At 28 days post immunization, the mice received a boost with the targeting antibodies and 25 µg αCD40. 14 days later, the mice were infected with EBOV OVA. Serial sacs of 3 mice from each group were performed at 3 and 7 days post infcetion. Monitoring was done for 21 days and mice that reached the humane endpoint criteria were euthanised. Blood was obtained at intervals of 3-4 days to determine viremia and liver enzyme levels. Graphs show Kaplan Meier survival curves (B), weight (C), viremia (D) viral titers in the the spleen, liver, lungs and kidney at endpoint (E), liver AST levels (F) and temperature (G). Values are reported as mean ± SEM. Statistical significance was determined using Mantel-Cox test (B) or unpaired two-tailed Student's *t*-test (C-G). (ns – not significant, *$p \leq 0.05$, **$p \leq 0.01$, ***$p \leq 0.001$).

Immunization with αmDEC205 OVA protected mice form lethal infection with EBOV OVA. 100 % of the mice immunized with the targeting antibody survived whereas three out of eight mice (75 %) in the control group reached the predetermined humane endpoint criteria and had to be euthanised (figure 21B). Additionally, the mice in the control group lost more weight in comparison to mice in the experimental group (figure 21C). Mice immunized with the isotype control also had higher viral titres in the organs with the highest titres being detected in the lungs (figure 21E). The isotype control group had higher levels of viremia between 9 and 14 days after infection and had not cleared the virus by the termination of the experiment at day 21 (figure 21D). In conrast, mice in the experimental group had lower viremia levels and did not have detectable virus in the blood from day 14 day onwards (figure 21D). AST levels were similar between the two groups albeit slightly higher levels were observed in the control group on day 7 and 11 (figure 21F).

4.5.4 Profile of the T cell response after antibody-mediated delivery

4.5.4.1 OT-I T cells expand and proliferate after immunization with αmDEC205 OVA and challenge with EBOV OVA

The induction of antigen-specific T cells is a main feature of DC-based vaccination. The endogenous T-cell response to vaccination and infection begins from low numbers of naïve precursors and is very diverse even when generated in response to a single antigen. TCR-transgenic T cells are specific for a single epitope of an antigen and are 1,000 to 100,000-fold higher than the corresponding endogenous naïve T cell frequency. This makes them easier to identify or track after vaccination or infection (Harty and Badovinac, 2008).

To better elucidate the phenotype of the cells involved in conferring protection to virus challenge, experiments to track the effector CD8 T cell populations after infection with EBOV OVA were performed. WT → IFNAR$^{-/-}$ were infected as described in section 4.5.3. 3 mice from each group were sacrificed 3 and 7 days after infection. The lungs and spleen were harvested and processed to obtain cells.

OT-I T cells were identified using MHC class I tetramers and the OT-I T cell response was assessed by flow cytometry.

A

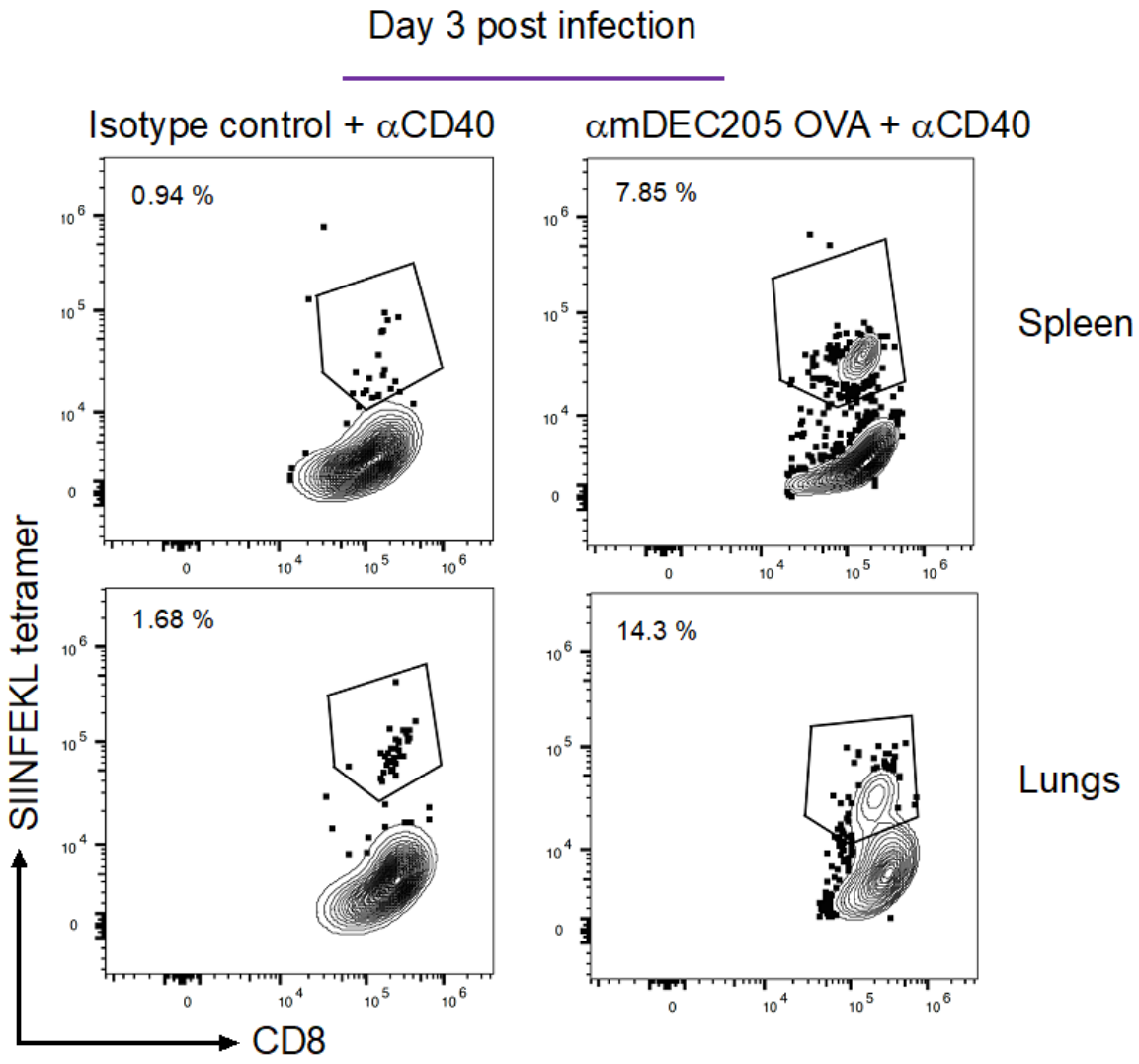
Day 3 post infection
Isotype control + αCD40
αmDEC205 OVA + αCD40
0.94 %
7.85 %
1.68 %
14.3 %
Spleen
Lungs
SIINFEKL tetramer
CD8

B

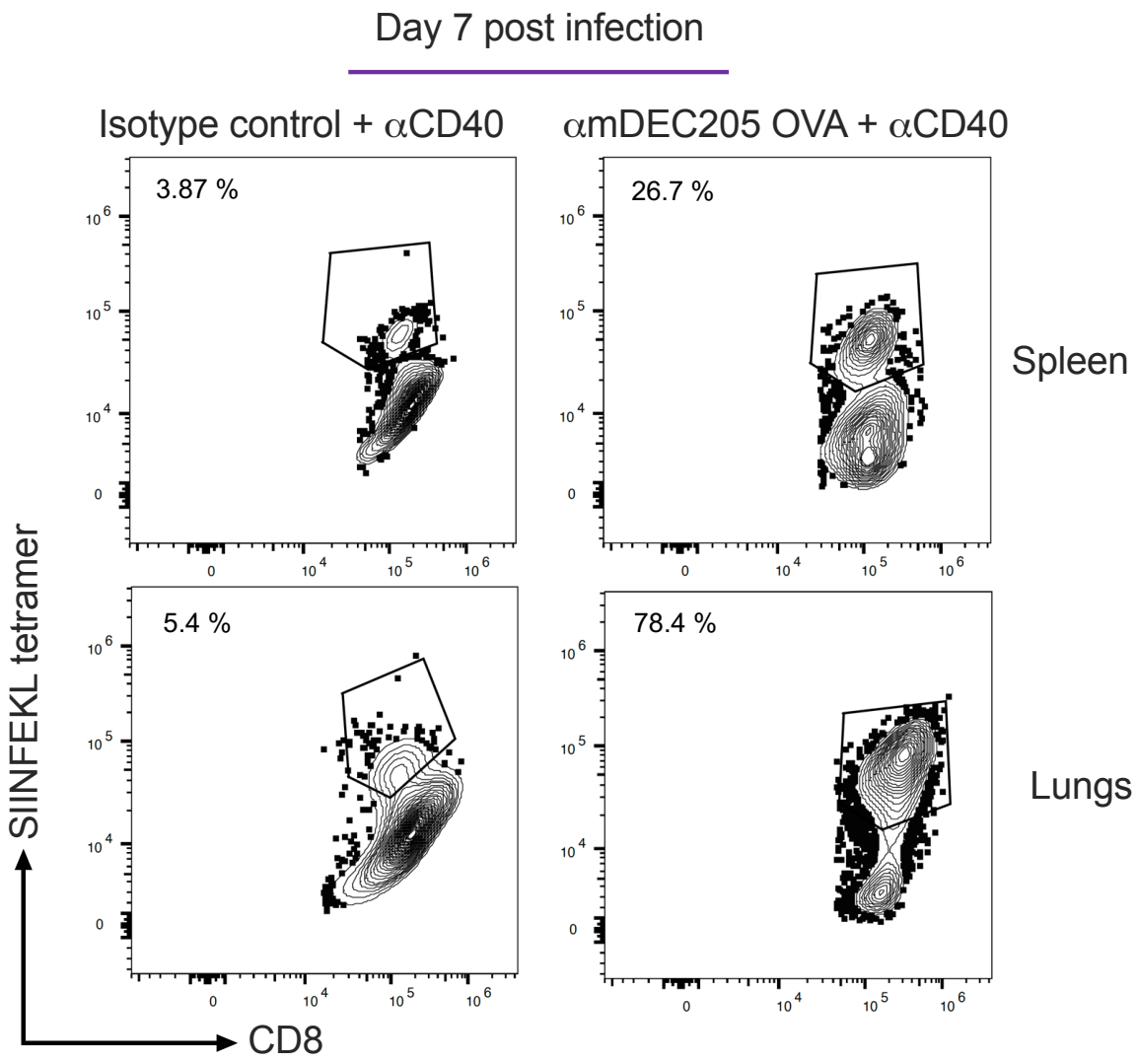
Day 7 post infection
Isotype control + αCD40
αmDEC205 OVA + αCD40
3.87 %
26.7 %
5.4 %
78.4 %
Spleen
Lungs
SIINFEKL tetramer
CD8

C

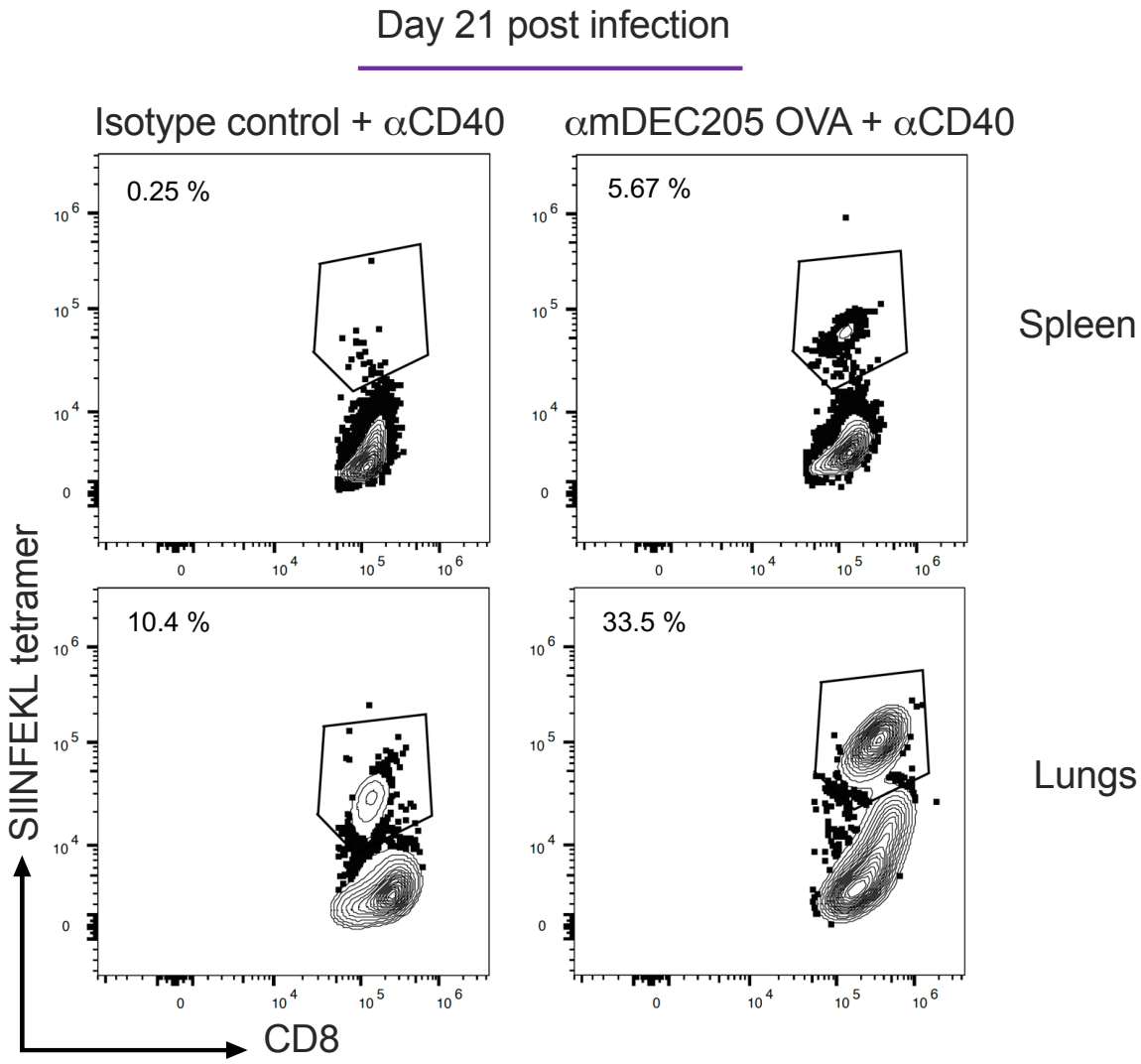
Day 21 post infection
Isotype control + αCD40
αmDEC205 OVA + αCD40
0.25 %
5.67 %
10.4 %
33.5 %
Spleen
Lungs
SIINFEKL tetramer
CD8

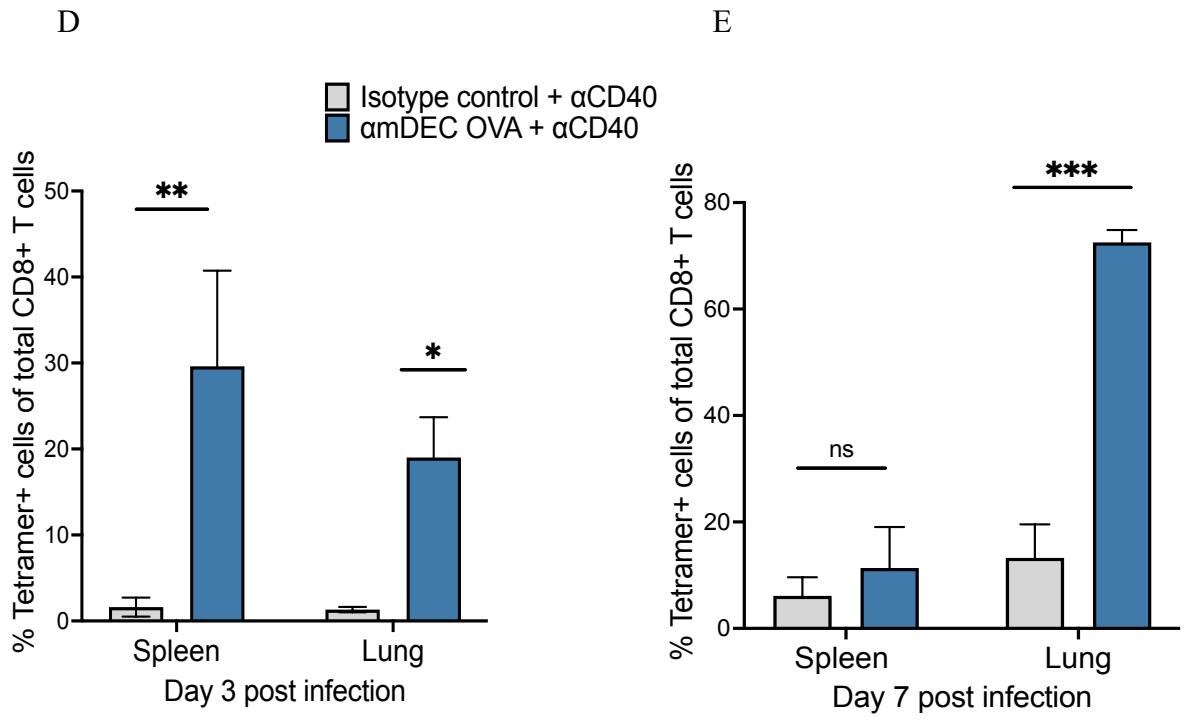

Figure 23: OT-I T cells in mice immunized with αmDEC205 OVA robustly expand after infection with EBOV OVA.

Mice were euthanized at 3- and 7-days post infection and at endpoint and the spleen and lung obtained and processed for flow cytometric analysis. Representative dot plots show the percentage of tetramer positive (SIINFEKL) $CD8^+$ T cells in the spleen and in the lungs (figure 22A-C) of mice immunized with the isotype control or αmDEC205 OVA. Bar graphs show the percentage of OT-I T cells in total $CD8^+$ T cells at day 3 and 7 post infection and the values are reported as mean ± SEM (figure 22D & E). Statistical significance was determined using unpaired Student's t-test. (ns – not significant, $*p \leq 0.05$, $**p \leq 0.01$, $***p \leq 0.001$).

OT-I T cells from mice immunized with αmDEC205 OVA robustly proliferated and expanded after infection both in the spleen and lungs. At day 3 post infection, the percentage of antigen-specific OT-I T cells both in the spleen and lung was more than double that observed in mice immunized with the isotype control antibody (figure 22A and D). The frequency of OT-I T cells was higher in the lungs compared to the spleen at day 7 post infection in both groups (figure 22E). However, the frequency of OT-I T cells was still significantly higher in the group that got the targeting antibody with the frequency of OT-I T cells in mice immunized with αmDEC205 OVA almost being triple that observed in the lungs of the mice in the isotype control group (figure 22E).

4.5.4.2 There is a higher frequency of MPECs after antibody-mediated delivery of antigen to DCs

Having shown that there is a strong and sustained expansion of OT-I T cells after immunization with αmDEC205 OVA and subsequent infection with EBOV OVA, the T cell response involved in protection was further elaborated by phenotyping the responding T cells. Viral infections drive $CD8^+$ T cells to differentiate into effector cells. Activation of $CD8^+$ T cells undergo metabolic and transcriptional changes which determine the effector status upon differentiation (Verdon et al., 2020). SLECs are characterised by the expression of KLRGI and undergo terminal differentiation. These cells are short-lived and are responsible for clearing viral infections following which they contract by apoptosis (Joshi et al., 2007). During the peak of an acute infection, a proportion of the responding CD8 T cells upregulate or retain CD127. CD8 T cells that upregulate this marker during an ongoing infection continue on to form the functional memory CD8 T cell pool (Kaech et al., 2003; Plumlee et al., 2015; Schluns et al., 2000).

MPECs are retained within secondary lymphoid organs, are long-lived and are able to robustly expand upon secondary antigen encounter (Kaech et al., 2003). To determine the phenotype of responding OT-I T cells, flow cytometry staining was done.

A

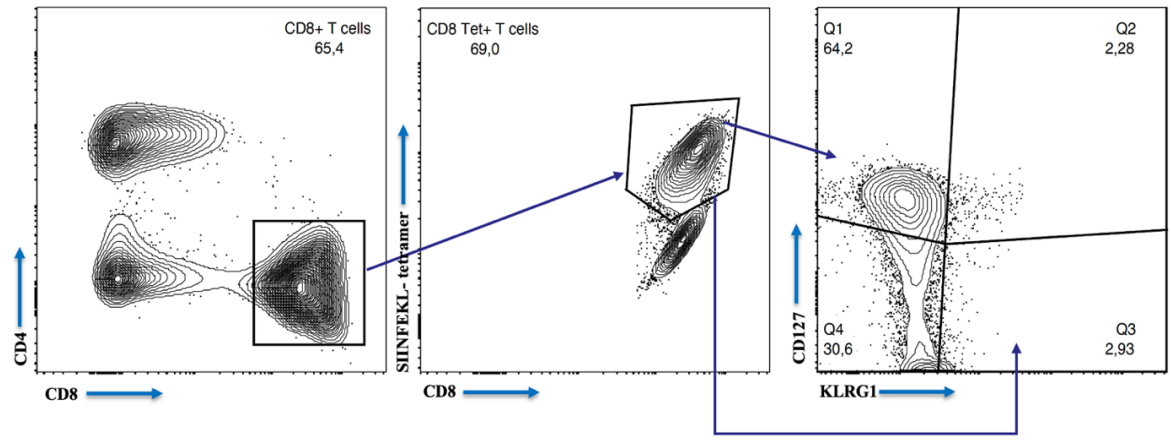

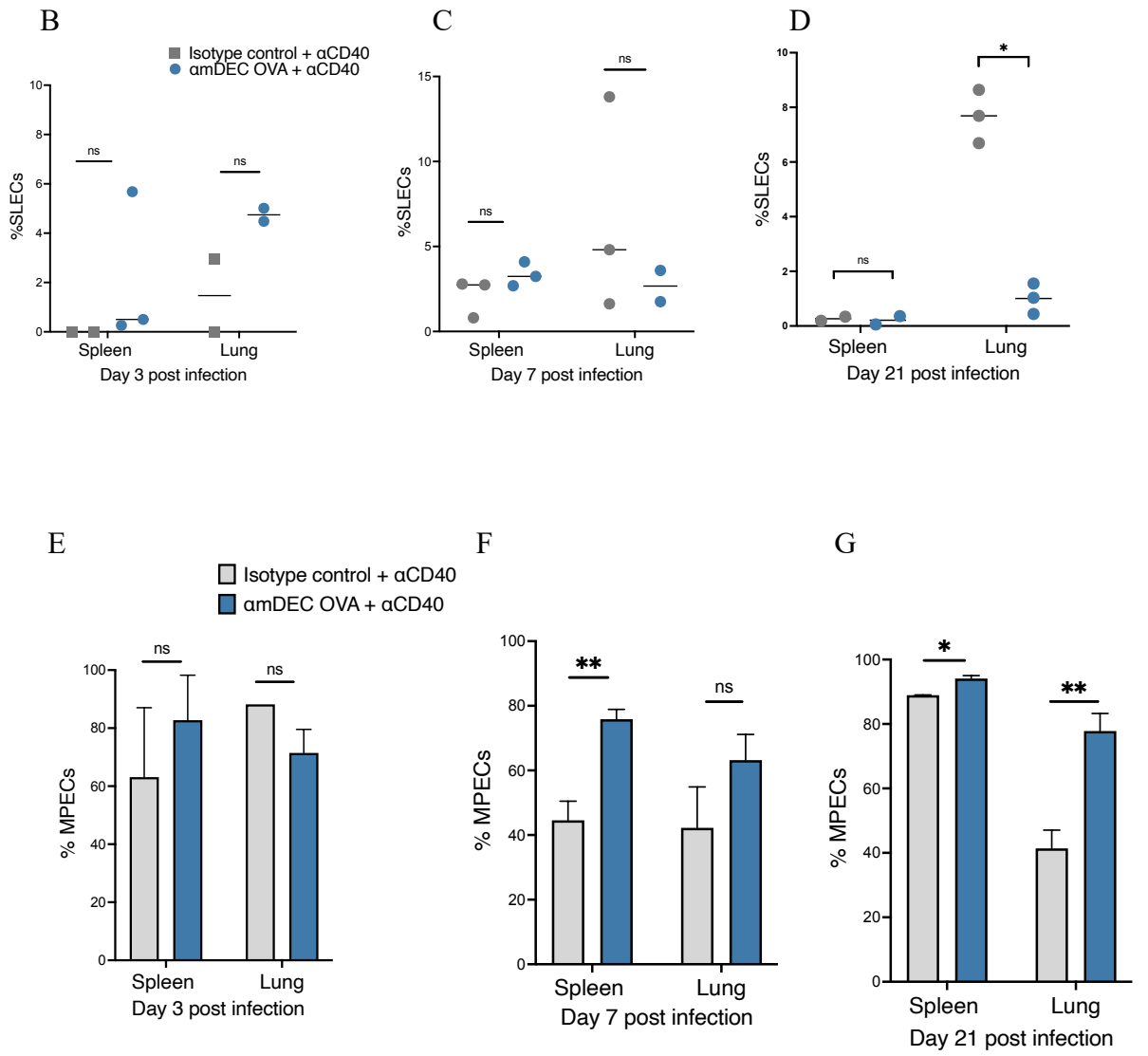

Figure 24: Antigen-specific T cells differentiate into memory cells after antibody-mediated delivery of OVA.

Differentiation of OT-I T cells into memory T cells was monitored in the spleen and lung following infection with EBOV OVA (A-E). Representative flow cytometry dot plots showing the expression of KLRG1 and CD127 markers used to delineate SLECs ($KLRG1^{+}CD127^{-}$) and MPECs ($KLRG1^{-}CD127^{+}$) (A). Graphs showing the frequencies of SLECs (B, C, D) and MPECs (E, F, G) in the indicated tissues at 3-, 7- and 21-days post infection. Values in the scatter and bar graphs are reported as mean ± SEM. Statistical significance was determined using unpaired Student's t-test (ns – not significant, $*p \leq 0.05$, $**p \leq 0.01$, $***p \leq 0.001$).

Flow cytometric analysis of the OT-I T cells from immunized mice revealed that there was a preponderance of memory precursor effector cells following infection. The frequency of SLECs in the spleen and lungs, though similar in both groups trended slightly higher in the αmDEC205

OVA immunized group on day 3 and 7 post infection (figure 23A and B). Interestingly, the frequency of SLECs was overall lower compared to the frequency of MPECs (figure 23B-G). The frequency of MPECs was similar in both groups 3 days after infection. However, this changed at day 7 post infection, which coincides with the start of the peak of EBOV infection. A higher frequency of OT-I T cells expressing CD127 was observed in both the lung and spleen of mice immunized with αmDEC205 OVA at 7- and 21-days post infection.

Acute infections in both humans and mice result in $CD127^{hi}$ virus specific-$CD8^+$ T cells. At the peak of infection, approximately 5 % - 20 % of antigen-specific effector $CD8^+$ T cells express CD127.

This indicates that antibody mediated delivery of EBOV NP to $DEC205^+$ DCs program activated $CD8^+$ T cells to predominantly differentiate into MPECs.

4.5.4.3 $CD8^+$ T cells differentiate into tissue resident memory T cells after infection

A major component of vaccine induced protection is the generation of memory T cells. Resident memory T cells were recently identified and have been shown to populate non-lymphoid tissue where they reside without recirculating in the blood (Wu, Shen, Jiang and Lu, 2018). T_{RM} T cells are able to rapidly respond to infection curtailing its spread to other sites. CD103 and CD69 are markers that are frequently used to delineate T_{RM} populations. Various studies have shown that CD8 T_{RM} are generated and retained in different tissues and are involved in protection against viral infections such as herpes simplex virus in the skin and restrict the spread of influenza virus from the upper respiratory tract to the lungs (Gebhardt et al., 2009; Pizzolla et al., 2017).

To determine whether $CD8^+$ T_{RM} are generated and retained in the lungs after antibody-mediated delivery of antigen, the expression of T_{RM} markers by $CD8^+$ T cells in the lung and spleen was assessed by flow cytometry.

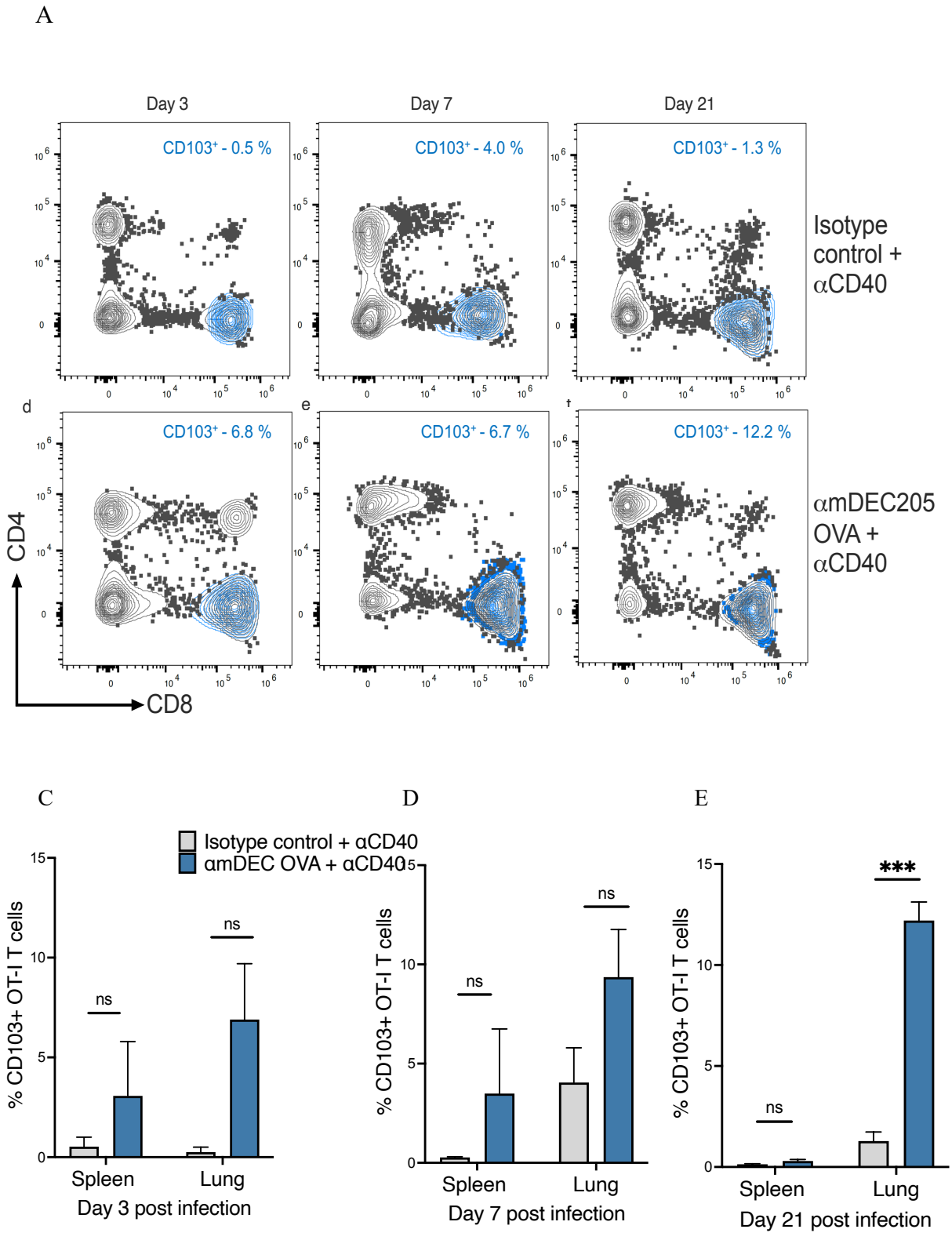

Figure 25: Targeting OVA to dendritic cells results in the generation of tissue resident memory cells.

Generation of $CD8^+$ T_{RM} cells in the spleen and lung was monitored after infection with EBOV OVA (A-F). Representative flow cytometry dot plots showing the proportion of $CD103^+$ T_{RM} cells in the lung at day 3, 7 and 21 post infection. Bar graphs showing the frequency of $CD8^+$ T_{RM} in the spleen and lungs at 3, 7 and 21 days after infection. Bar graphs represent the mean ± SEM. Statistical significance was determined using unpaired Student's t-test (ns – not significant, *$p \leq 0.05$, **$p \leq 0.01$, ***$p \leq 0.001$).

There was a higher induction of $CD8^+CD103^+$ memory T cells in the mice that were immunized with the targeting antibody (figure 24 C-E). The frequency of T_{RM} in the lungs increased from day 3 to day 7. The frequency of T_{RM} was significantly higher at day 21 which coincides with the convalescent phase and the resolution of infection (figure 24 E). The frequency of T_{RM} in the lungs of αmDEC205 OVA immunized mice was almost triple that observed in the isotype control group. These findings suggest that targeting EBOV NP to DCs is a useful strategy for the induction of antigen specific T_{RM} and indicates vaccination success. This highly suggests that these T_{RM} would be able to mediate protection in the event of a second exposure to EBOV.

4.5.4.4 Antibody-mediated antigen delivery results in the induction of Granzyme B^+ memory effector T cells.

Granzyme B (GrB) is a serine protease that plays major role in the response of $CD8^+$ T cells to viral infections. GrB is secreted by activated $CD8^+$ T cells and mediates cellular apoptosis of virus infected cells. GrB is stored in cytolytic granules in $CD8^+$ T cells and is released upon antigenic stimulation, however only a small fraction is secreted per cell, which allows $CD8^+$ T cells to act as "serial killers" (Nowacki et al., 2007). In combination with tetramer staining, it is possible to identify *in vivo* activated antigen-specific T cells by detecting intracellular stored GrB (Appay and Rowland-Jones, 2002).

To identify *in vivo* activated memory $CD8^+$ T cells, the expression of GrB was assessed by intracellular staining of cells obtained from the spleen and the lungs of immunized and infected mice.

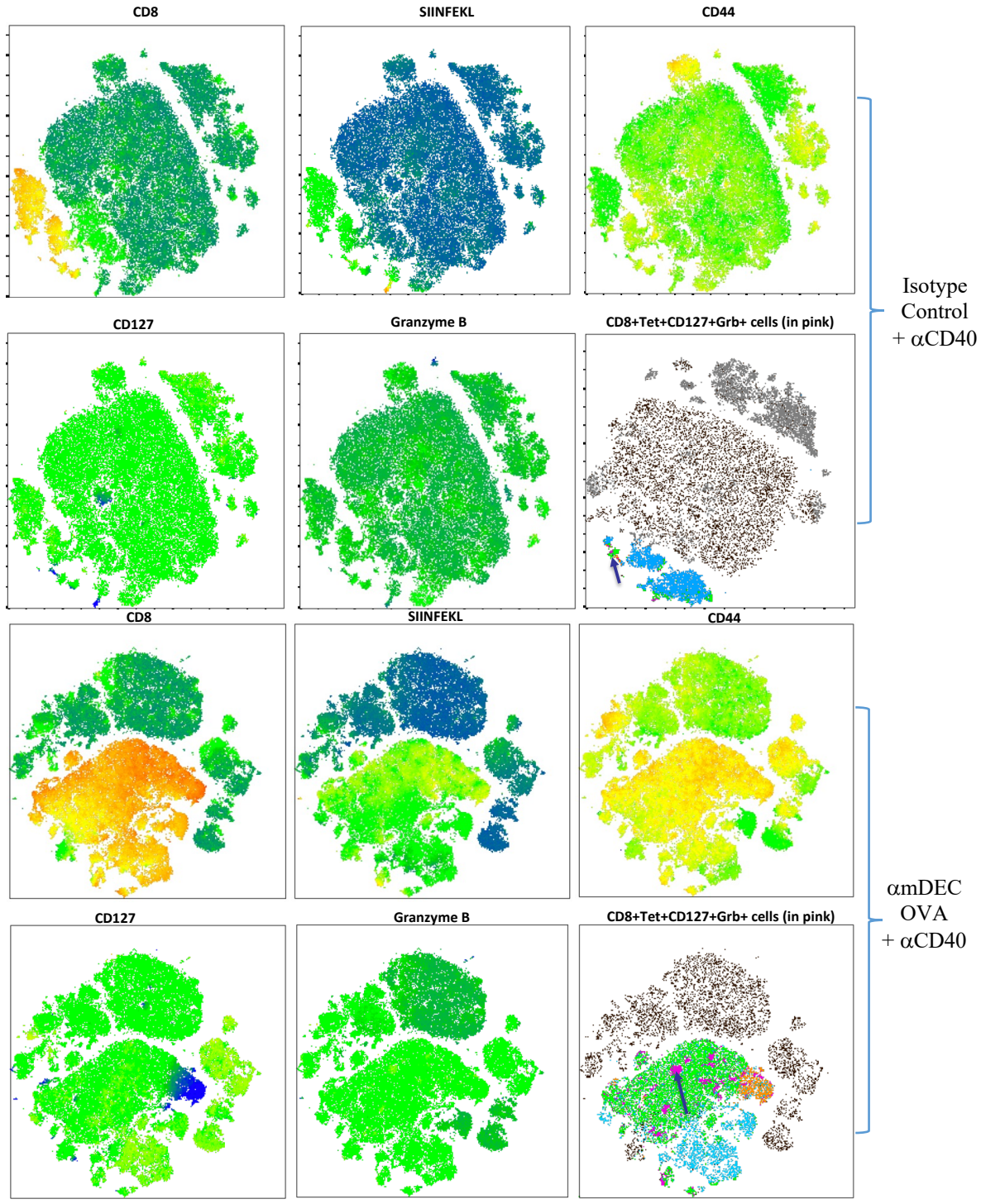

Figure 26: CD127^{+}OT-I T cells express the effector molecule Granzyme B at the peak of infection. The lungs and spleen were obtained from mice infected with EBOV OVA as described in prior sections. The cells were processed and intracellular staining for flow cytometry analysis performed. tSNE plots built on antigen specific CD8, CD44, CD127 and GrB. Plots show the lungs of mice sacrificed at day 7 post infection immunized with the isotype control (A) or αmDEC205 OVA (B).

Higher expression of GrB by antigen-specific CD8+ T cells was detected in mice immunized with αmDEC205 OVA in comparison to those immunized with the isotype control. Additionally, the highest amounts of GrB were detected at day, which coincides with the peak of infection.

Taken together, the results described above indicate that delivery of antigens using monoclonal antibodies is a viable strategy to induce the generation and retention of functional memory T cells and that these memory T cells play a role in protecting mice from lethal EBOV challenge.

4.6 Mice immunized with αmDEC205 EBOV NP develop anti-EBOV NP IgG antibodies

The magnitude of GP binding and neutralising antibodies generated during the course of infection is correlated with survival during EVD. Potent pan-EBOV GP neutralising antibodies have been isolated from EVD survivors and the administration of these antibodies after infection resulted in the survival of lethally-challenged ferrets and macaques (Bornholdt et al., 2019; Wec et al., 2017). Virus-specific antibodies have been detected in survivors up to a decade after initial infection, however it is not yet known whether these antibodies can protect against reinfection (Sobarzo et al., 2013; Corti et al., 2016) Anti-NP and anti-VP40 IgG antibodies are the most abundantly produced during natural infection, which in turn could be explained by the high concentration of these proteins produced in the course of infection (Davis et al., 2019; Ilinykh and Bukreyev, 2021) and the virus load decreases about 1 week following infection, which coincides with development of virus-specific IgG (Vernet et al., 2017).

DC targeting in the presence of an adjuvant induces the development of T helper cells including $CD4^+$ Tfh cells that interact with B cells providing the appropriate help resulting in the development of antigen-specific B cells that can differentiate into antibody-secreting cells. Tfh cells also produce cytokines that are necessary for antibody class switching.

To investigate whether DC targeting would result in the development of EBOV NP specific IgG antibodies, sera was obtained from infected mice at euthanasia endpoint and a direct ELISA was performed to determine antibody titres.

A

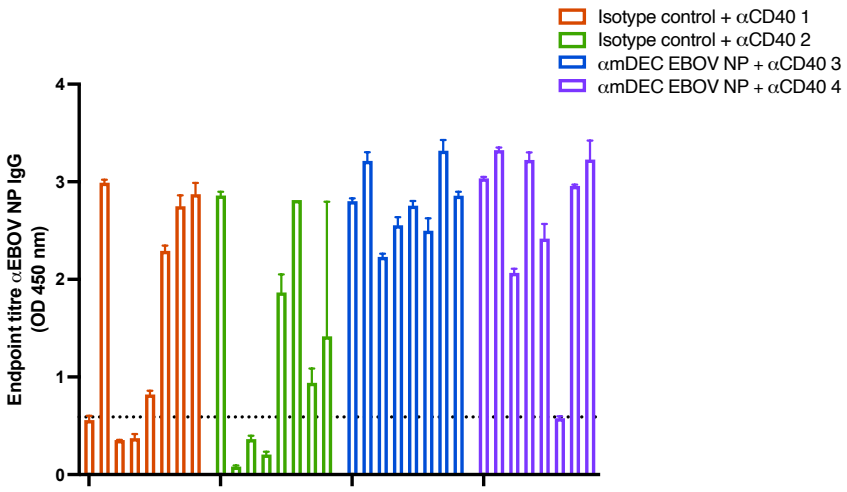
Isotype control + αCD40 1
Isotype control + αCD40 2
αmDEC EBOV NP + αCD40 3
αmDEC EBOV NP + αCD40 4
Endpoint titre αEBOV NP IgG (OD 450 nm)
0
1
2
3
4

B

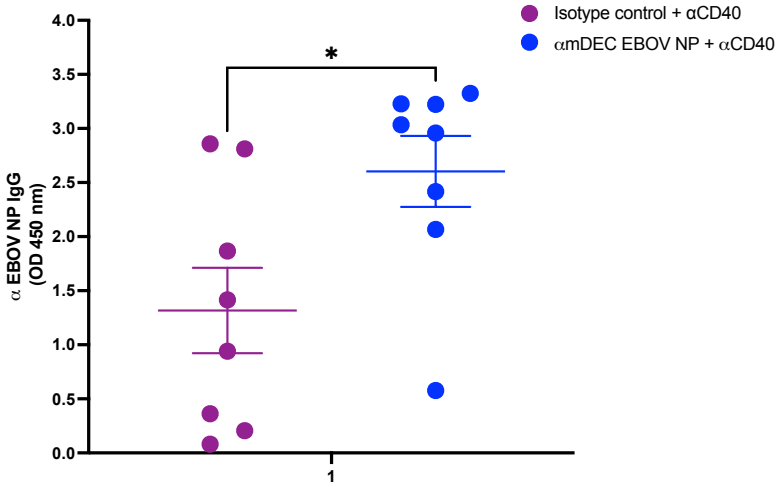
Isotype control + αCD40
αmDEC EBOV NP + αCD40
α EBOV NP IgG (OD 450 nm)
*
0.0
0.5
1.0
1.5
2.0
2.5
3.0
3.5
4.0
1

C

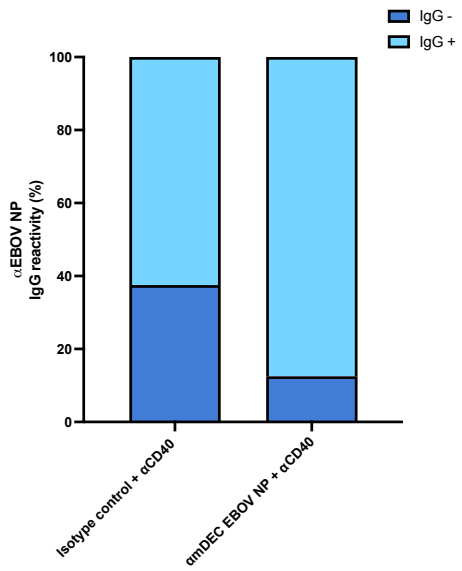

Figure 27: αmDEC205 EBOV NP have higher titres of EBOV NP-specific IgG.

Endpoint IgG titres were determined using ELISA. Endpoint IgG titres are expressed as OD values against EBOV NP determined from positive and negative serum samples. Cut-off value = 0.59 (dotted horizontal line) (A) Absorbance values obtained from individual serum samples of the control or treatment groups (B). Values are reported in the form of bar and scatter graphs displaying mean ± SEM. Statistical significance was calculated using the Mann-Whitney test (*$p \leq 0.05$, **$p \leq 0.01$, ***$p \leq 0.001$) (C). Total percentage of serum samples showing IgG positive (light blue) or negative (dark blue) OD values against EBOV NP. Data are from 2 independent experiments.

All the mice except one in the αmDEC205 EBOV NP immunized group developed anti-EBOV NP specific antibodies higher than the determined cut-off value while five out of eight mice in the control group had measurable antibodies against NP (figure 18 A). Mice in the experimental group had significantly higher anti-EBOV NP IgG titres (figure 18 B) and a higher proportion of IgG positive mice in comparison to the control group (figure 18 C).

Taken together, these results show that targeting EBOV NP to DEC205$^+$ DCs confers protection against EBOV challenge and that the protection is in part mediated by the generation of antibodies against EBOV NP.

4.7 Evaluation of the cross-protective capacity of αmDEC205 EBOV NP

Based on the results in previous sections, the capacity of the αmDEC205 antibodies to protect against other members of the filovirus family was evaluated. SUDV has been responsible for outbreaks in Uganda and South Sudan with CFRs of up to 50 %. Another outbreak of SUDV occurred beginning in September of 2022. There is currently no licensed vaccine against SUDV.

MARV was the first filovirus to be discovered and has been responsible for outbreaks in Eastern and Southern Africa with CFRs of up to 90 % and as of 2022 and similar to SUDV there is no licensed vaccine against MARV.

Broadly protective vaccines are highly desirable and could play a vital role in the reduction and ultimate elimination of filovirus outbreaks. It was hypothesised that the DC targeting platform could potentially be used for pan-filovirus prophylaxis.

4.7.1 Multiple sequence alignment to determine similarity between EBOV NP and SUDV NP

The protein-coding sequences of filovirus nucleoproteins are highly conserved and to determine the level of similarity in the NP sequence between the viruses, multiple sequence alignments were performed to visualize the percentage of conserved sequences.

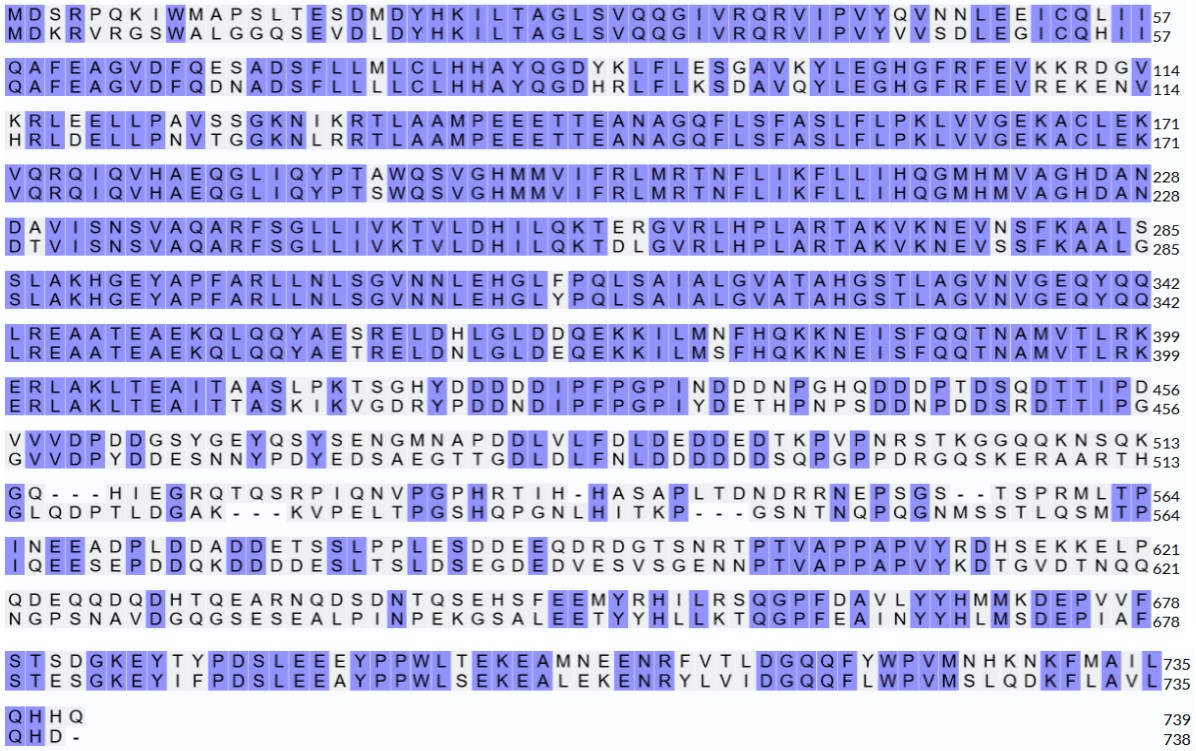

Figure 28: There is a high degree of similarity between the nucleoprotein of EBOV and SUDV.

The reference protein sequences of EBOV NP and SUDV NP were obtained from NCBI protein and aligned using the Align tool on Uniprot. Regions of similarity are shown in blue.

Multiple alignment of the sequences reveals that there is approximately 70 % (67.2 %) sequence identity in the NP of the two viruses.

In view of this, experiments to establish whether the targeting antibodies could confer protection to mice challenged with SUDV were performed.

4.7.2 αmDEC205 EBOV NP is not cross-protective

To assess the cross-protective capacity of αmDEC205 EBOV NP against SUDV, mice immunized with αmDEC205 EBOV NP were challenged with SUDV Gulu strain and monitored for 21 days.

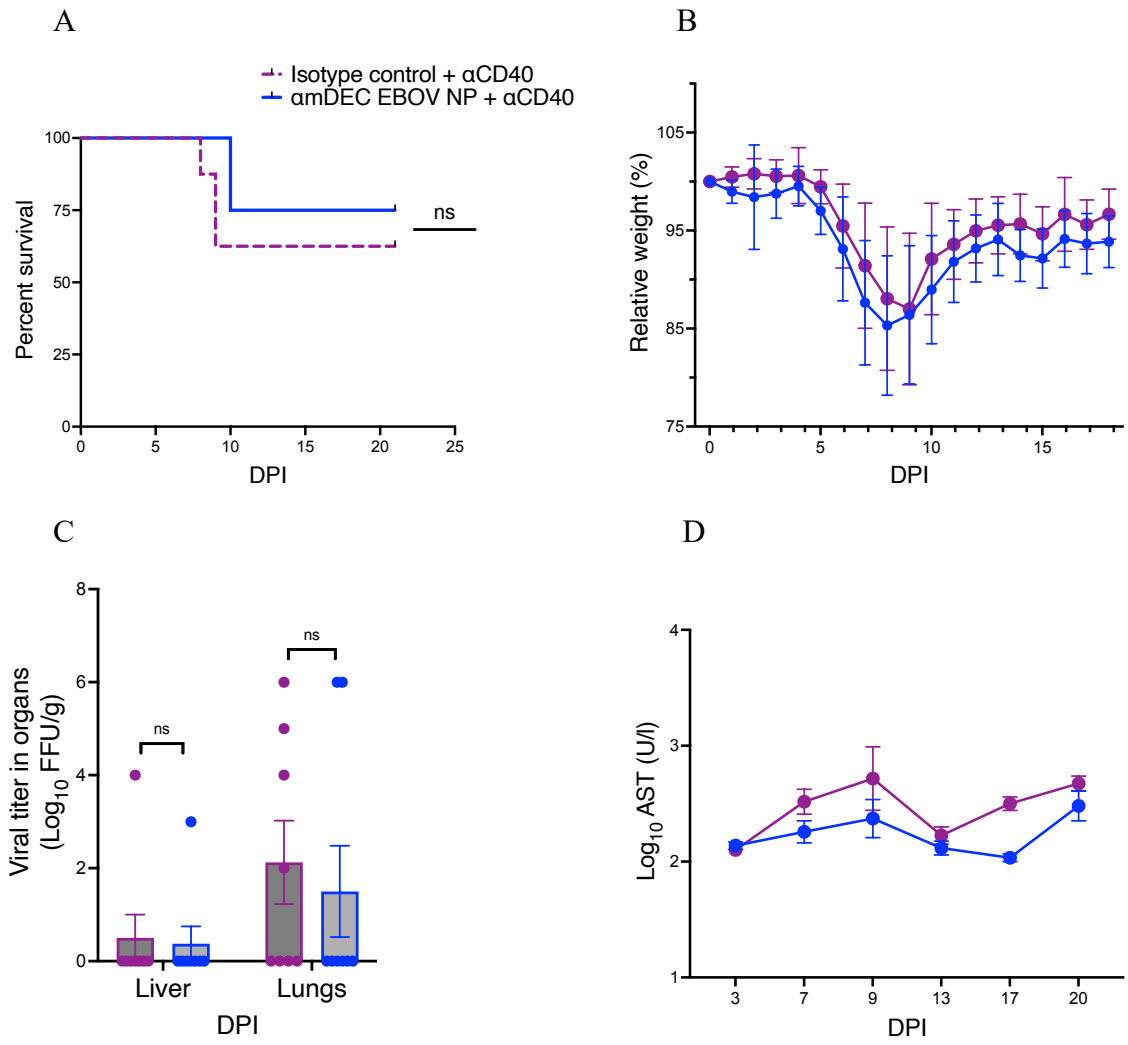

Figure 29: Targeting EBOV NP to DEC205$^+$ T cells does not confer protection to challenge with SUDV.

Male and female WT → IFNAR$^{-/-}$ mice (n = 8) were immunized with either the isotype control or αmDEC205 EBOV NP together with 25 µg αCD40 according to the immunization regimen previously described. At 28 days post immunization, the mice received a boost with the targeting antibodies and 25 µg αCD40. 14 days later, mice were infected intranasally with 10,000 FFU SUDV. Mice were monitored for 21 days and those that reached humane endpoint criteria were euthanised. Blood was obtained at intervals of 3-4 days to determine viremia and liver enzyme levels. Graphs show Kaplan Meier survival curves (A), weight (B), viral titres in the organs (C) and liver AST levels (D). Values are reported as mean ± SEM. Statistical significance was determined using Mantel-Cox test (A) or unpaired two-tailed Student's *t*-test (C and D) (ns – not significant, *$p \leq 0.05$, **$p \leq 0.01$, ***$p \leq 0.001$).

There were no significant differences in survival nor viral titres between the control group and the treated group. Targeting DCs with αmDEC205 EBOV NP resulted in 75 % survival after infection with SUDV. Four out of eight mice immunized with the isotype control had detectable viral titres in the lungs while virus was detected in only two out of eight mice immunized with αmDEC205 EBOV NP.

4.8 Evaluation of MARV in the WT → IFNAR$^{-/-}$ mouse model

There is a dearth of mouse models for use in studies on experimental MARV infection. The gold standard are non-human primates, which recapitulate the classical hallmarks of MVD in humans. Ferrets and hamsters are also commonly used but due to space and ethical constraints it is still necessary to evaluate other models. The IFN chimaera model allows the evaluation of morbidity, mortality as well as the immune response elicited to EBOV infection. To determine whether this model could be used in subsequent immunological studies involving MARV and whether the model would be suitable for vaccine studies, IFNAR$^{-/-}$ mice were first infected with MARV to determine its lethality in these mice. This would allow a baseline to be set thus allowing for a better characterisation of changes in survival.

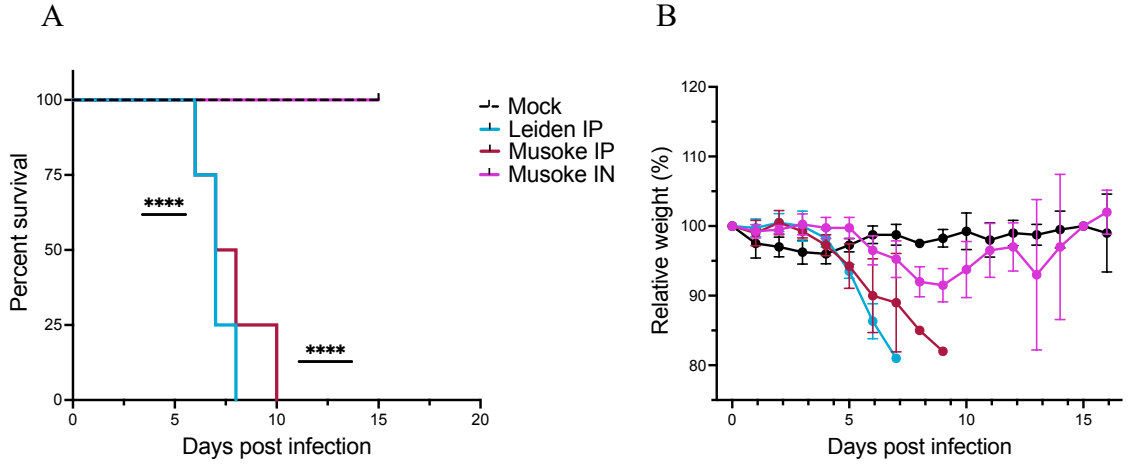

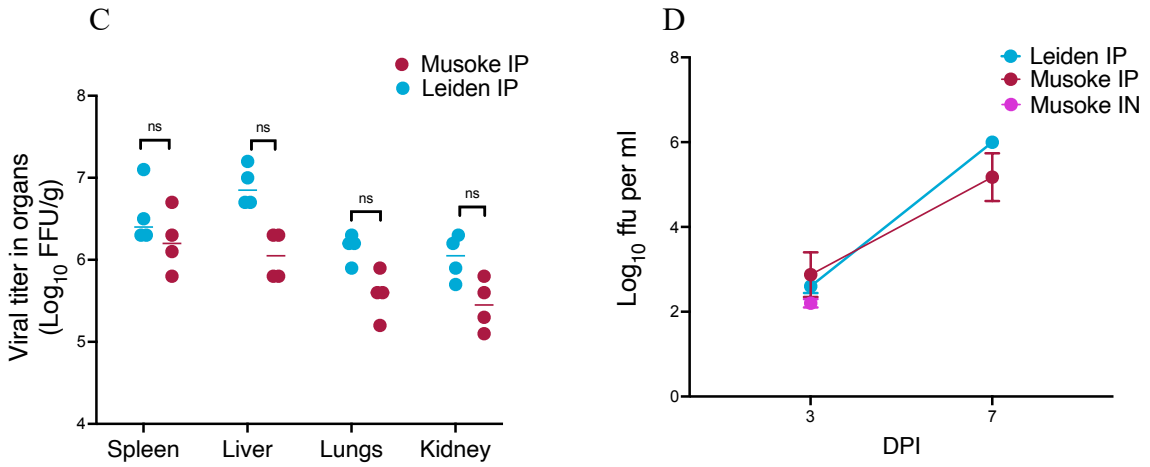

Figure 30: Intraperitoneal infection results in 100 % lethality in IFNAR$^{-/-}$ mice.

5-6 IFNR$^{-/-}$ mice were infected via different routes with 10,000 FFU MARV Musoke or MARV Leiden. Mice were monitored for 15 days and those that reached humane endpoint criteria were euthanised. Blood was obtained at intervals of 3-4 days to determine viremia and liver enzyme levels. Graphs show Kaplan Meier survival curves (A), weight (B), viral titres in the organs, (C) viremia (D) and liver AST levels (E). Values are reported as mean ± SEM. Statistical significance was determined using Mantel-Cox test (A) or Kruskall-Wallis test followed by Dunn's post-test (B and D) or unpaired two-tailed Student's *t*-test (C) (ns – not significant, *$p \leq 0.05$, **$p \leq 0.01$, ***$p \leq 0.001$).

Infection via the intraperitoneal route with both strains of MARV resulted in 100 % lethality in IFNAR$^{-/-}$ mice (figure 28 A). The virus replicated to high titres in these mice and was detectable in all the organs assessed (figure 28 C & D). MARV Leiden replicated to higher titres in the blood and organs compared to MARV Musoke. However, the difference in titres between the two strains was not significant (figure 28 C and D). Interestingly, all the mice infected intranasally survived the infection (figure 28 A). Transient weight loss was however observed in these mice (figure 28 B).

Based on these results, the level of lethality caused by MARV Musoke in IFN chimaeras was determined. WT → IFNAR$^{-/-}$ mice were infected intraperitoneally with MARV Musoke and monitored for 21 days.

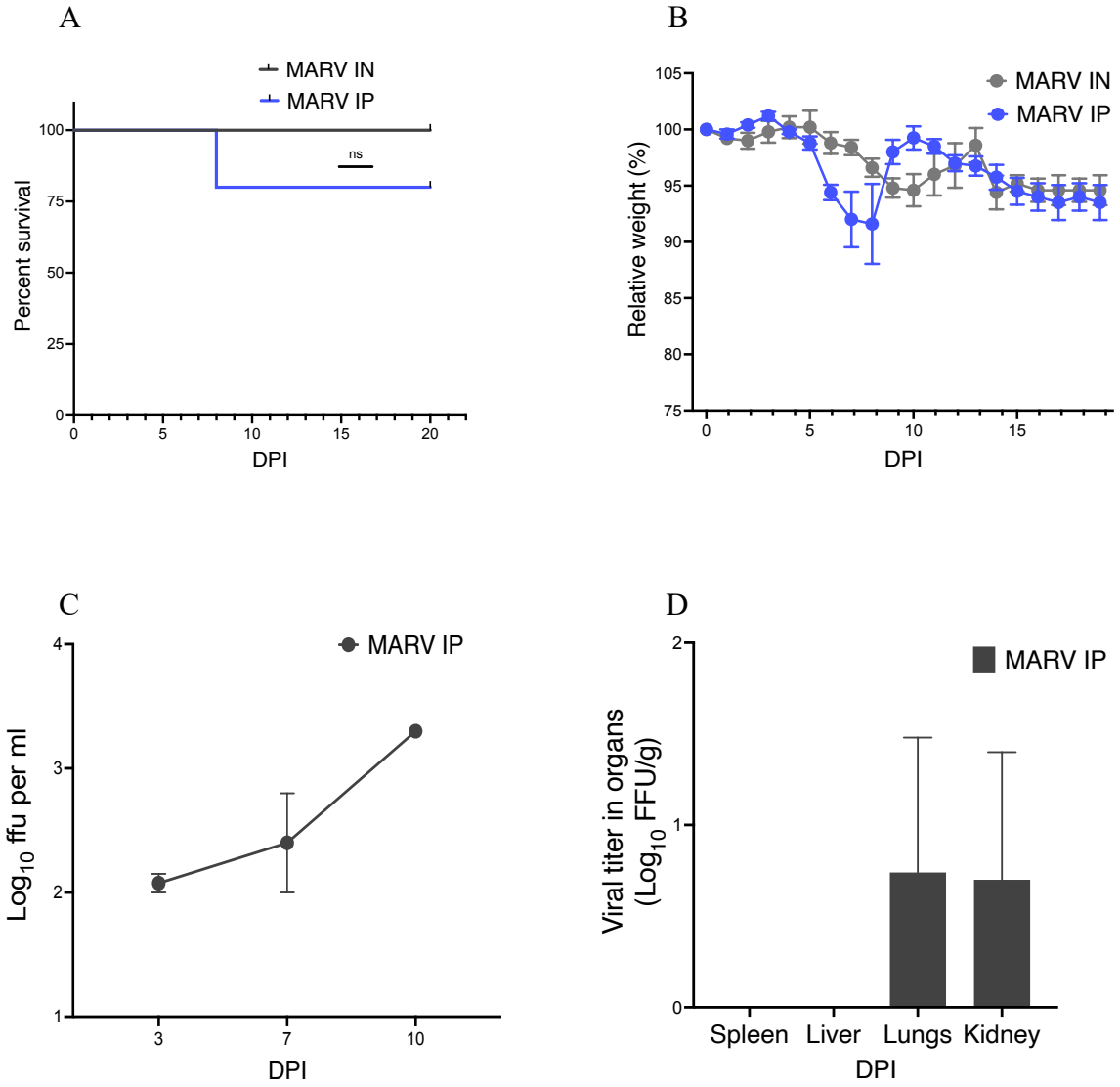

Figure 31: Intraperitoneal infection with MARV Musoke results in 20 % lethality in WT → IFNAR$^{-/-}$ mice.

5 IFNAR$^{-/-}$ mice were infected intranasally or intraperitoneally with 10,000 FFU MARV Musoke or MARV Leiden. Mice were monitored for 21 days and those that reached humane endpoint criteria were euthanised. Blood was obtained at intervals of 3-4 days to determine viremia and liver enzyme levels. Graphs show Kaplan Meier survival curves (A), weight (B), viral titres in the organs, (C) viremia (D) and liver AST levels (E). Values are reported as mean ± SEM. Statistical significance was determined using Mantel-Cox test (A) or unpaired two-tailed Student's *t*-test (B) (ns – not significant, *$p \leq 0.05$, **$p \leq 0.01$, ***$p \leq 0.001$).

All the mice challenged with MARV Musoke via the intranasal route survived the infection while MARV Musoke resulted in only 20 % lethality in the mice that were infected intraperitoneally. Transient weight loss was observed in both groups (figure 29 B). The mice that had been intranasally inoculated had a delayed onset of weight loss while mice inoculated intraperitoneally started losing weight at day 5 post infection ~3 days earlier and similar to what was observed for EBOV and SUDV infections (figure 29 B). Only the mice infected intraperitoneally had detectable viremia and virus was also detected in the organs albeit only in the lungs and kidney (figure 29 C and D).

4.8.1 Evaluation of the cross-protective capacity of αmDEC205 EBOV NP against other filoviruses

These findings show that MARV does indeed cause morbidity as displayed by the transient weight loss and is also lethal in the WT → IFNAR$^{-/-}$ model albeit causing much lower mortality compared to EBOV. Additionally, the virus also replicates in these mice resulting in detectable viral titres in the blood and some organs. Experiments to determine whether αmDEC205 EBOV NP had the capacity to not only protect mice after challenge with MARV but also whether there would be any effect on morbidity and virus titres after targeting were performed. To this end, WT → IFNAR$^{-/-}$ mice were immunized with αmDEC205 EBOV NP following the already established prime boost regimen.

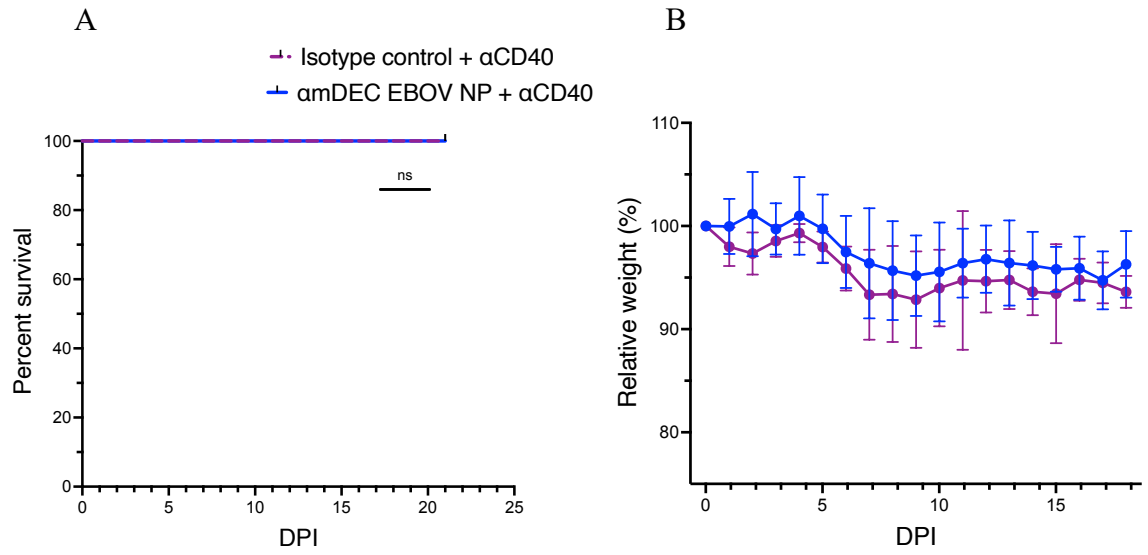

Figure 32: There are no significant differences between the control group and the experimental group after challenge with MARV.

Male and female WT → IFNAR$^{-/-}$ mice (n = 8) were immunized with either the isotype control or αmDEC205 EBOV NP together with 25 µg αCD40 according to the immunization regimen as previously described. At 28 days post immunization, the mice received a boost with the targeting antibodies and 25 µg αCD40. 14 days later, mice were infected intranasally with 10,000 FFU MARV. Mice were monitored for 21 days and those that reached humane endpoint criteria were euthanised. Blood was obtained at intervals of 3-4 days to determine viremia and liver enzyme levels. Graphs show Kaplan Meier survival curves (A), weight (B) and liver AST levels Values are reported as mean ± SEM. Statistical significance was determined using Mantel-Cox test (A) or unpaired two-tailed Student's *t*-test (B) (ns – not significant, *$p \leq 0.05$, **$p \leq 0.01$, ***$p \leq 0.001$).

Mice immunized with αmDEC205 EBOV NP displayed fewer signs of morbidity compared to the isotype control immunized mice as evidenced by the difference in weight loss (figure 30B). No virus was detected in the blood nor the organs.

5. Discussion

5.1 Summary

The objective of this study was to determine whether targeting of antigens to DCs could be used as a strategy to generate a T-cell based filovirus vaccine.

The main aim was to develop a vaccine that could be used to augment the T cell response during EBOV infection and to determine the role of T cell immunity in protection from secondary EBOV challenge.

Immunization with a DEC205 specific antibody conjugated to EBOV NP induced the development of functional EBOV NP specific $CD8^+$ T cells that secreted effector cytokines such as IFNγ and IL-2 upon re-stimulation. Immunization with αmDEC205 EBOV NP also conferred protection to susceptible mice challenged with EBOV. Immunized mice had reduced or no detectable viral titres in the organs as well as reduced viremia and AST levels in comparison to mice immunized with the isotype control vaccine. In addition, mice immunized with αmDEC205 EBOV NP developed high anti-EBOV NP IgG titres.

Using a novel recombinant EBOV harbouring the model antigen OVA, it was demonstrated that mice immunized with αmDEC205 OVA and subsequently infected with EBOV OVA had higher frequencies of OVA-specific T cells (OT-I) with the highest percentage at all time points observed in the lungs at the peak of infection. Flow cytometry analyses revealed that responding OT-I T cells predominantly differentiated into MPECs and that these cells were more abundant than SLECs. In addition, a high frequency of $CD103^+$ $CD8^+$ T cells, so called $T_{RM,}$ was observed in the lungs of vaccinated mice with the highest frequency detected at 21 days post infection. The induction of mucosal memory T cells is a major determinant of vaccination success, and the data from this study suggests that T_{RM} cells generated after immunization with αmDEC205 EBOV NP may mediate protection in case of re-exposure. Having shown the efficacy of αmDEC205 EBOV NP against EBOV, the question arose as to whether the DC targeting platform could be used to offer broad protection against other filoviruses.

Although it was expected that immunization with αmDEC205 EBOV NP would elicit cross-protective responses to other filoviruses, immunization with αmDEC205 EBOV NP did not confer protection against SUDV.

No real differences were observed after challenge with MARV, which can in part be explained by the constraints associated with the mouse model used.

Additional research is required to investigate whether DC targeting is a viable platform for the development of a vaccine against MARV.

5.2 Targeting EBOV NP to DEC205$^+$ DCs induces antigen-specific CD8$^+$ T cells

EBOV impedes the activation of DCs in turn interfering with T cell priming leading to poor cellular immunity against the virus. T cells have been shown to undergo mass apoptosis during EVD (Baize et al., 1999; Wauquier et al., 2010). Other studies show that proper T cell priming does indeed occur, however, these T cells are unable to clear the virus. This T cell dysfunction may in part be due to defective negative immune checkpoints which results in the high expression of T cell inhibitory molecules such as CTLA-4 and PD-1. This induces T cell exhaustion thus interfering with the ability of T cells to mediate viral clearance (Mohamadzadeh et al., 2007).Various studies have shown that survivors differ from fatal cases in that they are capable of mounting a well-coordinated immune response characterised by the induction of EBOV-specific T cells (Ruibal et al., 2016; McElroy et al., 2015).

EBOV GP-based vaccines induce strong humoral responses but generally do not induce robust T cell immunity (Agnandji et al., 2016; Ewer et al., 2016a; Muñoz-Fontela and McElroy, 2017; Zhu et al., 2019). Vaccinated individuals develop high titres of anti-EBOV GP specific IgG antibodies following vaccination with rVSV-ZEBOV and Ad.26.ZEBOV MVA-BN-FILO (Ewer et al., 2016b; Milligan et al., 2016). A recent study has shown that antibody responses from survivors fluctuate and that EBOV antibody reactivity wanes over a period of 0.5 – 2 years following recovery (Adaken et al., 2021). This brings into question the durability and efficacy of the vaccine induced response and underlines the necessity for additional vaccines that induce potent adaptive cell-mediated immunity. Of the two licensed vaccines, only Ad.26.ZEBOV MVA-BN-FILO has been shown to induce T cell responses (Milligan et al., 2016). However, the T cell response has not yet been conclusively elucidated. Data obtained from NHP studies point to cellular immunity mediated in part by IFNγ, TNFα and IL-2 secreting CD8$^+$ T cells as a correlate of protection against EBOV infection (Stanley et al., 2014; Sullivan et al., 2011).

EBOV NP is the major driver of CD8$^+$ T cell immunity in survivors and its incorporation in vaccines could have positive implications with regard to the induction of EBOV-specific cytotoxic T cells (McElroy et al., 2015; McElroy and Muñoz-Fontela, 2017; Ruibal et al., 2016; Sundar et al., 2007).

In this study, the EBOV NP was conjugated to αmDEC205 monoclonal antibodies to determine the consequences of antigen targeting to DCs in mice including the initiation of protective systemic immunity.

The initial observation was that antigen-specific $CD8^+$ T cells that were incubated with αmDEC205 EBOV NP robustly proliferated indicating that the targeting antibodies were able to successfully deliver antigen to $DEC205^+$ DCs and that these cells were able to cross-present antigen resulting in the proliferation of EBOV NP specific $CD8^+$ T cells.

Antibody-mediated delivery of EBOV NP to DCs thus appears to improve the efficiency of antigen presentation.

The antibody-mediated delivery of EBOV NP via intraperitoneal injection of mice results in the generation of EBOV-NP-specific CD8 T cells. Due to the fact that antigen delivery is in the form of extracellular antigen (antibody-antigen complexes), this indicates that the antigen is cross-presented to CD8 T cells by the targeted DCs *in vivo*. Furthermore, the results also indicate that the presence of an adjuvant is necessary to induce immunogenic responses against EBOV NP. This is in agreement with results from other studies whereby targeting to DEC205 resulted in the robust proliferation of $CD8^+$ T cell only when an adjuvant was supplied (Bonifaz et al., 2004; Henriques et al., 2013; Mahnke et al., 2005b).

5.2.1 Targeting EBOV NP to DCs *in vivo* induces $CD8^+$ T cell proliferation only in the presence of adjuvant

Targeting antigens to DCs in the steady state results in non-polarized T cells that are unresponsive to subsequent stimulation with adjuvants and highly reduced numbers of antigen-specific T cells for a few days. A subset of DCs in the steady-state are unable to process protein antigens when mature. Co-injection of DC targeting antibodies together with agonistic αCD40 antibody reverses this state from tolerance to immunity (Bonifaz et al., 2002; Hawiger et al., 2001).

Similar to the studies by Hawiger and Bonifaz, T cells from mice that received the targeting antibodies without additional stimuli did not proliferate while those that received the targeting antibodies together with Poly IC and agonistic αCD40 robustly proliferated. T cells from mice that received the isotype control antibody did not proliferate in both cases. The number of proliferation peaks were fewer after DC targeting with αmDEC205 EBOV NP compared to what has been previously observed after targeting with αmDEC205 OVA, which may be due to the low frequency of endogenous EBOV NP-specific T cell precursors.

This indicates that additional stimuli are necessary to induce DC maturation. Targeting EBOV NP to DEC205$^+$ DCs *in vivo* in the presence of adjuvants resulted in the development of immunity.

5.3 αmDEC205 antibodies are systemically distributed in WT → IFNAR$^{-/-}$ mice after IP injection

Common mouse strains such as C57BL/6J mice are not susceptible to EBOV and other filoviruses. Mouse adapted EBOV Mayinga and Makona strains have been developed by serial passaging and the introduction of mutations. The disease caused by the mouse adapted strains is similar to that caused by the wild-type virus but does not completely recapitulate the disease. Lüdtke et al., 2016, developed a mouse model that is susceptible to the wild-type virus (EBOV). All subsequent experiments were performed in these mice in order to limit the amount of variation that may arise as a result of using different mouse strains.

Target cells were identified in these mice using a commercial αDEC205 antibody conjugated to APC that was shown to be capable of binding DEC205$^+$ DCs in the spleen and lymph nodes just 30 min after intraperitoneal injection. Binding of CD8α DCs in the spleen shows that the targeting antibodies gained access to the blood. In addition, binding of DCs in the lymph nodes indicates that the targeting antibodies make use of the well-structured lymphatic network, which ensures that they are distributed systematically to other tissues. DCs are loaded for 3 days after injection (Bonifaz et al., 2004). Surface staining of DEC205$^+$ cells with APC in the liver and lungs was not observed which may be explained by the short amount of time between injection of the αDEC205 APC antibodies and euthanasia. The antibodies likely did not have enough time to circulate and penetrate these organs. Counterstaining with αDEC205$^+$ antibody conjugated to PerCP-eFluor 710 showed that cells in the lungs also expressed DEC205 (data not shown).

5.4 Targeting EBOV NP to DEC205$^+$ DCs induces functional antigen-specific CD8$^+$ T cells

The generation of antigen-specific T cells after targeting DCs can be used as an indicator of vaccination success. The responsiveness of such T cells to challenge with their cognate peptide and the secretion of effector cytokines can be used to determine the magnitude of the immune response.

The secretion of effector cytokines such as IL-2, IFNγ, and TNFα together with other effector molecules such as GrB and perforin can be used to measure the quality of the CD8$^+$ T cell response. Effector cytokines promote the T helper cell response and enhance the differentiation

of CTLs (Nutt and Huntington, 2019). Degranulation markers such as CD107a can be used to determine the level of activation following peptide re-stimulation. Degranulation is the first step of GrB and perforin-mediated killing and is a direct measure of CTL activity. Degranulation is necessary for immediate lytic killing mediated by antigen-specific T cells (Betts and Koup, 2004).

EBOV NP-specific $CD8^+$ T cells were detected in the spleen following intraperitoneal injection of the targeting antibodies when administered together with poly IC and αCD40 pointing to the importance of providing an additional stimulus during targeting.

The $CD8^+$ T cell response with αCD40 and poly IC as adjuvants was polyfunctional. The T cells from mice targeted with αmDEC205 EBOV NP produced IFNγ and IL-2 and expressed CD107a following re-stimulation with an MHC I restricted EBOV NP peptide. TNFα producing $CD8^+$ T cells were not detected in any mice, which may have been due to the type of cytokine secretion inhibitor used. Brefeldin A and Monensin inhibit the secretion of cytokines during peptide re-stimulation allowing their detection via flow cytometry. A combination of Monensin and Brefeldin A has been shown to be superior for the detection of TNFα due to the role that Monensin plays in pH neutralization in endosomal and lysosomal compartments (Betts and Koup, 2004). Brefeldin A was used for ICS in all the experiments.

Targeting EBOV NP to DCs induced high frequencies of both IFNγ producing $CD4^+$ and $CD8^+$ T cells. Mice immunized with αmDEC EBOV NP and αCD40 had 2-3-fold higher IFNγ secreting cells in comparison to the mice immunized with the isotype control at day 28 post immunization and the number of spot-forming units increased overall after boosting indicating a durable and poly-functional response. IFNγ can be spontaneously released by T cells, which may explain the background observed in the isotype control group.

There is a correlation between increased frequencies of IFNγ producing $CD4^+$ T cells and better outcome in HIV infected patients (Trumpfheller et al., 2008). Additionally, the induction of IFNγ producing $CD8^+$ T cells correlates with immunity to viral infections such as Influenza.

Targeting EBOV NP to $DEC205^+$ DCs resulted in the induction of multi-functional CTLs, which are necessary for protective immunity and are crucial for the containment of viral infections.

5.5 Antibody-mediated delivery of EBOV NP confers protection from lethal challenge with EBOV.

Section 5.3, 5.4.1 and 5.4.2 described above indicate that targeting DCs is a viable platform for the induction and modulation of the T cell response.

A prime and boost regimen was used to ensure an optimal immune response and both Poly IC and αCD40 were used as adjuvants. All the mice in the experimental group survived lethal challenge while ~13 % of the mice in the isotype control group had to be euthanised due to reaching the endpoint criteria. The difference in survival was, however, not significant which may have been due to the dose used for infection which was 10-fold lower than that required in the chimeric model.

Poly IC is a synthetic analogue of double stranded RNA and is used in vaccine formulations to enhance the immune response. It binds to TLR3 activating signalling pathways that lead to the production of Type I IFNs (Alexopoulou et al., 2001; Matsumoto et al., 2002).

The role of type I IFNs such as IFNα and IFNβ as pertaining to filovirus infections has not been completely elucidated. Clinical data obtained from an outbreak showed that elevated levels of IFNα coincided with a poor outcome, conversely the early production of type I IFNs has been shown to correlate with protection against other viruses such as West Nile virus. Since the effect that Poly IC may have had on the survival of the mice in the control group after challenge with EBOV could not be ruled out, only αCD40 was used in subsequent experiments.

Mice in the control group displayed significantly higher viral titres in the organs and blood and had higher levels of AST in comparison to the αmDEC205 EBOV NP immunized group suggesting that the CTLs induced after DC targeting were better able to control viral dissemination by killing virus infected cells.

An immunization regimen consisting of a prime and boost with αmDEC205 EBOV NP together with αCD40 adjuvant conferred protection to αmDEC205 EBOV NP immunized mice from lethal EBOV challenge. Keeping in mind that EBOV causes 50 % lethality in our mouse model, 50 % of the mice in the control group had to be euthanised due to reaching the endpoint criteria. Additionally, virus was only detected in the organs of the mice immunized with the isotype control. These mice displayed more weight loss, peaking between 5- and 10-days post infection. They also had higher levels of viremia and AST indicating higher viral replication and liver damage, respectively. On the other hand, αmDEC205 EBOV NP immunized mice showed no lethality, had lower AST and viremia levels and lost comparatively less weight corresponding to a less severe infection course. This suggests that immunized mice were able to mount an adequate adaptive immune response. Viral replication appears to have been better controlled in the mice immunized with αmDEC205 EBOV NP with no virus detectable in the blood from day 11 after infection. High AST levels and a high viral load are correlated with a poor EVD prognosis with liver damage being associated with disease severity (Vernet et al., 2017).

These findings suggested that antibody-mediated delivery of EBOV NP is a viable vaccination strategy against EBOV and that the antigen-specific CTLs induced by targeting EBOV NP to DEC205$^+$ DCs mediated effects that contributed to a positive outcome. Cytotoxic killing of virus infected cells is a major function of antigen-specific CTLs and this may explain the observed differences. The higher frequency of CTLs observed after immunization may in part explain this phenomenon as CTLs play a role in viral clearance through cytolysis of virus infected cells. CTLs also produce pro-inflammatory cytokines such as IFNγ that contribute to the maintenance of an antiviral state.

Immunization with αmDEC205 EBOV NP elicited significantly higher titres of anti-EBOV NP IgG antibodies. 100 % of the mice immunized with the targeting antibody developed high IgG titres above the baseline while only ~60 % of mice in the control group developed antibody titres after EBOV infection.

Targeting EBOV NP to DEC205$^+$ DCs is thus a viable platform that can be used to improve vaccine design. Targeting of antigens αmDEC205 antibodies to DCs enhances CD8$^+$ T cell immunity and confers systemic protective immunity. Cytotoxic T cells and antiviral antibodies are both required to mediate protection against EBOV and this study further substantiates findings by others that point to T cell immunity as a correlate of protection against EVD.

5.6 Characterisation of the T cell response after DC targeting

One of the main objectives of this study was to characterise the T cell response involved in immunity to experimental EBOV infection after DC targeting. The endogenous response is usually difficult to characterise due to the low frequency of antigen-specific T cells in bulk splenocytes or lung cells. The OT-I OVA model system enables the identification and tracking of antigen-specific T cells via tetramer staining.

5.6.1 Recombinant OVA-expressing EBOV is similar to wild-type EBOV

Recombinant EBOV viruses such as those that express GFP or luciferase are useful tools that can be used to study early pathogenic events and for high throughput compound/drug screening (Towner et al., 2005). There are, however, no recombinant viruses that can be used to study the cellular immune response to filovirus infections. A novel recombinant EBOV expressing ovalbumin by inserting the OVA ORF as an extra transcription unit between the NP and VP35 genes into the full-length EBOV Mayinga clone was generated to enable more in-depth studies of the immune response after.

EBOV OVA grew to similar titres as the wildtype virus and EBOV GFP and showed very slight attenuation in the growth rate. EBOV OVA caused CPE and morphological changes in the cells infected with EBOV OVA were clearly evident.

5.6.2 Antibody-mediated delivery of OVA protects mice from lethal infection with EBOV OVA

Targeting OVA to DEC205 DCs enhances the efficiency of antigen presentation and even a low dose of the vaccine is enough to charge DCs for long periods (Bonifaz et al., 2004).
Immunization of WT → IFNAR$^{-/-}$ mice with αmDEC205 OVA generated systemic protective immunity to lethal challenge with EBOV OVA. Mice immunized with αmDEC205 OVA remained stable for the duration of the experiment and displayed lower levels of viremia and viral titres in all the organs assessed indicating that viral replication and dissemination was curbed to a greater degree than in mice that received the isotype control antibodies.

5.6.3 OVA-specific CD8^{+} T cells expand and respond to challenge with EBOV OVA

Tetramers enable the direct *ex vivo* identification of antigen-specific T cells. However, they lack sensitivity when evaluating rare events due to the background staining usually observed.
The TCR-Transgenic adoptive transfer is an elegant approach to studying T cell immunity. The large numbers of transferred T cells enable their identification early after infection. The number of antigen-specific T cells is 1,000 -100,000 that of the endogenous naïve precursor T cells, which allows for easier detection using tetramers despite the background staining (Harty and Badovinac, 2008). Using EBOV OVA and complementary adoptive transfer experiments in WT → IFNAR$^{-/-}$ mice after immunization with αmDEC205 OVA, it was observed that OT-I T cells expand and are maintained at elevated levels following infection with EBOV OVA.
OT-I T cells expanded and migrated in large numbers to the lungs after intranasal infection with EBOV OVA. The frequency of OT-I T cells was highest in the spleen at day 3 post infection and was more than 10-fold that observed in the isotype control group. An increased frequency was observed in the lungs at day 7 post infection, which coincides with the start of the peak of the acute phase during which vigorous viral replication occurs. Indeed, the frequency of OT-I T cells more than quadrupled in the lungs indicating that the responding T cells migrated to the lungs. This data indicates that antibody-mediated delivery of EBOV NP does not only induce the proliferation of antigen-specific T cells but also serves to sustain them and that these T cells are capable of robust expansion upon infection.

The frequency of responding $CD8^+$ T cells began decreasing in the spleen from day 7 post infection but remained high in the lungs. The frequency of OT-I T cells contracted in both the lung and spleen during the convalescent phase, which coincides with the resolution of infection and recovery. The contraction of the immune response is a key component of immune balance and the reduction in the frequency of OT-I T cells observed in surviving mice at day 21 indicates that targeting antigens to DCs results in the modulation of the $CD8^+$ T cell response and the induction of a balanced immune response. This contraction phase is especially important for the prevention of non-specific tissue damage which may result from CTL activity.

5.6.4 OT-I T cells differentiate into memory effector cells after infection with EBOV OVA

Naive $CD8^+$ T cells rapidly proliferate and differentiate into effector cells following encounter with an antigen. These responding cells are able to mediate pathogen clearance after which a vast majority, ~90-95 % die via apoptosis. The remaining population of antigen-specific T cells, ~5 %, have the potential to become long-lived memory cells (Yuzefpolskiy et al., 2015). Vaccination can be used to bypass the initial step by training the immune response to respond to invading pathogens even before the first encounter. As mentioned in previous sections, targeting antigens to DCs enables the modulation of the immune response and the induction of potent CTLs that mediate protection to EBOV. MPECs and SLECs are generated during the effector expansion phase and are delineated by the inverse expression of KLRG1 and CD127. SLECs are short-lived, terminally differentiated and die following the resolution of the infection while MPECs are long-lived, capable of self-renewal and respond robustly to secondary infection (Chen et al., 2018).

A preferential accumulation of MPECs after infection with EBOV OVA was observed, which is in agreement with what has been described in the literature with regard to acute viral infections. There was a higher frequency of MPECs at day 3 post infection in the spleen of the mice that received the targeting antibody. At day 7 and day 21 post infection, the frequency of MPECs was higher both in the spleen and the lungs of αmDEC205 OVA immunized mice suggesting that MPECs are maintained in both SLOs and non-lymphoid peripheral tissues where they can develop into T_{RM}, T_{CM} or T_{EM} on secondary pathogen exposure.

Plumlee et al. showed that early effector cells have remarkable plasticity and are capable of differentiating into SLECs or MPECs depending on the availability of antigen and the inflammatory milieu induced by the pathogen. They showed that infection with LM resulted in the induction of more SLECs while infection with VSV drove EECs to differentiate into MPECs (Plumlee et al., 2015). The fate to which EECs are driven has not yet been determined in the

case of EBOV infection. VSV is a member of the order *mononegavirales*, the same order under which filoviruses are classified. Based on the data of this study, which shows the preponderance of MPECs following vaccination and infection with EBOV OVA, it appears that infection with EBOV may thus drive EECs to differentiate into MPECs similar to VSV. More studies are however required to establish whether this is also the case for natural EBOV infection.

5.6.5 Targeting antigens to DEC205$^+$ DCs results in mucosal resistance to EBOV infection

Developing and sustaining memory T cell populations is a cornerstone for protective vaccination against viral infections (Harty and Badovinac, 2008).

The induction of tissue-resident memory cells (T_{RM}) is one of the main hallmarks of vaccine induced immunity. These cells are found at the major sites of pathogen entry or replication where they restrict infection within the local tissue and mediate protection against pathogen re-exposure highlighting the importance of memory T cells in peripheral tissues. Oral infection with LM has been shown to result in a strong CD8$^+$ T cell response in the intestinal epithelium, which is predominantly composed of MPECs that upregulate CD103, one of the markers routinely used to identify T_{RM} (Sheridan et al., 2014).

Immunization with αmDEC205 OVA resulted in a higher frequency of CD8$^+$ T cells expressing CD103 in the lungs. The lungs had the highest measured frequency of T_{RM} at all time points suggesting that T_{RM} developed from responding T cells that seeded the site of infection (figure 24E). Strong T_{RM} responses appear to be linked to the route of infection i.e., robust protective T_{RM} responses in the skin are linked to skin infections and intranasal infections result in strong protective T_{RM} in the lungs (Gebhardt et al., 2009; Wu et al., 2014, 2018). Responding OT-I T cells that have already encountered antigen during vaccination can rapidly differentiate into memory cells and migrate to peripheral tissues where they mediate protection against EBOV.

The early and accelerated formation of T_{RM} in the lungs could in part be due to antibody-mediated DC targeting. There is a report that DC NK lectin group receptor (DNGR)$^+$ DCs may prime naïve CD8$^+$ T cells to become T_{RM} precursors and that CD24, a marker expressed by DCs is essential for the optimal formation of T_{RM} (Iborra et al., 2016). It would be interesting to determine the role, if any, that the priming of CD8$^+$ T cells by DEC205$^+$ DCs has on T_{RM} formation.

These findings strongly suggest that antibody-mediated delivery of antigens to DEC205$^+$ DCs is an attractive approach for the rational design of filovirus vaccines as it enhances the development of MPECs and T_{RM} that confer protection to lethal EBOV challenge.

5.6.6 DC targeting induces cytotoxic MPECs

Analysis of the CD8 T cell response also revealed that antigen-specific memory T cells expressed higher levels of GrB after immunization with αmDEC205 OVA. The highest levels of GrB were observed in the lungs 7 days after infection coinciding with the onset of the peak of infection.

Grb together with CD107a are good indicators of the ability of CTLs to kill infected cells. Antigen-specific T cells that express these two markers together with the effector cytokines IFNγ, IL-2 and TNFα are potent killers. Following infection, GrB is synthesized de novo and is stored in cytolytic granules for up to a month after the initial contact with antigen. Intracellular cytokine staining which requires a 6–7 h incubation step in addition to FACS staining was not performed due to the constraints of working in a BSL-4 environment.

5.7 Evaluation of the cross-protective capacity of αmDEC205 EBOV NP

The unprecedented EBOV outbreak that occurred from 2013-2016 spurred greater efforts than ever before to develop and advance vaccines and therapeutics against filoviruses. The reemergence of EBOV in Guinea and the Democratic Republic of the Congo and SUDV in Uganda and MARV in Ghana underscores the need for more effective vaccines against all filoviruses. There is also the possibility of new filoviruses emerging that could pose a risk to the general population. Of the five filovirus vaccines that have progressed to phase II or III clinical trials, only one is a multivalent vaccine that incorporates antigens from various filoviruses. This vaccine however is indicated for use as a boost in a heterologous regimen. The vaccine targets EBOV, SUDV TAFV and MARV but is only indicated for EBOV and there is no data on the vaccine's efficacy against SUDV and MARV.

The RNA-dependent RNA polymerase (RdRp) is required by RNA viruses with the exception of retroviruses for replication and transcription of the viral genome, which ensures their survival (Aftab et al., 2020). The RdRp, however, lacks fidelity and has high error rates that may lead to intraspecies mutations. Such mutations may not only impact vaccine efficacy but may even render them ineffective in the long run. Multivalent vaccines are a salient factor in the efforts to eliminate filovirus outbreaks.

The data described herein indicate that delivering antigens to cross-presenting DCs confers protection to lethal EBOV infection.

5.7.1 Targeting EBOV NP to DEC205$^+$ DCs does not confer protection against *Sudan ebolavirus*

25 % more mice survived after immunization with αmDEC205 EBOV NP in comparison to the isotype control group. Interestingly, the mice immunized with the targeting antibody displayed slightly worse signs of disease and lost more weight in comparison to the isotype control group. A possible explanation might be that the presence of EBOV NP specific T cells may have led to off target effects contributing to a more severe disease course. Pre-existing non-specific memory T cells can be activated by cytokines during an ongoing viral infection caused by a different pathogen. This phenomenon, termed bystander activation may exert detrimental effects on the host depending on the pathogens involved Indeed, bystander CD8$^+$ T cells activation has been shown to promote disease severity leading to tissue destruction following *Leishmania major* infection (Crosby et al., 2014). Two mechanisms that result in non-specific T cell activation have been elucidated and these may help explain the results seen after SUDV challenge of αmDEC205 EBOV NP immunized mice. The first mechanism involves the cross-linking of the TCR by a second pathogen that is closely related to the first similar to what may be expected with EBOV and SUDV. TCR-dependent activation results in the production of monoclonal or oligoclonal cross-reactive T cells with a weaker TCR affinity to the peptide-MHC I complex (Lee et al., 2022). It stands to reason that such weak MHC -TCR interaction may result in insufficient priming of responding T cells resulting in the induction of cross-reactive T cells that may have a low activation potential and that are unable to completely eliminate the pathogen. This may explain the differences in outcome observed after immunization with αmDEC205 EBOV NP followed by challenge with EBOV versus SUDV.

The second mechanism involves the bystander activation of CD8$^+$ T cells by cytokines resulting in the transient polyclonal activation of memory T cells. The polyclonal activation of T cells may lead to an exaggerated production of cytokines by other immune cells and this could result in deleterious effects (Lee et al., 2022). A hallmark of EVD is the cytokine storm, the advent of which is thought to be a marker for a worse prognosis. The role of bystander activation after infection with different filoviruses has not yet been described.

Various studies have shown that the non-specific activation of T cells may be beneficial or disadvantageous depending on the type of pathogen involved. Vigorous T cell responses are associated with liver injury during HBV and IL-15 induced memory CD8$^+$ T cells are thought to play a role in liver injury during HBV infection (Sandalova et al., 2010). Activated non-hepatitis B virus-specific (HBV) CD8$^+$ T cells are recruited in addition to HBV-specific CD8$^+$

T cells during acute HBV infection and are thought to contribute to immunopathology (Sandalova et al., 2010; Shin et al., 2016). A study by Ostler et al., in 2003 demonstrated that the "recruitment of lymphocytic choriomeningitis virus (LCMV) -specific bystander T cells failed to enhance immunity to respiratory syncytial virus (RSV), significantly delayed virus elimination and slightly enhanced RSV induced weight loss in BALB/c mice" (Ostler et al., 2003). Interestingly, this correlated with a delay in the recruitment of RSV-specific T cells to the lung. Indeed, enhanced SUDV-induced weight loss in the mice immunized with αmDEC205 EBOV NP was observed. A major assumption could be that the presence of EBOV NP induced $CD8^+$ T cells after targeting may have had a bystander effect similar to the one observed by Ostler et al during RSV infection.

It would be interesting to determine the effect of bystander activation during filovirus infections as well as the mechanism involved.

Another explanation for the lower level of effectiveness seen is that the incorporated antigen is simply from a different virus species. The immune dominant epitopes may vary considerably not only between viruses of the same family but also of the same genus.

Even though there were no significant differences in survival, mice immunized with αmDEC205 EBOV NP had lower SUDV titers in the organs and lower AST levels compared to the mice immunized with the isotype control.

Further studies will be required to further clarify the differences seen after vaccination with αmDEC205 EBOV NP and challenge with SUDV.

5.8 Evaluating the cross-protective capacity of αmDEC205 EBOV NP

In contrast to EBOV, there are fewer vaccine candidates in development against MARV. MVD outbreaks have been rare and sporadic in the past, however the disease recently re-emerged in Ghana resulting in a CFR of 67 % (WHO). The only licensed vaccine that can be used against MARV is Mvabea, which is a multivalent vaccine consisting of MARV GP among other filovirus antigens. The vaccine is administered as a boost and is currently only indicated against EBOV. There is no clinical data on the effectiveness nor the elicited immune response to MARV.

5.8.1 Development of a mouse model for the study of other filoviruses

Few animal models exist for not only filoviruses but also other haemhorrhagic fever causing viruses. Studies on SUDV and MARV are few and far between and mostly rely on data

extrapolated from studies with EBOV. In order to test vaccines or therapeutics, an animal model in which the major aspects of the disease are recapitulated is of paramount importance.

IFNAR$^{-/-}$ mice were inoculated via different routes to determine the best route of infection. Previous studies in our lab with EBOV, SUDV, RESTV and LASV have relied on intranasal administration to mice (Escudero-Pérez et al., 2019; Port et al., 2020; Rottstegge et al., 2022). This route of infection has proved adequate and results in a fulminant disease course in IFNAR$^{-/-}$ mice that culminates in death if no intervention is applied. Contrary to our expectations, intranasal infection only resulted in mild signs of clinical disease such as hunched posture, piloerection and transient weight loss. There was no detectable virus in the organs nor in the blood, suggesting that these mice mounted an adaptive immune response and were able to control viral replication and dissemination without any intervention. In contrast, intraperitoneal infection resulted in 100 % lethality with both strains of MARV. The disease course was more severe and infected mice had to be euthanised between day 5 and 8 post infection. Mice infected via the intraperitoneal route also rapidly lost weight and had extremely high viral titers in the order of 10^5 - 10^7 in all the organs assessed. Additionally, these mice had high levels of viremia indicating that the virus vigorously replicated.

Intraperitoneal injection of MARV allows faster systematic distribution, which may explain the extremely high viral titers observed after infection via this route. The IFNAR$^{-/-}$ mouse strain was raised on a C57BL/6J background and requires backcrossing with wild-type mice to refresh the colonies ensuring that issues that arise from inbreeding are kept to a minimum. Issues with the mouse colony cannot be ruled out, however all experiments described in section 4.6.3 were performed with mice from the same colony under the same conditions and at the same time. There may be an underlying mechanism that is yet to be elucidated that may explain the lack of lethality observed after intranasal MARV infection. Determining the mechanism involved was deemed outside the purview of this study and requires further elaboration. Factors such as the age and the sex of the mice may have had an impact on the outcome and should be investigated in future experiments.

5.8.2 Targeting EBOV NP to DEC205$^+$ DCs ameliorates signs of morbidity associated with MARV infection

The intraperitoneal route of infection was chosen for further experiments with MARV since it provided a baseline against which an effect on survival or viral replication could be measured. Infection of WT → IFNAR$^{-/-}$ mice with MARV Musoke resulted in 20 % lethality and more weight loss after intraperitoneal infection compared to intranasal infection. Infection via the

intraperitoneal route also resulted in a high level of viremia. Virus was however only detected in the lungs and kidneys.

There were no differences in survival after DC targeting. All the mice in both groups survived the infection, however mice immunized with the isotype control lost more weight than those immunized with αmDEC205 EBOV NP. Bearing in mind that in previous experiments, MARV only caused 20 % lethality in the WT → IFNAR$^{-/-}$ mice, it would be difficult to determine whether the survival of the control mice was a result of the low lethality observed with the mouse model. More studies are required to refine the model before it can be used for vaccine or therapeutic studies against MARV.

6. Outlook

This study showed that antibody-mediated delivery of EBOV NP is a valid approach for the generation of potent adaptive cellular immunity. Targeting antigens to CD8α DCs resulted in strong and protective EBOV NP-specific effector immune responses as well as antigen-specific antibodies after EBOV infection. Characterisation of the T cell response using the model antigen – OVA revealed that antigen-specific $CD8^+$ T cells acquire a memory phenotype that would enhance the immune response in the event of pathogen exposure. Additionally, vaccination induced the generation of tissue resident memory cells in the lungs that mediated mucosal resistance to EBOV.

Developing vaccines based on different platforms and that elicit different immune responses from those of the currently licensed vaccines would be beneficial in the fight to eliminate filoviruses. DC-targeted vaccines could be used in heterologous prime boost regimens to foster a well-rounded immune response. αmDEC205 EBOV NP can be used with the currently licensed vaccines to augment the immune response. Other groups have shown that fusing the protein of interest to αDEC205 antibodies preserves the native structure of the protein thus ensuring immunogenicity. Additionally, the vaccine is non-replicative, which ensures that the probability of vaccine shedding is nil.

More studies are still required to define the immune correlates of protection. Studies whereby either $CD4^+$ or $CD8^+$ T cells are depleted could help shed light on whether a polyfunctional response is required to mediate protection against filovirus infections. Delving even further and characterizing the immune response elicited after vaccination and infection, including single cell and transcriptomic analyses of both innate and adaptive immune cells would be interesting. Improving the vaccine by incorporating other filovirus antigens or the use of bispecific antibodies could help make this platform more attractive for further development and possible advancement to clinical trial contingent on the success of NHP studies.

The targeting antibodies were administered intraperitoneally in this study. This route of administration is not translatable to humans as it is rarely used in clinical settings. Intradermal administration has been shown to modulate protective immune responses against various pathogens and is more comparable to the routine method of vaccine administration in clinical studies (Pereira et al., 2020). Using a more translatable method of vaccine administration is a future goal. The vaccine is easily customizable in that other filovirus antigens can easily be incorporated, and different receptors can be targeted which makes it especially appealing.

7. References

Adaken, C., Scott, J.T., Sharma, R., Gopal, R., Dicks, S., Niazi, S., Ijaz, S., Edwards, T., Smith, C.C., and Cole, C.P. (2021). Ebola virus antibody decay–stimulation in a high proportion of survivors. Nature *590*, 468–472.

Adjemian, J., Farnon, E.C., Tschioko, F., Wamala, J.F., Byaruhanga, E., Bwire, G.S., Kansiime, E., Kagirita, A., Ahimbisibwe, S., and Katunguka, F. (2011). Outbreak of Marburg hemorrhagic fever among miners in Kamwenge and Ibanda Districts, Uganda, 2007. J. Infect. Dis. *204*, S796–S799.

Aftab, S.O., Ghouri, M.Z., Masood, M.U., Haider, Z., Khan, Z., Ahmad, A., and Munawar, N. (2020). Analysis of SARS-CoV-2 RNA-dependent RNA polymerase as a potential therapeutic drug target using a computational approach. J. Transl. Med. *18*, 1–15.

Agnandji, S.T., Huttner, A., Zinser, M.E., Njuguna, P., Dahlke, C., Fernandes, J.F., Yerly, S., Dayer, J.-A., Kraehling, V., and Kasonta, R. (2016). Phase 1 trials of rVSV Ebola vaccine in Africa and Europe. N. Engl. J. Med. *374*, 1647–1660.

Ahmed, E.H., Brooks, E., Sloan, S., Schlotter, S., Jeney, F., Hale, C., Mao, C., Zhang, X., Mclaughlin, E., Shindiapina, P., et al. (2021). Targeted Delivery of BZLF1 to DEC205 Drives EBV-Protective Immunity in a Spontaneous Model of EBV-Driven Lymphoproliferative Disease. 1–20.

Ahonen, C.L., Doxsee, C.L., McGurran, S.M., Riter, T.R., Wade, W.F., Barth, R.J., Vasilakos, J.P., Noelle, R.J., and Kedl, R.M. (2004). Combined TLR and CD40 triggering induces potent CD8+ T cell expansion with variable dependence on type I IFN. J. Exp. Med. *199*, 775–784.

Aleksandrowicz, P., Marzi, A., Biedenkopf, N., Beimforde, N., Becker, S., Hoenen, T., Feldmann, H., and Schnittler, H.-J. (2011). Ebola virus enters host cells by macropinocytosis and clathrin-mediated endocytosis. J. Infect. Dis. *204*, S957–S967.

Alexopoulou, L., Holt, A.C., Medzhitov, R., and Flavell, R.A. (2001). Recognition of double-stranded RNA and activation of NF-κB by Toll-like receptor 3. Nature *413*, 732–738.

Altman, J.D., Moss, P.A.H., Goulder, P.J.R., Barouch, D.H., McHeyzer-Williams, M.G., Bell, J.I., McMichael, A.J., and Davis, M.M. (1996). Phenotypic analysis of antigen-specific T lymphocytes. Science (80-.). *274*, 94–96.

Alvarez, C.P., Lasala, F., Carrillo, J., Muñiz, O., Corbí, A.L., and Delgado, R. (2002). C-type lectins DC-SIGN and L-SIGN mediate cellular entry by Ebola virus in cis and in trans. J. Virol. *76*, 6841–6844.

Amman, B.R., Bird, B.H., Bakarr, I.A., Bangura, J., Schuh, A.J., Johnny, J., Sealy, T.K., Conteh, I.,

Koroma, A.H., Foday, I., et al. (2020). Isolation of Angola-like Marburg virus from Egyptian rousette bats from West Africa. Nat. Commun. *11*, 1–9.

Amman, B.R., Schuh, A.J., Albariño, C.G., and Towner, J.S. (2021). Marburg virus persistence on fruit as a plausible route of bat to primate filovirus transmission. Viruses *13*, 1–12.

Appay, V., and Rowland-Jones, S.L. (2002). The assessment of antigen-specific CD8+ T cells through the combination of MHC class I tetramer and intracellular staining. J. Immunol. Methods *268*, 9–19.

Baize, S., Leroy, E.M., Georges-Courbot, M.-C., Capron, M., Lansoud-Soukate, J., Debré, P., Fisher-Hoch, S.P., McCormick, J.B., and Georges, A.J. (1999). Defective humoral responses and extensive intravascular apoptosis are associated with fatal outcome in Ebola virus-infected patients. Nat. Med. *5*, 423–426.

Banchereau, J., and Steinman, R.M. (1998). Dendritic cells and the control of immunity. *392*, 245–252.

Baseler, L., Chertow, D.S., Johnson, K.M., Feldmann, H., and Morens, D.M. (2017). The pathogenesis of Ebola virus disease. Annu. Rev. Pathol. Mech. Dis. *12*, 387–418.

Behr, F.M., Parga-Vidal, L., Kragten, N.A.M., van Dam, T.J.P., Wesselink, T.H., Sheridan, B.S., Arens, R., van Lier, R.A.W., Stark, R., and van Gisbergen, K.P.J.M. (2020). Tissue-resident memory CD8+ T cells shape local and systemic secondary T cell responses. Nat. Immunol. *21*, 1070–1081.

Bermejo-Jambrina, M., Eder, J., Helgers, L.C., Hertoghs, N., Nijmeijer, B.M., Stunnenberg, M., and Geijtenbeek, T.B.H. (2018). C-type lectin receptors in antiviral immunity and viral escape. Front. Immunol. *9*, 1–12.

Betts, M.R., and Koup, R.A. (2004). Detection of T-cell degranulation: CD107a and b. Methods Cell Biol. *2004*, 497–512.

Bonifaz, L., Bonnyay, D., Mahnke, K., Rivera, M., Nussenzweig, M.C., and Steinman, R.M. (2002). Efficient Targeting of Protein Antigen to the Dendritic Cell Receptor DEC-205 in the Steady State Leads to Antigen Presentation on Major Histocompatibility Complex Class I Products and Peripheral CD8 $^{+}$ T Cell Tolerance. J. Exp. Med. *196*, 1627–1638.

Bonifaz, L.C., Bonnyay, D.P., Charalambous, A., Darguste, D.I., Fujii, S.-I., Soares, H., Brimnes, M.K., Moltedo, B., Moran, T.M., and Steinman, R.M. (2004). In Vivo Targeting of Antigens to Maturing Dendritic Cells via the DEC-205 Receptor Improves T Cell Vaccination. J. Exp. Med. *199*, 815–824.

Den Boon, S., Marston, B.J., Nyenswah, T.G., Jambai, A., Barry, M., Keita, S., Durski, K., Senesie,

S.S., Perkins, D., Shah, A., et al. (2019). Ebola virus infection associated with transmission from survivors. Emerg. Infect. Dis. *25*, 240–246.

Bornholdt, Z.A., Herbert, A.S., Mire, C.E., Qiu, X., Geisbert, T.W., Dye, J.M., Bornholdt, Z.A., Herbert, A.S., Mire, C.E., He, S., et al. (2019). Clinical and Translational Report A Two-Antibody Pan-Ebolavirus Cocktail Confers Broad Therapeutic Protection in Ferrets and Clinical and Translational Report A Two-Antibody Pan-Ebolavirus Cocktail Confers Broad Therapeutic Protection in Ferrets and Nonhu. Cell Host Microbe *25*, 49-58.e5.

Borrow, P., Tishon, A., Lee, S., Xu, J., Grewal, I.S., Oldstone, M.B., and Flavell, R.A. (1996). CD40L-deficient mice show deficits in antiviral immunity and have an impaired memory CD8+ CTL response. J. Exp. Med. *183*, 2129–2142.

Bosio, C.M., Aman, M.J., Grogan, C., Hogan, R., Ruthel, G., Negley, D., Mohamadzadeh, M., Bavari, S., and Schmaljohn, A. (2003). Ebola and Marburg Viruses Replicate in Monocyte-Derived Dendritic Cells without Inducing the Production of Cytokines and Full Maturation. J. Infect. Dis. *188*, 1630–1638.

Brauburger, K., Hume, A.J., Mühlberger, E., and Olejnik, J. (2012). Forty-five years of marburg virus research. Viruses *4*, 1878–1927.

Cabeza-Cabrerizo, M., Cardoso, A., Minutti, C.M., Pereira Da Costa, M., and Reis E Sousa, C. (2021). Dendritic Cells Revisited. Annu. Rev. Immunol. *39*, 131–166.

Cantoni, D., Hamlet, A., Michaelis, M., Wass, M.N., and Rossman, J.S. (2016). Risks posed by Reston, the forgotten ebolavirus. Msphere *1*, e00322-16.

Carette, J.E., Raaben, M., Wong, A.C., Herbert, A.S., Obernosterer, G., Mulherkar, N., Kuehne, A.I., Kranzusch, P.J., Griffin, A.M., and Ruthel, G. (2011). Ebola virus entry requires the cholesterol transporter Niemann–Pick C1. Nature *477*, 340–343.

Caviness, K., Kuhn, J.H., and Palacios, G. (2017). Ebola virus persistence as a new focus in clinical research. Curr. Opin. Virol. *23*, 43–48.

Ceredig, R., and Rolink, T. (2002). A positive look at double-negative thymocytes. Nat. Rev. Immunol. *2*, 888–896.

Chan, Y.K., and Gack, M.U. (2016). Viral evasion of intracellular DNA and RNA sensing. Nat. Rev. Microbiol. *14*, 360–373.

Changula, K., Yoshida, R., Noyori, O., Marzi, A., Miyamoto, H., Ishijima, M., Yokoyama, A., Kajihara, M., Feldmann, H., Mweene, A.S., et al. (2013). Mapping of conserved and species-specific antibody epitopes on the Ebola virus nucleoprotein. Virus Res. *176*, 83–90.

Chen, Y., Zander, R., Khatun, A., Schauder, D.M., and Cui, W. (2018). Transcriptional and epigenetic regulation of effector and memory CD8 T cell differentiation. Front. Immunol. *9*, 2826.

Cheong, C., Matos, I., Choi, J., Dandamudi, D.B., Longhi, M.P., Jeffrey, K.L., Anthony, R.M., Kluger, C., Koh, H., Rodriguez, A., et al. (2011). NIH Public Access. *143*, 416–429.

Connor, J.H., Yen, J., Caballero, I.S., Garamszegi, S., Malhotra, S., Lin, K., Hensley, L., and Goff, A.J. (2015). Transcriptional profiling of the immune response to Marburg virus infection. J. Virol. *89*, 9865–9874.

Cooper, T.K., Sword, J., Johnson, J.C., Bonilla, A., Hart, R., Liu, D.X., Bernbaum, J.G., Cooper, K., Jahrling, P.B., and Hensley, L.E. (2018). New Insights into Marburg Virus Disease Pathogenesis in the Rhesus Macaque Model. J. Infect. Dis. *218*, S423–S433.

Corti, D., Misasi, J., Mulangu, S., Stanley, D.A., Kanekiyo, M., Wollen, S., Ploquin, A., Doria-Rose, N.A., Staupe, R.P., Bailey, M., et al. (2016). Protective monotherapy against lethal Ebola virus infection by a potently neutralizing antibody. Science (80-.). *351*, 1339–1342.

Crosby, E.J., Goldschmidt, M.H., Wherry, E.J., and Scott, P. (2014). Engagement of NKG2D on bystander memory CD8 T cells promotes increased immunopathology following Leishmania major infection. PLoS Pathog. *10*, e1003970.

Curtsinger, J.M., Valenzuela, J.O., Agarwal, P., Lins, D., and Mescher, M.F. (2005). Cutting Edge: Type I IFNs Provide a Third Signal to CD8 T Cells to Stimulate Clonal Expansion and Differentiation1. J. Immunol. *174*, 4465–4469.

Dahlke, C., Lunemann, S., Kasonta, R., Kreuels, B., Schmiedel, S., Ly, M.L., Fehling, S.K., Strecker, T., Becker, S., Altfeld, M., et al. (2017). Comprehensive characterization of cellular immune responses following ebola virus infection. J. Infect. Dis. *215*, 287–292.

Davis, C.W., Jackson, K.J.L., McElroy, A.K., Halfmann, P., Huang, J., Chennareddy, C., Piper, A.E., Leung, Y., Albariño, C.G., Crozier, I., et al. (2019). Longitudinal Analysis of the Human B Cell Response to Ebola Virus Infection. Cell *177*, 1566-1582.e17.

Dhodapkar, M. V, Sznol, M., Zhao, B., Wang, D., Carvajal, R.D., Keohan, M.L., Chuang, E., Sanborn, R.E., Lutzky, J., Powderly, J., et al. (2014). HHS Public Access.

Diehl, L., den Boer, A.T., Schoenberger, S.P., van der Voort, E.I.H., Schumacher, T.N.M., Melief, C.J.M., Offringa, R., and Toes, R.E.M. (1999). CD40 activation in vivo overcomes peptide-induced peripheral cytotoxic T-lymphocyte tolerance and augments anti-tumor vaccine efficacy. Nat. Med. *5*, 774–779.

Drouin, M., Saenz, J., and Chiffoleau, E. (2020). C-type lectin-like receptors: head or tail in cell death

immunity. Front. Immunol. *11*, 251.

Eiz-Vesper, B., and Schmetzer, H.M. (2020). Antigen-presenting cells: Potential of proven und new players in immune therapies. Transfus. Med. Hemotherapy *47*, 429–431.

Emanuel, J., Marzi, A., and Feldmann, H. (2018). Filoviruses: Ecology, Molecular Biology, and Evolution. Adv. Virus Res. *100*, 189–221.

Escudero-Pérez, B., Ruibal, P., Rottstegge, M., Lüdtke, A., Port, J.R., Hartmann, K., Gómez-Medina, S., Müller-Guhl, J., Nelson, E. V, and Krasemann, S. (2019). Comparative pathogenesis of Ebola virus and Reston virus infection in humanized mice. JCI Insight *4*.

Ewer, K., Rampling, T., Venkatraman, N., Bowyer, G., Wright, D., Lambe, T., Imoukhuede, E.B., Payne, R., Fehling, S.K., and Strecker, T. (2016a). A monovalent chimpanzee adenovirus Ebola vaccine boosted with MVA. N. Engl. J. Med. *374*, 1635–1646.

Ewer, K.J., Lambe, T., Rollier, C.S., Spencer, A.J., Hill, A.V.S., and Dorrell, L. (2016b). Viral vectors as vaccine platforms: from immunogenicity to impact. Curr. Opin. Immunol. *41*, 47–54.

Farooq, F., Beck, K., Paolino, K.M., Phillips, R., Waters, N.C., Regules, J.A., and Bergmann-leitner, E.S. (2016). Circulating follicular T helper cells and cytokine profile in humans following vaccination with the rVSV-ZEBOV Ebola vaccine. Nat. Publ. Gr. 1–9.

Feldmann, H., and Geisbert, T.W. (2011). Ebola haemorrhagic fever. Lancet *377*, 849–862.

Feldmann, H., Sprecher, A., and Geisbert, T.W. (2020). Ebola. N. Engl. J. Med. *382*, 1832–1842.

Flacher, V., Tripp, C.H., Mairhofer, D.G., Steinman, R.M., Stoitzner, P., Idoyaga, J., and Romani, N. (2014). Murine Langerin + dermal dendritic cells prime CD 8 + T cells while Langerhans cells induce cross-tolerance. *6*, 1191–1204.

Forero-Torres, A., Furman, R.R., Rosenblatt, J.D., Younes, A., Harrop, K., Drachman, J.G., and Advani, R. (2006). A humanized antibody against CD40 (SGN-40) is well tolerated and active in non-Hodgkin's lymphoma (NHL): results of a phase I study. J. Clin. Oncol. *24*, 7534.

Friedrich, B.M., Trefry, J.C., Biggins, J.E., Hensley, L.E., Honko, A.N., Smith, D.R., and Olinger, G.G. (2012). Potential vaccines and post-exposure treatments for filovirus infections. Viruses *4*, 1619–1650.

Furuyama, W., and Marzi, A. (2019). Ebola Virus: Pathogenesis and Countermeasure Development. Annu. Rev. Virol. *6*, 435–458.

Gasper, D.J., Tejera, M.M., and Suresh, M. (2014). CD4 T-cell memory generation and maintenance. Crit. Rev. Immunol. *34*, 121–146.

Gebhardt, T., Wakim, L.M., Eidsmo, L., Reading, P.C., Heath, W.R., and Carbone, F.R. (2009). Memory T cells in nonlymphoid tissue that provide enhanced local immunity during infection with herpes simplex virus. Nat. Immunol. *10*, 524–530.

Gehad, A., Al-Banna, N.A., Vaci, M., Issekutz, A.C., Mohan, K., Latta, M., and Issekutz, T.B. (2012). Differing Requirements for CCR4, E-Selectin, and α4β1 for the Migration of Memory CD4 and Activated T Cells to Dermal Inflammation. J. Immunol. *189*, 337–346.

Geisbert, T.W., Hensley, L.E., Larsen, T., Young, H.A., Reed, D.S., Geisbert, J.B., Scott, D.P., Kagan, E., Jahrling, P.B., and Davis, K.J. (2003a). Pathogenesis of Ebola Hemorrhagic Fever in Cynomolgus Macaques: Evidence that Dendritic Cells are Early and Sustained Targets of Infection. Am. J. Pathol. *163*, 2347–2370.

Geisbert, T.W., Hensley, L.E., Larsen, T., Young, H.A., Reed, D.S., Geisbert, J.B., Scott, D.P., Kagan, E., Jahrling, P.B., and Davis, K.J. (2003b). Pathogenesis of Ebola Hemorrhagic Fever in Cynomolgus Macaques. Am. J. Pathol. *163*, 2347–2370.

Godfrey, D.I., Kennedy, J., Suda, T., and Zlotnik, A. (1993). A developmental pathway involving four phenotypically and functionally distinct subsets of CD3-CD4-CD8- triple-negative adult mouse thymocytes defined by CD44 and CD25 expression. J. Immunol. *150*, 4244–4252.

Goldstein, T., Anthony, S.J., Gbakima, A., Bird, B., Bangura, J., Tremeau-Bravard, A., Belaganahalli, M., Wells, H., Dhanota, J., and Liang, E. (2019). The discovery of a new Ebolavirus, Bombali virus, adds further support for bats as hosts of Ebolaviruses. Int. J. Infect. Dis. *79*, 4–5.

Graham, J.P., Authie, P., Yu, C.I., Zurawski, S.M., Li, X.-H., Marches, F., Flamar, A.-L., Acharya, A., Banchereau, J., and Palucka, A.K. (2016). Targeting dendritic cells in humanized mice receiving adoptive T cells via monoclonal antibodies fused to Flu epitopes. Vaccine *34*, 4857–4865.

Grant-Klein, R.J., Van Deusen, N.M., Badger, C. V, Hannaman, D., Dupuy, L.C., and Schmaljohn, C.S. (2012). A multiagent filovirus DNA vaccine delivered by intramuscular electroporation completely protects mice from ebola and Marburg virus challenge. Hum. Vaccin. Immunother. *8*, 1703–1706.

Greenberg, R.N., Hurley, Y., Dinh, D. V, Mraz, S., Vera, J.G., von Bredow, D., von Krempelhuber, A., Roesch, S., Virgin, G., and Arndtz-Wiedemann, N. (2015). A multicenter, open-label, controlled phase II study to evaluate safety and immunogenicity of MVA smallpox vaccine (IMVAMUNE) in 18–40 year old subjects with diagnosed atopic dermatitis. PLoS One *10*, e0138348.

Grewal, I.S., and Flavell, R.A. (1998). CD40 and CD154 in cell-mediated immunity. Annu. Rev. Immunol. *16*, 111–135.

Grewal, I.S., Xu, J., and Flavell, R.A. (1995). Impairment of antigen-specific T-cell priming in mice lacking CD40 ligand. Nature *378*, 617–620.

Grewal, I.S., Foellmer, H.G., Grewal, K.D., Xu, J., Hardardottir, F., Baron, J.L., Janeway Jr, C.A., and Flavell, R.A. (1996). Requirement for CD40 ligand in costimulation induction, T cell activation, and experimental allergic encephalomyelitis. Science (80-.). *273*, 1864–1867.

Grindebacke, H., Stenstad, H., Quiding-Järbrink, M., Waldenström, J., Adlerberth, I., Wold, A.E., and Rudin, A. (2009). Dynamic Development of Homing Receptor Expression and Memory Cell Differentiation of Infant CD4+CD25high Regulatory T Cells1. J. Immunol. *183*, 4360–4370.

Groseth, A., Marzi, A., Hoenen, T., Herwig, A., Gardner, D., Becker, S., Ebihara, H., and Feldmann, H. (2012). The Ebola Virus Glycoprotein Contributes to but Is Not Sufficient for Virulence In Vivo. *8*.

Harty, J.T., and Badovinac, V.P. (2008). Shaping and reshaping CD8+ T-cell memory. Nat. Rev. Immunol. *8*, 107–119.

Hawiger, D., Inaba, K., Dorsett, Y., Guo, M., Mahnke, K., Rivera, M., Ravetch, J. V., Steinman, R.M., and Nussenzweig, M.C. (2001). Dendritic Cells Induce Peripheral T Cell Unresponsiveness under Steady State Conditions in Vivo. J. Exp. Med. *194*, 769–780.

Heath, W.R., Belz, G.T., Behrens, G.M.N., Smith, C.M., Forehan, S.P., Parish, I.A., Davey, G.M., Wilson, N.S., Carbone, F.R., and Villadangos, J.A. (2004). Cross-presentation, dendritic cell subsets, and the generation of immunity to cellular antigens. Immunol. Rev. *199*, 9–26.

Heil, F., Hemmi, H., Hochrein, H., Ampenberger, F., Kirschning, C., Akira, S., Lipford, G., Wagner, H., and Bauer, S. (2004). Species-Specific Recognition of Single-Stranded RNA via Toll-like Receptor 7 and 8. Science (80-.). *303*, 1526–1529.

Henriques, H.R., Rampazo, E. V., Gonçalves, A.J.S., Vicentin, E.C.M., Amorim, J.H., Panatieri, R.H., Amorim, K.N.S., Yamamoto, M.M., Ferreira, L.C.S., Alves, A.M.B., et al. (2013). Targeting the Non-structural Protein 1 from Dengue Virus to a Dendritic Cell Population Confers Protective Immunity to Lethal Virus Challenge. PLoS Negl. Trop. Dis. *7*, e2330.

Herbert, J.A., and Panagiotou, S. (2022). Immune Response to Viruses. Encycl. Infect. Immun. 429.

Hoenen, T., and Feldmann, H. (2017). Reverse Genetics Systems for Filoviruses BT - Reverse Genetics of RNA Viruses: Methods and Protocols. D.R. Perez, ed. (New York, NY: Springer New York), pp. 159–170.

Hoenen, T., Groseth, A., de Kok-Mercado, F., Kuhn, J.H., and Wahl-Jensen, V. (2011). Minigenomes, transcription and replication competent virus-like particles and beyond: reverse

genetics systems for filoviruses and other negative stranded hemorrhagic fever viruses. Antiviral Res. *91*, 195–208.

Homann, D., Teyton, L., and Oldstone, M. (2001). Differential regulation of antiviral T-cell immunity results in stable CD8+ but declining CD4+ T-cell memory. Nat. Med. *7*, 913–919.

Iborra, S., Martínez-López, M., Khouili, S.C., Enamorado, M., Cueto, F.J., Conde-Garrosa, R., del Fresno, C., and Sancho, D. (2016). Optimal Generation of Tissue-Resident but Not Circulating Memory T Cells during Viral Infection Requires Crosspriming by DNGR-1+ Dendritic Cells. Immunity *45*, 847–860.

Idoyaga, J., Lubkin, A., Fiorese, C., Lahoud, M.H., Caminschi, I., Huang, Y., Rodriguez, A., Clausen, B.E., Park, C.G., Trumpfheller, C., et al. (2011). Comparable T helper 1 (Th1) and CD8 T-cell immunity by targeting HIV gag p24 to CD8 dendritic cells within antibodies to Langerin, DEC205, and Clec9A. Proc. Natl. Acad. Sci. U. S. A. *108*, 2384–2389.

Ilinykh, P.A., and Bukreyev, A. (2021). Antibody responses to filovirus infections in humans: protective or not? Lancet Infect. Dis. *21*, e348–e355.

Jahrling, P.B., Geisbert, T.W., Johnson, E.D., Peters, C.J., Dalgard, D.W., and Hall, W.C. (1990). Preliminary report: isolation of Ebola virus from monkeys imported to USA. Lancet *335*, 502–505.

Jiang, X., Clark, R.A., Liu, L., Wagers, A.J., Fuhlbrigge, R.C., and Kupper, T.S. (2012). Skin infection generates non-migratory memory CD8+ TRM cells providing global skin immunity. Nature *483*, 227–231.

Jones, S.M., Feldmann, H., Ströher, U., Geisbert, J.B., Fernando, L., Grolla, A., Klenk, H.-D., Sullivan, N.J., Volchkov, V.E., and Fritz, E.A. (2005). Live attenuated recombinant vaccine protects nonhuman primates against Ebola and Marburg viruses. Nat. Med. *11*, 786–790.

Kaech, S.M. Generation of effector CD8 + T cells and their conversion to memory T cells.

Kaech, S.M., Tan, J.T., Wherry, E.J., Konieczny, B.T., Surh, C.D., and Ahmed, R. (2003). Selective expression of the interleukin 7 receptor identifies effector CD8 T cells that give rise to long-lived memory cells. Nat. Immunol. *4*, 1191–1198.

Kajihara, M., Hang'ombe, B.M., Changula, K., Harima, H., Isono, M., Okuya, K., Yoshida, R., Mori-Kajihara, A., Eto, Y., and Orba, Y. (2019). Marburgvirus in Egyptian fruit bats, Zambia. Emerg. Infect. Dis. *25*, 1577.

Kato, H., Takeuchi, O., Mikamo-Satoh, E., Hirai, R., Kawai, T., Matsushita, K., Hiiragi, A., Dermody, T.S., Fujita, T., and Akira, S. (2008). Length-dependent recognition of double-stranded ribonucleic acids by retinoic acid–inducible gene-I and melanoma differentiation–associated gene 5 .

J. Exp. Med. *205*, 1601–1610.

Kawai, T., and Akira, S. (2008). Toll-like receptor and RIG-1-like receptor signaling. Ann. N. Y. Acad. Sci. *1143*, 1–20.

Kell, A.M., and Gale, M. (2015). Since January 2020 Elsevier has created a COVID-19 resource centre with free information in English and Mandarin on the novel coronavirus COVID- 19 . The COVID-19 resource centre is hosted on Elsevier Connect , the company ' s public news and information. Virology *479–480*, 110–121.

Kemenesi, G., Kurucz, K., Dallos, B., Zana, B., Földes, F., Boldogh, S., Görföl, T., Carroll, M.W., and Jakab, F. (2018). Re-emergence of Lloviu virus in Miniopterus schreibersii bats, Hungary, 2016. Emerg. Microbes Infect. *7*, 1–4.

Kemenesi, G., Tóth, G.E., Mayora-Neto, M., Scott, S., Temperton, N., Wright, E., Mühlberger, E., Hume, A.J., Suder, E.L., Zana, B., et al. (2022). Isolation of infectious Lloviu virus from Schreiber's bats in Hungary. Nat. Commun. *13*, 1–11.

Khalil, M., and Vonderheide, R.H. (2007). Anti-CD40 agonist antibodies: preclinical and clinical experience. Update Cancer Ther. *2*, 61–65.

Kincaid, E.Z., Che, J.W., York, I., Escobar, H., Reyes-Vargas, E., Delgado, J.C., Welsh, R.M., Karow, M.L., Murphy, A.J., Valenzuela, D.M., et al. (2012). Mice completely lacking immunoproteasomes show major changes in antigen presentation. Nat. Immunol. *13*, 129–135.

Kok, L., Masopust, D., and Schumacher, T.N. (2022). The precursors of CD8+ tissue resident memory T cells: from lymphoid organs to infected tissues. Nat. Rev. Immunol. *22*, 283–293.

Kortepeter, M.G., Bausch, D.G., and Bray, M. (2011). Basic clinical and laboratory features of filoviral hemorrhagic fever. J. Infect. Dis. *204*, S810–S816.

Ksiazek, T.G., Rollin, P.E., Williams, A.J., Bressler, D.S., Martin, M.L., Swanepoel, R., Burt, F.J., Leman, P.A., Khan, A.S., Rowe, A.K., et al. (1999). Clinical virology of Ebola hemorrhagic fever (EHF): Virus, virus antigen, and IgG and IgM antibody findings among EHF patients in Kikwit, Democratic Republic of the Congo, 1995. J. Infect. Dis. *179*, 177–187.

Kuhn, J.H., Becker, S., Ebihara, H., Geisbert, T.W., Johnson, K.M., Kawaoka, Y., Lipkin, W.I., Negredo, A.I., Netesov, S. V, and Nichol, S.T. (2010). Proposal for a revised taxonomy of the family Filoviridae: classification, names of taxa and viruses, and virus abbreviations. Arch. Virol. *155*, 2083–2103.

Kuhn, J.H., Amarasinghe, G.K., Basler, C.F., Bavari, S., Bukreyev, A., Chandran, K., Crozier, I., Dolnik, O., Dye, J.M., and Formenty, P.B.H. (2019). ICTV virus taxonomy profile: Filoviridae. J.

Gen. Virol. *100*, 911.

Kumar, B. V., Connors, T.J., and Farber, D.L. (2018). Human T Cell Development, Localization, and Function throughout Life. Immunity *48*, 202–213.

Kuzmin, I. V, Niezgoda, M., Franka, R., Agwanda, B., Markotter, W., Breiman, R.F., Shieh, W.-J., Zaki, S.R., and Rupprecht, C.E. (2010). Marburg virus in fruit bat, Kenya. Emerg. Infect. Dis. *16*, 352.

Lam, J.H., Smith, F.L., and Baumgarth, N. (2020). B Cell Activation and Response Regulation during Viral Infections. Viral Immunol. *33*, 294–306.

Lanzavecchia, A., and Sallusto, F. (2009). Human B cell memory. Curr. Opin. Immunol. *21*, 298–304.

Lee, H., Jeong, S., and Shin, E.C. (2022). Significance of bystander T cell activation in microbial infection. Nat. Immunol. *23*, 13–22.

Leone, P., Shin, E.C., Perosa, F., Vacca, A., Dammacco, F., and Racanelli, V. (2013). MHC class i antigen processing and presenting machinery: Organization, function, and defects in tumor cells. J. Natl. Cancer Inst. *105*, 1172–1187.

Leroy, E.M., Kumulungui, B., Pourrut, X., Rouquet, P., Hassanin, A., Yaba, P., Délicat, A., Paweska, J.T., Gonzalez, J.-P., and Swanepoel, R. (2005). Fruit bats as reservoirs of Ebola virus. Nature *438*, 575–576.

Leroy, E.M., Epelboin, A., Mondonge, V., Pourrut, X., Gonzalez, J.-P., Muyembe-Tamfum, J.-J., and Formenty, P. (2009). Human Ebola outbreak resulting from direct exposure to fruit bats in Luebo, Democratic Republic of Congo, 2007. Vector-Borne Zoonotic Dis. *9*, 723–728.

LH, P., and K, V. (2016). Antibody-Mediated Delivery of Antigen to Dendritic Cells. Immunother. Open Access *02*.

Li, D.-K., and Wang, W. (2020). Characteristics and clinical trial results of agonistic anti-CD40 antibodies in the treatment of malignancies. Oncol. Lett. *20*, 1.

Lin, K.L., Twenhafel, N.A., Connor, J.H., Cashman, K.A., Shamblin, J.D., Donnelly, G.C., Esham, H.L., Wlazlowski, C.B., Johnson, J.C., and Honko, A.N. (2015). Temporal characterization of Marburg virus Angola infection following aerosol challenge in rhesus macaques. J. Virol. *89*, 9875–9885.

Liu, Q., Fan, C., Li, Q., Zhou, S., Huang, W., Wang, L., Sun, C., Wang, M., Wu, X., Ma, J., et al. (2017). Antibody-dependent-cellular-cytotoxicity-inducing antibodies significantly affect the post-exposure treatment of Ebola virus infection. Sci. Rep. *7*, 1–11.

Longhi, M.P., Trumpfheller, C., Idoyaga, J., Caskey, M., Matos, I., Kluger, C., Salazar, A.M., Colonna, M., and Steinman, R.M. (2009). Dendritic cells require a systemic type I interferon response to mature and induce CD4+ Th1 immunity with poly IC as adjuvant. J. Exp. Med. *206*, 1589–1602.

Lubaki, N.M., Ilinykh, P., Pietzsch, C., Tigabu, B., Freiberg, A.N., Koup, R.A., and Bukreyev, A. (2013). The Lack of Maturation of Ebola Virus-Infected Dendritic Cells Results from the Cooperative Effect of at Least Two Viral Domains. J. Virol. *87*, 7471–7485.

Lüdtke, A., Ruibal, P., Wozniak, D.M., Pallasch, E., Wurr, S., Bockholt, S., Gómez-Medina, S., Qiu, X., Kobinger, G.P., Rodríguez, E., et al. (2017). Ebola virus infection kinetics in chimeric mice reveal a key role of T cells as barriers for virus dissemination. Sci. Rep. *7*, 43776.

Lund, J.M., Alexopoulou, L., Sato, A., Karow, M., Adams, N.C., Gale, N.W., Iwasaki, A., and Flavell, R.A. (2004). Recognition of single-stranded RNA viruses by Toll-like receptor 7. Proc. Natl. Acad. Sci. U. S. A. *101*, 5598–5603.

Macri, C., Dumont, C., Johnston, A.P., and Mintern, J.D. (2016). Targeting dendritic cells: a promising strategy to improve vaccine effectiveness. Clin. Transl. Immunol. *5*, e66.

Mahnke, K., Qian, Y., Fondel, S., Brueck, J., Becker, C., and Enk, A.H. (2005a). Targeting of antigens to activated dendritic cells in vivo cures metastatic melanoma in mice. Cancer Res. *65*, 7007–7012.

Mahnke, K., Qian, Y., Fondel, S., Brueck, J., Becker, C., and Enk, A.H. (2005b). Targeting of antigens to activated dendritic cells in vivo cures metastatic melanoma in mice. Cancer Res. *65*, 7007–7012.

Marongiu, L., Valache, M., Facchini, F.A., and Granucci, F. (2021). How dendritic cells sense and respond to viral infections. Clin. Sci. *135*, 2217–2242.

Martín-Fontecha, A., Lanzavecchia, A., and Sallusto, F. (2009). Dendritic cell migration to peripheral lymph nodes. Handb. Exp. Pharmacol. *188*, 31–49.

Martinez, O., Johnson, J.C., Honko, A., Yen, B., Shabman, R.S., Hensley, L.E., Olinger, G.G., and Basler, C.F. (2013). Ebola Virus Exploits a Monocyte Differentiation Program To Promote Its Entry. J. Virol. *87*, 3801–3814.

Martins, K.A.O., Cooper, C.L., Stronsky, S.M., Norris, S.L.W., Kwilas, S.A., Steffens, J.T., Benko, J.G., van Tongeren, S.A., and Bavari, S. (2016). Adjuvant-enhanced CD4 T Cell Responses are Critical to Durable Vaccine Immunity. EBioMedicine *3*, 67–78.

Marzi, A., and Mire, C.E. (2019). Current Ebola Virus Vaccine Progress. BioDrugs *33*, 9–14.

Marzi, A., Engelmann, F., Feldmann, F., Haberthur, K., Shupert, W.L., Brining, D., Scott, D.P.,

Geisbert, T.W., Kawaoka, Y., Katze, M.G., et al. (2013). Antibodies are necessary for rVSV/ZEBOV-GP-mediated protection against lethal Ebola virus challenge in nonhuman primates. Proc. Natl. Acad. Sci. U. S. A. *110*, 1893–1898.

Matsumoto, M., Kikkawa, S., Kohase, M., Miyake, K., and Seya, T. (2002). Establishment of a monoclonal antibody against human Toll-like receptor 3 that blocks double-stranded RNA-mediated signaling. Biochem. Biophys. Res. Commun. *293*, 1364–1369.

Matz, K.M., Marzi, A., and Feldmann, H. (2019). Ebola vaccine trials: progress in vaccine safety and immunogenicity. Expert Rev. Vaccines *18*, 1229–1242.

Mayr, A., Stickl, H., Müller, H.K., Danner, K., and Singer, H. (1978). The smallpox vaccination strain MVA: marker, genetic structure, experience gained with the parenteral vaccination and behavior in organisms with a debilitated defence mechanism (author's transl). Zentralbl. Bakteriol. B. *167*, 375–390.

McElroy, A.K., Akondy, R.S., Davis, C.W., Ellebedy, A.H., Mehta, A.K., Kraft, C.S., Lyon, G.M., Ribner, B.S., Varkey, J., Sidney, J., et al. (2015). Human Ebola virus infection results in substantial immune activation. Proc. Natl. Acad. Sci. *112*, 4719–4724.

Meager, A. (1998). 25. - Interferons Alpha, Beta, and Omega. In Handbook of Immunopharmacology, A.R. Mire-Sluis, and R.B.T.-C. Thorpe, eds. (San Diego: Academic Press), pp. 361–389.

Mehedi, M., Groseth, A., Feldmann, H., and Ebihara, H. (2011). Clinical aspects of Marburg hemorrhagic fever. Future Virol. *6*, 1091–1106.

Mescher, M.F., Curtsinger, J.M., Agarwal, P., Casey, K.A., Gerner, M., Hammerbeck, C.D., Popescu, F., and Xiao, Z. (2006). Signals required for programming effector and memory development by CD8+ T cells. Immunol. Rev. *211*, 81–92.

Messaoudi, I., Amarasinghe, G.K., and Basler, C.F. (2015a). Filovirus pathogenesis and immune evasion: Insights from Ebola virus and Marburg virus. Nat. Rev. Microbiol. *13*, 663–676.

Messaoudi, I., Amarasinghe, G.K., and Basler, C.F. (2015b). Filovirus pathogenesis and immune evasion: Insights from Ebola virus and Marburg virus. Nat. Rev. Microbiol. *13*, 663–676.

Miller, E.H., Obernosterer, G., Raaben, M., Herbert, A.S., Deffieu, M.S., Krishnan, A., Ndungo, E., Sandesara, R.G., Carette, J.E., and Kuehne, A.I. (2012). Ebola virus entry requires the host-programmed recognition of an intracellular receptor. EMBO J. *31*, 1947–1960.

Milligan, I.D., Gibani, M.M., Sewell, R., Clutterbuck, E.A., Campbell, D., Plested, E., Nuthall, E., Voysey, M., Silva-Reyes, L., and McElrath, M.J. (2016). Safety and immunogenicity of novel adenovirus type 26–and modified vaccinia ankara–vectored ebola vaccines: a randomized clinical

trial. Jama *315*, 1610–1623.

Miyauchi, K., Sugimoto-Ishige, A., Harada, Y., Adachi, Y., Usami, Y., Kaji, T., Inoue, K., Hasegawa, H., Watanabe, T., Hijikata, A., et al. (2016). Protective neutralizing influenza antibody response in the absence of T follicular helper cells. Nat. Immunol. *17*, 1447–1458.

Mohamadzadeh, M., Chen, L., and Schmaljohn, A.L. (2007). How Ebola and Marburg viruses battle the immune system. Nat. Rev. Immunol. *7*, 556–567.

Mohan, G.S., Li, W., Ye, L., Compans, R.W., and Yang, C. (2012). Antigenic Subversion: A Novel Mechanism of Host Immune Evasion by Ebola Virus. PLoS Pathog. *8*.

Monteiro, J.T., and Lepenies, B. (2017). Myeloid C-type lectin receptors in viral recognition and antiviral immunity. Viruses *9*, 59.

Mühlberger, E. (2007). Filovirus replication and transcription.

Muñoz-Fontela, C., and McElroy, A.K. (2017). Ebola Virus Disease in Humans: Pathophysiology and Immunity BT - Marburg- and Ebolaviruses: From Ecosystems to Molecules. E. Mühlberger, L.L. Hensley, and J.S. Towner, eds. (Cham: Springer International Publishing), pp. 141–169.

Nowacki, T.M., Kuerten, S., Zhang, W., Shive, C.L., Kreher, C.R., Boehm, B.O., Lehmann, P. V, and Tary-Lehmann, M. (2007). Granzyme B production distinguishes recently activated CD8+ memory cells from resting memory cells. Cell. Immunol. *247*, 36–48.

Nutt, S.L., and Huntington, N.D. (2019). Cytotoxic T Lymphocytes and Natural Killer Cells (Elsevier Ltd).

O'Donnell, K., and Marzi, A. (2020). The Ebola virus glycoprotein and its immune responses across multiple vaccine platforms. Expert Rev. Vaccines *19*, 267–277.

Obar, J.J., Jellison, E.R., Sheridan, B.S., Blair, D.A., Pham, Q.-M., Zickovich, J.M., and Lefrançois, L. (2011). Pathogen-Induced Inflammatory Environment Controls Effector and Memory CD8+ T Cell Differentiation. J. Immunol. *187*, 4967–4978.

Oestereich, L., Lüdtke, A., Ruibal, P., Pallasch, E., Kerber, R., Rieger, T., Wurr, S., Bockholt, S., Perez-Giron, J. V, and Krasemann, S. (2016). Chimeric mice with competent hematopoietic immunity reproduce key features of severe Lassa fever. PLoS Pathog. *12*, e1005656.

Okumura, A., Pitha, P.M., Yoshimura, A., and Harty, R.N. (2010). Interaction between Ebola Virus Glycoprotein and Host Toll-Like Receptor 4 Leads to Induction of Proinflammatory Cytokines and SOCS1. J. Virol. *84*, 27–33.

Ostler, T., Pircher, H., and Ehl, S. (2003). " Bystander" recruitment of systemic memory T cells

delays the immune response to respiratory virus infection. Eur. J. Immunol. *33*, 1839–1848.

Owen, D.L., Sjaastad, L.E., and Farrar, M.A. (2019). Regulatory T Cell Development in the Thymus. J. Immunol. *203*, 2031–2041.

Di Paola, N., Sanchez-Lockhart, M., Zeng, X., Kuhn, J.H., and Palacios, G. (2020). Viral genomics in Ebola virus research. Nat. Rev. Microbiol. *18*, 365–378.

Paweska, J.T., Jansen van Vuren, P., Fenton, K.A., Graves, K., Grobbelaar, A.A., Moolla, N., Leman, P., Weyer, J., Storm, N., and McCulloch, S.D. (2015). Lack of Marburg virus transmission from experimentally infected to susceptible in-contact Egyptian fruit bats. J. Infect. Dis. *212*, S109–S118.

Pawęska, J.T., van Vuren, P.J., Kemp, A., Storm, N., Grobbelaar, A.A., Wiley, M.R., Palacios, G., and Markotter, W. (2018). Marburg virus infection in Egyptian rousette bats, South Africa, 2013–2014. Emerg. Infect. Dis. *24*, 1134.

Pawęska, J.T., Storm, N., Markotter, W., Di Paola, N., Wiley, M.R., Palacios, G., and van Vuren, P.J. (2020). Shedding of marburg virus in naturally infected egyptian rousette bats, South Africa, 2017. Emerg. Infect. Dis. *26*, 3051.

Perdomo-celis, F., Salvato, M.S., Medina-moreno, S., and Zapata, J.C. (2019). vaccines T-Cell Response to Viral Hemorrhagic Fevers. 1–29.

Pereira, L.R., Cristina, E., Vicentin, M., Pereira, S.A., Lina, D., Fabris, N., Alves, S., Andreata-santos, R., Tramontini, F., Sousa, G. De, et al. Intradermal Delivery of Dendritic Cell-Targeting Chimeric mAbs Genetically Fused to Type 2 Dengue Virus Nonstructural Protein 1. 1–19.

Pizzolla, A., Nguyen, T.H.O., Smith, J.M., Brooks, A.G., Kedzierska, K., Heath, W.R., Reading, P.C., and Wakim, L.M. (2017). Resident memory CD8+ T cells in the upper respiratory tract prevent pulmonary influenza virus infection. Sci. Immunol. *2*, eaam6970.

Plumlee, C.R., Obar, J.J., Colpitts, S.L., Jellison, E.R., Haining, W.N., Lefrancois, L., and Khanna, K.M. (2015). Early Effector CD8 T Cells Display Plasticity in Populating the Short-Lived Effector and Memory-Precursor Pools Following Bacterial or Viral Infection. Sci. Rep. *5*, 1–13.

Poetsch, J.H., Dahlke, C., Zinser, M.E., Kasonta, R., Lunemann, S., Rechtien, A., Ly, M.L., Stubbe, H.C., Krähling, V., Biedenkopf, N., et al. (2019). Detectable Vesicular Stomatitis Virus (VSV)-Specific Humoral and Cellular Immune Responses Following VSV-Ebola Virus Vaccination in Humans. J. Infect. Dis. *219*, 556–561.

Port, J.R., Wozniak, D.M., Oestereich, L., Pallasch, E., Becker-Ziaja, B., Müller, J., Rottstegge, M., Olal, C., Gómez-Medina, S., Oyakhliome, J., et al. (2020). Severe human Lassa fever is characterized by nonspecific T-cell activation and lymphocyte homing to inflamed tissues. J. Virol. *94*, e01367-20.

Pourrut, X., Souris, M., Towner, J.S., Rollin, P.E., Nichol, S.T., Gonzalez, J.-P., and Leroy, E. (2009). Large serological survey showing cocirculation of Ebola and Marburg viruses in Gabonese bat populations, and a high seroprevalence of both viruses in Rousettus aegyptiacus. BMC Infect. Dis. *9*, 1–10.

Ramírez de Arellano, E., Sanchez-Lockhart, M., Perteguer, M.J., Bartlett, M., Ortiz, M., Campioli, P., Hernández, A., Gonzalez, J., Garcia, K., and Ramos, M. (2019). First evidence of antibodies against Lloviu virus in Schreiber's bent-winged insectivorous bats demonstrate a wide circulation of the virus in Spain. Viruses *11*, 360.

Rehwinkel, J., and Gack, M.U. (2020). RIG-I-like receptors: their regulation and roles in RNA sensing. Nat. Rev. Immunol. *20*, 537–551.

Reinhardt, R.L., Liang, H.-E., and Locksley, R.M. (2009). Cytokine-secreting follicular T cells shape the antibody repertoire. Nat. Immunol. *10*, 385–393.

Reynolds, P., and Marzi, A. (2017). Ebola and Marburg virus vaccines. Virus Genes *53*, 501–515.

Richman, D.D., Cleveland, P.H., McCormick, J.B., and Johnson, K.M. (1983). Antigenic analysis of strains of Ebola virus: identification of two Ebola virus serotypes. J. Infect. Dis. *147*, 268–271.

Rivera, A., and Messaoudi, I. (2016). Molecular mechanisms of Ebola pathogenesis. J. Leucoc. Biol. *100*, 889–904.

Robert-Guroff, M. (2007). Replicating and non-replicating viral vectors for vaccine development. Curr. Opin. Biotechnol. *18*, 546–556.

Rose, N.F., Roberts, A., Buonocore, L., and Rose, J.K. (2000). Glycoprotein Exchange Vectors Based on Vesicular Stomatitis Virus Allow Effective Boosting and Generation of Neutralizing Antibodies to a Primary Isolate of Human Immunodeficiency Virus Type 1. J. Virol. *74*, 10903–10910.

Rottstegge, M., Tipton, T., Oestereich, L., Ruibal, P., Nelson, E. V, Olal, C., Port, J.R., Seibel, J., Pallasch, E., and Bockholt, S. (2022). Avatar Mice Underscore the Role of the T Cell-Dendritic Cell Crosstalk in Ebola Virus Disease and Reveal Mechanisms of Protection in Survivors. J. Virol. *96*, e00574-22.

Rowe, A.K., Bertolli, J., Khan, A.S., Mukunu, R., Muyembe-Tamfum, J.J., Bressler, D., Williams, A.J., Peters, C.J., Rodriguez, L., Feldmann, H., et al. (1999). Clinical, virologic, and immunologic follow-up of convalescent Ebola hemorrhagic fever patients and their household contacts, Kikwit, Democratic Republic of the Congo. J. Infect. Dis. *179*, 28–35.

Ruibal, P., Oestereich, L., Ludtke, A., Becker-Ziaja, B., Wozniak, D.M., Kerber, R., Korva, M., Cabeza-Cabrerizo, M., Bore, J.A., Koundouno, F.R., et al. (2016). Unique human immune signature

of Ebola virus disease in Guinea. Nature *533*, 100–104.

Sallusto, F., Lenig, D., Förster, R., Lipp, M., and Lanzavecchia, A. (1999). Two subsets of memory T lymphocytes with distinct homing potentials and effector functions. Nature *401*, 708–712.

Sandalova, E., Laccabue, D., Boni, C., Tan, A.T., Fink, K., Ooi, E.E., Chua, R., Shafaeddin Schreve, B., Ferrari, C., and Bertoletti, A. (2010). Contribution of herpesvirus specific CD8 T cells to anti-viral T cell response in humans. PLoS Pathog. *6*, e1001051.

Saravia, J., Chapman, N.M., and Chi, H. (2019). Helper T cell differentiation. Cell. Mol. Immunol. *16*, 634–643.

Schluns, K.S., Kieper, W.C., Jameson, S.C., and Lefrançois, L. (2000). Interleukin-7 mediates the homeostasis of naive and memory CD8 T cells in vivo. Nat. Immunol. *1*, 426–432.

Schnell, M.J., Buonocore, L., Kretzschmar, E., Johnson, E., and Rose, J.K. (1996). Foreign glycoproteins expressed from recombinant vesicular stomatitis viruses are incorporated efficiently into virus particles. Proc. Natl. Acad. Sci. *93*, 11359–11365.

Schnittler, H.-J., Mahner, F., Drenckhahn, D., Klenk, H.-D., and Feldmann, H. (1993). Replication of Marburg virus in human endothelial cells. A possible mechanism for the development of viral hemorrhagic disease. J. Clin. Invest. *91*, 1301–1309.

Schuh, A.J., Amman, B.R., Jones, M.E.B., Sealy, T.K., Uebelhoer, L.S., Spengler, J.R., Martin, B.E., Coleman-McCray, J.A.D., Nichol, S.T., and Towner, J.S. (2017). Modelling filovirus maintenance in nature by experimental transmission of Marburg virus between Egyptian rousette bats. Nat. Commun. *8*, 14446.

Shabman, R.S., Hoenen, T., Groseth, A., Jabado, O., Binning, J.M., Amarasinghe, G.K., Feldmann, H., and Basler, C.F. (2013). An Upstream Open Reading Frame Modulates Ebola Virus Polymerase Translation and Virus Replication. *9*.

Sheridan, B.S., Pham, Q.M., Lee, Y.T., Cauley, L.S., Puddington, L., and Lefrançois, L. (2014). Oral infection drives a distinct population of intestinal resident memory cd8+ t cells with enhanced protective function. Immunity *40*, 747–757.

Shifflett, K., and Marzi, A. (2019). Marburg virus pathogenesis - Differences and similarities in humans and animal models. Virol. J. *16*, 1–12.

Shin, E.-C., Sung, P.S., and Park, S.-H. (2016). Immune responses and immunopathology in acute and chronic viral hepatitis. Nat. Rev. Immunol. *16*, 509–523.

Shortman, K., and Heath, W.R. (2010). The CD8+ dendritic cell subset. Immunol. Rev. *234*, 18–31.

Sijts, A.J.A.M., Ruppert, T., Rehermann, B., Schmidt, M., Koszinowski, U., and Kloetzel, P.M. (2000). Efficient generation of a hepatitis B virus cytotoxic T lymphocyte epitope requires the structural features of immunoproteasomes. J. Exp. Med. *191*, 503–513.

Simmons, G., Reeves, J.D., Grogan, C.C., Vandenberghe, L.H., Baribaud, F., Whitbeck, J.C., Burke, E., Buchmeier, M.J., Soilleux, E.J., Riley, J.L., et al. (2003). DC-SIGN and DC-SIGNR bind Ebola glycoproteins and enhance infection of macrophages and endothelial cells. Virology *305*, 115–123.

Simon, J.K., Kennedy, S.B., Mahon, B.E., Dubey, S.A., Grant-Klein, R.J., Liu, K., Hartzel, J., Coller, B.-A.G., Welebob, C., and Hanson, M.E. (2022). Immunogenicity of rVSVΔG-ZEBOV-GP Ebola vaccine (ERVEBO®) in African clinical trial participants by age, sex, and baseline GP-ELISA titer: A post hoc analysis of three Phase 2/3 trials. Vaccine *40*, 6599–6606.

Smith, L.M., Hensley, L.E., Geisbert, T.W., Johnson, J., Stossel, A., Honko, A., Yen, J.Y., Geisbert, J., Paragas, J., and Fritz, E. (2013). Interferon-β therapy prolongs survival in rhesus macaque models of Ebola and Marburg hemorrhagic fever. J. Infect. Dis. *208*, 310–318.

Sobarzo, A., Groseth, A., Dolnik, O., Becker, S., Lutwama, J.J., Perelman, E., Yavelsky, V., Muhammad, M., Kuehne, A.I., and Marks, R.S. (2013). Profile and persistence of the virus-specific neutralizing humoral immune response in human survivors of Sudan ebolavirus (Gulu). J. Infect. Dis. *208*, 299–309.

Stanley, D.A., Honko, A.N., Asiedu, C., Trefry, J.C., Lau-Kilby, A.W., Johnson, J.C., Hensley, L., Ammendola, V., Abbate, A., Grazioli, F., et al. (2014). Chimpanzee adenovirus vaccine generates acute and durable protective immunity against ebolavirus challenge. Nat. Med. *20*, 1126–1129.

Stonier, S.W., Herbert, A.S., Kuehne, A.I., Sobarzo, A., Habibulin, P., Dahan, C.V.A., James, R.M., Egesa, M., Cose, S., Lutwama, J.J., et al. (2017). Marburg virus survivor immune responses are Th1 skewed with limited neutralizing antibody responses. J. Exp. Med. *214*, 2563–2572.

Storm, N., Jansen Van Vuren, P., Markotter, W., and Paweska, J.T. (2018). Antibody responses to marburg virus in Egyptian rousette bats and their role in protection against infection. Viruses *10*, 73.

Sullivan, N.J., Geisbert, T.W., Geisbert, J.B., Shedlock, D.J., Xu, L., Lamoreaux, L., Custers, J.H.H.V., Popernack, P.M., Yang, Z.Y., Pau, M.G., et al. (2006). Immune protection of nonhuman primates against Ebola virus with single low-dose adenovirus vectors encoding modified GPs. PLoS Med. *3*, 0865–0873.

Sullivan, N.J., Martin, J.E., Graham, B.S., and Nabel, G.J. (2009). Correlates of protective immunity for Ebola vaccines: implications for regulatory approval by the animal rule. Nat. Rev. Microbiol. *7*, 393–400.

Sullivan, N.J., Hensley, L., Asiedu, C., Geisbert, T.W., Stanley, D., Johnson, J., Honko, A., Olinger, G., Bailey, M., and Geisbert, J.B. (2011). CD8+ cellular immunity mediates rAd5 vaccine protection against Ebola virus infection of nonhuman primates. Nat. Med. *17*, 1128–1131.

Sundar, K., Boesen, A., and Coico, R. (2007). Computational prediction and identification of HLA-A2. 1-specific Ebola virus CTL epitopes. Virology *360*, 257–263.

Swanepoel, R., Smit, S.B., Rollin, P.E., Formenty, P., Leman, P.A., Kemp, A., Burt, F.J., Grobbelaar, A.A., Croft, J., and Bausch, D.G. (2007). Studies of reservoir hosts for Marburg virus. Emerg. Infect. Dis. *13*, 1847.

Swenson, D.L., Wang, D., Luo, M., Warfield, K.L., Woraratanadharm, J., Holman, D.H., Dong, J.Y., and Pratt, W.D. (2008). Vaccine to confer to nonhuman primates complete protection against multistrain Ebola and Marburg virus infections. Clin. Vaccine Immunol. *15*, 460–467.

Tai, Y.-T., Catley, L.P., Mitsiades, C.S., Burger, R., Podar, K., Shringpaure, R., Hideshima, T., Chauhan, D., Hamasaki, M., and Ishitsuka, K. (2004). Mechanisms by which SGN-40, a humanized anti-CD40 antibody, induces cytotoxicity in human multiple myeloma cells: clinical implications. Cancer Res. *64*, 2846–2852.

Takeda, K., and Akira, S. (2005). Toll-like receptors in innate immunity. Int. Immunol. *17*, 1–14.

Tao, X., Constant, S., Jorritsma, P., and Bottomly, K. (1997). Strength of TCR signal determines the costimulatory requirements for Th1 and Th2 CD4+ T cell differentiation. J. Immunol. *159*, 5956–5963.

Thomas, R., Al-Khadairi, G., Roelands, J., Hendrickx, W., Dermime, S., Bedognetti, D., and Decock, J. (2018). NY-ESO-1 based immunotherapy of cancer: current perspectives. Front. Immunol. *9*, 947.

Tortorella, D., Gewurz, B.E., Furman, M.H., Schust, D.J., and Ploegh, H.L. (2000). Viral subversion of the immune system. Annu. Rev. Immunol. *18*, 861–926.

Towner, J.S., Paragas, J., Dover, J.E., Gupta, M., Goldsmith, C.S., Huggins, J.W., and Nichol, S.T. (2005). Generation of eGFP expressing recombinant Zaire ebolavirus for analysis of early pathogenesis events and high-throughput antiviral drug screening. Virology *332*, 20–27.

Towner, J.S., Pourrut, X., Albariño, C.G., Nkogue, C.N., Bird, B.H., Grard, G., Ksiazek, T.G., Gonzalez, J.-P., Nichol, S.T., and Leroy, E.M. (2007). Marburg virus infection detected in a common African bat. PLoS One *2*, e764.

Towner, J.S., Sealy, T.K., Khristova, M.L., Albariño, C.G., Conlan, S., Reeder, S.A., Quan, P.-L., Lipkin, W.I., Downing, R., and Tappero, J.W. (2008). Newly discovered ebola virus associated with hemorrhagic fever outbreak in Uganda. PLoS Pathog. *4*, e1000212.

Travieso, T., Li, J., Mahesh, S., Mello, J.D.F.R.E., and Blasi, M. (2022). The use of viral vectors in vaccine development. Npj Vaccines *7*, 75.

Trumpfheller, C., Caskey, M., Nchinda, G., Longhi, M.P., Mizenina, O., Huang, Y., Schlesinger, S.J., Colonna, M., and Steinman, R.M. (2008). The microbial mimic poly IC induces durable and protective CD4+ T cell immunity together with a dendritic cell targeted vaccine. Proc. Natl. Acad. Sci. *105*, 2574–2579.

Venkatraman, N., Ndiaye, B.P., Bowyer, G., Wade, D., Sridhar, S., Wright, D., Powlson, J., Ndiaye, I., Dièye, S., and Thompson, C. (2019). Safety and immunogenicity of a heterologous prime-boost Ebola virus vaccine regimen in healthy adults in the United Kingdom and Senegal. J. Infect. Dis. *219*, 1187–1197.

Verdon, D.J., Mulazzani, M., and Jenkins, M.R. (2020). Cellular and molecular mechanisms of CD8+ T cell differentiation, dysfunction and exhaustion. Int. J. Mol. Sci. *21*, 1–28.

Vernet, M.A., Reynard, S., Fizet, A., Schaeffer, J., Pannetier, D., Guedj, J., Rives, M., Georges, N., Garcia-Bonnet, N., Sylla, A.I., et al. (2017). Clinical, virological, and biological parameters associated with outcomes of Ebola virus infection in Macenta, Guinea. JCI Insight *2*, 1–14.

Vignali, D.A.A., Collison, L.W., and Workman, C.J. (2008). How regulatory T cells work. Nat. Rev. Immunol. *8*, 523–532.

Vonderheide, R.H. (2007). Prospect of targeting the CD40 pathway for cancer therapy. Clin. Cancer Res. *13*, 1083–1088.

Vonderheide, R.H. (2020). CD40 agonist antibodies in cancer immunotherapy. Annu. Rev. Med. *71*, 47–58.

Wamala, J.F., Lukwago, L., Malimbo, M., Nguku, P., Yoti, Z., Musenero, M., Amone, J., Mbabazi, W., Nanyunja, M., and Zaramba, S. (2010). Ebola hemorrhagic fever associated with novel virus strain, Uganda, 2007–2008. Emerg. Infect. Dis. *16*, 1087.

Wauquier, N., Becquart, P., Padilla, C., Baize, S., and Leroy, E.M. (2010). Human fatal zaire ebola virus infection is associated with an aberrant innate immunity and with massive lymphocyte apoptosis. PLoS Negl. Trop. Dis. *4*.

Wec, A.Z., Herbert, A.S., Murin, C.D., Nyakatura, E.K., Abelson, D.M., Fels, J.M., He, S., James, R.M., De, M.-A., Vega, L., et al. (2017). Antibodies from a Human Survivor Define Sites of Vulnerability for Broad Protection against Ebolaviruses AUTHOR CONTRIBUTIONS produced GPs and mAbs for structural and functional studies HHS Public Access. Cell *169*, 878–890.

Wherry, E.J. (2011). T cell exhaustion. Nat. Immunol. *12*, 492–499.

Wherry, E.J., and Kurachi, M. (2015). Molecular and cellular insights into T cell exhaustion. Nat. Rev. Immunol. *15*, 486–499.

Wong, G., Richardson, J.S., Pillet, S., Patel, A., Qiu, X., Alimonti, J., Hogan, J., Zhang, Y., Takada, A., Feldmann, H., et al. (2013). Virus Infection in Rodents and Nonhuman Primates. *4*.

Wong, G., Kobinger, G.P., and Qiu, X. (2014). Characterization of host immune responses in Ebola virus infections. Expert Rev. Clin. Immunol. *10*, 781–790.

Wu, T., Hu, Y., Lee, Y.-T., Bouchard, K.R., Benechet, A., Khanna, K., and Cauley, L.S. (2014). Lung-resident memory CD8 T cells (TRM) are indispensable for optimal cross-protection against pulmonary virus infection. J. Leukoc. Biol. *95*, 215–224.

Wu, X., Wu, P., Shen, Y., Jiang, X., and Xu, F. (2018). CD8+Resident memory T cells and viral infection. Front. Immunol. *9*.

Yuzefpolskiy, Y., Baumann, F.M., Kalia, V., and Sarkar, S. (2015). Early CD8 T-cell memory precursors and terminal effectors exhibit equipotent in vivo degranulation. Cell. Mol. Immunol. *12*, 400–408.

Zhu, W., Banadyga, L., Emeterio, K., Wong, G., and Qiu, X. (2019). The roles of ebola virus soluble glycoprotein in replication, pathogenesis, and countermeasure development. Viruses *11*.

Zúñiga-Pflücker, J.C. (2004). T-cell development made simple. Nat. Rev. Immunol. *4*, 67–72.

Internet sources:

https://www.who.int/news-room/fact-sheets/detail/marburg-virus-disease

https://www.who.int/news-room/fact-sheets/detail/ebola-virus-disease

Shah, D (2022). T cell development in the thymus. https://www.immunology.org/public-information/bitesized-immunology/immune-development/t-cell-development-thymus

Schematics in figure 8,10, 11, 12, 13, 16 and 22 were created with Biorender.

8. Appendix

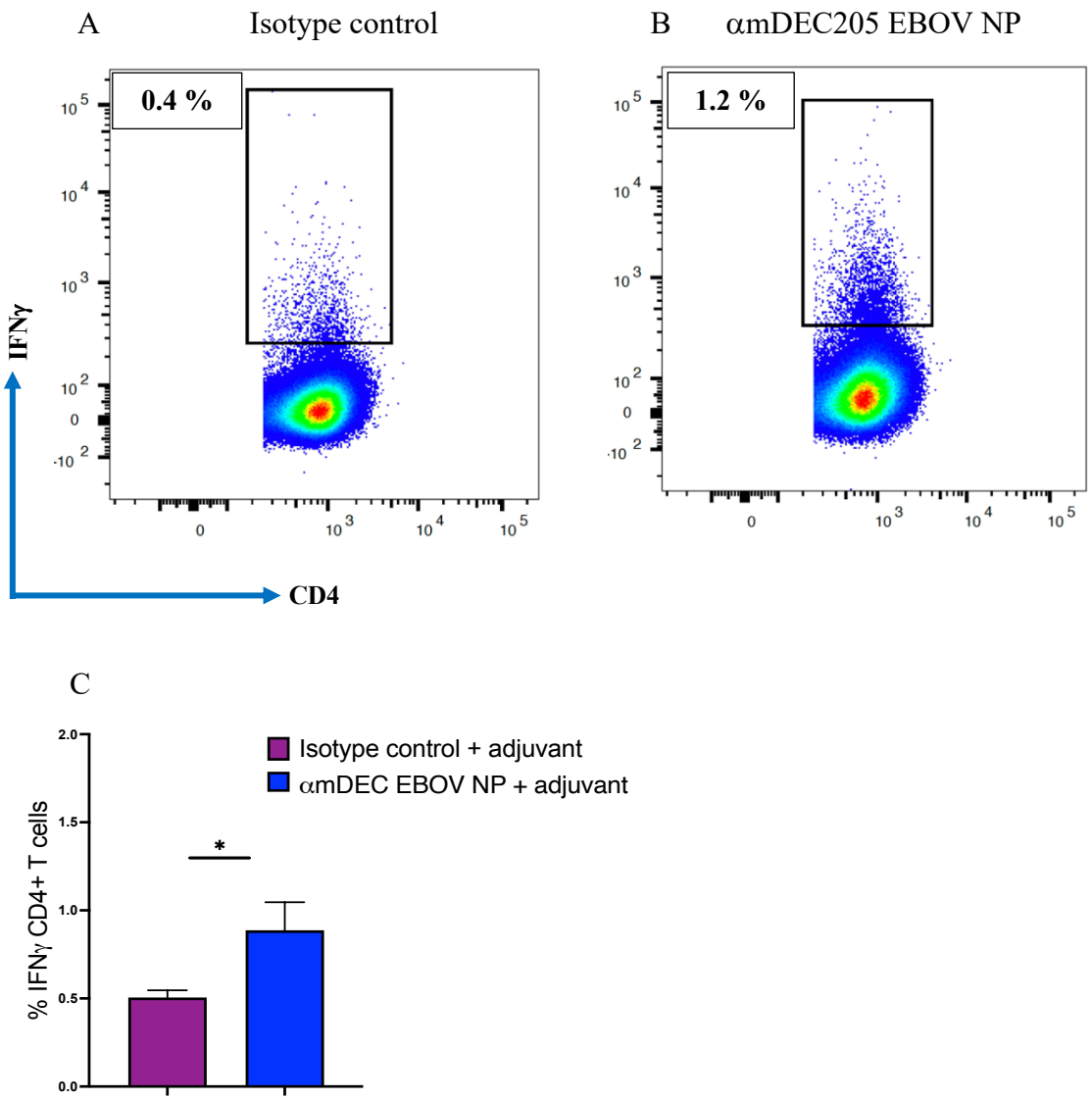

Supplementary figure 1: IFNγ secretion by CD4$^+$ T cells after targeting EBOV NP to DCs

Mice (n= 4) were immunized as described in figure 13. Splenocytes were obtained and restimulated with EBOV NP peptide - LSFASLSFASLFLPKLVVGEK. The frequency of T cells expressing IFNγ was determined by intracellular cytokine staining after peptide re-stimulation. Representative flow cytometry plots showing the percentage of CD4$^+$ T cells expressing IFNγ. Bar graphs represent mean values ± SEM of IFNγ (C). Statistical significance was calculated using student's t-test (ns – not significant, *$p \leq 0.05$, **$p \leq 0.01$, ***$p \leq 0.001$).

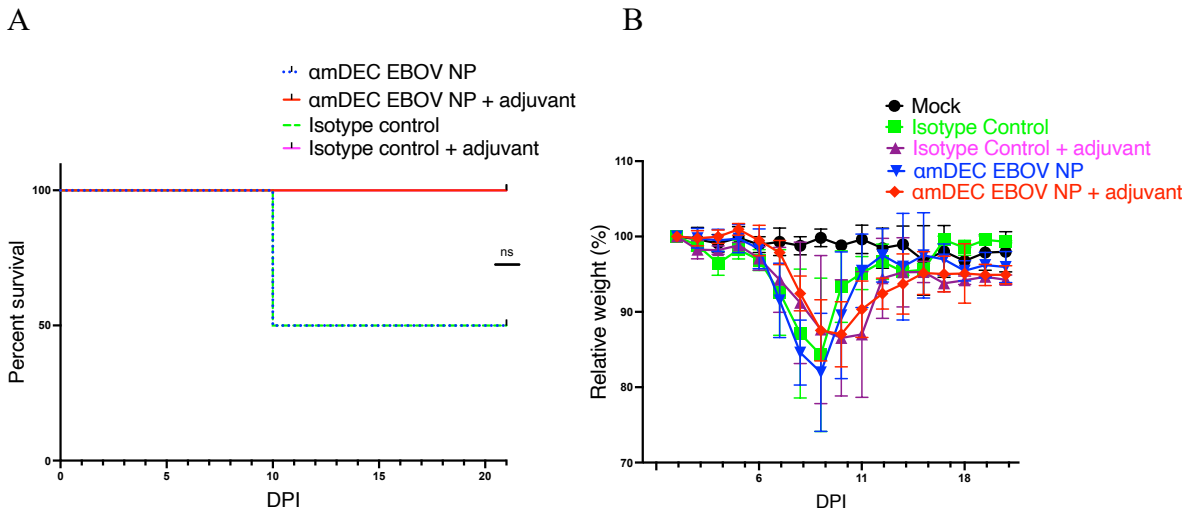

Supplementary figure 2: There is no difference in morbidity and survival after DC targeting without adjuvant.

Male and female WT → IFNAR$^{-/-}$ mice (n = 8) were immunized with either the isotype control or αmDEC205 EBOV NP together with 50 µg Poly IC and 25 µg αCD40 according to the immunization regimen as previously described. At 28 days post immunization, the mice received a boost with the targeting antibodies and the adjuvants. 14 days later, mice were infected intranasally with 10,000 FFU EBOV Mayinga. Mice were monitored for 21 days and those that reached humane endpoint criteria were euthanised. Graphs show Kaplan Meier survival curves (A), weight (B). Values are reported as mean ± SEM. Statistical significance was determined using Mantel-Cox test (A) or unpaired two-tailed Student's *t*-test (B) (ns – not significant, *$p \leq 0.05$, **$p \leq 0.01$, ***$p \leq 0.001$).